UNIVERSIDAD AUTÓNOMA DE MADRID
Departamento de Biología Molecular

BIOGÉNESIS Y REGULACIÓN DEL TRANSPORTADOR NEURONAL DE GLICINA GlyT2 Y MUTANTES RESPONSABLES DE HIPERPLEXIA HUMANA

Esther Arribas González

Madrid, 2017

UNIVERSIDAD AUTÓNOMA DE MADRID
Facultad de Ciencias
Departamento de Biología Molecular

BIOGÉNESIS Y REGULACIÓN DEL TRANSPORTADOR NEURONAL DE GLICINA GlyT2 Y MUTANTES RESPONSABLES DE HIPERPLEXIA HUMANA

Memoria presentada por la licenciada en Bioquímica
Esther Arribas González para optar al título de Doctora en Ciencias por compendio de publicaciones bajo la supervisión de:

Directora de la tesis:

Dra. Beatriz López Corcuera

Este trabajo ha sido realizado en el Departamento de Biología Molecular, Centro de Biología Molecular "Severo Ochoa" (C.S.I.C-U.A.M) y ha sido posible gracias a una ayuda predoctoral dentro del subprograma de Formación Personal de Investigación (FPI;BES- 2012-053800) asociada al proyecto SAF2011-28674 concedido por el Ministerio de Economía y Competitividad.

A mis padres
con todo mi cariño

"Todo hombre puede ser, si se lo propone, escultor de su propio cerebro"

Santiago Ramón y Cajal

"Somos lo que hacemos"

Ortega y Gasset

Ha llegado la hora. Aún no me lo creo. Son muchos años invertidos, ideas desarrolladas y experimentos realizados hasta ver realmente un resultado prometedor. Y es que aprendes a dormir con porqués sin resolver deseando despertarte y que te surja la solución al problema, pero el tiempo es limitado y cuando más realizado te sientes, te llega la hora de reunir todo y plasmar tu aportación en ciencia. No era de las niñas que soñaba con batas blancas ni pipetas, tampoco que haría una carrera universitaria, un máster y un doctorado para finalmente poder convertirme en doctora en ciencias sin una inculcación previa, pero el destino no está escrito.

Por eso, en primer lugar estaré eternamente agradecida a las doctoras Carmen Aragón Rueda y Beatriz López Corcuera por sobre todo, confiar en mí y haberme brindado la posibilidad de realizar la tesis doctoral en su laboratorio. Gracias a Carmen por estar siempre dispuesta a aconsejarme cuando la he necesitado desde la humildad que la caracteriza y muy especialmente a Beatriz por crear mi *yo científico*. Desde el primer momento que entré en el laboratorio como estudiante hace ahora ya unos cuantos años, has estado ahí cada día, supervisando los experimentos e ideas, revisando y redactando los artículos, animándome en momentos malos, apoyándome en asuntos personales y mucho más. Has escuchado mis ideas científicas dejándome volar sola pero siempre atenta por si me caía. Me has enseñado lo que es la ciencia. Es un honor haberte tenido como directora de tesis porque aunque estás a mil cosas siempre, y cuando digo siempre es siempre, tienes tiempo para nosotros sin importarte cuánto pase. Gracias Beatriz.

Gracias también al Dr. Francisco Zafra por sus excelentes consejos en los "clonajes peleones" con intermitentes notas de humor que te hacen más llevadero un difícil día y al Dr. Cecilio Giménez por el interés mostrado durante estos años. Son tantas las personas con las que he convivido en esta época de mi vida que ojalá no se me olvide reconocer a ninguna porque claramente esta tesis no habría sido la misma sin el apoyo, ayuda y consejos de todos vosotros.

Agradecer la dedicación de mis compañeros iniciales del 304 por aguantar mis preguntitas de novata. Espe me has transmitido tranquilidad para afrontar problemas entre *sushi* y dibujo ¡gracias por esa portada de tesis!, Gon eres la simpatía y sencillez personificada y sobretodo a JJ, el hombre tranquilo siempre dispuesto a ayudarme con esa templanza necesaria en ciencia, eres un genio ¡crucemos los dedos con la LNX! No, no me he olvidado de tí Enri, sabes bien qué mereces un párrafo aparte. Has sido mi guía experimental en todos estos años con una paciencia enorme con "la que no te escucha" resolviendo las cabezonerías que he ido teniendo día tras día.

Sabes que si me han salido experimentos sólo ha sido posible por tu meticulosa ayuda. Pero sobretodo, gracias por formar un equipo conmigo. Nunca olvidaré esas conversaciones con confianza que nos hemos echado, gracias amigo. Cuánto he disfrutado con los geles nativos pensando en azul contigo…toma, toma y toma! Gracias a Guille, Ernesto y con gran afecto al gijonés de Iván porque es un orgullo haberte conocido y ser amiga de alguien como tú, un tío de lo más llano que llegará muy lejos. Muchísimas gracias a todos los antiguos compañeros del antaño 303 como Kike, Noe, Jauma, Rachel, Inma, Aroa, Icíar, Irene, Sara por todos los momentos compartidos.

Por supuesto, infinitas gracias a los compis de ahora. Esos momentos-comedor en cuadrilla 304-306-307 con tan buena sintonía alegran el día a cualquiera. Sois geniales, gracias por esas conversaciones tan definidas jeje. Cris no tienes reemplazo como compañera de trabajo, gracias por ser persona en un laboratorio y por esas pedazo figuras de *Pymol*. Siempre con una gran sonrisa ofreciendo tu ayuda y prestando tus consejos sin esperar moneda a cambio. Eres una gran persona. Lucía gracias por tantas escuchas a pesar de aburrirte con mutantes y oligómeros. Al Dr. Ibáñez, gracias por tu aportación para conseguir un buen blot de ubiquitinación y sobre todo, gracias por estar siempre ahí cuando te necesito, eres un ejemplo a seguir allá donde vayas cruzando el charco o quedándote en la patria. A David, porque aunque se resistieron al sello las neuronas, me llevo el mejor sello que es tu nobleza, francamente en ciencia hay pocas personas tan dóciles y respetuosas como tú. A Lola por esas donaciones de cultivos de corteza y ¡por qué me encanta esa fuerte personalidad que desprendes!. A Andrés porque no se puede ser más pragmático y a mis chicas nuevas Raquel, Laura y Elena por lo risueñas y dispuestas que son. A la servicial Raquel 307 porque parece que te conocemos desde siempre y a Marina por ser una Arribas con esos grandes selfies. A Eva, Edu y Rubén por formar parte también del equipo.

Gracias al resto de familia del CBM: A mis vecinos del laboratorio de J. Esteban, a la sonrisa y optimismo de Almudena, a las charlas con Alberto Garrido en cultivos, a Vega porque sin tus consejos aún estaría pegándome con la obtención de lentivirus, a J.M. Requena por ese magnífico anticuerpo m-cherry, a Jose por el politrón y esos debates sobre ubiquitina, al majete de Pau, a Fulvio por adentrarnos en geles nativos, a las chicas del SMOC y en general a toda la gente que me ha facilitado la investigación ya sea a través de gentes (habéis sido muy generosos con mis solicitudes de reactivos y anticuerpos)o con una simple mueca de apoyo en el pasillo muy gratificante. Al servicio de bioinformática especialmente a Almudena Perona, por hacerme creer que resolver la estructura cuaternaria no es tan difícil. A los de instrumentación, informática

y secuenciación por su rápida disponibilidad. Y a Ilu porque se nota mucho cuando faltas y no se puede ser más espontánea y a MariJose porque tú si que eres maja.

A Charly, María y Pili porque estoy segura que allá donde estemos formaremos el cuarteto. Gracias chicos por animarme a seguir pese a sentir inicialmente que no valía para esto. Es una suerte haber coincidido con vosotros. Al resto de bioquímicos como Guada, Chus, Deivis, Adri, Chumi, Camero por los ratos compartidos y disfrutados que ojalá hubiesen sido más.

A todos mis amigos del mundo del toro, a mis amigos de mi querido pueblo Guadalix porque aunque GlyT2 os suena a chino confiáis en mí. Os adoro.

A mis padres, porque todo lo que soy es obra vuestra, sois mi referencia. Por haberme dirigido con tanta certeza en la vida, levantarme cuando me he caído y enseñarme que *el que la sigue la consigue*. Lo que está claro es que esta tesis no habría sido posible sin vuestra ayuda. Siempre conmigo al pie del cañón apoyándome en todo momento y ahora con vuestra nieta. Y a mi hermana, porque es el otro eslavón de mi vida siempre atenta de mí. Me siento tan afortunada. Sois muy grandes. Al resto de mi familia suegros, cuñados, tíos, primos y mis queridas sobrinitas (y al principito que viene en camino) porque reforzáis mi alegría. Y muy muy especialmente,

A Rober, porque sólo tú sabes lo que me ha costado esto, cuántos días de llamadas para ver cuándo salía. Porque día tras día, has aguantado mis altibajos, animado en momentos duros y confiado ciegamente en mí. Gracias por hacerme creer que puedo con todo. Has sido mi mejor compañero de viaje y me apunto a la vida eterna contigo.

¡Y a mi todo! mi hija Verónica, ¡qué buena fuiste en la barriguita permitiéndome investigar hasta la recta final! Aunque ahora no puedo tenerte 24 horas a mi lado no me imagino una vida sin tí burbujita, eres mi motor. Tenerte ha sido la motivación para mis éxitos y tú sin duda, mi mejor logro.

ARNm Ácido ribonucleico mensajero
BiP ó GRP78 Binding immunoglobulin protein (BiP)
CNX Calnexina
CNX/CRT Ciclo de calnexina/calreticulina
COS7 Línea celular de células epiteliales de riñón de mono verde
COPII Specific coat protein complex
DAT Transportador de dopamina
DMEM Medio Eagle modificado por Dulbecco
DMSO Dimetil sulfóxido
DN Dominante negativo
DTT Ditiotreitol
EAAT Transportador de aminoácidos excitadores
EC_{50} Concentración efectiva
EDTA Ácido etilendiamino tetraacético
EGFP Enhanced green fluorescent protein
EL Bucle extracelular
ERAD Endoplasmic-reticulum-associated protein degradation
ERK Quinasa regulada por señales extracelulares
FBS Suero fetal de ternera
FMG formas monoglucosiladas
GABA Ácido gamma amino butírico
GAT Transportador de GABA
GLT1 Transportador de glutamato
Gly Glicina
GlyR Receptor de glicina
GlyT Transportador de glicina
GPCR Receptores acoplados a proteínas G
IL Bucle intracelular
K_m Constante de Michaelis-Menten
LeuT Transportador de leucina bacteriano
MAMs Mitochondria-associated membranes
MesNa 2-mercapto-etanosulfonato sódico
MTSEA-Biotina N-biotinil aminoetilmetanotiosulfonato
NCX Intercambiador Na^+/Ca^{2+}
NFPS N[3-(4'-fluorofenil)-3-(4'-fenilfenoxi) propil]-sarcosina
NKA Bomba Na/K-ATPasa
NMDA N-metil-D-aspartato
NR(1,2,3) Subunidad del receptor NMDA
NSS neurotransmitter:sodium symporter family
BN-PAGE Blue Native Polyacrilamide Gel Electrophoresis
PBS Solución salina tamponada con fosfato
PCR Reacción en cadena de la polimerasa
PDI Proteína disulfuro isomerasa
PMSF Fenil metil sulfonil fluoruro
PMA Forbol 12-miristato 13-acetato
PMCA ATPasa de calcio de membrana plasmática
QCS Quality Control System
RE Retículo endoplasmático
SDS Dodecil sulfato sódico
Sec24D Componente de la cubierta COPII
SERCA Sarco/endoplasmic reticulum Ca^{2+}-ATPase
SERT Transportador de serotonina
SLC Solute carrier
SNC Sistema nervioso central
SNARE Soluble NSF attachment protein receptor
SSV Vesículas sinápticas pequeñas
TM Dominio transmembrana
UPR Unfolded protein response
VIAAT/VGAT Vesicular inhibitory amino acid transporter
Vmax Velocidad máxima

Resumen / Summary

La hiperplexia o "enfermedad de sobresalto" es un síndrome clínico raro caracterizado por una respuesta inesperada y exagerada a estímulos triviales acústicos o táctiles. Este trastorno neurológico puede tener consecuencias graves para los recién nacidos, incluyendo daño cerebral y/o muerte súbita causada por episodios de apnea y fallo cardiorrespiratorio. La enfermedad es causada por una deficiente neurotransmisión glicinérgica inhibidora siendo las mutaciones en el gen *SLC6A5* humano que codifica el transportador neuronal de glicina GlyT2 las responsables de la forma presináptica de la hiperplexia. GlyT2 retira la glicina sináptica, constituyendo la principal fuente de neurotransmisor liberado en las sinapsis glicinérgicas. En el presente trabajo hemos analizado los mecanismos moleculares subyacentes a la biogénesis del tipo silvestre de GlyT2, dada la importancia de su correcto progreso a membrana, y de dos mutantes de hiperplexia (S512R e Y705C). La cantidad de transportador activo puede modularse por variaciones en las concentraciones de calnexina (CNX) conseguidas mediante su depleción por siRNA o su sobreexpresión. Los niveles de CNX modulan el control de calidad del precursor de GlyT2 que se une transitoriamente a la chaperona mediante sus glicanos e interacciones proteína-proteína. La CNX puede aumentar la expresión en membrana y el transporte del mutante carente de asparaginas glicosiladas en virtud de su actividad chaperona independiente de lectina, probando que CNX selecciona los estados conformacionales más competentes del transportador. También, la sobreexpresión de la chaperona es capaz de resolver la retención detectada en el RE de GlyT2 por la presencia del mutante dominante negativo (DN) de hiperplexia S512R, recuperando así sus niveles en superficie y actividad. Un análisis de las propiedades y alteraciones estructurales de S512R, ha confirmado que la introducción de la arginina perturba el plegamiento del transportador, facilita la asociación con CNX y altera la unión a Sec24D, impidiendo la salida del RE. El efecto DN del mutante sobre el tráfico de GlyT2 puede explicarse por la formación de heterómeros entre moléculas de tipo mutante-silvestre que presentan mayor estabilidad que los homómeros entre tipos silvestre-silvestre. Con vistas a la terapia, hemos demostrado el efecto chaperona del 4-PBA en el rescate del efecto DN de S512R sobre GlyT2 en células heterólogas y neuronas primarias. Respecto a la regulación de la actividad de GlyT2, hemos establecido su modulación mediante el complejo funcional GlyT2-PMCA2/3-NCX exclusivamente presente en subdominios *lipid rafts*, cuya función podría ser el mantenimiento de la homeostasis local de Na^+ y Ca^{2+} en terminales glicinérgicos dotando a GlyT2 del gradiente electroquímico de Na^+ necesario para ejercer su función. Por último, se ha caracterizado la mutación Y705C encontrada por nuestro laboratorio en muestras de pacientes de hiperplexia y demostrado que ocasiona un defecto recesivo en el tráfico intracelular y una alteración dominante en la actividad de transporte pues interfiere en la acción del pH y el zinc como moduladores cruciales de la neurotransmisión glicinérgica inhibidora.

Hyperekplexia or "startle disease" is a rare clinical syndrome characterized by unexpected and exaggerated responses to trivial acoustic or tactile stimuli. This neurological disorder can have serious consequences for newborns, including brain damage and/or sudden death caused by episodes of apnea and cardiorespiratory failure. The disease is caused by deficient inhibitory glycinergic neurotransmission. Mutations in the human *SLC6A5* gene encoding the glycine neuronal transporter GlyT2 are responsible for the presynaptic form of hyperekplexia. GlyT2 recaptures the synaptic glycine, which constitutes the main source of neurotransmitter released in glycinergic synapses. In the present work we have analyzed the molecular mechanisms underlying GlyT2 wild type biogenesis, given the importance of its correct progression to membrane, and two hyperekplexia mutants (S512R and Y705C). The amount of active transporter can be modulated by variations in the concentrations of calnexin (CNX) achieved through siRNA depletion or cDNA overexpression. CNX levels modulate the quality control of the GlyT2 precursor that is transiently bound to the chaperone by its glycan and protein-protein interactions. CNX can increase membrane expression and transport of the mutant lacking glycosylated asparagines by virtue of lectin-independent chaperone activity, proving that CNX selects the most competent conformational states of the transporter. Also, the overexpression of the chaperone resolves the retention of GlyT2 in the RE due to the presence of the S512R dominant negative (DN) hyperekplexia mutant, thus, recovering its surface and activity levels. An analysis of the structural properties and alterations of S512R has confirmed that the introduction of arginine disrupts transporter folding, facilitates association with CNX and alters binding to Sec24D, what prevents ER exit. The DN effect of the mutant on the traffic of GlyT2 can be explained by the formation of heteromers between mutant-wild type molecules which present greater stability than the homomers between wild type-wild type. Focused to the therapy, we have demonstrated the chaperone effect of 4-PBA in the rescue of the DN effect of S512R on GlyT2 in heterologous cells and primary neurons. Regarding the regulation of GlyT2 activity, we have established its modulation by the functional complex GlyT2-PMCA2/3-NCX exclusively present in *lipid rafts* subdomains, whose function could be the maintenance of local homeostasis of Na^+ and Ca^{2+} in glycinergic terminals endowing GlyT2 of the Na^+ electrochemical gradient necessary to exert its function. Finally, we have characterized the Y705C mutation found by our laboratory in samples of hyperekplexia patients and demonstrated that it causes a recessive defect in the intracellular traffic and a dominant alteration in the transport activity since it interferes in the action of pH and zinc as crucial modulators of inhibitory glycinergic neurotransmission.

I. Introducción

El sistema nervioso es el encargado de coordinar todas las funciones del organismo a través de su función sensorial, integradora y motora. Su unidad básica es la neurona, célula excitable altamente especializada que es capaz de recibir e integrar una señal eléctrica y propagarla a lo largo de su membrana plasmática y permitir que esa información sea transmitida entre neuronas por medio de las sinapsis (Figura 1). La sinapsis es una diferenciación morfológica y funcional constituida por la terminación del axón de una neurona que se ensancha para formar el botón presináptico en aposición a una región de otra neurona (frecuentemente una dendrita), que recibe el nombre de región postsináptica. En el espacio resultante o hendidura sináptica se produce la comunicación interneuronal mediante un mecanismo de acción común: liberación de un compuesto químico o neurotransmisor, unión de éste a su receptor postsináptico específico, excitación (o inhibición) de la neurona postsináptica y finalización de la señal. La terminación se lleva a cabo principalmente por la recaptación del neurotransmisor a través de transportadores específicos neuronales y/o gliales.

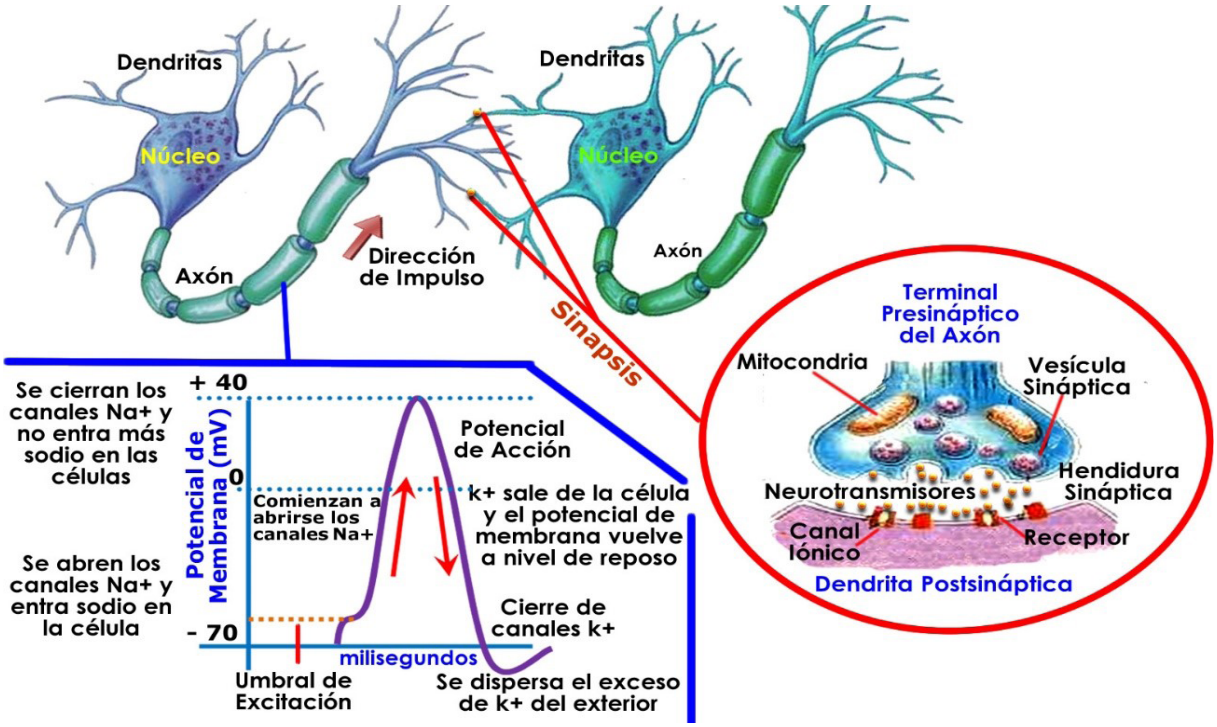

Figura 1. Esquema de la transmisión del impulso nervioso: excitabilidad neuronal y sinapsis.

1. LA GLICINA COMO NEUROTRANSMISOR

La glicina, el aminoácido proteinogenético más simple, es junto con el ácido gamma-aminobutírico (GABA), el principal neurotransmisor inhibidor en regiones caudales del sistema nervioso central (SNC) donde opera a través de receptores específicos de glicina (GlyRs) sensibles a estricnina (Legendre 2001). **La inhibición glicinérgica** es necesaria para la integración de la información sensorial y motora. Se ha descrito su papel en el procesamiento de la señal auditiva a través del núcleo coclear, el complejo olivar superior y el colículo inferior (Wenthold, Altschuler et al. 1990), en la transmisión de la información visual en las células ganglionares de la retina (Han, Zhang et al. 1997) y en la percepción del dolor neuropático e inflamatorio (Zeilhofer 2008). En el tallo cerebral y la médula espinal, las interneuronas glicinérgicas del tipo Ia tienen especial relevancia en el control del equilibrio postural y otros procesos de coordinación motora colocando al cuerpo en postura defensiva tras estímulos inesperados como un ruido súbito, un toque o una señal visual mediante circuitos reflejos de inhibición recíproca, permitiendo así la relajación de músculos antagónicos y la contracción coordinada de los músculos. Asimismo, las interneuronas de Renshaw regulan la excitabilidad de las motoneuronas mediante la producción de señales inhibidoras recurrentes a través de un sistema de retroalimentación negativa (Legendre 2001). La homeostasis del SNC depende principalmente del equilibrio entre los sistemas de neurotransmisión excitadores e inhibidores.

El glutamato es el principal neurotransmisor excitador del SNC de mamíferos y está implicado en el correcto funcionamiento del cerebro ejerciendo su efecto sobre cognición, aprendizaje y memoria con un importante papel durante el desarrollo del sistema nervioso (Danbolt 2001). La **excitación glutamatérgica** se produce cuando el glutamato liberado por el terminal presináptico interacciona con receptores específicos en la neurona postsináptica. Estos receptores pueden ser ionotrópicos como N metil-D-aspartato (NMDA) y α-amino-3-hidroxi-5-metilo-4-isoxazolpropiónico (AMPA) formando canales catiónicos operados por ligando, ó metabotrópicos (mGluR1) acoplados a diversas proteínas G que pueden ser también presinápticos. Ante este escenario, **la glicina adopta un segundo papel modulando la neurotransmisión excitadora** en vías glutamatérgicas al actuar como coagonista obligado del receptor de glutamato NMDA. Allí, la glicina es necesaria tanto para la unión del glutamato como para el reciclado del receptor en la membrana plasmática (Nong, Huang et al. 2003). Estos receptores forman heterómeros que contienen subunidades NR1 y NR2 (NR2A-D) y en ocasiones, subunidades NR3 (NR3A o NR3B). La glicina se une específicamente a la subunidad NR1 o NR3 mientras que el glutamato se une a la subunidad NR2 y la unión de ambos provoca la apertura eficiente de un canal catiónico

inespecífico que conduce a la excitación postsináptica (Madden 2002). Los receptores formados por NR1/NR3 detectados solo en nervio óptico, constituyen un nuevo tipo de receptor excitador regulado solo por glicina con una función en plasticidad neuronal aún desconocida (Rozeboom, Queenan et al. 2015). Para que tenga lugar la máxima activación del receptor de glutamato NMDA, se requiere aparentemente la unión de dos moléculas de glutamato y dos de glicina (Benveniste and Mayer 1991). Durante las últimas décadas ha habido una intensa investigación sobre la región en NR1 que reconoce glicina, ya que la modulación de la actividad del receptor NMDA mediante agonistas o antagonistas específicos de esta región puede resultar interesante como aproximación terapéutica en algunas enfermedades como la esquizofrenia (Labrie and Roder 2010).

2. LA NEUROTRANSMISIÓN GLICINÉRGICA INHIBIDORA

La despolarización producida por la llegada de un potencial de acción al terminal de una neurona glicinérgica inhibidora provoca la liberación de la glicina contenida en vesículas sinápticas mediante exocitosis regulada por calcio **(Figura 2)**. Tras su liberación en la hendidura sináptica, la glicina interacciona y activa receptores postsinápticos específicos (GlyRs) (Grenningloh, Rienitz et al. 1987). La activación del GlyR determina la apertura de un canal en la proteína que provoca un flujo de cloruro al citoplasma de la neurona postsináptica. La hiperpolarización resultante estabiliza el potencial de membrana alrededor del valor de reposo, alejándolo del umbral de excitación y, por tanto, inhibe a la neurona postsináptica (Betz and Laube 2006).

2.1. Receptores de glicina

Los GlyRs cuyo antagonista más potente es la estricnina, pertenecen a la superfamilia de los canales iónicos activados por ligando cuya estructura es heteropentamérica. La composición de subunidades del pentámero que se creía formado por tres subunidades alfa y dos subunidades beta (α3:β2) (Langosch, Thomas et al. 1988), ha sido recientemente determinada por microscopía de fuerza atómica como α2:β3 siguiendo una distribución β-α-β-α-β (Yang, Taran et al. 2012). Las subunidades α y β comparten una misma estructura formada por un largo extremo amino terminal, cuatro dominios transmembrana (TM1-4) y un gran bucle intracelular entre los TM3 y TM4 (Dutertre, Becker et al. 2012). Esta región tiene la capacidad de unir gefirina (Kirsch, Langosch et al. 1991), una proteína de andamiaje necesaria para la correcta posición del receptor en la postsinapsis. En cuanto al mecanismo de apertura del receptor, tras la unión de glicina los segmentos TM2 de cada monómero se orientan hacia el interior del pentámero para formar un canal selectivo a iones cloruro. La acción neurotransmisora de la glicina finaliza cuando su concentración en la sinapsis

disminuye y se recuperan los niveles anteriores a la estimulación. Los transportadores específicos (GlyTs, *Glycine transporters*) localizados en la membrana plasmática de las neuronas o de las células de glía adyacentes llevan a cabo esta fase final de la neurotransmisión al transportar glicina activamente hacia el interior celular. El ciclo iniciado por la despolarización del terminal se completa con el rellenado de las vesículas sinápticas con la glicina presente en el citoplasma, función que lleva a cabo el transportador vesicular, VIAAT/VGAT que intercambia la glicina por protones (McIntire, Reimer et al. 1997; Sagne, El Mestikawy et al. 1997). La glicina y el GABA comparten el mismo transportador vesicular, lo que permite que algunos terminales inhibidores (mixtos) almacenen conjuntamente ambos neurotransmisores en las mismas vesículas desde donde serán liberados simultáneamente (Gasnier 2004). Aunque el GABA y la glicina se co-liberan continuamente a lo largo del desarrollo (Keller, Coull et al. 2001),

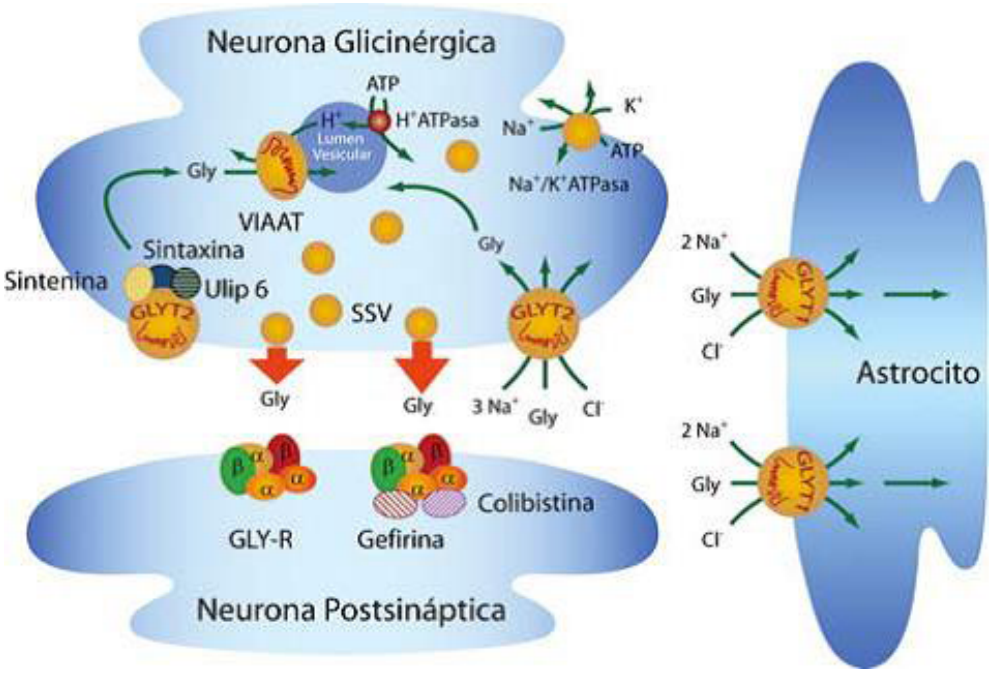

Figura 2. Esquema de una sinapsis glicinérgica. El transportador vesicular de aminoácidos inhibidores (VIAAT) produce acumulación de glicina (Gly) en vesículas sinápticas pequeñas (SSV) intercambiándolo por protones. Tras despolarización del terminal y entrada de Ca^{2+}, las SSV se fusionan con la membrana plasmática y liberan el neurotransmisor a la hendidura sináptica. Una vez que la glicina se une a receptores postsinápticos específicos (GlyRs), la acción sináptica del neurotransmisor es terminada por transportadores dependientes de Na^+ y Cl^-, GlyT1 (preferentemente glial) y GlyT2 (neuronal). La activación de GlyR por glicina abre un canal en la proteína receptora que crea una corriente de Cl^- en la neurona postsináptica generando un potencial postsináptico inhibidor.

parece que en la edad adulta existen mecanismos reguladores adicionales en el terminal que desplazan la competencia a favor de uno u otro neurotransmisor (Aubrey 2016)

2.2. Modulación por pH y zinc

Las condiciones existentes en el entorno de las sinapsis han de estar siempre controladas para la optimización de la comunicación interneuronal. Uno de los factores que afectan a la función de diversos componentes de las sinapsis glicinérgicas son los cambios de pH (Zafra and Gimenez 1989) que afectan tanto a neurotransportadores como GlyT1 (Aubrey, Mitrovic et al. 2000) o GAT1 (Grossman and Nelson 2002), como a receptores de glicina (Chen, Dillon et al. 2004) y GABA (Huang and Dillon 1999; Chen and Huang 2014). La secreción conjunta de los protones almacenados en las vesículas sinápticas y el neurotransmisor provoca acidificación del pH extracelular. Otras fuentes de protones en las sinapsis podrían proceder de la incorporación de la propia protón ATPasa a la membrana plasmática o fuentes extrasinápticas como canales o intercambiadores de protones que modulan la neurotransmisión glicinérgica (Chesler 2003). Se ha descrito que la recaptación de GABA desciende aproximadamente un 80% en oocitos de *Xenopus laevis* perfundidos con un medio extracelular a pH 5,5 (Grossman and Nelson 2002) y este efecto es más marcado cuando se reduce la concentración extracelular de $Na^{+,}$ lo cual puede ser debido a que ambos cationes podrían competir directa o indirectamente por sus sitios de unión en el transportador (Forlani, Bossi et al. 2001). Otros reguladores del entorno de las sinapsis son los metales dicatiónicos de transición como el zinc que se unen frecuentemente en sitios de unión solapantes con los de protones y modulan al GlyR (Han and Wu 1999; Chen, Dillon et al. 2004; Chen and Huang 2007), así como al transportador de glicina GlyT1 (Ju, Aubrey et al. 2004). El efecto sinérgico del Zn^{2+} inhibiendo a GlyT1 e incrementando la amplitud de la respuesta de GlyR, produce una alta ocupación de los receptores sinápticos y consigue un efecto potenciador de la respuesta. En concordancia, la generación del ratón *knock-in* α1GlyR-D80A, elimina el efecto potenciador del zinc sobre las corrientes generadas por GlyR produciendo un fenotipo similar a la hiperplexia (ver más adelante) demostrando que el Zn^{2+} es necesario para el correcto funcionamiento de la neurotransmisión glicinérgica *in vivo* (Hirzel, Muller et al. 2006).

3. TRANSPORTADORES DE GLICINA

Los GlyTs son los responsables de la terminación de la acción sináptica de la glicina finalizándola mediante recaptación con alta afinidad (K_m de orden μM) hacia el interior del terminal presináptico (Zafra, Aragon et al. 1995). Este proceso de

co-transporte activo de glicina, sodio y cloruro está acoplado al gradiente electroquímico de Na^+, es dependiente de cloruro y controla el nivel del neurotransmisor en la sinapsis (Kuhar and Zarbin 1978). La isoforma exclusivamente neuronal GlyT2 suministra glicina al terminal y asegura el mantenimiento de la neurosecreción inhibidora mientras que la isoforma predominantemente glial GlyT1 se encarga mayoritariamente de regular los niveles del neurotransmisor en la sinapsis, si bien ayudado por GlyT2.

3.1. Estructura. Oligomerización.

Los GlyTs pertenecen a la familia génica SLC6 (*solute carrier 6*), también denominada NSS (*neurotransmitter: sodium symporter family*), que engloba a los transportadores de neurotransmisores para serotonina (5-hidroxitriptamina), dopamina, noradrenalina y GABA, entre otros (Kristensen, Andersen et al. 2011). Estas proteínas poseen doce dominios transmembrana (TM) y presentan los extremos amino y carboxilo terminal orientados hacia el interior celular. Los TMs están conectados por cinco bucles intracelulares (IL) y seis extracelulares (EL). El bucle extracelular 2 (EL2) conecta los dominios transmembrana III y IV y contiene cuatro asparaginas glicosiladas en GlyT2 y tres en GlyT1. Los GlyTs comparten un patrón estructural de plegamiento descrito primeramente en el transportador homólogo bacteriano de leucina (LeuTAa) de *Aquifex aeolicus* (Yamashita, Singh et al. 2005) que fue cristalizado a alta resolución (1.65Å) en tres conformaciones diferentes en la presencia de varios inhibidores y sustratos (Krishnamurthy and Gouaux 2012). En el plegamiento de LeuT (también llamado de repetición invertida 5 + 5), cinco hélices (TM1-5) se orientan topológicamente invertidas a otras cinco (TM6-10), de modo que la proteína tiene un eje de simetría casi paralelo al plano de la membrana. Las dos repeticiones invertidas se entrelazan para formar dos haces de cuatro hélices cada uno: un haz llamado de andamiaje (*scaffold*) más estático y un haz llamado núcleo (*core o bundle*) que se mueve durante el transporte. Los sitios de unión a sustrato e iones (1 a 3 iones Na^+ y 1 ion Cl^-) se encuentran en la porción central de la proteína donde las hélices TM1 y TM6 se desenrollan parcialmente. Durante el transporte, la proteína transportadora se abre a un lado de la membrana para unir los sustratos y luego al lado opuesto para liberarlos experimentando rotación de un haz sobre el otro y cambios conformacionales durante esta conversión. Este modelo de "acceso alternante" es el más aceptado para explicar el funcionamiento de los transportadores (Forrest, Zhang et al. 2008) y predice la existencia de al menos dos conformaciones: una abierta hacia fuera (*outward-open conformation*) para la unión de sustrato/s y una abierta hacia dentro (*inward-open conformation*) para su liberación (Jardetzky 1966). Después, el transportador con los sitios de unión vacíos puede regresar a la conformación hacia

fuera e iniciar un nuevo ciclo de transporte. No obstante, la existencia de una o varias conformaciones intermedias ocluidas (*occluded)* está siendo constatada. El núcleo móvil en los SLC6 (*core o bundle*) está formado por los TMs 1, 2, 6, 7 y el haz de andamiaje (*scaffold*) por los TMs 3, 4, 5, 8, 9 y 10 (Rudnick, Kramer et al. 2014) **(Figura 3)**

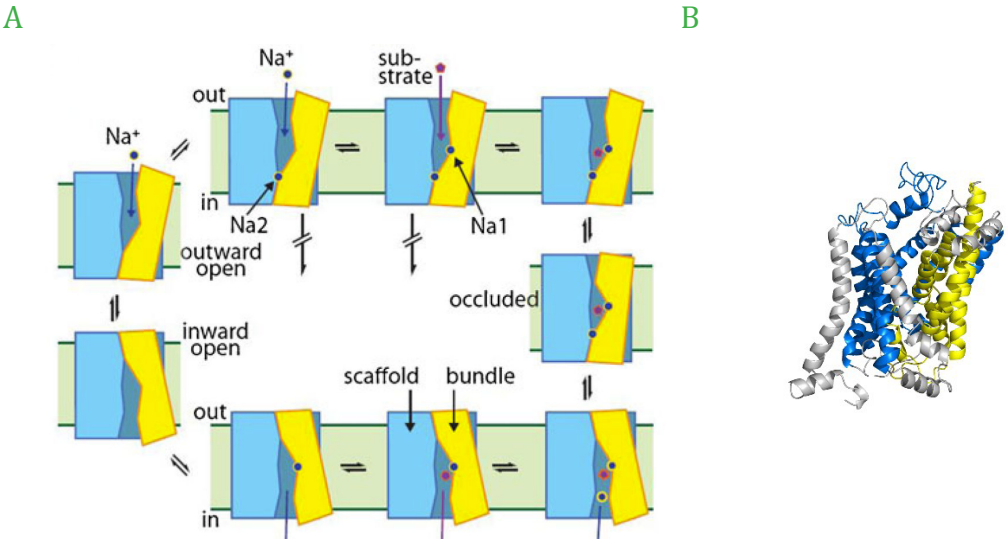

Figura 3. (A) Mecanismo de acceso alternante en LeuT. El ciclo de transporte es iniciado por la unión de un Na^+ (Na2, sitio de sodio 2) que estabilizaría la conformación hacia fuera (*outward-open conformation*). Tras esta unión se produce un cambio conformacional en la proteína. Esto expone los sitios de unión a glicina e iones que promueven la conformación hacia dentro (*inward-open conformation*) lo que permite su liberación al citosol. El transportador vacío tiene la capacidad de volver a la conformación hacia fuera para permitir un nuevo ciclo de transporte de glicina. Imagen de *Rudnick et. al. (2014) Pflugers Arch - Eur J Physiol (2014) 466:25–42* **(B)** Modelo tridimensional de GlyT2 basado en el cristal de dDAT motrándose en azul y amarillo los TM implicados en el scaffold y en el core o bundle respectivamente.

Recientemente, se han resuelto a alta resolución dos cristales de transportadores SLC6 eucariotas unidos a inhibidores antidepresivos: el transportador de dopamina de *Drosophila melanogaster* (dDAT) (Penmatsa, Wang et al. 2013) y el transportador de serotonina humano (hSERT) (Coleman, Green et al. 2016). Ambos cristales han confirmado la arquitectura general de la conformación hacia fuera descrita en la anterior estructura de LeuT. Se han validado los sitios de unión al sustrato e iones y el mecanismo de inhibición. Por primera vez, se puede visualizar una parte de la hélice carboxilo terminal que muestra una estructura similar a un pestillo que tapa la compuerta citoplasmática cerca del IL1 **(Figura 3B)**.

Otra faceta estructural destacada se refiere a la capacidad de **oligomerización.** Aunque LeuTAa fue cristalizado como dímero con subunidades unidas por residuos del TM11 y TM12, los residuos que forman parte del bolsillo de unión al sustrato e iones en cada monómero sugieren que son funcionales de modo independiente. Sin embargo, la

formación de oligómeros se ha observado en diferentes transportadores eucariotas de la familia SLC6/NSS (Farhan, Freissmuth et al. 2006). La resolución de las estructuras cristalinas dDAT y hSERT sugiere que las interfases de oligomerización no están conservadas respecto a los ortólogos procariotas. En los transportadores eucariotas se ha identificado un residuo de prolina que orienta hacia fuera la mitad citoplasmática del TM12, lo que parece descartar su implicación (Gether, Andersen et al. 2006; Broer and Gether 2012). Por lo tanto, los nuevos cristales sugieren una estructura cuaternaria única en eucariotas. Aunque la oligomerización no parece ser crucial para el transporte, es presumible su implicación en el tráfico del transportador desde su salida del retículo endoplasmático (RE) hacia la membrana plasmática como se ha descrito para GlyT1, GAT, SERT y DAT (Sorkina, Doolen et al. 2003; Farhan, Reiterer et al. 2007; Fernandez-Sanchez, Diez-Guerra et al. 2008; Anderluh, Klotzsch et al. 2014). Por tanto, cualquier alteración en el ensamblaje de multímeros podría impedir el correcto posicionamiento de los transportadores en la superficie celular y, en definitiva, afectar a su capacidad de transporte. Existen evidencias que sugieren que tanto DAT como SERT (Kilic and Rudnick 2000) (Milner, Beliveau et al. 1994; Hastrup, Sen et al. 2003) pueden existir como tetrámero y parece que las interacciones entre los protómeros ocurren dentro de cada uno de los dos dímeros en el tetrámero. Aunque no está claro si los protómeros funcionan independientemente en el oligómero, estudios recientes han revelado que la actividad de transporte en un protómero de DAT (cambiando desde *outward* a *inward conformation*) influye en la afinidad para inhibidores de otros protómeros, lo que sugiere que el estado conformacional de un protómero determina el de los demás y esto genera la afinidad resultante por el ligando (Zhen, Antonio et al. 2015). Además, un trabajo reciente ha establecido que la oligomerización de SERT está sujeta a un equilibrio dinámico caracterizado por un rápido intercambio de subunidades entre diferentes oligómeros en el RE y que tras el tráfico a la membrana, la estequiometría queda fijada y está mediada por la unión directa al fosfoinositido fosfatidilinositol-4,5-bifosfato (PIP2)(Anderluh, Hofmaier et al. 2017).
Otro aspecto novedoso aportado por el cristal de dDAT es la presencia de una molécula de colesterol asociada al transportador en un hueco entre el TM5 y TM7 donde el colesterol podría unirse regulando el movimiento del TM1a que es crucial para el transporte (Penmatsa, Wang et al. 2013; Coleman, Green et al. 2016). Este aspecto es de gran relevancia dada la dependencia de DAT del entorno lipídico rico en colesterol (Hong and Amara 2010), un aspecto también relevante para GlyT2 (ver punto 6). Sin embargo, en el cristal de hSERT la localización de la molécula de colesterol co-cristalizada es diferente y se sitúa en la región extracelular del TM12, lo que sugiere un papel en el mantenimiento de la conformación de este TM.

3.2 Expresión y localización

El gen humano de GlyT1 (*SLC6A9*) se compone de 14 exones distribuidos a lo largo de 44,1 mega bases (Mb) y está localizado en el cromosoma 1 (p31.3–p32)(Jones, Fernald et al. 1995). Hasta la fecha en humanos y otros mamíferos se han detectado 3 variantes de GlyT1 (GlyT1a-c) que difieren en su extremo amino terminal (Dohi, Morita et al. 2009). Mientras que GlyT1a y GlyT1b se generan por un uso alternativo de promotores, GlyT1c es un producto derivado del "splicing" producido sobre el ARN mensajero (ARNm) de GlyT1b que contiene un segmento inicial de 15 residuos (común con GlyT1b) seguido por una secuencia única de 54 residuos que no aparece en las otras dos variantes (Liu, Lopez-Corcuera et al. 1993; Kim, Kingsmore et al. 1994). Además, en bovinos (subfamilia Bovinae) se han descrito dos variantes

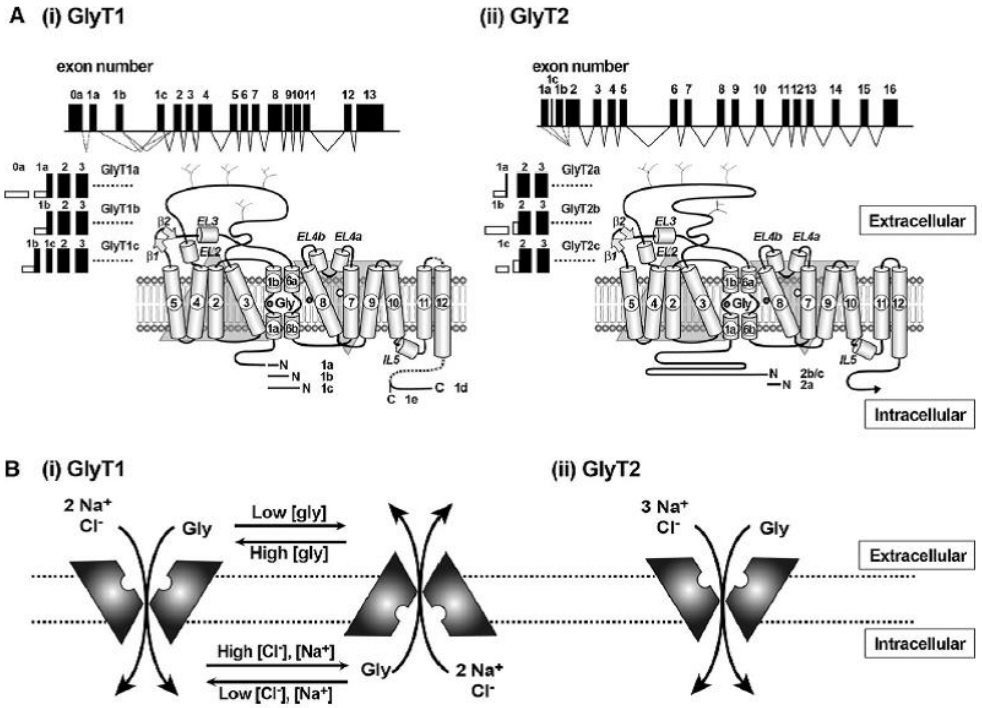

Figura 4. Diferencias estructurales, génicas y de transporte entre GlyT1 y GlyT2. **(A)** Estructura del gen de GlyT1 (SLC6A9, 14 exones) y GlyT2 (SLC6A5, 16 exones) mostrando sus variantes de splicing. Nótese la mayor longitud del extremo amino terminal de GlyT2 que posee unos 200 aminoácidos. **(B)** Diferencias en el ciclo de transporte de glicina por GlyT1 y GlyT2. GlyT1 necesita menor fuerza motriz para el transporte que GlyT2, lo que le permite funcionar en modo reverso dependiendo de los cambios en la concentración extracelular de sustrato o gradientes electroquímicos iónicos, mientras que este modo es menos probable para GlyT2. *Dohi T et. al. (2009) Pharmacol Ther 123, 54-79*.

de "splicing" del extremo carboxilo terminal (GlyT1d, e) que hasta la fecha no se han encontrado en otras especies (Hanley, Jones et al. 2000).

El gen humano que codifica GlyT2 (*SLC6A5*) se compone de 16 exones distribuidos a lo largo de 20,6 mega bases (Mb) y está localizado en el cromosoma 11 (p15.1–15.2)(Rees, Harvey et al. 2006). Sobre el tránscrito que produce, se han descrito 3 variantes de "splicing" del extremo amino terminal que da lugar a tres variantes, GlyT2a-c. Únicamente hay 5 aminoácidos de diferencia entre GlyT2a y GlyT2b/c, por lo que en la bibliografía lo más común es hablar de GlyT2 y englobar las tres isoformas. Entre GlyT2b y GlyT2c no existen diferencias en la secuencia de aminoácidos y lo único que se ha encontrado son diferencias en las regiones 5' no codificantes (5'-UTR, del inglés "*untranslated region*") de sus respectivos ARNm (Gomeza, Armsen et al. 2006). El papel funcional de las distintas isoformas es objeto de estudio.

En cuanto a la **localización**, GlyT1 se expresa a lo largo del SNC, principalmente en astrocitos (Adams, Sato et al. 1995), aunque puede ser hallado en determinadas poblaciones neuronales, como por ejemplo en neuronas glutamatérgicas de hipocampo (Cubelos, Gimenez et al. 2005) y también se localiza en hígado, páncreas e intestino. Por el contrario, GlyT2 tiene acotada su detección en interneuronas glicinérgicas y se expresa fundamentalmente en tallo cerebral y médula espinal (Jursky and Nelson 1995). La generación del ratón transgénico que expresa la proteína fluorescente EGFP bajo el control de un fragmento del promotor de GlyT2 (Zeilhofer, Studler et al. 2005; Punnakkal, von Schoultz et al. 2014) ha confirmado la inmunorreactividad de GlyT2 en terminales axónicos y de glicina en el soma neuronal. Esta excelente herramienta, junto con nuevos ratones que expresan la recombinasa Cre específicamente en neuronas glicinérgicas (Ishihara, Armsen et al. 2010; Giber, Diana et al. 2015), puede permitir la identificación de poblaciones de neuronas glicinérgicas en tejidos *in vivo* y contribuir al esclarecimiento de su papel en circuitos neuronales (Zafra 2016).

3.3 Papel fisiológico

Los primeros ratones en los que se eliminaron los genes de GlyTs pusieron de manifiesto la función *in vivo* de los transportadores (Gomeza, Ohno et al. 2003). Los ratones GlyT1$^{-/-}$ y GlyT2$^{-/-}$ presentaban un aspecto físico relativamente normal al nacer, lo que sugiere que la expresión de ambas proteínas no parece ser crucial para un correcto desarrollo embrionario. Sin embargo, los **ratones GlyT1$^{-/-}$** morían generalmente durante las primeras horas tras el nacimiento debido a que sufrían alteraciones respiratorias

y motosensoriales graves caracterizadas por letargia, hipotonía y falta de respuesta a estímulos sensoriales. Los registros funcionales se normalizaban con la adición de estricnina, el antagonista del GlyR. Las motoneuronas del núcleo hipogloso del tallo cerebral presentaban una actividad tónica elevada de GlyR debido a una concentración de glicina en la sinapsis superior a la normal. Estas observaciones revelaron que el papel de GlyT1 era el mantenimiento de los niveles submicromolares de glicina en las sinapsis requeridos para una neurotransmisión glicinérgica correcta, y que su función impedía el fallo respiratorio en el periodo neonatal. La concentración extracelular de glicina se controla mediante su retirada del medio extracelular por GlyT1 y su posterior suministro al sistema de ruptura de glicina (*Glycine Cleavage System*, GCS) presente mayoritariamente en mitocondrias de astrocitos, el cual la degrada mediante descarboxilación (Wang, Wu et al. 2013).

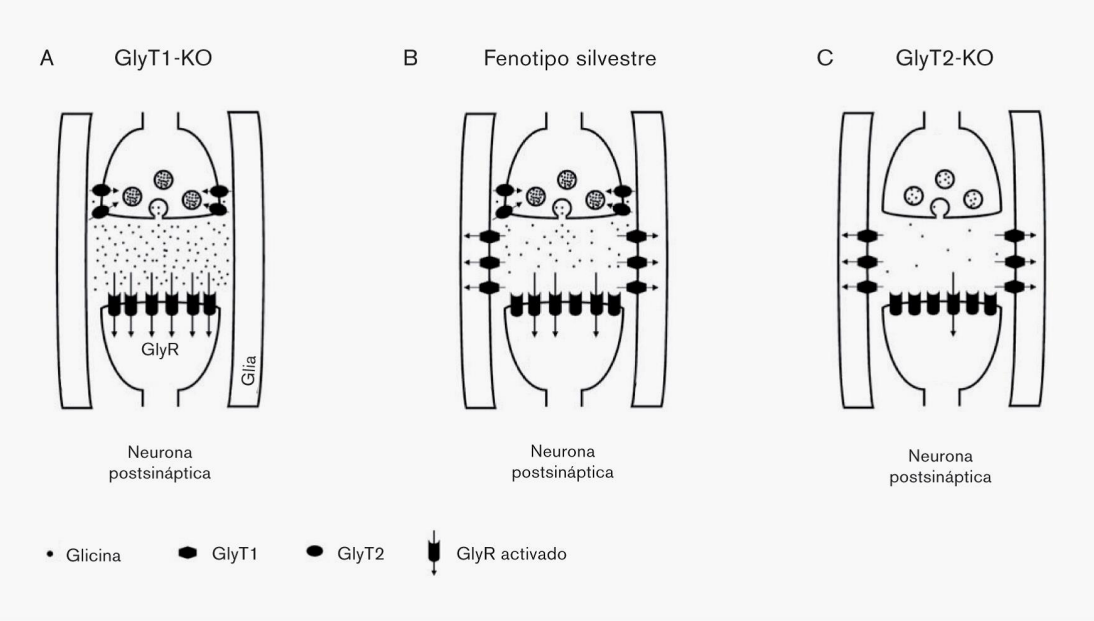

Figura 5. Modelos de la estructura sináptica en ratones deficientes en transportadores de glicina. El esquema muestra diferentes sinapsis glicinérgicas. **(A)** En ratones deficientes en GlyT1, **(B)** en ratones con fenotipo silvestre y **(C)** en ratones deficientes en GlyT2. En el fenotipo silvestre se observa que GlyT2 es esencial para la recaptación de glicina hacia la neurona presináptica, lo que permite el rellenado de las vesículas y que GlyT1 está retirando la glicina del espacio sináptico hacia las células gliales manteniendo una baja concentración de glicina en la hendidura sináptica. En el caso del ratón deficiente en GlyT1 **(A)**, se produce un aumento de la concentración de glicina en la hendidura sináptica, lo que resulta en una inhibición continuada de la neurona postsináptica. En el caso del ratón deficiente en GlyT2 **(C),** la deficiencia en el rellenado de vesículas reduce la cantidad de glicina liberada y, por tanto, la inhibición de la neurona postsináptica *Gomeza J, Armsen W, Betz H, Eulenburg V. Handb Exp Pharmacol. 2006;(175):457-83.*

La eliminación del gen de GlyT1 en ratones (*SLC6A9*) genera un fenotipo que reproduce síntomas de una enfermedad humana, la encefalopatía glicinérgica o hiperglicinemia no cetósica (NKH) que puede producirse también por mutaciones en las distintas subunidades proteicas del GCS. La NKH cursa con una acumulación masiva de glicina en el espacio extracelular en sangre, orina y cerebro que tiene graves consecuencias como hipotonía, crisis de apnea, episodios de hipo, aumento de los reflejos osteotendinosos. Las primeras manifestaciones pueden ocurrir tras el nacimiento o en las primeras semanas de vida, aunque el daño neurológico puede haberse iniciado ya en el periodo intrauterino. Además, como consecuencia del papel excitotóxico de la glicina pueden aparecer convulsiones, retraso mental y alteraciones del desarrollo cerebral. Recientemente, se han encontrado mutaciones en el gen humano de GlyT1 (*SLC6A9)* en pacientes de NKH (Alfadhel, Nashabat et al. 2016; Kurolap, Armbruster et al. 2016).

Los **ratones GlyT2$^{-/-}$** también presentaban un fenotipo letal pero la muerte ocurría generalmente durante la segunda semana postnatal debido a alteraciones neuromotoras graves caracterizadas por rigidez muscular, espasticidad, temblores y convulsiones. El registro electrofisiológico mostraba menor amplitud en las corrientes postsinápticas espontáneas inhibidoras (IPSCs) debido a una reducción de la liberación de glicina en la sinapsis. Estos resultados validaron el papel crucial que GlyT2 desempeña en el reciclaje de glicina aportando suficiente neurotransmisor para el mantenimiento de los quanta en las vesículas sinápticas necesarios para la neurosecreción glicinérgica inhibidora. Así pues, la ausencia de GlyT1 conduce a la acumulación del neurotransmisor en la hendidura sináptica produciéndose una activación constante de los GlyRs y, por el contrario, la eliminación completa de GlyT2 provoca una disminución de los niveles de glicina en la hendidura sináptica debido a una menor liberación vesicular de glicina y una menor estimulación de los GlyRs **(Figura 5)**. No obstante, la inhibición parcial no crónica de GlyT2 tiene el efecto opuesto de incrementar la concentración y tiempo de aclarado de la glicina en la sinapsis, como se ha comprobado posteriormente utilizando inhibidores (ver más adelante).

Las funciones diferenciales de los GlyTs están de acuerdo con el **distinto acoplamiento** termodinámico al gradiente de Na^+ para el transporte de glicina de GlyT1 y GlyT2. GlyT2 requiere la unión de tres iones Na^+ para transportar una molécula de glicina, mientras que GlyT1 sólo necesita dos iones Na^+ para llevar a cabo este proceso. Esta propiedad, hace de GlyT2 un transportador mucho más acumulativo, mientras que GlyT1 es más proclive a operar en modo reverso (Aragon, Gimenez et al. 1987; Roux and Supplisson 2000) **(Figura 4B)**. Otras diferencias funcionales entre los GlyTs incluyen diferente sensibilidad catiónica para el ion litio que ejerce efectos opuestos sobre ambas isoformas: inhibición

sobre GlyT1 y estimulación sobre GlyT2. Esta acción del litio se produce tras su unión a los sitios Na2 y a un nuevo sitio transitorio para sodio en el vestíbulo de GlyT2 que incluye el residuo Asp471 (Perez-Siles, Morreale et al. 2011; Perez-Siles, Nunez et al. 2012) . La capacidad de GlyT1 y GlyT2 para modular la neurotransmisión glicinérgica de modo complementario, ha despertado el interés del desarrollo de una farmacología selectiva para ambos. A pesar de que GlyT1 y GlyT2 comparten aproximadamente el 50% de su secuencia de aminoácidos, existen inhibidores selectivos que permiten diferenciar farmacológicamente a los dos transportadores (Eulenburg, Armsen et al. 2005; Dohi, Morita et al. 2009; Harvey and Yee 2013). La inhibición de GlyT1 por sarcosina y NFPS (N(3-(4´-fluorofenil)-3-(4´-fenilfenoxi)propil) sarcosina (Aubrey and Vandenberg 2001) tiene efectos antipsicóticos y antinociceptivos (Dohi, Morita et al. 2009), además de producir mejoras cognitivas en pacientes con esquizofrenia (Hashimoto 2011). La inhibición selectiva de GlyT2 mediante administración intratecal de ALX1393 (O-[(2-benziloxifenil-3-fluorofenil)metil]-L-serina), ha demostrado tener un efecto analgésico en modelos animales de dolor crónico y agudo (Haranishi, Hara et al. 2010).

4. FISIOPATOLOGÍA DE GlyT2 en la neurotransmisión glicinérgica:

4.1 Hiperplexia humana

La hiperplexia hereditaria (también denominada “síndrome del bebé entumecido” o “enfermedad del sobresalto”, OMIM 149400) es un desorden neurológico de baja prevalencia en la población, caracterizado por una respuesta exagerada a estímulos triviales somatosensoriales e hipertonía muscular (Saenz-Lope, Herranz-Tanarro et al. 1984). Los individuos afectados reaccionan inesperadamente con sobresaltos enérgicos y sostenidos manteniendo una apreciable rigidez de tronco y extremidades con temblores, recordando a las respuestas propias de ataques epilépticos tónicos. Sus síntomas aparecen tras el nacimiento y, aunque suelen mejorar con el tiempo, el riesgo de muerte súbita del bebé es alto como consecuencia de espasmos laríngeos y fallos cardiorrespiratorios (Praveen, Patole et al. 2001). Durante toda la vida subsisten en los pacientes alteraciones motoras más o menos incapacitantes generando inseguridad al caminar debido a la alta probabilidad de sufrir caídas repentinas, aunque el desarrollo mental de los afectados suele ser normal. En la actualidad este síndrome no tiene cura y sus síntomas son paliados en cierto modo utilizando fármacos que estimulan la neurotransmisión GABAérgica como *clonazepam* (Bakker, Peeters et al. 2009). La primera causa asociada con la enfermedad son mutaciones en los genes que codifican proteínas postsinápticas necesarias para la transmisión glicinérgica: la subunidad α (*Glra1*) del GlyR (Shiang, Ryan et al. 1993; Rees,

Andrew et al. 1994) que también puede estar afectada en GlyRs homoméricos presinápticos (Xiong, Chen et al. 2014). Algunas mutaciones en la subunidad β(*Glrb*) de GlyR o en proteínas como la gefirina (*GPNH*) y colibistina (*ARHGEF9*), son causa más rara de la enfermedad (Rees, Lewis et al. 2002; Harvey, Topf et al. 2008) **(Figura 6)**. Aproximadamente un 70% de los pacientes diagnosticados de hiperplexia hereditaria resultaron negativos para mutaciones de dichos genes lo que sugirió la implicación de otros genes en su etiología.

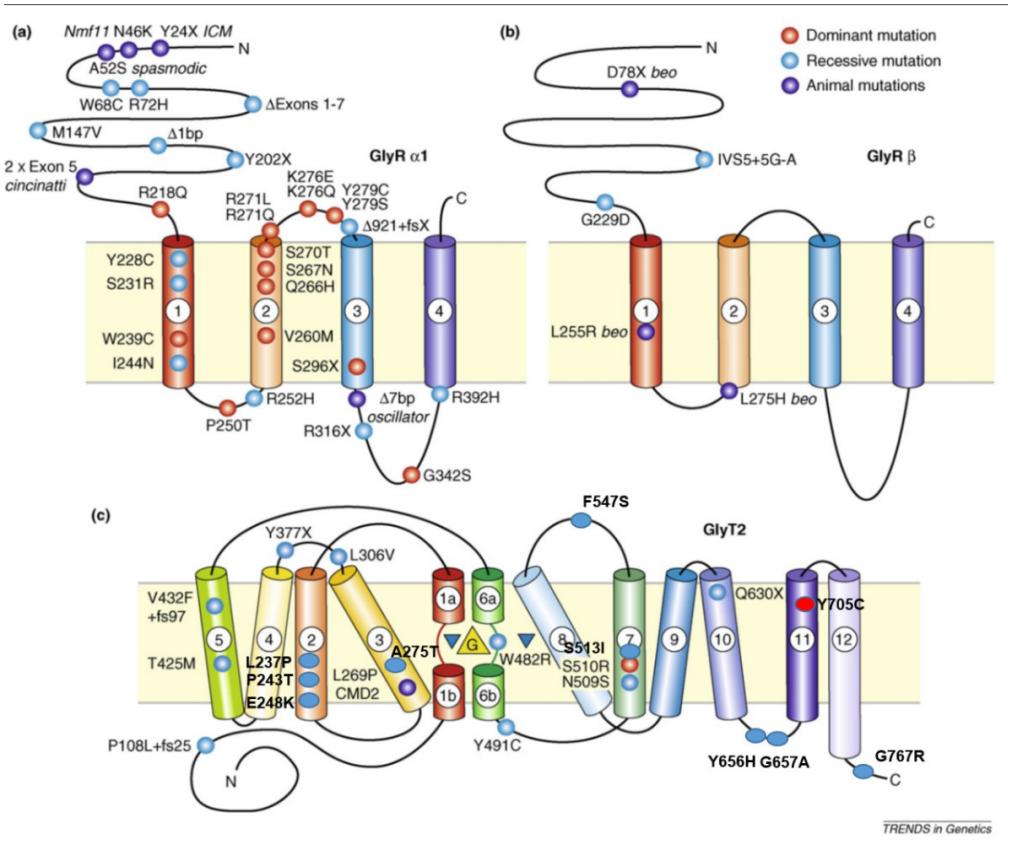

Figura 6. Diagrama esquemático que muestra las mutaciones asociadas a hiperplexia. **(a)** En la subunidad α y **(b)** en la subunidad β del receptor de glicina GlyR así como **(c)** en el transportador de glicina GlyT2. *Imagen modificada de (Harvey, R. et al. 2008).*

Los ratones GlyT2$^{-/-}$ reproducían los síntomas de los animales con mutaciones en *Glra1* y análisis genéticos recientes han permitido confirmar la implicación del GlyT2 mediante el descubrimiento de varias mutaciones causantes de la enfermedad (Eulenburg, Becker et al. 2006; Rees, Harvey et al. 2006). Un estudio de correlación genotipo-fenotipo ha mostrado que los pacientes con mutaciones en el gen *SLC6A5* tienen más probabilidades de tener retraso en el desarrollo, en particular en la adquisición del habla, que aquellos con mutaciones en Glra1, lo que indica que en ausencia de liberación presináptica de glicina se producen alteraciones en redes neuronales de desarrollo o defectos de migración neurogénica (Thomas, Chung et al. 2013).

A excepción de dos mutaciones dominantes (Rees, Harvey et al. 2006; Gimenez, Perez-Siles et al. 2012), la mayor parte de las mutaciones que afectan al gen *SLC6A5* asociadas a hiperplexia son autosómicas recesivas y producen pérdida bialélica de función (Rees, Harvey et al. 2006). Entre las mutaciones estudiadas (un total de 26), la mayoría producen un transportador truncado inactivo debido a la inserción de un codón de terminación "*non-sense mutation*" (W151X, R191X, Y297X, Y377X, R439X, V432F+fs97,Q630X, P108L+fs25). Otras mutaciones con cambio de sentido ("*missense mutations*") producen transportadores no funcionales que sí son capaces de alcanzar correctamente la superficie celular pero que poseen sustituciones en residuos importantes para el ciclo de transporte, como en sitios de unión a Na^+ (N509S, A275T), Cl^- (S513I), glicina (W482R) y otras sin identificar (L306V, G767R). Además se han detectado 8 mutaciones asociadas a hiperplexia que tienen (o podrían tener) actividad residual y su defecto estaría asociado a alteraciones del tráfico intracelular (L237P, P243T, E248K, T425M, Y491C, G657A, F547S o Y656H), así como otras 3 que afectan al procesamiento del RNAm del transportador por alteración de splicing (Carta, Chung et al. 2012)**(Figura 6)**.

Aunque en los ratones GlyT2$^{-/-}$ la transmisión sináptica está drásticamente reducida no está completamente ausente, lo que sugiere que existen otras formas de recaptación o la síntesis de novo de glicina en terminales presinápticos. Algunos estudios recientes han revelado que mutaciones en el gen *SLC7A10* que codifica para el antiportador de aminoácidos neutros Asc-1 podrían ser también causa de hiperplexia humana. El ratón Asc-1-KO exhibe una alteración en el metabolismo de la glicina y una disminución de sus niveles en cerebro que compromete la neurotransmisión glicinérgica (Safory, Neame et al. 2015).

4.2 Dolor

Diferentes estudios han demostrado que la inhibición farmacológica tanto de GlyT1 como de GlyT2 se asocia con el alivio del dolor neuropático e inflamatorio (Harvey and Yee 2013). Esto es debido a que la población de interneuronas glicinérgicas de las astas dorsales de la médula espinal constituyen la primera estación de la señal nociceptiva en su progreso hacia centros superiores del SNC donde se hace consciente (Melzack and Wall 1965). El dolor se relaciona con una disminución en la neurotransmisión inhibidora tanto GABAérgica como glicinérgica en las astas dorsales de la médula espinal que favorece la activación de interneuronas glutamatérgicas y el progreso del impulso doloroso al cerebro (Zeilhofer 2008; Foster, Wildner et al. 2015). La analgesia producida al aumentar la concentración de glicina en estas sinapsis manifiesta la importancia de la neurotransmisión glicinérgica inhibidora en la señalización nociceptiva.

5. CONTROL DE CALIDAD DE PROTEÍNAS EN LA RUTA SECRETORA

5.1 Proteostasis

Las actividades biológicas de la vida dependen de la correcta función de las proteínas responsables de múltiples procesos celulares como señalización, catálisis, transporte, fusión de membranas, defensa, regulación, apoptosis, etc. El sistema de control de calidad de las proteinas (*Quality Control System*, QCS) lleva a cabo el balance entre el plegamiento y la degradación proteica y contribuye al mantenimiento de la homeostasis proteica celular o proteostasis regulando mecanismos que controlan la síntesis, plegamiento, degradación y tráfico de proteínas (Balch, Morimoto et al. 2008). El RE es el orgánulo fundamental en el plegamiento, modificación postraduccional y control de calidad de las glicoproteínas de membrana que están siendo sintetizadas de novo. A pesar de que el RE está escasamente estudiado en neuronas, existen evidencias de que es más extenso que en otros tipos celulares y tiene una síntesis local de múltiples proteínas en dendritas y axón (Merianda, Lin et al. 2009; Ramirez, Hartel et al. 2011). Se calcula que solo el 30% de las proteínas recién sintetizadas superan el restrictivo control de calidad de proteínas y adquieren con éxito la conformación correcta final necesaria para su función (Kopito 1999; Sanders and Myers 2004). Así, el reconocimiento y eliminación de proteínas mal plegadas es un proceso esencial para la sustentación de la proteostasis celular, función crítica y especialmente relevante para las células postmitóticas como las neuronas que no pueden ser fácilmente reemplazadas (Gidalevitz, Kikis et al. 2010). Como proteínas de membrana, los GlyTs se sintetizan a través de la ruta secretora comenzando con su translocación cotraduccional al RE y reciben en las cuatro asparaginas de EL2 que se encuentran en secuencias consenso de N-glicosilación (Asn-X-Ser/Thr) el oligosacárido de 14 azúcares Glc3Man9GlcNAc2. Su biogénesis requiere la asistencia de chaperonas moleculares y enzimas residentes que promoverán su plegamiento, la formación de puentes disulfuro y otras modificaciones postraduccionales. El ciclo calnexina/calreticulina (CNX/CRT) supone el inicio del QCS de la ruta secretora. Mediante él, una proteína integral de membrana de tipo I, la chaperona calnexina (CNX), se une a formas monoglucosiladas (FMG) de intermediarios de N-glicosilación de las proteínas nacientes que son producidas por glucosidasas que retiran dos de las tres glucosas del oligosacárido inicialmente transferido al péptido naciente (Glc3Man9GlcNAc2). Ciclos de glucosilación–deglucosilación por las glucosidasas implican la unión-liberación de la chaperona para las glicoproteínas correctamente plegadas o la unión-degradación para las proteínas con plegamiento erróneo (Parodi 2000). Las proteínas con plegamiento apropiado salen del RE y viajan reclutadas en vesículas

COPII con un transporte anterógrado al aparato de Golgi donde continúan su maduración por glicosilación y son enviadas a la superficie celular (Routledge, Gupta et al. 2010).

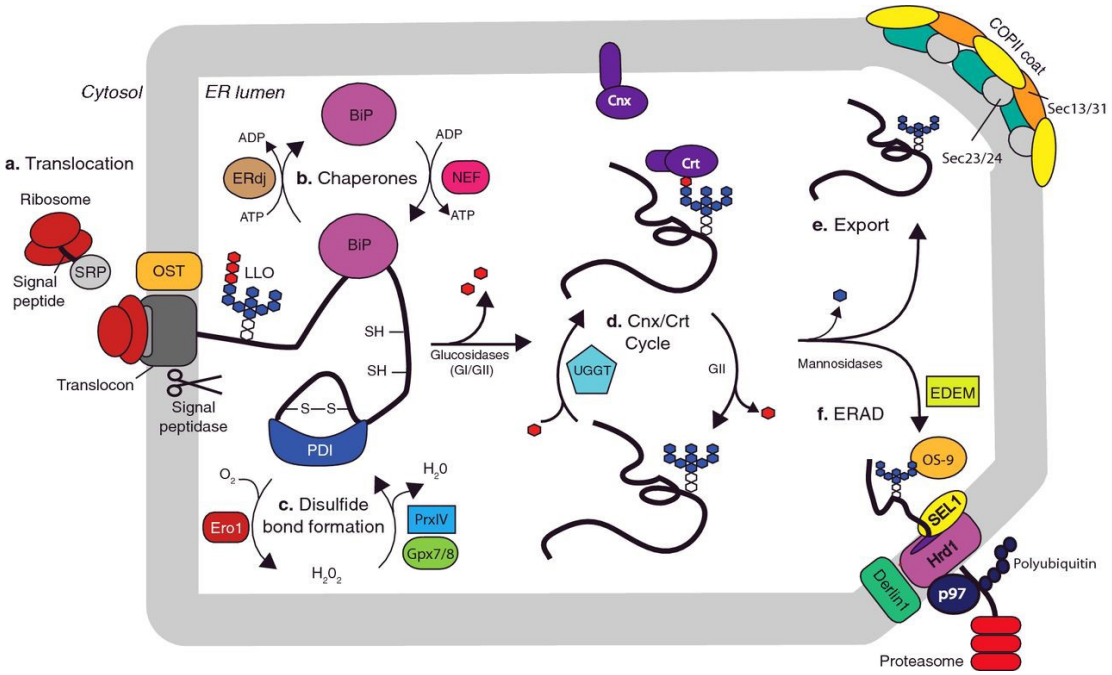

Figura 7. Control de calidad de glicoproteínas en la ruta secretora temprana. La síntesis proteica comienza con la translocación cotraduccional y la adición del oligosacárido Glc3Man9GlcNAc2 al péptido naciente. Las GI y GII retiran dos de las tres glucosas generando las FMG reconocidas por CNX. La chaperona participa en ciclos de glucosilación-deglucosilación sobre intermediarios de plegamiento hasta que adquieren la conformación correctamente plegada y continúan en vesículas COPII hacia el aparato de Golgi para completar su maduración y finalmente alcanzar la membrana plasmática. Los intermediarios que no superan el QCS son retrotranslocados al citosol, poliubiquitinados y degradados por el proteasoma a través de ERAD. La formación de puentes disulfuro es catalizada por las PDIs correspondientes. *Kathleen McCaffrey & Ineke Braakman Essays In Biochemistry, 2016.*

Se ha identificado un motivo dibásico (RL) conservado en el C-terminal de los miembros de la familia SLC6 responsable de la unión al adaptador Sec24 del complejo Sec24/Sec23 que forma la capa interna de la cubierta COPII y es el responsable de la exportación del RE tras el reconocimiento de la proteína cargo (Miller, Beilharz et al. 2003; Farhan, Reiterer et al. 2007; El-Kasaby, Just et al. 2010). Además, se ha descrito que un prerrequisito para la salida del RE de los transportadores SLC6 es que las distintas subunidades individuales sean estabilizadas mediante oligomerización (Springer, Malkus et al. 2014). Es más, la oligomerización parece facilitar el reclutamiento de los componentes de COPII, confirmando la necesidad de estructura cuaternaria para la exportación del RE (Sato and Nakano 2003; Farhan, Reiterer et al. 2007).

La acumulación de proteínas mal plegadas en el RE induce la llamada respuesta a proteínas mal plegadas o *Unfolded Protein Response*, (UPR), un mecanismo que contrarresta alteraciones de plegamiento (estrés) en el RE y que puede restaurar la proteostasis (Perri, Thomas et al. 2015). La activación de la **UPR** bajo condiciones moderadas señaliza la inhibición de la traducción, la expansión de la membrana del RE, el reclutamiento de chaperonas que corrigen los defectos de plegamiento y el aumento de la degradación de proteínas reduciendo de esta forma el estrés de RE (Hetz 2012). La unión de chaperonas específicas a los núcleos hidrofóbicos expuestos de intermediarios de plegamiento evita la agregación proteica y promueve su estabilización (Kim, Hipp et al. 2013). Sin embargo, bajo condiciones crónicas o de estrés de RE irreversible, la activación de UPR desencadena señales proapoptóticas que dan lugar a muerte celular (Hetz and Mollereau 2014). Los tres sensores principales de UPR son: *PKR-like endoplasmic reticulum kinase* (PERK), implicada en la inhibición de la traducción y posterior activación de vías pro-apoptóticas si fuera necesario; *inositol-requiring kinase 1* (IRE1) y *activating transcription factor 6* (ATF6), implicadas en el aumento de la capacidad de plegamiento y degradación de proteínas. En condiciones basales estos sensores están inactivos y unidos a la chaperona BiP (*binding immunoglobulin protein*). La acumulación de proteínas mal plegadas induce la disociación de BiP y la activación de los sensores, de modo que la chaperona puede también unirse a regiones hidrofóbicas expuestas de los intermediarios favoreciendo su plegamiento (Rutkowski, Arnold et al. 2006). Dentro del grupo de chaperonas que se sobreexpresan en UPR se encuentran las PDI, una familia de proteínas con dos funciones alternativas: actividad chaperona general (Ferrari and Soling 1999) y actividad de intercambio de disulfuros que tiene capacidad de oxidar, reducir e isomerizar enlaces disulfuro. Recientemente se han identificado otros papeles poco caracterizados que las implican en neurodegeneración (Woycechowsky and Raines 2000; Perri, Thomas et al. 2015). Entre las múltiples acciones iniciadas por las vías IRE1 y ATF6 para aliviar el estrés de RE se encuentra la expresión de genes implicados en la degradación de proteínas por el proteasoma dando lugar al sistema denominado *ER-associated degradation* (ERAD).

El proceso de **ERAD** requiere la retrotranslocación al citosol de las proteínas mal plegadas, su ubiquitinación y posterior degradadación por el proteasoma (Brodsky 2012; Christianson and Ye 2014)**(Figura 7)**. La ubiquitinación es una modificación postraduccional que consiste en la adición de una o varias moléculas de la proteína de 76 aminoácidos ubiquitina a uno o varios residuos de lisina de una proteína. Este proceso interviene en diversas funciones celulares como la reparación de ADN, regulación de la transcripción y tráfico de proteínas interviniendo en endocitosis

y degradación proteasomal y lisosomal (Komander and Rape 2012) controlando la estabilidad, actividad y localización de receptores y neurotransportadores modulando las conexiones sinápticas (DiAntonio and Hicke 2004). Cuando la producción de proteínas mal plegadas excede la capacidad de plegamiento de las chaperonas y satura el sistema de degradación del proteasoma, las proteínas mal plegadas son activamente transportadas para formar inclusiones especializadas llamadas agresomas que son eliminadas por **autofagia**. Cabe destacar que la limitación en el tamaño del poro del canal de retrotranslocación y de la subunidad 26S del proteasoma, acota la degradación de un gran número de agregados y complejos proteicos que sí pueden ser degradados por autofagia (Olzmann, Li et al. 2008; Hidvegi, Ewing et al. 2010). Si a pesar de esto la proteostasis no puede ser restaurada, la célula entrará en apoptosis (Wang and Kaufman 2014). Está comprobado que muchos agregados proteicos pueden resultar tóxicos para la célula y su acumulación puede causar enfermedades neurodegenerativas como Alzheimer, Parkinson, Huntington y enfermedades priónicas (Jucker and Walker 2013) (Scheper and Hoozemans 2015).

5.2 Chaperonas como agentes terapéuticos

Debido a que el proceso de plegamiento está inherentemente sujeto a errores (se calcula que una cadena de 100 aminoácidos puede adquirir más de 10^{30} conformaciones posibles)(Balchin, Hayer-Hartl et al. 2016), resulta necesario actuar en este proceso

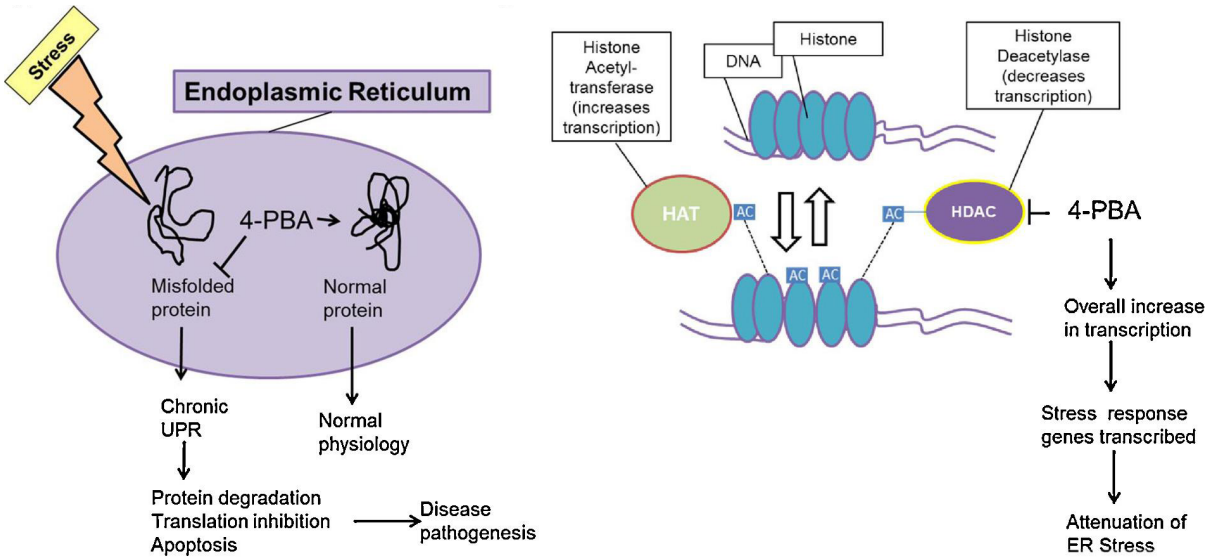

Figura 8. Modo de actuación del compuesto 4-ácido fenilbutírico (4-PBA) como sensor de estrés de RE con atenuación de UPR (izquierda) o como regulador transcripcional sobre la HDAC (derecha). *Imagen de Kolb, P.S. et al; 2015.*

para aumentar la eficiencia en la adquisición de la estructura tridimensional correcta. Partiendo de los estudios pioneros de *Sato et al* (Sato, Ward et al. 1996) sobre la eficacia de los osmolitos en la recuperación de los canales aniónicos mal plegados, cada vez hay más pruebas que apoyan la capacidad de moléculas pequeñas para estabilizar y/o inhibir la agregación de proteínas. Existen pequeñas moléculas que tanto *in vitro* como *in vivo* han demostrado prevenir la agregación proteica, facilitar el plegamiento proteico y reducir el estrés de RE mediante estabilización de intermediarios de plegamiento siendo posibles agentes terapéuticos para la acumulación de proteínas mal plegadas en enfermedades neurodegenerativas (Wang and Kaufman 2016). En consecuencia y mimetizando la función endógena de las chaperonas celulares o moleculares, las chaperonas químicas y farmacológicas representan una estrategia para corregir defectos en el QCS de las proteínas.

Las **chaperonas químicas** interactúan con el estado no nativo de proteínas y asisten a su plegamiento y ensamblaje representando la primera y más potente línea de defensa contra el mal plegamiento y agregación proteica (Muchowski and Wacker 2005). Por ejemplo, la sobreexpresión de las principales chaperonas celulares *heat sock proteins* (Hsps) ha mostrado tener un papel neuroprotector en enfermedades neurodegenerativas constituyendo una terapia potencial (Turturici, Sconzo et al. 2011). Recientemente, se ha establecido que SERT une (HSP) 70-1A, HSP90β, y co-chaperonas en su extremo C-terminal como parte del QCS de este transportador (El-Kasaby, Koban et al. 2014; Koban, El-Kasaby et al. 2015). De modo similar a las chaperonas celulares, las chaperonas químicas son moléculas que pueden ayudar en el plegamiento proteico. Pueden ser osmolitos como algunos derivados de aminoácidos (glicina, taurina, β-alanina), polioles (glicerol, sacarosa), metilaminas (trimetilamina-N-óxido (TMAO) o compuestos hidrofóbicos que generalmente tienen un modo de acción no específico sobre las proteínas. Estos compuestos inespecíficos, suelen ser eficaces a altas concentraciones (rango molar) pudiendo producir toxicidad celular. No obstante, debido a la complejidad en generar compuestos que corrijan defectos específicos en proteínas concretas, el uso de estos compuestos generales ha incrementado en los últimos años. Los que son hidrofílicos tienen un modo de acción basado fundamentalmente en alterar las propiedades del solvente secuestrando moléculas de agua originando un entorno hidrofóbico alrededor de la proteína que favorecerá su plegamiento. Los polioles protegen frente a la temperatura extrema y deshidratación celular, los aminoácidos protegen de un ambiente con alta concentración salina y las metilaminas protegen del efecto deletéreo de la urea sobre la estructura proteica (Cortez and Sim 2014). Los que son hidrofóbicos actúan a través de interacciones con segmentos hidrofóbicos expuestos en las proteínas

mal plegadas amortiguando la agregación proteica y se conocen como como chaperonas hidrofóbicas. Ejemplos de este tipo son el ácido fenilbutírico (4-PBA) y distintos ácidos biliares como el ácido tauroursodeoxicólico (TUDCA) y el ácido ursodeoxicólico (UDCA) (Cortez and Sim 2014). Recientemente, la bibliografía publicada sobre el uso del 4-PBA ha aumentado en varios sistemas biológicos y es ampliamente utilizado con el nombre clínico *Bufenil* para el tratamiento de enfermedades del ciclo de la urea (Diaz, Krivitzky et al. 2013). **4-PBA** es un ácido graso de cadena corta que puede rescatar el fenotipo de algunas proteínas mal plegadas *in vitro* e *in vivo* habiendo sido aprobado por la agencia estadounidense *Food Drug Administration* (FDA) para su uso clínico (Iannitti and Palmieri 2011). Se ha visto que 4-PBA es capaz de restaurar funcionalmente mutantes del canal de cloruro CFTR (Zeitlin, Diener-West et al. 2002), de la proteína surfactante A2 (Song, Fang et al. 2012), de la proteasa alfa-1 antitripsina (Burrows, Willis et al. 2000) de transportadores del tipo *ATP-binding cassette* (Cheong, Madesh et al. 2006), de uromodulina (Kemter, Sklenak et al. 2014), de canales regulados por nucleótidos cíclicos (CNG)(Duricka, Brown et al. 2012). También ha sido utilizado en distonía hereditaria (Cho, Zhang et al. 2014), así como en algunas enfermedades neurodegenerativas como Parkinson (Kubota, Niinuma et al. 2006) y Alzheimer (Kaneko 2012). Estos datos sugieren que 4-PBA reduce la agregación proteica y mejora el tráfico de una variedad de proteínas mal plegadas causadas por mutación genética o enfermedades neurodegenerativas asociadas con estrés de RE. Se proponen tres posibles modos de acción del compuesto como: sumidero de amonio, inhibidor de las histonas desacetilasas actuando como regulador transcripcional o inhibidor de estrés de RE actuando como chaperona (Kolb, Ayaub et al. 2015)**(Figura 8).**

Finalmente, las **chaperonas farmacológicas** son compuestos de bajo peso molecular que se unen específicamente a proteínas concretas e inducen su plegamiento, estabilización y recuperación funcional de manera selectiva (Bernier, Lagace et al. 2004). Pueden ser enzimas, receptores de ligando o moléculas que selectivamente unen una conformación nativa en particular de una proteína incrementando su estabilidad (Gupta, Neupane et al. 2016). La administración oral de un inhibidor competitivo en ratones transgénicos que expresan un mutante α-galactosidasa recupera la deficiente actividad contribuyendo a la patología de enfermedad de Fabry (Ishii 2012) así como otros compuestos específicos sobre la diabetes renal insípida (Bernier, Morello et al. 2006) o sobre la fenilcetonuria (Pey, Ying et al. 2008). La terapia basada en chaperonas farmacológicas representa una alternativa para reducir los grandes costes de la terapia de reemplazamiento enzimático y puede ser aplicada a trastornos de almacenamiento lisosomal y/o enfermedades conformacionales generadas por mutantes con defectos en plegamiento y tráfico como posibles mutantes de hiperplexia humana.

6. REGULACIÓN DE LA ACTIVIDAD DE GLYT2

6.1 Exocitosis y endocitosis. Modulación por balsas lipídicas.

Los cambios en la actividad de GlyT2 podrían modular la concentración de glicina en la hendidura sináptica y, por tanto, su acción postsináptica sobre los receptores. Por ello, la densidad y número de receptores de neurotransmisores o de transportadores en una sinapsis resulta crucial para determinar la fuerza e importancia de su respuesta. Así un mayor número de receptores permite una mayor respuesta de la neurona postsináptica al neurotransmisor liberado, mientras que un mayor número de transportadores producirá una recaptación más rápida del neurotransmisor, limitando su tiempo de acción en la sinapsis. Estos cambios pueden sustentar distintos aspectos de la plasticidad sináptica. La actividad de estas moléculas puede controlarse de una manera rápida y versátil mediante su tráfico intracelular, resultante del equilibrio entre exocitosis (llegada a la membrana plasmática) y endocitosis (retirada desde la membrana plasmática).

Los transportadores de neurotransmisores, como proteínas de membrana, están sujetos a un **tráfico constitutivo** resultante del equilibrio exocitosis/endocitosis como parte de su continuo reciclaje. En nuestro laboratorio, algunos experimentos han demostrado que la principal vía de endocitosis para GlyT2 está mediada por clatrina (Fornes, Nunez et al. 2008; de Juan-Sanz, Zafra et al. 2011) y constitutivamente el transportador recicla a través de endosomas que contienen Rab11, ya que un dominante negativo Rab11 impide el tráfico vesicular y su actividad de transporte (Nunez, Perez-Siles et al. 2009). Se ha comprobado para la mayoría de los neurotransportadores (GLT1, DAT, GAT1, GlyT1, GlyT2, SERT y NET) que el **tráfico** intracelular puede ser **regulado**. La activación de varias isoformas de PKC por el éster de forbol 12-miristato 13-acetato (PMA o TPA) produce un desplazamiento de este equilibrio hacia una mayor endocitosis con la consiguiente disminución de la presencia y actividad del transportador (Sato, Betz et al. 1995; Apparsundaram, Schroeter et al. 1998; Fornes, Nunez et al. 2004; Jayanthi, Samuvel et al. 2005; Boudanova, Navaroli et al. 2008; Fornes, Nunez et al. 2008; Gonzalez-Gonzalez, Garcia-Tardon et al. 2008; Fernandez-Sanchez, Martinez-Villarreal et al. 2009; Garcia-Tardon, Gonzalez-Gonzalez et al. 2012). Este mecanismo de endocitosis regulado por PKC se ha relacionado con procesos de ubiquitinación para algunos de los transportadores, como GlyT1, GLT1 y DAT, para los que se ha observado un considerable aumento de su grado de ubiquitinación tras la activación de PKC (Gonzalez-Gonzalez, Garcia-Tardon et al. 2008; Fernandez-Sanchez, Martinez-Villarreal et al. 2009; Martinez-Villarreal, Garcia Tardon et al. 2012). La implicación de varios residuos de lisina en el extremo carboxilo

terminal de GlyT2 en la endocitosis constitutiva y regulada dependiente de ubiquitinación ha sido recientemente confirmada (de Juan-Sanz, Nunez et al. 2013). Además, existe una modulación diferencial de GlyT1 y GlyT2 por la *glycogen synthase kinase 3* (GSK3b) disimuyendo e incrementando la expresión en superficie neuronal y la actividad de transporte respectivamente de ambos transportadores (Jimenez, Nunez et al. 2015).

Por otro lado, nuestro laboratorio ha demostrado que GlyT2 se asocia a balsas lipídicas o *lipid rafts* en la membrana plasmática. Estos subdominios caracterizados por ser ricos en colesterol y esfingolípidos, dan lugar a un entorno lipídico ordenado de una manera diferencial en la superficie celular. En el caso de GlyT2, este entorno lipídico produce variaciones en su actividad de transporte, de tal modo que alcanza su máxima actividad cuando reside en estos subdominios, pero si se produce una desestructuración de las balsas lipídicas por agentes que acomplejan colesterol, su actividad se reduce de manera drástica (Nunez, Alonso-Torres et al. 2008). Además, se ha visto que la activación de PKC produce un desplazamiento de GlyT2 desde los dominios raft a los no raft en la membrana, con la consiguiente disminución de actividad del transportador (Fornes, Nunez et al. 2008).

6.2 Interactoma

Los posibles mecanismos de regulación de proteínas transportadoras pueden ser iniciados a través de interacciones con otras moléculas que pueden modular directa o indirectamente la función de transporte modificando la localización celular, conformación molecular o actividad del transportador. Se han detectado las siguientes interacciones con GlyT2: la proteína SNARE **sintaxina1A** que está implicada en su llegada rápida a membrana y estimula la exocitosis de neurotransmisor (Geerlings, Lopez-Corcuera et al. 2000; Geerlings, Nunez et al. 2001); **sintenina-1**, cuya interacción con el dominio PDZ del carboxilo terminal de GlyT2 controla la correcta localización presináptica del transportador (Ohno, Koroll et al. 2004; Armsen, Himmel et al. 2007) y **Ulip6/CRMP5**, que interacciona con la región de aminoácidos 134-185 del amino terminal de GlyT2 y podría modular la endocitosis del transportador (Horiuchi, Loebrich et al. 2005). Esto se ha sugerido debido a su similitud con CRMP2, una proteína de la misma familia que comparte gran parte de su secuencia de aminoácidos con Ulip6/CRMP5 y que regula la endocitosis de algunas proteínas neuronales (Nishimura, Fukata et al. 2003).

A partir de un estudio proteómico, nuestro laboratorio ha podido detectar la interacción de GlyT2 con la **Na/K-ATPasa (NKA)**, interacción que se produce exclusivamente en lipid rafts. La bomba NKA es la encargada de la generación y

mantenimiento de los gradientes iónicos de Na^+ y K^+ en la membrana que permiten, entre otros procesos, el transporte de glicina acoplado a Na^+ llevado a cabo por GlyT2. Por otro lado, la bomba NKA puede comportarse como receptor de esteroides cardiotónicos como la ouabaína y activar una serie de cascadas de señalización que inducen la endocitosis y degradación del reservorio de GlyT2 asociado a *lipid rafts* en neuronas (de Juan-Sanz, Nunez et al. 2013).

Con estos datos, el transporte de glicina por GlyT2 podría ser mantenido y regulado por otras proteínas que controlan el gradiente electroquímico de los iones necesarios para la función del transportador y que podrían participar en las distintas situaciones y demandas de la neurotransmisión glicinérgica. El gradiente electroquímico de Na^+ puede verse influenciado por el intercambiador Na^+ /Ca^{2+} (NCX), cotransportador situado en la membrana plasmática con gran capacidad de transporte de Ca^{2+} desde el citosol al exterior celular, pero con baja afinidad por este ion. Funciona con estequiometría de $3Na^+$:$1Ca^{2+}$. Junto al intercambiador NCX, las Ca^{2+}-ATPasas o bombas de Ca^{2+} de membrana plasmática (PMCAs), exportan Ca^{2+} al exterior celular en contra de gradiente de concentración a expensas de la hidrólisis de ATP (intercambia $1Ca^{2+}$ por $1H^+$) representando los dos sistemas principales de extrusión del calcio celular (Brini and Carafoli 2011). Al contrario que el intercambiador NCX, las PMCAs tienen alta afinidad por Ca^{2+} pero baja capacidad de transporte. Aunque el acoplamiento a protones y extrusión de Ca^{2+} de la PMCA es frecuentemente ignorado en la bibliografía (Niggli and Sigel 2008) han existido discrepancias sobre si su estequiometría es electrogénica o electroneutra (Niggli, Sigel et al. 1982; Mata and Sepulveda 2005). Los últimos estudios apuntan a una estequiometría 1:1, siendo susceptible de cambios en el potencial de membrana (Thomas 2009). Además, su actividad es inhibida por alcalinización extracelular y acidificación intracelular (Thomas 2011). Se conocen tres familias con distinta localización subcelular: la Ca^{2+}-ATPasa del retículo sarco(endo)plásmico (SERCA), la Ca^{2+}-ATPasa de las vías secretoras (SPCA) y las PMCAs. Las cuatro isoformas de PMCA muestran diferentes patrones de expresión siendo PMCA1/4 ubicuas y las PMCA2/3 predominantemente expresadas en SNC (Mata and Sepulveda 2005) con una alta proporción asociada a *lipid rafts* (Jiang, Bechtel et al. 2012). Al igual que GlyT2, NCX y PMCA muestran una actividad óptima cuando están incluidas en estos subdominios de membrana (Marques-da-Silva and Gutierrez-Merino 2014).

II. Introducción y aportación original del autor

La apropiada función de GlyT2 requiere el correcto posicionamiento de la proteína en la membrana plasmática de las neuronas glicinérgicas donde se expresa. De igual modo, para que la retirada del neurotransmisor sea efectiva y también el aporte de glicina al terminal, la proteína transportadora ha de tener un apropiado tráfico intracelular y estar sujeta a un correcto equilibrio exocitosis/endocitosis y una adecuada regulación del mismo que mantenga los niveles necesarios de transportador en superficie en cada momento. Algunas de las mutaciones en el gen de GlyT2 asociadas a hiperplexia humana producen alteraciones en su tráfico intracelular y dejan retenido al transportador en distintos estadíos de la ruta secretora durante el proceso de exocitosis. Resulta de crucial importancia explorar cuáles son las moléculas que ocasionan este comportamiento y su modo de actuación, con el objetivo final de conseguir un mejor acceso a la superficie y explorar aplicaciones terapéuticas.

En el ***artículo #1*** se han examinado algunos requerimientos para la síntesis de GlyT2 en la ruta secretora temprana para establecer un marco de estudio de la síntesis de transportadores con mutaciones asociadas a hiperplexia. El trabajo se centra en el estudio de la implicación de CNX en la biogénesis de GlyT2. GlyT2 se sintetiza en el RE como un precursor inmaduro parcialmente glicosilado que va madurando y adquiriendo azúcares hasta la forma madura funcional presente en membrana plasmática. Hemos descrito la cinética y los determinantes moleculares de la interacción GlyT2-CNX y demostrado el papel de los azúcares en la unión, así como la función dependiente e independiente de la actividad lectina que tiene la chaperona en el plegamiento y maduración de GlyT2. Por otro lado, utilizando bloqueantes del proteasoma y/o el lisosoma, se han establecido las principales vías de degradación para ambas formas de GlyT2.

El ***artículo #2*** es un estudio pormenorizado de las bases moleculares del efecto dominante negativo (DN) de uno de los dos mutantes no recesivos de hiperplexia identificados en el gen de GlyT2 humano (Rees, Harvey et al. 2006). Este mutante retiene al genotipo silvestre en el interior celular retirándolo de la superficie que es su lugar de actuación. El trabajo investiga el mecanismo de retención, así como la eliminación de este efecto por chaperonas en modelos celulares donde mutante y silvestre son co-expresados emulando las condiciones de heterocigosis presente en los pacientes.

Dada la relevancia de la función de GlyT2 como regulador de la neurotransmisión glicinérgica en el SNC, resulta clave identificar mecanismos reguladores que pudieran controlar su actividad en la membrana plasmática. Las interacciones con otras moléculas reguladoras representan un mecanismo utilizado por la mayoría de las

proteínas. Un estudio proteómico realizado por nuestro grupo a partir de sinaptosomas provenientes de médula espinal de rata adulta inmunoprecipitados con un anticuerpo específico de GlyT2 permitió detectar nuevos componentes del interactoma de GlyT2. En el ***artículo #3*** se ha investigado el complejo funcional GlyT2-NCX-PMCA2/3 cuya función podría ser el mantenimiento de la homeostasis local de Na^+ y Ca^{2+} en terminales glicinérgicos dotando a GlyT2 del gradiente electroquímico de Na^+ necesario para ejercer su función.

En el ***artículo #4*** de esta tesis, nuestro laboratorio junto al grupo del Dr. Cecilio Giménez y en colaboración con el equipo del Dr. Robert Harvey (de la UCL School of Pharmacy del Reino Unido), identificó una nueva mutación dominante asociada a hiperplexia encontrada en el exón 15 de muestras de pacientes de España y Reino Unido facilitadas por el profesor Dr. Pablo Lapunzina del Hospital Universitario La Paz, Madrid. La sustitución Y705C (c.2114A⟶G) presenta menor actividad de transporte debido a la retención intracelular de transportador y a una alteración funcional en la regulación por protones y zinc. Este trabajo identificó y caracterizó el primer mutante de hiperplexia humana que es dominante para la función de transporte y recesivo para el tráfico del transportador y cuyo defecto puede alterar la neurotransmisión glicinérgica de los pacientes heterocigotos que lo portan.

APORTACIÓN ORIGINAL DEL AUTOR MEDIANTE LOS TRABAJOS PRESENTADOS EN ESTA TESIS DOCTORAL

1) Papel de la N-glicosilación en la expresión de GlyT2 en la ruta secretora. Papel en la biogénesis y actividad del transportador mediante mutantes: la glicosilación es necesaria pero no imprescindible para la llegada a membrana de GlyT2 (***Artículo #1***). Papel de los azúcares en la selección de la vía degradativa de GlyT2 y mutantes (***Artículo 1# y #2***).

2) Demostración de que CNX asiste la biogénesis de GlyT2 y caracterización de la interacción GlyT2-CNX: facilita el procesamiento del transportador actuando sobre el precursor; está mediada por N-glicosilación y por interacciones proteína-proteína; los niveles de CNX correlacionan positivamente con la expresión de GlyT2 activo (***Artículo #1***).

3) Determinación de la actividad chaperona de CNX independiente de lectina y su acción selectiva sobre el genotipo silvestre y mutantes. Demostración de que CNX puede discriminar los intermediarios de plegamiento más competentes tanto en el transportador silvestre como en el carente de sitios de glicosilación. La sobrexpresión de CNX puede rescatar la acción de un mutante con defecto de tráfico que retiene al genotipo silvestre de manera dominante. (***Articulo #1 y #2***).

4) Caracterización de un mutante de hiperplexia humana y explicación de su efecto DN sobre el tipo silvestre. Rescate por la chaperona química 4-PBA en neuronas primarias (***Artículo #2***).

5) Establecimiento de la interacción funcional exclusiva de *lipid rafts* entre GlyT2 y las proteínas de membrana plasmática NCX y PMCA2/3 (***Artículo #3***).

6) Análisis de una nueva mutación dominante en el gen de GlyT2 (*SLC6A5*) encontrada en pacientes de hiperplexia humana con defectos en el tráfico del transportador y en la actividad de transporte (***Artículo #4***).

7) Estudio de la relevancia estructural y funcional del puente disulfuro presente en el EL2 de GlyT2 sobre su tráfico intracelular y durante el ciclo de transporte (***Artículo #4***).

8) Descubrimiento de la regulación de la actividad de GlyT2 por protones y zinc y alteración de esta modulación del transporte por inclusión de una cisteína en posición 705 en pacientes de hiperplexia (***Artículo #4***).

9) Se han establecido los determinantes estructurales de la interfase de oligomerización de GlyT2 ***(Anexo Artículo #5).***

REFERENCIAS DE LOS ARTÍCULOS COMPENDIADOS

Artículo #1

Arribas-González E, Alonso-Torres P, Aragón C y López-Corcuera B (2013)
Calnexin-assisted biogenesis of the neuronal glycine transporter 2 (GlyT2)
PLoS One. May 1;8(5):e63230

Artículo #2

Arribas-González E, de Juan-Sanz J, Aragón C, López-Corcuera B (2015)
Molecular basis of the dominant negative effect of a glycine transporter 2 mutation associated with hyperekplexia.
J Biol Chem 290(4):2150-65

Artículo #3

de Juan-Sanz J, Núñez E, Zafra F, Berrocal M, Corbacho I, Ibáñez I, **Arribas-González E**, Marcos D, López-Corcuera B, Mata A.M. and Aragón C (2014)
Presynaptic control of glycine transporter 2 (GlyT2) by physical and functional association with plasma membrane Ca2+-ATPase (PMCA) and Na+-Ca2+ exchanger (NCX)
J Biol Chem 289(49):34308-24

Artículo #4

Giménez C, Pérez-Siles G, Martínez-Villarreal J, **Arribas-González E**, Jiménez E, Núñez E, de Juan-Sanz J, Fernández-Sánchez E, García-Tardón N, Ibáñez I, Romanelli V, Nevado J, James VM, Topf M, Chung SK, Thomas RH, Desviat LR, Aragón C, Zafra F, Rees MI, Lapunzina P, Harvey RJ, López-Corcuera B (2012)
A novel dominant hyperekplexia mutation Y705C alters trafficking and biochemical properties of the presynaptic glycine transporter GlyT2
J Biol Chem. 287(34):28986-9002

Anexo Artículo #5

Arribas-González E, Núñez E, Benito-Muñoz C, Dos Santos HG, Perona A, Aragón C and López-Corcuera B (En preparación, 2017)
Oligomer assembly of the neuronal glycine transporter GlyT2

III. Artículos compendiados

Artículo #1

Arribas-González E, Alonso-Torres P, Aragón C y López-Corcuera B (2013)
Calnexin-assisted biogenesis of the neuronal glycine transporter 2 (GlyT2)
PLoS One. May 1;8(5):e63230

OPEN ACCESS Freely available online

PLOS ONE

Calnexin-Assisted Biogenesis of the Neuronal Glycine Transporter 2 (GlyT2)

Esther Arribas-González[1,3], Pablo Alonso-Torres[1], Carmen Aragón[1,2,3], Beatriz López-Corcuera[1,2,3]*

1 Departamento de Biología Molecular and Centro de Biología Molecular "Severo Ochoa", Consejo Superior de Investigaciones Científicas, Universidad Autónoma de Madrid, Madrid, Spain, **2** Centro de Investigación Biomédica en Red de Enfermedades Raras, Instituto de Salud Carlos III, Madrid, Spain, **3** IdiPAZ-Hospital Universitario La Paz, Universidad Autónoma de Madrid, Madrid, Spain

Abstract

The neuronal transporter GlyT2 is a polytopic, 12-transmembrane domain, plasma membrane glycoprotein involved in the removal and recycling of synaptic glycine from inhibitory synapses. Mutations in the human GlyT2 gene (*SLC6A5*) that cause deficient glycine transport or defective GlyT2 trafficking are the second most common cause of hyperekplexia or startle disease. In this study we examined several aspects of GlyT2 biogenesis that involve the endoplasmic reticulum chaperone calnexin (CNX). CNX binds transiently to an intermediate under-glycosylated transporter precursor and facilitates GlyT2 processing. In cells expressing GlyT2, transporter accumulation and transport activity were attenuated by siRNA-mediated CNX knockdown and enhanced by CNX overexpression. GlyT2 binding to CNX was mediated by glycan and polypeptide-based interactions as revealed by pharmacological approaches and the behavior of GlyT2 *N*-glycan-deficient mutants. Moreover, transporter folding appeared to be stabilized by *N*-glycans. Co-expression of CNX and a fully non-glycosylated mutant rescues glycine transport but not mutant surface expression. Hence, CNX discriminates between different conformational states of GlyT2 displaying a lectin-independent chaperone activity. GlyT2 wild-type and mutant transporters were finally degraded in the lysosome. Our findings provide further insight into GlyT2 biogenesis, and a useful framework for the study of newly synthesized GlyT2 transporters bearing hyperekplexia mutations.

Citation: Arribas-González E, Alonso-Torres P, Aragón C, López-Corcuera B (2013) Calnexin-Assisted Biogenesis of the Neuronal Glycine Transporter 2 (GlyT2). PLoS ONE 8(5): e63230. doi:10.1371/journal.pone.0063230

Editor: Jeffrey L. Brodsky, University of Pittsburgh, United States of America

Received October 8, 2012; **Accepted** March 30, 2013; **Published** May 1, 2013

Funding: This work was supported by the Spanish 'Dirección General de Enseñanza Superior e Investigación Científica' (BFU2005-05931/BMC and BIO2005-05786), 'Ministerio de Ciencia e Innovación' (SAF2008-05436), 'Comunidad Autónoma de Madrid' (11/BCB/010 and S-SAL-0253/2006), Ministerio de Economia y Competitividad (SAF2011-28674), CIBERER (intramural project U-751/U-753), by an institutional grant from the 'Fundación Ramón Areces'. The funders had no role in study design, data collection and analysis, decision to publish, or preparation of the manuscript.

Competing Interests: The authors have declared that no competing interests exist.

* E-mail: blopez@cbm.uam.es

Introduction

Glycine is the major inhibitory neurotransmitter in caudal areas of the vertebrate central nervous system, participating in the motor and sensory information processing involved in movement, vision and audition [1,2]. Moreover, glycinergic inhibition also modulates nociceptive signaling [3]. The synaptic action of glycine is terminated by its reuptake via specific plasma membrane transporters (GLyTs), which perform high-affinity, active co-transport coupled to the electrochemical gradient of Na^+ and dependent on Cl^- [4]. The neuronal GlyT2 transporter is involved in the removal and recycling of synaptic glycine from inhibitory synapses by supplying substrate to the low-affinity vesicular transporter VIAAT (VGAT) [5–8]. Presynaptic glycine taken up by GlyT2 has been demonstrated to be the sole source of releasable transmitter at glycinergic synapses [9], and inactivation of the GlyT2 gene in mice generates a complex postnatal neuromotor phenotype that reproduces the symptoms of human hyperekplexia [6].

Hyperekplexia or startle disease (OMIM 149400) is characterized by neonatal hypertonia and an exaggerated startle response to trivial stimuli [10]. This disorder can lead to brain damage and/or sudden infant death caused by apneic episodes. Genetic analysis of hyperekplexia patients has identified mutations in the human GlyT2 gene (*SLC6A5*) as the second most common cause of the disease, after mutations affecting the glycine receptor and other key proteins in glycinergic synapses [11,12]. A model of the 3-dimensional structure of GlyT2 was recently developed [13,14] using as a template the leucine transporter from *Aequifex aeolicus* ($LeuT_{Aa}$), a prokaryotic homologue of the solute carrier 6 (SLC6) family to which GlyT2 belongs [15]. This model provides an explanation for the effects of selected missense mutations on Na^+- and glycine-binding residues crucial for transport [12,16–19]. The majority of GlyT2 mutations are recessive and cause bi-allelic loss of function due to the absence of the protein in the plasma membrane or the generation of inactive transporters [12]. Only one dominant mutation affecting GlyT2 intracellular trafficking has been described to date (S510R), which is proposed to block the arrival of the transporter to the plasma membrane [16]. However, recently a dominantly inherited mutation that causes complex alterations in transport function and that hinders the proper expression of the transporter at the cell membrane was described [18]. While the trafficking of GlyT2 to and from the plasma membrane along the late secretory pathway has been studied largely [20–22], similar analyses of the biogenesis of GlyT2 and its trafficking along the early secretory pathway have not been performed, despite the importance of these processes in the physiology and pathologies of glycinergic neurotransmission.

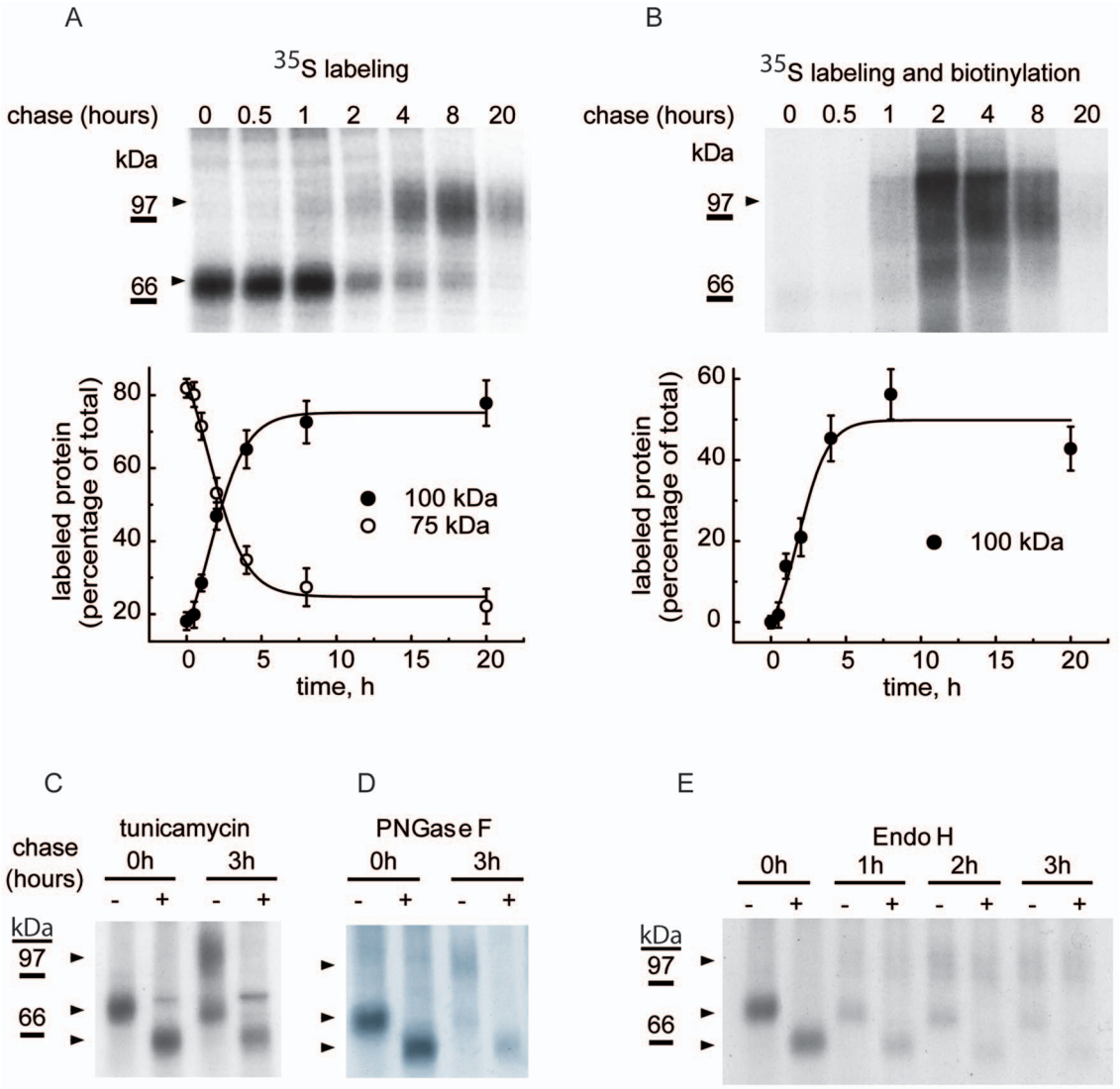

Figure 1. GlyT2 expression after a pulse-chased in culture cells. COS7 cells transfected with GlyT2 cDNA in pCDNA3 were pulse-labeled for 15 min with [^{35}S]methionine/cysteine and chased for the times indicated in the conditions given in Material and Methods. The cells were then surface biotinylated, lysed and the protein lysate was either immunoprecipitated with GlyT2 antibody (total transporter, A) or bound to streptavidin-agarose and sequentially immunoprecipitated with GlyT2 antibody (biotinylated fraction, B). Proteins extracted from the beads were resolved in SDS-PAGE. (A) Kinetics of GlyT2 expression. (B) Kinetics of GlyT2 plasma membrane expression in the same cells as in A. Lower panels: (A) densitometry of the 100 kDa and 75 kDa bands in the fluorograms. (B) Biotinylated bands are represented as a percentage of each of the lanes labeled in A. Bars represent the S.E.M. (n = 3). (C) Cells were treated overnight with the vehicle alone (DMSO) or with 10 μg/ml tunicamycin, and then pulse-chased as described above. (D, E) Immunoprecipitates were treated overnight with the vehicle alone (endoglycosidase buffer, -) or with the indicated endoglycosidase (+) in denaturing conditions, and then resolved by SDS-PAGE as described in the Materials and Methods. The transporter proteins (100 kDa, 75 kDa and 60 kDa) are indicated with arrowheads.
doi:10.1371/journal.pone.0063230.g001

The synthesis of GlyT2, a polytopic plasma membrane protein, begins with its co-translational translocation to the endoplasmic reticulum (ER) [23]. The biogenesis of these proteins requires interactions with ER chaperones, such as calnexin (CNX), calreticulin (CRT), BiP (GRP78), and oxidoreductases like ERp57 and PDI [24]. CNX is a type I integral membrane protein responsible for the folding and quality control of newly-synthesized glycoproteins [25]. The ER luminal domain of calnexin is responsible for lectin-like activity and interaction with nascent polypeptide chains [26]. Protein-protein interactions may also mediate the interaction with CNX [27,28]. The second extracellular loop (EL2) of GlyT2 contains 4 asparagines (N345, N355, N360 and N366) that are *N*-glycosylated in the mature protein. The *N*-glycosylation of GlyT2 is partially responsible for its arrival to the plasma membrane, and its asymmetric distribution in polarized cells [29]. In addition, oligomer assembly of neurotransmitter transporters appears to be a prerequisite for export to the plasma membrane and their asymmetric targeting to the neuronal synapse [30].

Here, we confirm a role for CNX in GlyT2 biogenesis, and we describe the kinetics and determinants of the GlyT2-CNX interaction. Our data identify some of the key features of GlyT2 biogenesis in the early secretory pathway. These findings may help to decipher the effects of hyperekplexia mutations on the plasma membrane expression of newly synthesized GlyT2 transporters.

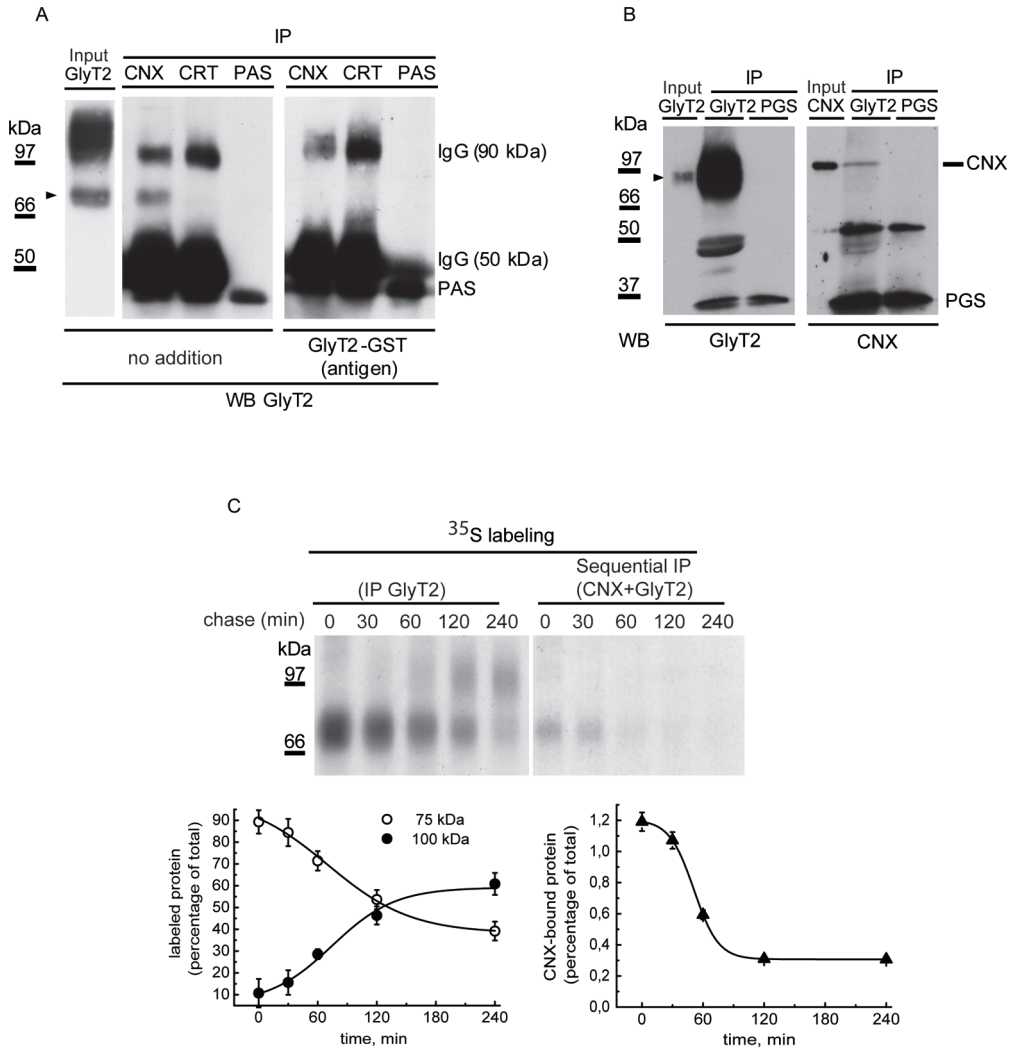

Figure 2. GlyT2 co-immunoprecipitates with CNX. (A) Lysates of COS7 cells expressing GlyT2 were immunoprecipitated with anti-CNX (CNX), anti-calreticulin (CRT) or no antibody (PAS) and then analyzed in Western blots (WB) to detect GlyT2 in the presence or absence (no addition) of 100 μg/ml of the GlyT2 fusion protein used as antigen to generate the rabbit GlyT2 antibody (GlyT2-GST) [30]. The input GlyT2 lane contains 10% of the protein loaded for immunoprecipitation (IP). PAS: protein A sepharose (~45 kDa). (B) Rat brain stem primary neurons were immunoprecipitated with anti-GlyT2 antibody made in rat [20] and then analyzed in WBs to detect the endogenous immunoprecipitated GlyT2 or CNX by using antibodies made in rabbit. The input lanes contain 5% of the protein loaded for immunoprecipitation (IP). Arrowheads indicate GlyT2. PGS: protein G sepharose (~17 kDa). (C) COS7 cells expressing GlyT2 were pulse-labeled for 15 min with [^{35}S]methionine/cysteine, chased for the times indicated and subjected to sequential immunoprecipitation with CNX and GlyT2 antibodies, as described in the Materials and Methods. Lower panel: densitometry of the fluorograms.
doi:10.1371/journal.pone.0063230.g002

Materials and Methods

Cell Growth and Protein Expression

COS7 cells (American Type Culture Collection) were grown at 37°C and 5% CO_2 in Dulbecco's modified Eagle's medium supplemented with 10% fetal bovine serum. Transient expression was achieved using Neofectin^{TM} (MidAtlantic Biolabs), according to the manufacturer's protocol. Reproducible results were obtained with 50–60% confluent cells on 60 mm or 6 well plates using 5.5 μg and 2.5 μg of total DNA, respectively. Cells were incubated for 48 h at 37°C until used. Transfection efficiency was determined by co-transfecting the cDNAs with the pSV-β-galactosidase plasmid (Promega) and measuring β-galactosidase activity 24 h later after cell solubilization with 25 mM glycylglycine pH 7.8, 0.5% Triton X-100, 1 mM DTT (100 μl/well). After centrifugation (15,000×g) for 2 min, supernatants (15 μl) were transferred to a 96 well plate together with 1 volume of assay buffer (2 mM $MgCl_2$, 120 mM $NaPO_4$, 80 mM Na_2HPO_4, 100 mM β-mercaptoethanol and 1.33 mg/ml O-nitophenyl-β-D-galactopyranoside) and incubated for 20 min at 37°C. Absorbance was measured at 420 nm in an ELISA Dynatech MR5000 and normalized to the protein concentration. Rat brain stem primary neuronal cultures were performed as previously described [29].

Plasmid Constructs

N-glycosylation mutants of rat GlyT2 were inserted into a pCDNA3 vector either as described previously [31] or constructed by site-directed mutagenesis using the QuikChange kit (Stratagene) [32]. Two independent *Escherichia coli* colonies

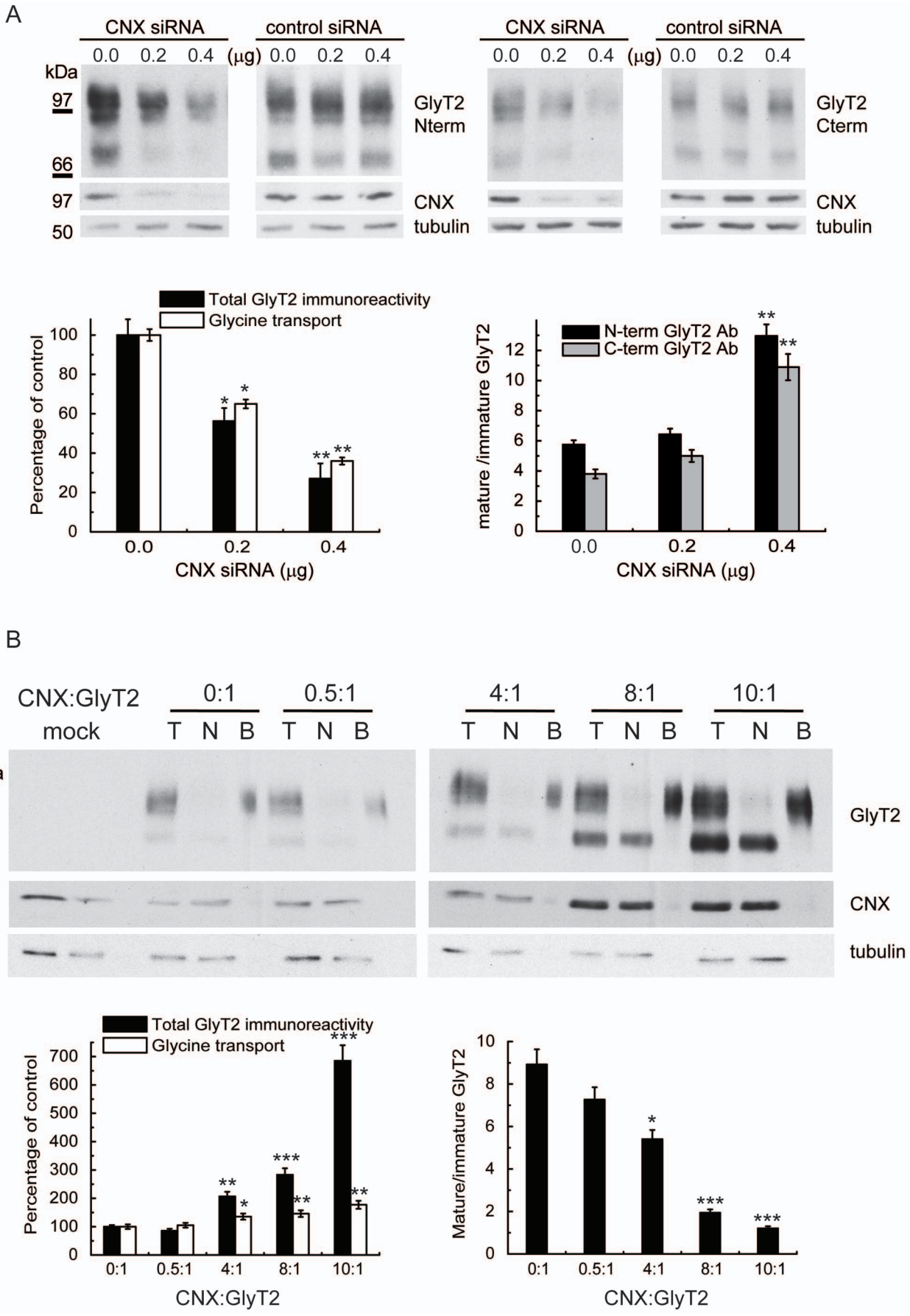
A
CNX siRNA
control siRNA
CNX siRNA
control siRNA
0.0 0.2 0.4 (μg) 0.0 0.2 0.4
0.0 0.2 0.4 (μg) 0.0 0.2 0.4
kDa
97
66
97
50
GlyT2 Nterm
CNX
tubulin
GlyT2 Cterm
CNX
tubulin
Total GlyT2 immunoreactivity
Glycine transport
Percentage of control
CNX siRNA (μg)
N-term GlyT2 Ab
C-term GlyT2 Ab
mature /immature GlyT2
CNX siRNA (μg)
B
CNX:GlyT2
mock
0:1
0.5:1
4:1
8:1
10:1
T N B T N B T N B T N B T N B
kDa
97
66
97
50
GlyT2
CNX
tubulin
Total GlyT2 immunoreactivity
Glycine transport
Percentage of control
CNX:GlyT2
Mature/immature GlyT2
CNX:GlyT2

Figure 3. Expression of GlyT2 following CNX knockdown/overexpression. (A) COS7 cells were co-transfected with 0.5 μg of GlyT2 cDNA in pCDNA3 and the indicated amount of control (HPRT) or CNX siRNA. At 48 h post-transfection, the cells were analyzed in Western blots (upper panel) or assayed for glycine transport (open bars, left graph). The specific CNX d-siRNA reduced CNX protein levels by 62% (0.2 μg) and 85% (0.4 μg), respectively, as compared with endogenous levels. Control d-siRNA increased total GlyT2 levels by 10% and 15%, respectively. Right graph: ratio of mature (100 kDa) to immature (75 kDa) band at the different amounts of CNX siRNA transfected. The bands were detected with GlyT2 antibodies against N- or C-terminal epitopes (Fig. S1). (B) COS7 cells were co-transfected with 0.5 μg of GlyT2 cDNA together with a CNX cDNA at the indicated mass ratio (CNX:GlyT2). At 48 h post-transfection the cells were biotinylated (T = total transporter; N = non-biotinylated transporter; B = biotinylated transporter, 3-fold the protein amount in T or N) or glycine transport was assayed (open bars, left histogram). Solid bars in the left histogram represent total GlyT2 normalized to tubulin immunoreactivity. Verification of CNX overexpression by densitometry revealed the following increases at increasing mass ratios: 0:1, 1-fold (endogenous CNX); 0.5:1, 1.8-fold; 4:1, 2.4-fold; 8:1, 9.3-fold; 10:1, 12.9-fold. Right graph: the ratio of the mature (100 kDa) to immature (75 kDa) protein decreased with the amount of CNX expressed. Bars represent the S.E.M (n = 6). *$p<0.05$, **$p<0.01$, ***$p<0.001$ with respect to control (Student's t-test).
doi:10.1371/journal.pone.0063230.g003

carrying the mutant plasmids were characterized by DNA sequencing and [^{3}H]glycine transport activity. We sequenced the complete coding region of each construct to verify that only the desired mutation had been introduced. Mouse cDNA CNX clone (IMAGE number 2582119) was purchased from Source Bioscience Lifesciences.

Pulse and Chase

Cells cultured to 80–90% confluence in p60 or p100 plates were incubated with methionine-free medium for 1 hour. The cells were then pulse-labeled for 15 min with 0.25 mCi/ml [^{35}S]methionine/cysteine (Redivue Promix, Amersham) and chased for varying periods in Dulbecco's modified Eagle's medium 10% fetal calf serum containing 1 mM cycloheximide to quickly stop the elongation of nascent polypeptide chains. Labeling was stopped by the addition of ice-cold phosphate-buffered saline (PBS) containing 20 mM freshly prepared N-ethylmaleimide to prevent oxidation of free sulfhydryl groups. Proteins were immunoprecipitated with GlyT2 antibody [33] or sequentially with anti-CNX (Stressgen) and anti-GlyT2 antibodies, as described below. Samples were resolved in SDS-polyacrylamide gels (SDS-PAGE), fixed and treated with Amplify fluorography reagent (Amersham). The gels were dried and exposed for 4–12 days at −70°C, and the protein bands were quantified after densitometry.

Carbohydrate Modification

Pulse-chased GlyT2 immunoprecipitates were digested with the desired endoglycosidase (PNGase F, New England Biolabs; or Endoglycosidase H or D, Roche) in a small volume of the appropriate buffer, following the manufacturer's instructions. For tunicamycin treatment, GlyT2-expressing cells were treated with 1–10 μg/ml tunicamycin or the vehicle alone (DMSO) for the time and the temperature indicated in the figure legends, immunoprecipitated with the desired antibodies and resolved by SDS-PAGE.

Surface Biotinylation

Pulse-chased (or non-labeled) transfected COS7 cells growing in 6 well plates (Nunc) were washed 3 times with complete PBS (PBSc) containing 0.1 mM $CaCl_2$ and 1 mM $MgCl_2$, and they were incubated for 30 minutes with Sulfo-NHS-Biotin in PBSc (1.0 mg/ml, Pierce) at a temperature that blocks trafficking (4°C). After two 30 min washes at 4°C, 100 mM L-lysine in PBSc was added to block free biotin, cells were rinsed with 150 mM NaCl and 50 mM Tris-HCl (pH 7.4) containing protease inhibitors (0.4 mM PMSF and 4 μM pepstatin) and lysed by end-over-end agitation for 30 minutes at 4°C with 1x lysis buffer (150 mM NaCl, 50 mM Tris-HCl [pH 7.4], 5 mM EDTA, 1% Triton-X, 0.1% SDS, 0.25% deoxycholate sodium, 0.4 mM PMSF and 4 μM pepstatin). A portion of the lysate was saved for total protein determination and the remainder was incubated with streptavidin-agarose for 2 h at room temperature with rotary shaking. After centrifugation, the supernatant was removed (except for an aliquot - not biotinylated), and the agarose beads were washed 3 times with 1x lysis buffer. The bound proteins (biotinylated) were eluted with Laemmli buffer (65 mM Tris, 10% glycerol, 2.3% SDS, 100 mM DTT, 0.01% bromophenol blue) for 10 minutes at 75°C. Samples were analyzed by SDS-PAGE, immunoblotting (Western blot) and densitometry.

Electrophoresis and Western Blotting

Samples were subjected to SDS-PAGE using a 4% stacking gel and 6% or 7.5% resolving gels. The samples were transferred to nitrocellulose by semi-dry electrotransfer (Life Technologies Inc.: 1.2 mA/cm^2 for 2 h) and the membranes were then blocked with 5% milk in PBS for 4 h at 25°C. The membranes were probed overnight at 4°C with the desired primary antibody: anti-GLYT2 (1:1,000), anti-CNX (1:1,000) or anti-PERK (C33E10, 1:1,000, Cell Signaling Technology Inc., Danvers, MA). After several washes, the antibodies bound were detected with peroxidase coupled anti-rat or anti-rabbit IgG respectively (1:6,000), which were visualized by ECL (Amersham Corp.). Subsequently, the antibodies were stripped from the membrane (Thermo Scientific) and it was re-probed with anti-tubulin (1:3000; Sigma), which was detected with peroxidase-coupled anti-rabbit IgG. The protein bands were quantified by densitometry.

Inmunoprecipitation Assays

Transfected COS7 cells were washed twice with 20 mM N-ethylmaleimide in PBS and solubilized for 15 min at 4°C in 1 ml of 1% 3-((3-Cholamidopropyl) dimethylammonio)-1-propanesulfonic acid (CHAPS) in HEPES-buffered saline (HBS) buffer (10 mM HEPES-NaOH [pH 7.4], 150 mM NaCl, 1 mM EDTA, 1% CHAPS, 0.4 mM PMSF and 4 μM pepstatin). The CNX-GlyT2 complexes were also maintained in both Triton X-100 and digitonin at the same concentration, although CHAPS displayed the highest solubilization potency. The solubilized material was centrifuged at 10,000×g for 15 min. A portion of the lysate was retained (total protein, input or lysate) and the remainder was incubated with 30 μl of 50% protein A or G cross-linked to sepharose beads in lysis buffer (PAS or PGS: Sigma, St Louis, MO, USA). The mixture was precleared by incubation for 30 min at 4°C with continuous rotation, the samples were centrifuged and the supernatants were incubated for 2 hours at 4°C with 1.5 μg of anti-GlyT2 [33] or anti-CNX antibody (Stressgen Biotechnologies Corp., Victoria, Canada). Subsequently, 30 μl of beads were added and the mixture was incubated for 1 h at 4°C with constant rotation. The beads were washed 3 times with 0.5% CHAPS in ice-cold HBS before adding SDS-PAGE sample buffer to each sample (30 μl). The bound proteins were dissociated from the beads by heating at 75°C for 15 min before SDS-PAGE resolution. For sequential immunoprecipitation, the immunopre-

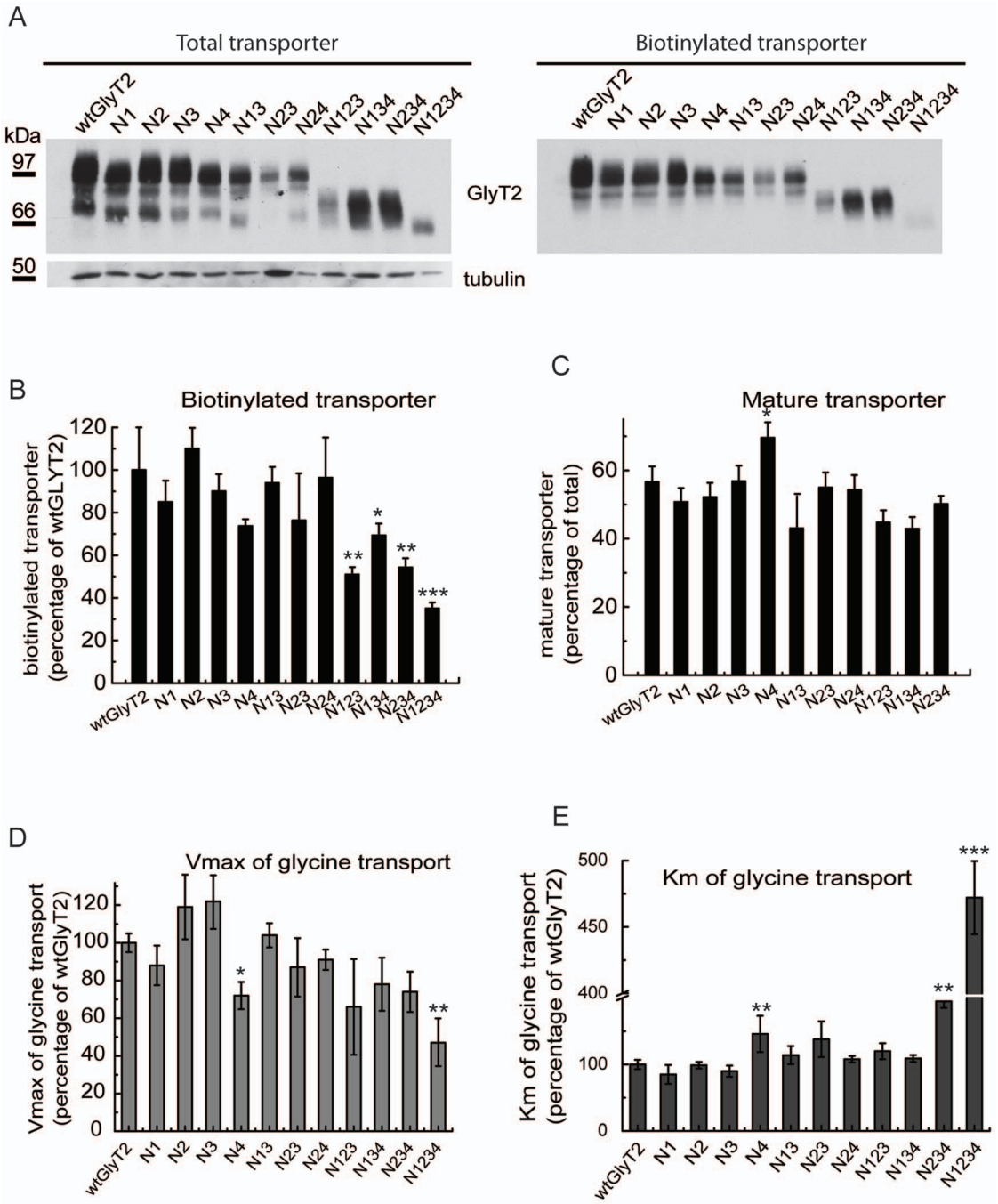

Figure 4. Characterization of GlyT2 *N*-glycan site mutants. (A) COS7 cells expressing the indicated GlyT2 *N*-glycosylation mutants were biotinylated and processed as described in the Materials and Methods. (A) Lysates (6 μg, total transporter, left) or biotinylated protein (18 μg, biotinylated transporter, right) were resolved by SDS-PAGE and analyzed in Western blots to detect GlyT2. Tubulin immunoreactivity was used as a loading control. Immunoblots were quantified by densitometry. (B) Densitometry representing the proportion of mutant biotinylated transporter as a percentage of the biotinylated fraction of wild-type GlyT2. (C) Densitometry of the Western blots expressing the fraction of mature transporter (upper band) as a percentage of the total transporter for each mutant. (D,E) COS7 cells expressing the indicated GlyT2 *N*-glycosylation mutants were assayed for glycine transport (as described in the Materials and Methods) in the presence of increasing concentrations of glycine from 1 to 1000 μM. Kinetic data were fitted to hyperbolae and V_{max} and K_m parameters were calculated from the best fit. For wild-type GlyT2, $V_{max} = 17 \pm 3.8$ nmol gly/mg prot/4 min and $K_m = 171 \pm 20$ μM. Bars represent the S.E.M (n = 3). *p<0.05, **p<0.01, ***p<0.001 with respect to wild-type GlyT2 (ANOVA with Tukey's post-hoc test).
doi:10.1371/journal.pone.0063230.g004

cipitated proteins were eluted from the beads by adding 150 μl of 1% SDS in HBS at 75°C for 30 min and centrifuged. The supernatant was diluted with 1.35 ml 1% CHAPS in HBS to decrease the SDS concentration to 0.1% and transferred to a new tube containing 1.5 μg of anti-GlyT2 antibody and incubated overnight at 4°C. The immunocomplexes were bound to beads and eluted as described above. Samples were subsequently subjected to SDS-PAGE.

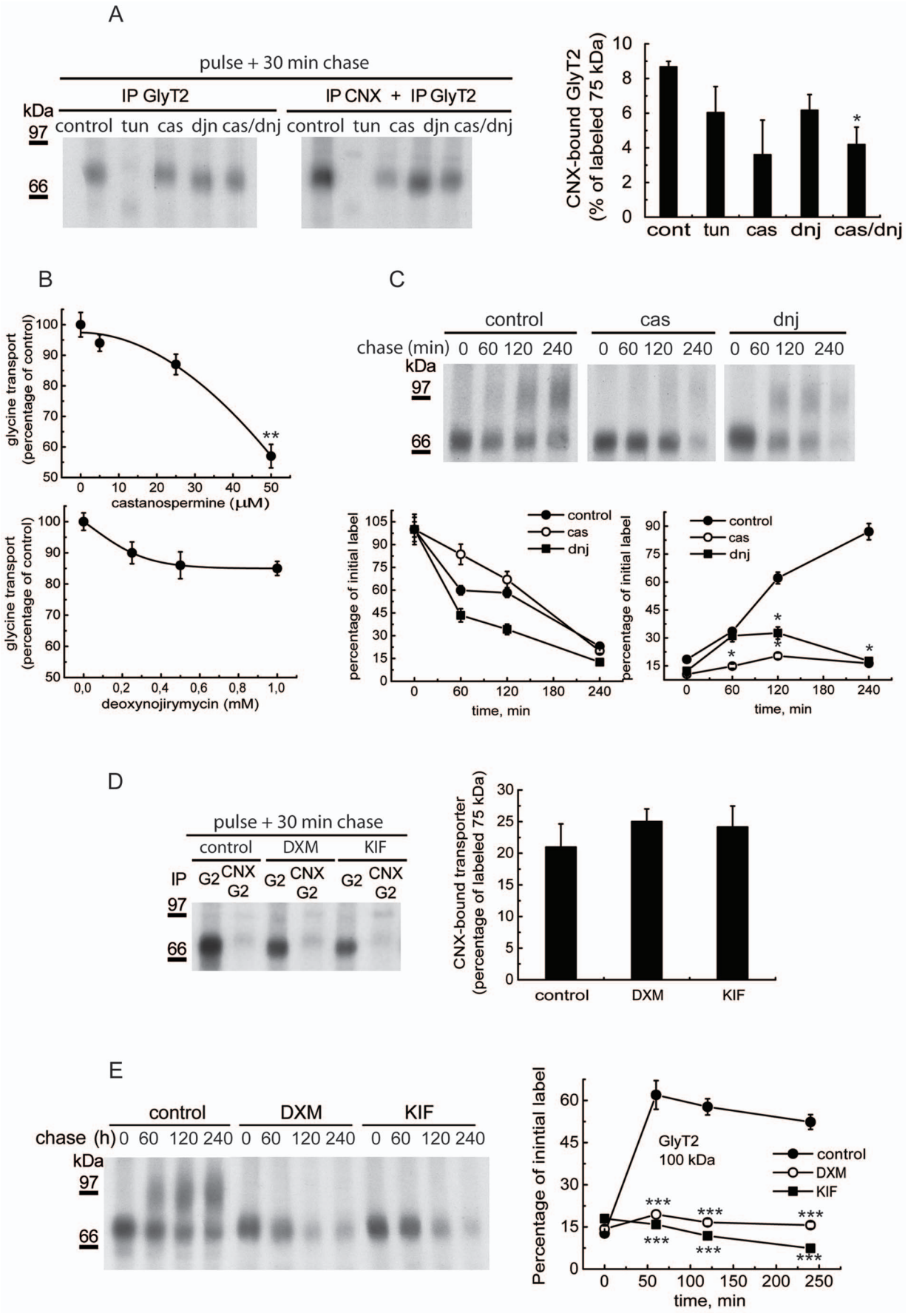
A
pulse + 30 min chase
IP GlyT2
IP CNX + IP GlyT2
kDa
97
66
control tun cas djn cas/dnj control tun cas djn cas/dnj
CNX-bound GlyT2
(% of labeled 75 kDa)
cont tun cas dnj cas/dnj
B
glycine transport
(percentage of control)
castanospermine (μM)
deoxynojirymycin (mM)
C
control
cas
dnj
chase (min) 0 60 120 240 0 60 120 240 0 60 120 240
percentage of initial label
time, min
D
pulse + 30 min chase
control
DXM
KIF
IP G2 CNX G2 G2 CNX G2 G2 CNX G2
CNX-bound transporter
(percentage of labeled 75 kDa)
E
chase (h) 0 60 120 240 0 60 120 240 0 60 120 240
Percentage of inintial label
GlyT2
100 kDa

Figure 5. Effects of glucosidase and mannosidase inhibitors on CNX binding and GlyT2 maturation. (A) COS7 cells expressing GlyT2 were treated for 2 h with the vehicle alone (DMSO), 1 μg/ml tunicamycin, 1 mM castanospermine (cas), 1 mM deoxynojirimycin (dnj) or 1 mM castanospermine plus 1 mM deoxynojirimycin (cas/dnj), and then pulse-labeled for 15 min with [^{35}S]methionine/cysteine and chased for 30 min. The cell lysates were then immunoprecipitated with a GlyT2 antibody or subjected to sequential immunoprecipitation with CNX and GlyT2 antibodies (as described in the Materials and Methods) and resolved by SDS-PAGE. Right panel: densitometry of the fluorograms (n = 3) showing the percentage of total GlyT2 precursor bound to CNX in each condition (± S.E.M). (B) COS7 cells expressing GlyT2 were treated for 2 h with the vehicle alone (water), 1–50 μM castanospermine (upper graph) or 0.2–1 mM deoxynojirimycin (lower graph) and then glycine transport was assayed in the cells. (C) COS7 cells expressing GlyT2 were treated for 2 h with the vehicle alone (control), 1 mM castanospermine or 2 mM deoxynojirimycin and then pulse-labeled for 15 min with [^{35}S]methionine/cysteine, chased for the times indicated. The cell lysates were immunoprecipitated with GlyT2 antibody and analyzed by SDS-PAGE. Lower graphs: densitometry. (D,E) The experimental conditions applied were as described in A and C, except the cells were treated with 1 mM deoxymannojirimycin (DXM) or 10 μM kifunensin (KIF). *$p<0.05$, **$p<0.01$, ***$p<0.001$ with respect to controls (Student's t-test).
doi:10.1371/journal.pone.0063230.g005

siRNA Generation and Transfection

CNX mRNA silencing was achieved by generating and transfecting CNX-specific small d-siRNA into COS7 cells as indicated below. A 300-base pair CNX amplification product (IMAGE number 2582119) flanked by a T7 promoter (RZPD, German Resource Center for Genome Research) was transcribed *in vitro* using the X-tremeGENE siRNA Dicer Kit (Roche) following the manufacturer's instructions. The resulting annealed dsRNA was subsequently digested with recombinant Dicer enzyme, and the digested RNA was purified and d-siRNA was transfected into COS7 cells using the X-tremeGENE siRNA Transfection Reagent (Roche) with 2.5 μl/0.2 μg d-siRNA. Knockdown efficiency of the CNX-siRNA was assessed in Western blots 48 h post-transfection and it was 85–90%. The siRNA from hypoxanthine phosphoribosyltransferase (HPRT) served as a control.

Glycine Transport Assays

The day before the assay, the cells transfected with pcDNA3 (control) and/or the cDNAs under study were seeded at 80% confluence in 24 well plates (Nunc). The culture medium was then removed. The cells were washed with PBS (137 mM NaCl, 0.9 mM $CaCl_2$, 2.68 mM KCl, 1.47 mM KH_2PO_4, 0.49 mM $MgCl_2$, 7.37 mM Na_2HPO_4 [pH 7.4] and 10 mM glucose) and tempered at 37°C. After a further 10 minute incubation at 37°C with 250 μl of transport medium (2 μl/ml [2-^{3}H]-glycine [PerkinElmer Life Sciences], 1.6 TBq/mmol, isotopically diluted to a concentration of 10 μM in PBS), the cells were washed with 750 μl PBS and lysed with 250 μl of 0.2 M NaOH. The protein concentration was determined in aliquots taken from each well by the Bradford method (Biorad) and [2-^{3}H]-glycine was measured by liquid scintillation (LKB 1219 Rackbeta). GlyT2 transport was measured as the difference between glycine accumulation in cDNA-transfected cells and that observed in mock-transfected cells. Assays were performed in triplicate or quadruplicate.

Membrane Isolation

Cells were recovered with PBS 1 mM EDTA and by centrifugation at 1,000 rpm for 5 minutes, resuspended in PBS-EDTA and lysed mechanically by passing the sample 5 times through a needle of 0.5 mm diameter. The lysate was cleared by centrifugation (3,500 rpm for 10 minutes) and the supernatant was collected. The pellet was resuspended in PBS-EDTA and passed 5 times through a needle of 0.3 mm diameter, a step that was repeated twice more. The pellet was discarded and the supernatant collected in the 3 steps above was centrifuged at 18,000 rpm for 45 minutes. The supernatant was discarded and the membrane-enriched pellet was resuspended in a minimal volume of PBS-EDTA. The protein concentration was determined by the Bradford method and adjusted to 0.5 mg/ml.

Limited Proteolysis

Membranes (25 μl) from an enriched fraction obtained by subcellular fractionation were incubated with 0–100 μg/ml of Papain (Roche) and 0.8 mM DTT in a final volume of 50 μl PBS for 15 minutes at room temperature (22°C). The digestion was stopped by adding 5 mM E-64 (Roche) for 5 minutes on ice and the sample was centrifuged for 90 min at 4°C and 14,000 rpm. The supernatant was discarded and the pellet was resuspended in Laemmli buffer and incubated for 20 minutes at 37°C. Finally, samples were separated by SDS-PAGE and the proteins were visualized by Western blot.

Data Analysis and Densitometric Quantitation

Protein bands visualized by ECL (Amersham) or by fluorography were quantified in a GS-800 Calibrated Imaging Densitometer using the BioRad Quantity One program with film exposures in the linear range. Non-linear regression fits of experimental transport data were performed using ORIGIN software (Microcal Software, Northampton, MA). The bars represent the S.E.M. of triplicate samples and the representative experiments shown were repeated at least 3 times with comparable results.

Results

To better understand the requirements for the expression of newly synthesized GlyT2 transporters at the plasma membrane, we measured the kinetics of GlyT2 expression in COS7 cells by [^{35}S]methionine/cysteine pulse-chase assays, from which GlyT2 was immunoprecipitated with a specific antibody [33]. According to the presence of *N*-glycans attached to GlyT2 at the cell surface [29], electrophoretic separation of the transporter recovered from cultured cells revealed a protein doublet composed of a glycosylated surface and intracellular forms [29,34]. In our experimental conditions, biosynthesized GlyT2 initially appeared as a 75 kDa metabolic precursor with a half-life of about 1 hour, which then gave rise to a 100 kDa mature transporter (Fig. 1A). The 100 kDa mature protein was present at the plasma membrane and could be labeled with the membrane-impermeant reagent NHS-SS-biotin. The biotinylation of this band increased exponentially during the first 2 hours, reaching a plateau at which it remained for more than 20 hours, suggesting a half-life for this mature protein of over 24 hours (Fig. 1B).

We next employed carbohydrate modification to confirm the glycosylation state of the 75 kDa precursor and to determine its location within the secretory pathway (Fig. 1D, E). Complete enzymatic removal of *N*-linked glycans with PNGase F from both the 75 kDa and the 100 kDa forms after pulse-labeling and subsequent immunoprecipitation yielded a 60-kDa band (Fig. 1D). A protein of the same size was obtained from the 2 protein bands upon treatment of the pulse-chased cells with the *N*-glycosylation blocker tunicamycin, indicating that the 60 kDa form corresponds to the deglycosylated protein core (Fig. 1C). In contrast to the

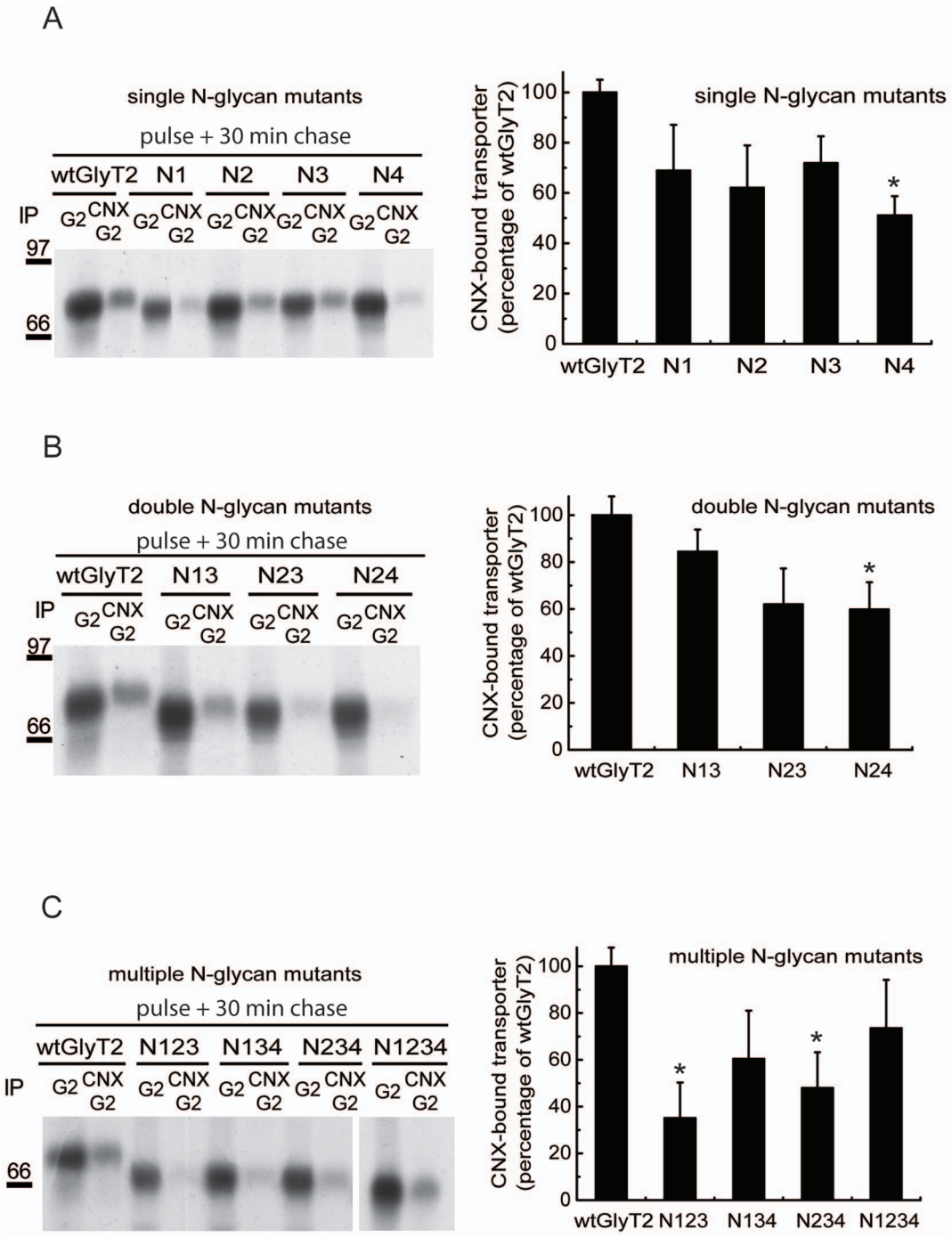

Figure 6. Co-immunoprecipitation of GlyT2 *N*-glycan mutants and CNX. COS7 cells expressing the indicated single (A), double (B) or multiple (C) *N*-glycan mutants were pulse-labeled for 15 min with [^{35}S]methionine/cysteine and chased for 30 min. The cell lysates were immunoprecipitated with GlyT2 antibody or subjected to sequential immunoprecipitation with CNX and GlyT2 antibodies (as described in the Materials and Methods) and analyzed by SDS-PAGE. Right panels: densitometric analysis of the fluorograms (n = 3) showing the percentage of total GlyT2 precursor bound to CNX in each condition (± S.E.M). *$p<0.05$ with respect to wild-type GlyT2 (ANOVA with Tukey's post-hoc test).
doi:10.1371/journal.pone.0063230.g006

mature transporter, which was resistant to endoglycosidase H (EndoH) digestion, the 75 kDa precursor was EndoH-sensitive at all the time points assayed. This is to be expected for a protein transported via the early secretory pathway. The amount of EndoH-digested protein suggests total EndoH sensitivity, although a general decrease in total GlyT2 labeling, probably due to some contaminant protease activity, was also observed (Fig. 1E). Moreover, the transporter was not sensitive to endoglycosidase D at any time points assayed (data not shown). Taken together, these data indicate that the 75 kDa immature form of GlyT2 is likely to be an underglycosylated form located in the ER or *cis* Golgi [35].

The ER is the site at which quality control of the glycoproteins synthesized takes place, with the assistance of molecular chaper-

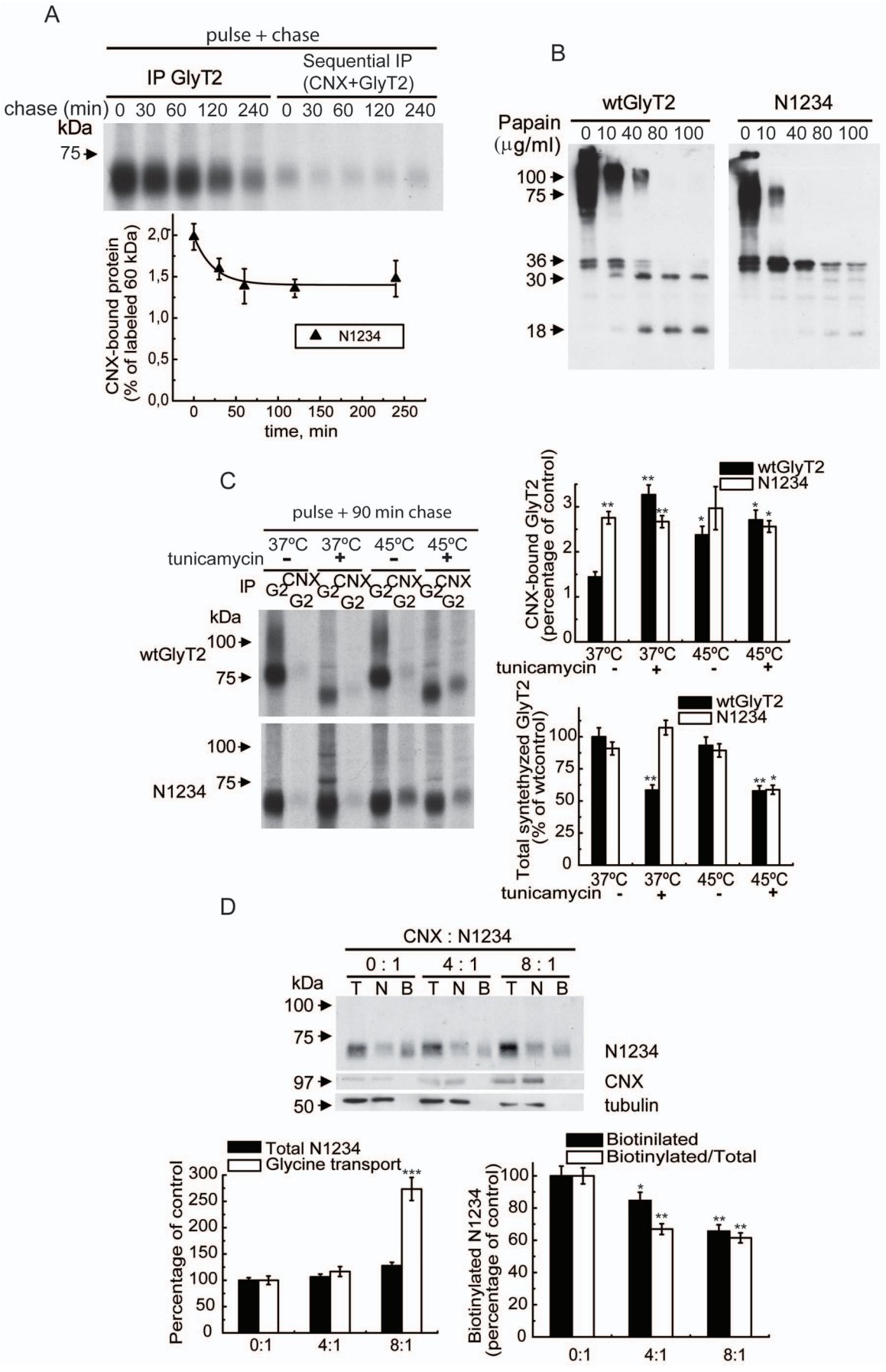
A
pulse + chase
IP GlyT2
Sequential IP (CNX+GlyT2)
chase (min) 0 30 60 120 240 0 30 60 120 240
kDa
75
CNX-bound protein (% of labeled 60 kDa)
N1234
time, min
B
wtGlyT2
N1234
Papain (μg/ml)
0 10 40 80 100
100
75
36
30
18
C
pulse + 90 min chase
37ºC 37ºC 45ºC 45ºC
tunicamycin - + - +
IP G2 CNX G2 CNX G2 CNX G2 CNX G2
kDa
wtGlyT2
N1234
CNX-bound GlyT2 (percentage of control)
Total syntethyzed GlyT2 (% of wtcontrol)
D
CNX : N1234
0 : 1 4 : 1 8 : 1
T N B T N B T N B
N1234
CNX
tubulin
Total N1234
Glycine transport
Percentage of control
0:1 4:1 8:1
Biotinilated
Biotinylated/Total
Biotinylated N1234 (percentage of control)

Figure 7. CNX-binding and folding properties of the *N*-glycan-deficient GlyT2 mutant. (A) COS7 cells expressing the N1234 *N*-glycan-deficient mutant were pulse-labeled for 15 min with [^{35}S]methionine/cysteine and chased for the indicated time. The cell lysates were immunoprecipitated with GlyT2 antibody or subjected to sequential immunoprecipitations with CNX and GlyT2 antibodies as described in the Materials and Methods and resolved by SDS-PAGE. Lower graph: densitometry of the fluorograms (n = 2) showing the percentage of N1234 bound to CNX in each condition (± S.E.M). (B) The membrane enriched fraction from COS7 cells expressing GlyT2 or the N1234 *N*-glycan-deficient mutant (12.5 µg) was digested for 15 min at 22°C with the concentrations of papain indicated as described in the Materials and Methods and analyzed in Western blots probed with antibodies against the GlyT2 N-terminus. (C) COS7 cells expressing wild-type GlyT2 or the N1234 mutant were treated with the vehicle alone (-) or 10 µg/ml tunicamycin (+) for 3 h at 37°C, pulse-labeled for 15 min with [^{35}S]methionine/cysteine and then chased for 90 min at the temperature indicated. The cell lysates were immunoprecipitated with GlyT2 antibody or subjected to sequential immunoprecipitation with CNX and GlyT2 antibodies as described in the Materials and Methods and resolved by SDS-PAGE. Right panels: densitometry of the fluorograms (n = 3) showing the percentage of total GlyT2 precursor bound to CNX in each condition (up) and the total synthesized transporter (down). Bars represent the S.E.M. (n = 3). *$p<0.05$, **$p<0.01$ with respect to wild-type control (Student's t-test). (D) The experimental conditions applied were as described in Figure 3B except that cells expressed the N1234 mutant and CNX overexpression was achieved by co-expressing CNX and N1234 at ratios of 0:1, 4:1 and 8:1. *$p<0.05$, **$p<0.01$, ***$p<0.001$ with respect to the wild-type control (Student's t-test).
doi:10.1371/journal.pone.0063230.g007

ones such as calnexin (CNX) [36]. The 75 kDa GlyT2 precursor co-immunoprecipitated with an antibody against CNX and its immunodetection in Western blots was prevented by antigen preadsorption with an excess of the GlyT2 fusion protein (GlyT2-GST) previously used to generate the GlyT2 antibody [33]. These observations confirmed the immunoprecipitated 75 kDa band to be the transporter precursor (Fig. 2A). The co-immunoprecipitation of GlyT2 and CNX also occurred in primary neurons in which GlyT2 appeared as a lower molecular weight band that overlapped with that of the precursor (Fig. 2B). However, GlyT2 did not immunoprecipitate with calreticulin in any of the conditions assayed (Fig. 2A). We next measured the kinetics of the GlyT2-CNX interaction by performing sequential immunoprecipitation of GlyT2-expressing pulse-chased COS7 cells using CNX and GlyT2 antibodies (Fig. 2C). The 75 kDa precursor transiently associated with CNX to form a complex with a half-life of about 60 min, which agreed with the onset of the expression of the 100 kDa mature transporter, suggesting that CNX facilitates GlyT2 biogenesis. The CNX-bound GlyT2 was deglycosylated by PNGaseF, it was sensitive to Endo H and was Endo D resistant, as expected of the GlyT2 precursor present in the ER or *cis* Golgi (not shown). In agreement with a facilitatory role of CNX in GlyT2 biogenesis, total expression of the transporter was sensitive to the expression of the chaperone (Fig. 3). Knockdown of CNX in COS7 cells using a specific RNAi reduced the total transporter expression (as evident in Western blots) and decreased glycine transport activity in a dose-dependent manner (Fig. 3A), indicating that the low levels of remaining CNX limit GlyT2 synthesis. Consequently, accumulation of the mature form of the transporter was observed, resulting in a progressive increase in the mature (100 kDa)/immature (75 kDa) ratio in steady state conditions. This increase is not due to a differential recognition of the immature protein by the used GlyT2 antibody, since the same result was obtained with an antibody against the C-terminus of GlyT2 (Fig. 3A and Fig. S1). Conversely, with an optimized co-transfection protocol in COS7 cells we found that CNX over-expression dramatically increased total GlyT2 expression and glycine transport. Furthermore, in agreement with the increased number of binding sites for the GlyT2 precursor following CNX overexpression, we also detected an increased proportion of immature transporter (Fig. 3B). Together, these results confirm that GlyT2 biosynthesis is assisted by CNX.

We previously demonstrated that GlyT2 contains 4 *N*-glycan chains attached to asparagines 345, 355, 360 and 366 in the mature protein [29]. As a monovalent lectin, CNX has affinity for monoglucosylated intermediaries but it can also associate via protein-protein interactions [27,28]. We constructed various mutants with deficiencies in single or multiple *N*-glycan acceptor sites by substituting the asparagines 345, 355, 360 or 366 with aspartates [29]. The single (N1, N2, N3 and N4) and double (N13, N23, N24) mutants maintained a wild-type-like time course of expression in [^{35}S] pulse-chased COS7 cells (data not shown). The onset of the appearance of the glycosylated protein in the singly glycosylated triple mutants (N123, N134, N234) could not be accurately determined in pulse-chased cells due to the small size of the mature transporter close to the [^{35}S]labeled immature precursor. However, we observed a decrease in the amount of biotinylated plasma membrane transporter (Fig. 4A–C) that paralleled transporter activity (Fig. 4D,E). The Vmax of glycine transport diminished progressively and the Km increased markedly, reaching levels in the fully deglycosylated mutant (N1234) that were 5-fold higher than those of the wild-type GlyT2. This increase in Km was also observed when *N*-glycosylation mutants were generated by replacing the asparagines with glutamines rather than aspartates (data not shown), indicating that the sugar rather than the charge removal caused the increase in Km. One important exception in this series of mutants was the N4 mutant (N366). Although its time course of expression was comparable with that of the wild-type, this mutant exhibited slightly slower mature protein synthesis (Fig. S2), reduced levels of total biotinylated surface transporter (Fig. 4A,B), an increased proportion of glycosylated versus total transporter (Fig. 4C), a lower Vmax (Fig. 4D) and a higher Km than the other related mutants (Fig. 4E). In addition, the glycosylated N4 band was of a lower apparent weight than N2 and N3 (Fig. 4A), suggesting that either the *N*-glycans attached to N366 have a greater molecular mass or that their removal affects GlyT2 folding. We hypothesized that some of the features displayed by the N4 mutant were sustained by reduced binding to CNX (see below). We therefore further investigated the factors that influence GlyT2 binding to the chaperone.

Glucosidases I and II (GI and GII) give rise to monoglucosylated CNX substrates [37]. Treatment of GlyT2-expressing COS cells with the glucosidase inhibitors castanospermine and deoxynojirimycin resulted in a partial but consistent reduction in the levels of CNX-bound transporter recovered by sequential immunoprecipitations (Fig. 5A). CNX binding was also sensitive to low concentrations of tunicamycin, an inhibitor of *N*-glycosylation. Moreover, glucosidase inhibition impaired glycine transport activity (Fig. 5B) as a consequence of decreased transporter maturation (Fig. 5C). By contrast, mannosidase inhibition did not reduce the amount of CNX-bound GlyT2, although it fully prevented the generation of the mature 100 kDa transporter (Fig. 5D,E). The latter observation was expected as mannose trimming is not required for the generation of CNX substrates but it is necessary for the further processing of glycans in the Golgi [28]. The increased specificity and membrane permeability of mannosidase versus glucosidase inhibitors may explain the greater efficiency of the former in preventing the expression of the mature transporter [38]. The loss of sugar following mutagenesis also

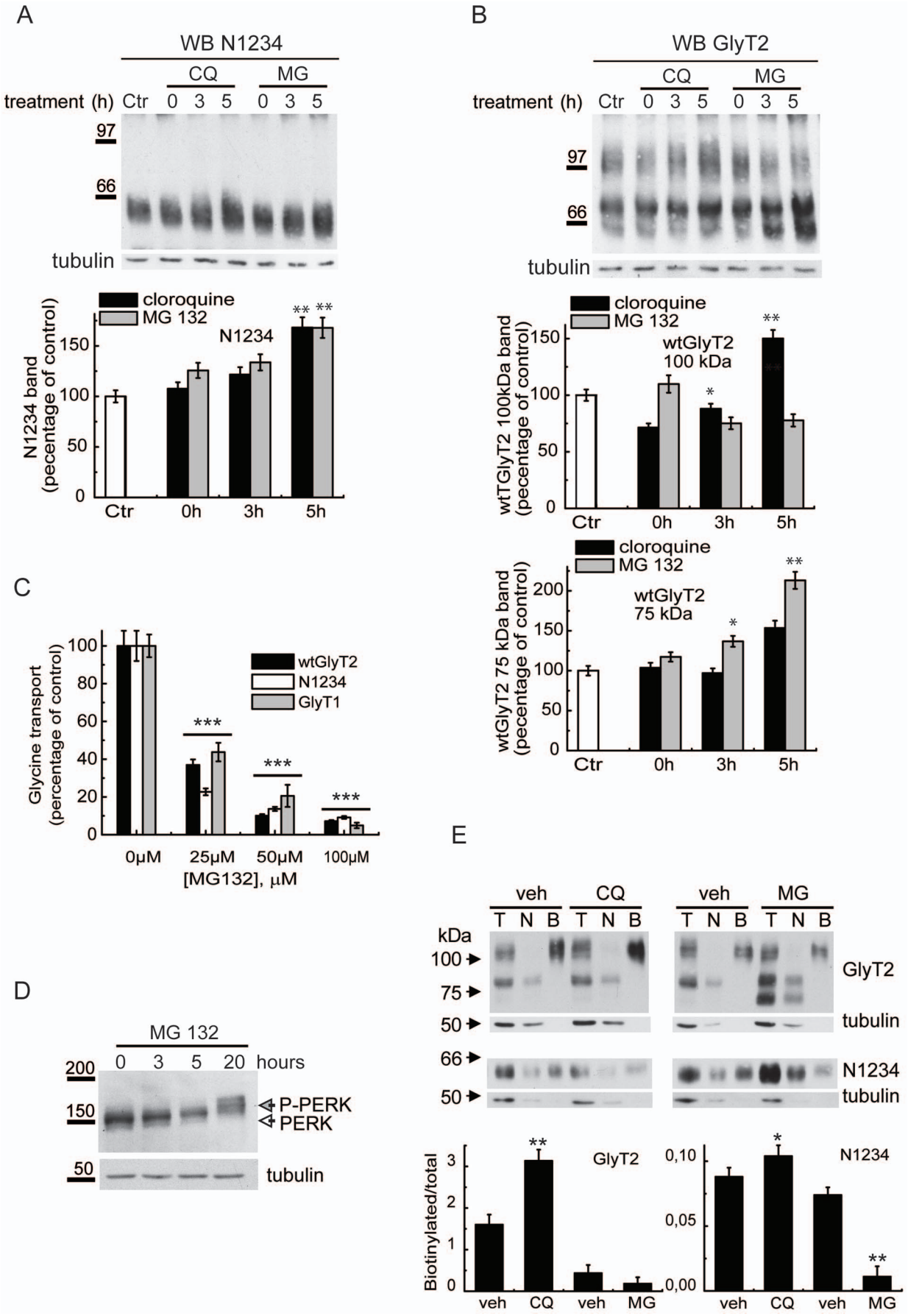
A
WB N1234
CQ
MG
treatment (h) Ctr 0 3 5 0 3 5
97
66
tubulin
cloroquine
MG 132
N1234
N1234 band (pecentage of control)
Ctr
0h
3h
5h
B
WB GlyT2
wtGlyT2 100 kDa
wtGlyT2 75 kDa
C
Glycine transport (percentage of control)
wtGlyT2
N1234
GlyT1
0μM
25μM
50μM
100μM
[MG132], μM
D
MG 132
0 3 5 20 hours
200
150
50
P-PERK
PERK
tubulin
E
veh
CQ
MG
T N B
kDa
100
75
50
66
GlyT2
N1234
Biotinylated/total
veh
CQ
MG

Figure 8. Degradation of GlyT2. (A,B) COS7 cells expressing the N1234 mutant or wild-type GlyT2 were treated with 0.1 mM chloroquine (CQ), 50 μM MG132 (MG) or the corresponding vehicles (water and DMSO, respectively) for the times indicated, resolved by SDS-PAGE and GlyT2 was analyzed in Western blots. Densitometry (n = 2–4) is shown in the histograms in A and B. *$p<0.05$, **$p<0.01$ with respect to control at the corresponding time points (Student's t-test). (C) COS7 cells expressing wtGlyT2, N1234 or a control protein (GlyT1) were treated with vehicle or MG132 for 16 h at the concentrations indicated and glycine transport was then assayed in the cells. Bars represent the S.E.M. (n = 3). ***$p<0.001$ with respect to control (Student's t-test). (D) COS cells were treated with vehicle or 5 μM MG132 for the times indicated and then resolved in SDS-PAGE and PERK was analyzed in Western blots. Tubulin immunoreactivity was used as a loading control in A, B and D. (E) COS7 cells expressing the N1234 mutant or wild-type GlyT2 were treated for 5 hours with 0.1 mM chloroquine (CQ), 50 μM MG132 (MG) or the corresponding vehicle solutions (water and DMSO, respectively), biotinylated and GlyT2 was analyzed in Western blots. *$p<0.05$ with respect to wild-type control (Student's t-test).
doi:10.1371/journal.pone.0063230.g008

hampered the interaction with CNX measured after a 15-min pulse and a 30-min chase. However, these experiments revealed no correlation between glycan removal and CNX binding. Indeed, depending on the single or multiple *N*-glycan-deficient mutant chosen, 60–80% of the CNX binding observed in the wild-type was obtained (Fig. 6A,B). Moreover, the removal of 3 or 4 *N*-glycosylation sites did not further impair CNX interaction. In fact, a considerable amount of *N*-glycosylation-deficient GlyT2 mutant was bound to CNX and recovered by sequential immunoprecipitation (Fig. 6C), suggesting that the association of GlyT2 with CNX is mediated by interactions involving both sugars and polypeptides. Accordingly, the reduced CNX binding exhibited by the N4 mutant was possibly due to the involvement of N366 in CNX binding or to an alteration in the conformation of GlyT2 following *N*-glycan removal.

The behavior of the N1234 mutant, which lacks *N*-glycan acceptor sites, provided further evidence of the involvement of protein-protein interactions in GlyT2 binding to CNX (Figs. 4 and 7). In contrast to wtGlyT2, which associated transiently with CNX (Fig. 2C), the mutant engaged in a more persistent interaction with the chaperone, as revealed by sequential immunoprecipitation of pulse-chased cells with CNX and GlyT2 antibodies (Fig. 7A). This finding was consistent with the reduced surface expression and V_{max} of glycine transport shown by this mutant (Fig. 4A,B,D), and suggests that the unglycosylated transporter does not easily pass CNX quality control, an ER check point for newly synthesized glycoproteins [39]. This longer lasting binding may reflect an alteration to the 3-dimensional structure of the mutant that is detected by CNX. Indeed, the mutant displayed increased proteolytic sensitivity in a limited proteolysis experiment using the wild-type and N1234 mutant and increasing concentrations of papain, such that low molecular weight proteolytic fragments (36, 34, 30 and 18 kDa) that could be detected with an antibody against the N-terminal region of GlyT2 were produced at different protease concentrations (Fig. 7B). This may be indicative of misfolding in the mutant, although glycan-mediated protection from proteolysis is also possible.

As well as inhibiting *N*-glycosylation, tunicamycin may also trigger the unfolded protein response (UPR) and therefore act as a misfolding agent when used at high concentrations or long incubation times [40]. Hence, we performed pulse-chase experiments in the presence of this inhibitor with longer chase times (90 min) and at different temperatures (Fig. 7C). In the presence of high concentrations of tunicamycin, the association of wild-type GlyT2 to CNX was enhanced at 37°C and to a much lesser extent at 45°C, suggesting that this association is enhanced by tunicamycin-induced unfolding. The effect of tunicamycin was less evident at 45°C as both tunicamycin and high temperature treatment trigger general unfolding (Fig. 7C, upper histogram). By contrast, the N1234 mutant displayed greater CNX binding in all the conditions assayed, and its association to CNX was insensitive to tunicamycin or the increase in temperature. The same pattern was observed in assays using thapsigargin, another inducer of UPR (data not shown). Moreover, the total amount of wild-type transporter synthesized at 37°C was reduced in the presence of tunicamycin, while that of the mutant was tunicamycin-insensitive. As expected, there was a general reduction in total protein synthesis at 45°C (Fig. 7C, lower histogram). These results strongly suggest that the 3-dimensional structure of the N1234 mutant lacking sugar chains is altered, consistent with its proteolytic pattern and with the dramatic increase in the K_m for glycine transport shown by this mutant (Fig. 7B and 4E).

To determine whether CNX can act as a *bona-fide* chaperone independently of its lectin activity, we investigated the effect of CNX overexpression in cells expressing the N1234 mutant using the experimental conditions shown in Fig. 3B for wtGlyT2 (Fig. 7D). In agreement with the effect of CNX on the wild-type GlyT2, total expression of the mutant and its glycine transport were enhanced by CNX overexpression, albeit to a lesser extent (Fig. 7D, left histogram). Conversely, surface expression of the mutant transporter was reduced by overexpressing the chaperone (Fig. 7D, right histogram), suggesting that it was more efficiently folded although less of the mutant transporter reached the plasma membrane. These findings suggest that CNX can discriminate between different conformational states in a glycan-independent manner and select the most functionally competent structure required.

The long-term binding of the glycosylation-deficient mutant to CNX suggests that it fails to progress past a quality control check point. This may result in the transporter being sent for proteasomal degradation, the ultimate fate of deficiently-folded membrane proteins [41–43], or it may be resolved by correct folding and subsequent progression through the secretory pathway. Treatment of N1234-expressing COS7 cells with the lysosome inhibitor chloroquine, or with high concentrations of the proteasome inhibitors MG132 and lactacystin (data not shown), resulted in comparable increases in the amount of mutant transporter (Fig. 8A). This may indicate that the mutant uses both lysosomal and proteasomal pathways for degradation. However, the same treatments applied to wild-type cells expressing GlyT2 produced opposite effects: while treatment with the lysosome inhibitor chloroquine augmented the mature (100 kDa) transporter, proteasome inhibition reduced the amount of mature transporter (Fig. 8B). In addition, a band of ~60 kDa visibly augmented in immunoprecipitates from cells treated with proteasome inhibitor. The apparent molecular weight of this band coincided with that of the deglycosylated protein core (Fig. 1), suggesting that it represents an early arrested form of the transporter. This raises the possibility that proteasome inhibition in our experimental conditions induced ER stress and affected general ER protein folding.

To further investigate this possibility we studied the effect of increasing MG132 concentrations on glycine transport by wtGlyT2, the N1234 mutant and a control protein (GlyT1). All 3 transporters were similarly sensitive, suggesting that off-target secondary effects of proteasome inhibition may produce a general folding defect (Fig. 8C). Indeed, the phosphorylated form of protein kinase-like endoplasmic reticulum kinase (PERK), a well-

established ER stress marker that is activated during UPR and that attenuates mRNA translation by phosphorylating eIF2α [44], was already visible when the cells were treated for 3 h with a low concentration of MG132 (5 μM; Fig. 8D). Thus, a clearly involved degradation pathway for both wtGlyT2 and the N1234 mutant appears to be the lysosome, as both seem to accumulate in the presence of lysosome inhibitors (Fig. 8E). However, this effect was more evident for the wild-type especially over longer chase times (Fig. S3), leading us to consider a contribution of the proteasome in the degradation of the mutant.

Discussion

According to the validated LeuTAa homology model for the SLC6 family of sodium- and chloride-dependent transporters, the plasma membrane GlyT2 has 12 transmembrane domains (TM) oriented such that TMs 1–5 are positioned in an antiparallel conformation relative to TMs 6–10 [13–15]. While resolving the crystal structure of the prokaryote transporter has furthered our understanding of the underlying protein structure significantly, the biosynthesis of polytopic plasma membrane proteins like GlyT2 and the role of the *N*-glycans attached to its EL2 remain poorly understood. Nascent GlyT2 is translocated to the lumen of the ER and oligosaccharide moieties are co-translationally attached to 4 EL2 asparagines in *N*-glycosylation consensus sequences (N345, N355, N360 and N366) [29]. CNX/CRT retains glycoproteins in the ER by re-binding to the lectin site until a folded conformation of the substrate is achieved. Properly folded glycoproteins are incorporated into transport vesicles and exported to the Golgi, while terminally misfolded glycoproteins that persist in CNX/CRT cycles are targeted for degradation by the ER-associated degradation (ERAD) pathway [28,36].

Our electrophoretic analysis of GlyT2-expressing cells revealed a 75 kDa precursor that disappeared as the chase times following [^{35}S]-labeling increase. This protein represents the ER precursor that has received the initial 14-sugar chain from dolichol and carbohydrate removal with PNGase F or tunicamycin yielded a 60 kDa protein core. This is smaller in size than the protein predicted by summing the molecular weights of the individual amino acid residues (78.9 kD), although packing of the protein fraction may account for this weight difference, as previously described for other related transporters [45]. At longer chase times, the fully glycosylated transporter appeared as a 100 kDa diffuse band, which may contain a mixture of glycosylated species in different states of trimming. We investigated several aspects of GlyT2 biogenesis in which CNX plays a facilitatory role. By performing sequential immunoprecipitation with CNX followed by GlyT2 antibodies, we captured the pulse-labeled 75 kDa CNX-bound precursor in the ER. The CNX-bound precursor reached maximal levels immediately after the pulse, before the appearance of the mature 100 kDa transporter, and then decayed to basal levels. As expected for CNX-assisted biogenesis, GlyT2 was very sensitive to CNX concentrations, and siRNA-mediated CNX knockdown in GlyT2-expressing cells reduced membrane expression and transport function by limiting the amount of the available precursor. These results are in good agreement with the phenotype of CNX knockout mice, which die after 4 weeks due to the inability of CRT to fully substitute CNX activity [46]. We detected no GlyT2 binding to CRT in any of the conditions assayed, which included a range of different detergents and chase times. On the other hand, optimizing the co-transfection protocol to use low levels of transfected cDNA and prevent competition for the cell translation machinery, we demonstrated that the access of GlyT2 to the membrane was facilitated dramatically following CNX overexpression. CNX made possible the maturation of a greater proportion of immature transporter and increased levels of transporter at the cell surface and thus transport activity. These results are in good agreement with earlier studies of other SLC6 transporters [47], and strongly support the role of CNX as a chaperone in GlyT2 biogenesis.

GlyT2 binding to CNX is mediated by glycans and protein-protein interactions, as revealed by disruption of transporter binding with pharmacological treatments and through the behavior of GlyT2 mutants lacking *N*-glycan acceptor sites. GlyT2 binding to CNX is sensitive to GI and GII inhibitors. Deoxinojirimycin is a more potent GII inhibitor than castanospermine, yet the latter inhibits the activity of both GI and GII [48,49]. The differential effect of these inhibitors on GlyT2 biosynthesis may be linked to the crucial role of GI in rapid glucose trimming after glycan addition or the modulation of GII activity by neighboring *N*-glycans, which may attenuate the inhibition of GlyT2 [36,37]. However, the cell permeability of both these compounds is poor, and although IC_{50} values in the low micromolar range have been measured in cell-free systems, these values increase by several orders of magnitude in cell cultures [38]. This may explain why these glucosidase inhibitors exhibited variable effects and why high concentrations were required to prevent GlyT2 maturation. However, even using concentrations in the high mM range, we were unable to fully prevent GlyT2 binding to CNX, indicating that CNX binding requires polypeptide- as well as lectin-based interactions [36,39].

The binding of GlyT2 to CNX was also sensitive to the removal of single or multiple *N*-glycan sites, although it increased most when all *N*-glycan binding sites were removed. This is consistent with the hypothesis that initial binding to calnexin requires monoglucosylated *N*-linked oligosaccharides until the mature protein conformation is achieved, although the retention of bound proteins is not mediated by the glycans but by polypeptide motifs [50,51]. Furthermore, for GII to generate the monoglucosylated oligosaccharide in mammalian cells, at least 2 oligosaccharide chains on the substrate glycoprotein are required [37]. The removal of multiple glycosylation sites may alter the protein conformation and unmask unfolded peptide regions that are detected by CNX, thereby increasing binding. This may be due to a chaperone-independent pro-folding effect of *N*-glycosylation, as reported for the cystic fibrosis transmembrane regulator [52]. We previously demonstrated that PNGase F treatment of the purified and reconstituted GlyT2 impairs glycine transport, probably due to the anomalous conformation of the deglycosylated protein [29]. In the present study we show that the GlyT2 N1234 mutant, which lacks all 4 *N*-glycan acceptor sites, exhibits anomalous folding as revealed by differential papain and pronase (not shown) proteolysis patterns. Accordingly, this mutant displays deficient glycine transport in functional assays, as revealed by a low Vmax and high Km. Moreover, membrane expression of the mutant was significantly impaired, while its binding to CNX was increased, long-lasting and temperature-independent. The glycan bound to N366 may crucially contribute to the N1234 phenotype, as the phenotype of the N4 mutant (which lacks the N366-linked glycan) shares several features with that of the N1234 mutant. The present findings point to a lectin-independent chaperone activity of CNX on GlyT2, as inferred by its interaction with the N1234 mutant. Co-expression of CNX and N1234 rescued the mutant activity, although not the surface transporter, suggesting that CNX selectively facilitates the surface expression of the more competent conformational state in a glycan-independent manner.

The final degradation of GlyT2 and the N1234 mutant transporter occurs via the lysosomal pathway. The greater increase

in the amount of mature transporter observed for the wild type in the presence of lysosomal inhibitors may indicate the existence of more than one degradation pathway for the mutant. However, given the side effects produced by proteasome inhibition, it remains unclear whether the mutant is more prone to proteasomal degradation. In summary, we describe some of the processes involved in GlyT2 biogenesis in the early secretory pathway, including CNX assistance and binding interactions, and we reveal a key role for CNX in the selection of functionally-competent GlyT2 folding intermediates. In the light of this framework, it may now be possible to decipher the effects of hyperekplexia mutations on the plasma membrane expression of newly synthesized GlyT2 transporters.

Supporting Information

Figure S1 GlyT2 immunodetection with antibodies against N-terminal and C-terminal epitopes. COS7 cells expressing wt-GlyT2 or GlyT2 N-terminal (ΔN-GlyT2) or C-terminal (ΔC-GlyT2) deletion mutants were lysed and subjected to Western blot with antibodies against GlyT2 N-terminus (Nt-GlyT2 Ab) or C-terminus (Ct-GlyT2 Ab). ΔC-GlyT2 mutant lacks last 53 amino acids in the GlyT2 C-terminus. ΔN-GlyT2 mutant lacks first 140 N-terminal amino acids of GlyT2 (Poyatos et al., 2000 Molecular and Cellular Neuroscience 15, 99–111). Tubulin immunoreactivity was used as a loading control.
(TIF)

Figure S2 Time course of expression of N4 mutant. COS7 cells expressing wtGLYT2 or the N366D (N4) mutant were pulse-labeled for 15 min with [^{35}S]methionine/cysteine, chased for the indicated times, immunoprecipitated with GlyT2 antibody and resolved in SDS-PAGE. (A) Kinetics of expression of total synthesized protein. (B) Densitometric analysis of the fluorographies representing labeled bands as a percentage of total synthesized protein.
(TIF)

Figure S3 Long term lysosomal degradation of GlyT2. COS7 cells expressing GlyT2 were treated with vehicle or 0.1 mM chloroquine (CQ) during 1 h and then pulse-labeled for 15 min with [^{35}S]methionine/cysteine, chased for the indicated times in the absence or presence of the inhibitor, immunoprecipitated with GlyT2 antibody and resolved in SDS-PAGE. Histograms: densitometric analysis of the fluorographies (n = 2–4). Significantly different from the control at the corresponding chase time: *$p<0.05$ and **$p<0.01$ in Student's t-test.
(TIF)

Acknowledgments

The authors thank Enrique Núñez for expert technical assistance, Jaime de Juan-Sanz for helpful comments and Professor Francisco Zafra (Centro de Biología Molecular Severo Ochoa, Madrid) for assistance with siRNA synthesis.

Author Contributions

Conceived and designed the experiments: BLC. Performed the experiments: EAG PAT. Analyzed the data: EAG PAT CA BLC. Contributed reagents/materials/analysis tools: CA. Wrote the paper: BLC.

References

1. Lynch JW (2004) Molecular structure and function of the glycine receptor chloride channel. Physiol Rev 84 (4): 1051–1095.
2. Legendre P (2001) The glycinergic inhibitory synapse. Cell Mol Life Sci 58 (5–6): 760–793.
3. Harvey RJ, Depner UB, Wassle H, Ahmadi S, Heindl C, et al. (2004) GlyR alpha3: an essential target for spinal PGE2-mediated inflammatory pain sensitization. Science 304 (5672): 884–887.
4. Aragón C, López-Corcuera B (2003) Structure, function and regulation of glycine neurotransporters. Eur J Pharmacol 479 (1–3): 249–262.
5. Gomeza J, Hulsmann S, Ohno K, Eulenburg V, Szoke K, et al. (2003) Inactivation of the glycine transporter 1 gene discloses vital role of glial glycine uptake in glycinergic inhibition. Neuron 40 (4): 785–796.
6. Gomeza J, Ohno K, Hulsmann S, Armsen W, Eulenburg V, et al. (2003) Deletion of the mouse glycine transporter 2 results in a hyperekplexia phenotype and postnatal lethality. Neuron 40 (4): 797–806.
7. Aragón C, López-Corcuera B (2005) Glycine transporters: crucial roles of pharmacological interest revealed by gene deletion. Trends Pharmacol Sci 26 (6): 283–286.
8. McIntire SL, Reimer RJ, Schuske K, Edwards RH, Jorgensen EM (1997) Identification and characterization of the vesicular GABA transporter. Nature 389 (6653): 870–876.
9. Rousseau F, Aubrey KR, Supplisson S (2008) The glycine transporter GlyT2 controls the dynamics of synaptic vesicle refilling in inhibitory spinal cord neurons. J Neurosci 28 (39): 9755–9768.
10. Suhren O, Bruyn G, Tynman J (1966) Hyperekplexia. A hereditary startle syndrome. J Neurol Sci 3: 577–605.
11. Chung SK, Vanbellinghen JF, Mullins JG, Robinson A, Hantke J, et al. (2010) Pathophysiological mechanisms of dominant and recessive GLRA1 mutations in hyperekplexia. J Neurosci 30 (28): 9612–9620.
12. Harvey RJ, Topf M, Harvey K, Rees MI (2008) The genetics of hyperekplexia: more than startle! Trends Genet 24 (9): 439–447.
13. Pérez-Siles G, Morreale A, Leo-Macias A, Pita G, Ortiz AR, et al. (2011) Molecular basis of the differential interaction with lithium of glycine transporters GLYT1 and GLYT2. J Neurochem 118 (2): 195–204.
14. Pérez-Siles G, Núñez E, Morreale A, Jiménez E, Leo-Macías A, et al. (2012) An aspartate residue in the external vestibule of GLYT2 (glycine transporter 2) controls cation access and transport coupling. Biochem J 442 (2): 323–334.
15. Yamashita A, Singh SK, Kawate T, Jin Y, Gouaux E (2005) Crystal structure of a bacterial homologue of Na+/Cl–dependent neurotransmitter transporters. Nature 437 (7056): 215–223.
16. Rees MI, Harvey K, Pearce BR, Chung SK, Duguid IC, et al. (2006) Mutations in the gene encoding GlyT2 (SLC6A5) define a presynaptic component of human startle disease. Nat Genet 38 (7): 801–806.
17. Eulenburg V, Becker K, Gomeza J, Schmitt B, Becker CM, et al. (2006) Mutations within the human GLYT2 (SLC6A5) gene associated with hyperekplexia. Biochem Biophys Res Commun 348 (2): 400–405.
18. Giménez C, Pérez-Siles G, Martinez-Villarreal J, Arribas-González E, Jiménez E, et al. (2012) A Novel Dominant Hyperekplexia Mutation Y705C Alters Trafficking and Biochemical Properties of the Presynaptic Glycine Transporter GlyT2. J Biol Chem 287 (34): 28986–29002.
19. Carta E, Chung SK, James VM, Robinson A, Gill JL, et al. (2012) Mutations in the GlyT2 Gene (SLC6A5) Are a Second Major Cause of Startle Disease. J Biol Chem 287 (34): 28975–28985.
20. Núñez E, Pérez-Siles G, Rodenstein L, Alonso-Torres P, Zafra F, et al. (2009) Subcellular localization of the neuronal glycine transporter GLYT2 in brainstem. Traffic 10 (7): 829–843.
21. de Juan-Sanz J, Zafra F, López-Corcuera B, Aragón C (2011) Endocytosis of the neuronal glycine transporter GLYT2 is clathrin and ubiquitin mediated from different cell surface subdomains. Traffic 12: 1850–1867.
22. Núñez E, Alonso-Torres P, Fornés A, Aragón C, López-Corcuera B (2008) The neuronal glycine transporter GLYT2 associates with membrane rafts: functional modulation by lipid environment. J Neurochem 105: 2080–2090.
23. Walter P, Johnson AE (1994) Signal sequence recognition and protein targeting to the endoplasmic reticulum membrane. Annu Rev Cell Biol 10: 87–119.
24. Hebert DN, Molinari M (2007) In and out of the ER: protein folding, quality control, degradation, and related human diseases. Physiol Rev 87 (4): 1377–1408.
25. Parodi AJ (2000) Protein glucosylation and its role in protein folding. Annu Rev Biochem 69: 69–93.
26. Schrag JD, Bergeron JJ, Li Y, Borisova S, Hahn M, et al. (2001) The Structure of calnexin, an ER chaperone involved in quality control of protein folding. Mol Cell 8 (3): 633–644.
27. Brockmeier A, Williams DB (2006) Potent lectin-independent chaperone function of calnexin under conditions prevalent within the lumen of the endoplasmic reticulum. Biochemistry 45 (42): 12906–12916.
28. Lederkremer GZ (2009) Glycoprotein folding, quality control and ER-associated degradation. Curr Opin Struct Biol 19 (5): 515–523.
29. Martinez-Maza R, Poyatos I, López-Corcuera B, Núñez E, Giménez C, et al. (2001) The role of N-glycosylation in transport to the plasma membrane and sorting of the neuronal glycine transporter GLYT2. J Biol Chem 276 (3): 2168–2173.

30. Bartholomaus I, Milan-Lobo L, Nicke A, Dutertre S, Hastrup H, et al. (2008) Glycine transporter dimers: evidence for occurrence in the plasma membrane. J Biol Chem 283 (16): 10978–10991.
31. López-Corcuera B, Núñez E, Martínez-Maza R, Geerlings A, Aragón C (2001) Substrate-induced conformational changes of extracellular loop 1 in the glycine transporter GLYT2. J Biol Chem 276 (46): 43463–43470.
32. Jiménez E, Zafra F, Pérez-Sen R, Delicado EG, Miras-Portugal MT, et al. (2011) P2Y purinergic regulation of the glycine neurotransmitter transporters. J Biol Chem 286 10712–10724.
33. Zafra F, Gomeza J, Olivares L, Aragón C, Giménez C (1995) Regional distribution and developmental variation of the glycine transporters GLYT1 and GLYT2 in the rat CNS. Eur J Neurosci 7 (6): 1342–1352.
34. López-Corcuera B, Martínez-Maza R, Núñez E, Roux M, Supplisson S, et al. (1998) Differential properties of two stably expressed brain-specific glycine transporters. J Neurochem 71 (5): 2211–2219.
35. Freeze H, HaK C (2010) Endoglycosidase and Glycoamidase Release of N-Linked Glycans. Current Protocols in Immunology. Wiley Interscience. John Wiley & Sons, Inc.
36. Rutkevich LA, Williams DB (2011) Participation of lectin chaperones and thiol oxidoreductases in protein folding within the endoplasmic reticulum. Curr Opin Cell Biol 23 (2): 157–166.
37. Deprez P, Gautschi M, Helenius A (2005) More than one glycan is needed for ER glucosidase II to allow entry of glycoproteins into the calnexin/calreticulin cycle. Mol Cell 19 (2): 183–195.
38. Compain P, Martin OR (2007) Iminosugars: From synthesis to therapeutic applications. John Wiley and Sons Ltd, Chichester, West Sussex, England.
39. Korkhov VM, Milan-Lobo L, Zuber B, Farhan H, Schmid JA, et al. (2008) Peptide-based interactions with calnexin target misassembled membrane proteins into endoplasmic reticulum-derived multilamellar bodies. J Mol Biol 378 (2): 337–352.
40. Kaufman RJ (1999) Stress signaling from the lumen of the endoplasmic reticulum: coordination of gene transcriptional and translational controls. Genes Dev 13 (10): 1211–1233.
41. Morello JP, Salahpour A, Petaja-Repo UE, Laperriere A, Lonergan M, et al. (2001) Association of calnexin with wild type and mutant AVPR2 that causes nephrogenic diabetes insipidus. Biochemistry 40 (23): 6766–6775.
42. Esapa CT, McIlhinney RA, Blake DJ (2005) Fukutin-related protein mutations that cause congenital muscular dystrophy result in ER-retention of the mutant protein in cultured cells. Hum Mol Genet 14 (2): 295–305.
43. Molinari M, Calanca V, Galli C, Lucca P, Paganetti P (2003) Role of EDEM in the release of misfolded glycoproteins from the calnexin cycle. Science 299 (5611): 1397–1400.
44. Yan W, Frank CL, Korth MJ, Sopher BL, Novoa I, et al. (2002) Control of PERK eIF2alpha kinase activity by the endoplasmic reticulum stress-induced molecular chaperone P58IPK. Proc Natl Acad Sci U S A 99 (25): 15920–15925.
45. Olivares L, Aragón C, Giménez C, Zafra F (1994) Carboxyl terminus of the glycine transporter GLYT1 is necessary for correct processing of the protein. J Biol Chem 269 (45): 28400–28404.
46. Denzel A, Molinari M, Trigueros C, Martin JE, Velmurgan S, et al. (2002) Early postnatal death and motor disorders in mice congenitally deficient in calnexin expression. Mol Cell Biol 22 (21): 7398–7404.
47. Tate CG, Whiteley E, Betenbaugh MJ (1999) Molecular chaperones improve functional expression of the serotonin (5-hydroxytryptamine) transporter in insect cells. Biochem Soc Trans 27 (6): 932–936.
48. Kaushal GP, Pastuszak I, Hatanaka K, Elbein AD (1990) Purification to homogeneity and properties of glucosidase II from mung bean seedlings and suspension-cultured soybean cells. J Biol Chem 265 (27): 16271–16279.
49. Elbein AD, Tropea JE, Mitchell M, Kaushal GP (1990) Kifunensine, a potent inhibitor of the glycoprotein processing mannosidase I. J Biol Chem 265 (26): 15599–15605.
50. Hammond C, Braakman I, Helenius A (1994) Role of N-linked oligosaccharide recognition, glucose trimming, and calnexin in glycoprotein folding and quality control. Proc Natl Acad Sci U S A 91 (3): 913–917.
51. Solda T, Galli C, Kaufman RJ, Molinari M (2007) Substrate-specific requirements for UGT1-dependent release from calnexin. Mol Cell 27 (2): 238–249.
52. Glozman R, Okiyoneda T, Mulvihill CM, Rini JM, Barriere H, et al. (2009) N-glycans are direct determinants of CFTR folding and stability in secretory and endocytic membrane traffic. J Cell Biol 184 (6): 847–862.

Artículo #2

Arribas-González E, de Juan-Sanz J, Aragón C, López-Corcuera B (2015)

Molecular basis of the dominant negative effect of a glycine transporter 2 mutation associated with hyperekplexia.

J Biol Chem 290(4):2150-65

THE JOURNAL OF BIOLOGICAL CHEMISTRY VOL. 290, NO. 4, pp. 2150–2165, January 23, 2015

Molecular Basis of the Dominant Negative Effect of a Glycine Transporter 2 Mutation Associated with Hyperekplexia*

Received for publication, June 6, 2014, and in revised form, December 4, 2014 Published, JBC Papers in Press, December 5, 2014, DOI 10.1074/jbc.M114.587055

Esther Arribas-González[‡§], **Jaime de Juan-Sanz**[‡§¶1], **Carmen Aragón**[‡§¶], **and Beatriz López-Corcuera**[‡§¶2]

From the [‡]*Departamento de Biología Molecular and Centro de Biología Molecular "Severo Ochoa," Consejo Superior de Investigaciones Científicas-Universidad Autónoma de Madrid, Madrid 28049, Spain, the* [¶]*Centro de Investigación Biomédica en Red de Enfermedades Raras, Instituto de Salud Carlos III, Madrid 28029, Spain, and the* [§]*IdiPAZ-Hospital Universitario La Paz, Universidad Autónoma de Madrid, Madrid 28046, Spain*

Background: Hyperekplexia is caused by defective glycinergic neurotransmission.
Results: A dominant negative glycine transporter-2 mutant is trapped in a calnexin-bound state and retains wild type GlyT2 in the endoplasmic reticulum.
Conclusion: Chemical chaperones rescue the folding defect of the mutant and overcome its dominant negative effect.
Significance: This opens the way to revert the dominant negative effect exerted by the mutant associated with hyperekplexia in neurons.

Hyperekplexia or startle disease is a rare clinical syndrome characterized by an exaggerated startle in response to trivial tactile or acoustic stimuli. This neurological disorder can have serious consequences in neonates, provoking brain damage and/or sudden death due to apnea episodes and cardiorespiratory failure. Hyperekplexia is caused by defective inhibitory glycinergic neurotransmission. Mutations in the human *SLC6A5* gene encoding the neuronal GlyT2 glycine transporter are responsible for the presynaptic form of the disease. GlyT2 mediates synaptic glycine recycling, which constitutes the main source of releasable transmitter at glycinergic synapses. Although the majority of GlyT2 mutations detected so far are recessive, a dominant negative mutant that affects GlyT2 trafficking does exist. In this study, we explore the properties and structural alterations of the S512R mutation in GlyT2. We analyze its dominant negative effect that retains wild-type GlyT2 in the endoplasmic reticulum (ER), preventing surface expression. We show that the presence of an arginine rather than serine 512 provoked transporter misfolding, enhanced association to the ER-chaperone calnexin, altered association with the coat-protein complex II component Sec24D, and thereby impeded ER exit. The S512R mutant formed oligomers with wild-type GlyT2 causing its retention in the ER. Overexpression of calnexin rescued wild-type GlyT2 from the dominant negative effect of the mutant, increasing the amount of transporter that reached the plasma membrane and dampening the interaction between the wild-type and mutant GlyT2. The ability of chemical chaperones to overcome the dominant negative effect of the disease mutation on the wild-type transporter was demonstrated in heterologous cells and primary neurons.

The extracellular concentration of synaptic glycine is regulated by Na^+-and Cl^--dependent glycine reuptake (1). The neuronal GlyT2 transporter is involved in the removal and recycling of glycine from inhibitory synapses, generating a flux from the synaptic cleft to the presynaptic terminal and supplying substrate to the low affinity vesicular inhibitory amino acid transporter (2, 3). Therefore, the synaptic glycine taken up by GlyT2 is the main source of the releasable transmitter at glycinergic synapses (4, 5). Accordingly, inactivation of the mouse GlyT2 gene generates a complex postnatal neuromotor phenotype that mimics clinical signs of human hyperekplexia (2).

Hyperekplexia or startle disease (OMIM 149400) is a rare neurological disorder characterized by neonatal hypertonia and exaggerated startle responses to trivial but unexpected tactile or acoustic stimuli (6). The most severe consequences of the disease include brain damage and even sudden death from lapses in cardiorespiratory function. Although the majority of patients survive, they may suffer unprotected falls throughout their entire life that could result in injury (7). Startle disease is a glycinergic synaptopathy that disrupts postsynaptic or presynaptic inhibitory glycinergic neurotransmission. The main genes implicated in startle disease are those corresponding to the glycine receptor and related postsynaptic proteins (8, 9), with genetic analyses revealing mutations in the human GlyT2 gene (*SLC6A5*; solute carrier 6A5) to be the most common cause of presynaptic hyperekplexia (10–12) and a very common cause of the disease. The majority of GlyT2 mutations found in hyperekplexia patients are recessive and cause biallelic loss of function due to the absence of the protein from the plasma membrane or to the generation of inactive transporters. Recently, a dominantly inherited mutation affecting the function that also reduces the expression of the transporter at the cell membrane was identified and characterized (13). In addition, one interesting mutation is S512R, the sole dominant negative disease-as-

* This work was supported by Spanish "Ministerio de Economia y Competitividad" Grant SAF2011-28674, by the Centro de Investigación Biomédica en Red de Enfermedades Raras (CIBERER), and by an institutional grant from the "Fundación Ramón Areces."
[1] Present address: Dept. of Biochemistry, Weill Cornell Medical College, New York, NY 10065.
[2] To whom correspondence should be addressed: Dept. de Biología Molecular, Centro de Biología Molecular "Severo Ochoa", Universidad Autónoma de Madrid, 28049 Madrid, Spain. Tel.: 34-91-1964631; Fax: 34-91-1964420; E-mail: blopez@cbm.csic.es.

sociated mutation affecting transporter trafficking. This mutant transporter prevents the wild-type protein from reaching the plasma membrane, although its exact mechanism of action has yet to be fully defined (10).

GlyT2 belongs to the SLC6 solute carrier family of neurotransmitter sodium symporters. This family groups together 12-transmembrane domain transport proteins including the GABA (γ-aminobutyric acid) and monoamine transporters (14, 15). A model of the three-dimensional structure of GlyT2 was recently generated (16) based on the leucine transporter from *Aquifex aeolicus* ($LeuT_{Aa}$), a prokaryotic SLC6 homologue (18). This model provided important clues to explain the effects of selected missense mutations on critical residues involved in Na^+ and glycine binding (8, 10–13). More recently, the crystal structure of a eukaryotic SLC6, the dopamine transporter (DAT)[3] from *Drosophila*, was resolved (19). Among the differences from the prokaryotic model, the presence of a cholesterol binding site is particularly relevant in the context of DAT and GlyT2, which are lipid-raft-associated transporters (20).

During GlyT2 synthesis, the nascent polypeptide is co-translationally translocated to the membrane of the endoplasmic reticulum (ER) (21). Correct folding of the transporter is stabilized by its four *N*-glycan chains, but it also requires an interaction with several ER chaperones (22). For example, calnexin (CNX) transiently binds to an intermediate hypoglycosylated transporter precursor, and it facilitates GlyT2 processing. The binding of GlyT2 to CNX is mediated by glycan- and polypeptide-based interactions, allowing CNX to discriminate between different GlyT2 conformational states through a lectin-independent chaperone activity (23, 24). In addition, oligomer assembly is a prerequisite to export the SLC6 transporters from the ER and for their subsequent delivery to the plasma membrane (25). Accordingly, a model has been proposed in which transporter intermediates are engaged by ER chaperones, and they are delivered to the coatomer protein II (COPII) prior to forming oligomers that can subsequently be exported out of the ER (25, 26). In the present study, we characterize the features and behavior of the dominant negative hyperekplexia mutant in the early secretory pathway. We confirmed its dominant negative effect on the trafficking of wild-type GlyT2 by means of an interaction in common oligomers. We found that this mutant transporter provoked the retention of the wild-type GlyT2 in the ER, an effect that could be reverted by the overexpression of CNX. An excess of this chaperone increased the amount of wild-type transporter that reaches the plasma membrane by preventing the interaction between wild-type and mutant GlyT2. The effect of pharmacological chaperones in the rescue of GlyT2 was analyzed in heterologous cells and transfected cortical neurons.

EXPERIMENTAL PROCEDURES

Cell Growth and Protein Expression—COS7 cells (American Type Culture Collection) were grown at 37 °C and 5% CO_2 in Dulbecco's modified Eagle's medium (DMEM) supplemented with 10% fetal bovine serum. Transient expression was achieved using Neofectin™ (MidAtlantic Biolabs), according to the manufacturer's protocol (24), and the cells were then incubated for 48 h at 37 °C. Reproducible results were obtained with 50–60% confluent cells on 60-mm or 6-well plates, using 5 and 2 μg of total DNA, respectively. In co-transfection experiments, 25% of the total DNA was wild-type DNA. The transfection efficiency was determined by co-transfecting the cDNAs with the pSV-β-galactosidase plasmid (Promega) and measuring β-galactosidase activity 24 h later, as described elsewhere (24).

Plasmid Constructs—The pRFP vector (27) was a generous gift of José Antonio Esteban (Centro de Biología Molecular Severo Ochoa, Madrid, Spain). The Myc-Sec24D and HA-GlyT2 constructs in the pcDNA3 plasmid (Invitrogen) were generously provided by Francisco Zafra (Centro de Biología Molecular Severo Ochoa). GlyT2 (28) was subcloned into pcDNA3 or pRFP (BglII-SalI sites), and the GlyT2 mutants were constructed by site-directed mutagenesis using the QuikChange kit (Stratagene) (29). S512R was subcloned in the unique EcoRI and XbaI sites flanking HA-GlyT2. The complete coding region of all of the constructs was sequenced to verify that only the desired mutation had been introduced. Plasmids from two independent *Escherichia coli* colonies were transfected into eukaryotic cells, and [^{3}H]glycine transport was measured in the cells for verification. The GFP-GlyT2 plasmid was constructed and characterized as described previously (30, 31). The RFP and HA tags were fused in frame with GlyT2 at the N terminus, and they did not interfere either with the uptake capacity in [^{3}H]glycine uptake assays or its expression at the plasma membrane as assessed by biotinylation (see Fig. 5*A*). C-terminal tagging was avoided because previous reports indicated that this region of the transporter might be involved in specific interactions and intracellular trafficking (32). The CNX cDNA clone (IMAGE number 2582119) in pCMV.SPORT6 was purchased from Source Bioscience Lifesciences (24).

Transport Assays—Glycine transport assays on COS7 cells were performed at 37 °C in phosphate-buffered saline (PBS) containing 10 mM glucose and 2 μCi/ml 2-^{3}H-labeled glycine (1.6 TBq/mmol; PerkinElmer Life Sciences), diluted to a final concentration of 10 μM, as described previously (24). For glutamate transport assays, the radiolabeled glycine was substituted with the same amount of ^{3}H-labeled glutamate. These reactions were run for 10 min and then terminated by aspiration. The protein concentration was determined in aliquots taken from each well (Bradford), and the uptake of [2-^{3}H]glycine was measured by liquid scintillation (LKB 1219 Rackbeta). Transport was quantified by subtracting the glycine accumulated in mock-transfected COS7 cells (or in the presence of the specific GlyT2 inhibitor, ALX1393) from that of the transporter-transfected cells and normalized to the protein concentration. Assays were performed in triplicate or quadruplicate.

Surface Biotinylation—COS7 cells expressing wild type or mutant GlyT2 were grown in 6-well plates (Nunc), washed, and labeled with Sulfo-NHS-Biotin (1.0 mg/ml in PBS; Pierce) at 4 °C, a temperature that blocks membrane trafficking of proteins. After quenching with 100 mM L-lysine to inactivate the

[3] The abbreviations used are: DAT, dopamine transporter; CNX, calnexin; COPII, coatomer protein II; ER, endoplasmic reticulum; ERAD, ER-associated degradation; MDCK, Madin-Darby canine kidney; PBA, sodium 4-phenylbutyrate; TM, transmembrane domain; ANOVA, analysis of variance.

free biotin, the cells were lysed with 1× lysis buffer as described elsewhere (24). A portion of the lysate was saved to determine the total protein content, and the remainder was incubated with streptavidin-agarose beads for 2 h at room temperature with rotary shaking. After centrifugation, the supernatant was removed, and an aliquot was used to quantify the non-biotinylated fraction. The agarose beads recovered were washed three times with 1× lysis buffer, and the bound proteins (biotinylated) were eluted with Laemmli buffer (65 mM Tris, 10% glycerol, 2.3% SDS, 100 mM DTT, 0.01% bromphenol blue) for 10 min at 75 °C. The samples were then analyzed in Western blots.

Immunofluorescent Staining of Cultured Cells—Immunocytochemistry was performed as described (31). Briefly, MDCK II cells, COS7 cells, or primary neurons were fixed with 4% paraformaldehyde in PBS, washed three times with 1 ml of PBS, and then blocked for 30 min with 10% serum in TNT (0.1 M Tris/HCl (pH 7.5), 0.3 M NaCl, and 0.2% Triton X-100). The cells were then incubated for 2 h with the desired primary antibodies (E-cadherin (rat, 1:200), CNX (rabbit, 1:500), GFP (mouse, 1:200), or RFP (rabbit, 1:1000)) diluted in TNT containing 1% serum (TNT-S), after which they were washed three times with TNT buffer and incubated for 2 h with the appropriate secondary antibody diluted in TNT-S (anti-mouse Alexa Fluor 488 (1:200), anti-rabbit Alexa Fluor 555 (1:200), or anti-rat or anti-rabbit Alexa Fluor 647 (1:200)). After three washes with TNT, the coverslips were mounted on microscope slides with Vectashield (Vector Laboratories, Burlingame, CA), and the cells were visualized by confocal microscopy on an inverted microscope AXIOVERT200 (Zeiss). At least 30 images for each condition were quantified using ImageJ software (National Institutes of Health) (as in Ref. 33). The images were processed with a 2.0-pixel median filter, and the threshold applied was automatically determined by the JACoP plugin (34). Pearson's value of correlation was obtained with JACoP by comparing the two thresholded channels and measuring the correlation between them. The value can range from −1 to 1, the latter representing maximal co-localization (two identical images).

Electrophoresis and Western Blotting—Protein samples were separated by SDS-PAGE using a 4% stacking gel and 6 or 7.5% resolving gels. The samples were transferred to nitrocellulose (Invitrogen) (1.2 mA/cm^2 for 2 h), and the membranes were then blocked for 4 h with 5% milk in PBS at 25 °C. The membranes were probed overnight at 4 °C with the desired primary antibody: anti-GlyT2 (rabbit, 1:1,000) (35); anti-GlyT2 (rat, 1:500) (36); anti-CNX (1:1,000; Stressgen Biotechnologies Corp.); anti-ubiquitin (P4D1, 1:200; Santa Cruz Biotechnology, Inc.); anti-HA (monoclonal antiserum 12CA5, 1:500; Sigma); anti-GFP (green fluorescent protein, 1:1,000; Invitrogen); or anti-RFP (red fluorescent protein, 1:2,000; a generous gift of José María Requena, Centro de Biología Molecular Severo Ochoa). After several washes, the antibodies bound were detected with peroxidase-coupled anti-rat (1:8,000; Sigma) or anti-rabbit IgG (1:10,000; Bethyl), which were visualized by enhanced chemiluminescence (ECL; Amersham Biosciences). Subsequently, the antibodies were stripped from the membrane (Thermo Scientific), which was reprobed with anti-tubulin (1:3,000; Sigma), and antibody binding was detected with a peroxidase-coupled anti-mouse IgG. The protein bands were quantified by densitometry.

Carbohydrate Modification—COS7 cells expressing GlyT2 or the desired mutants were lysed in 1× lysis buffer (150 mM NaCl, 50 mM Tris-HCl (pH 7.4), 5 mM EDTA, 1% Triton X-100, 0.1% SDS, 0.25% deoxycholate sodium, 0.4 mM PMSF, and 4 μM pepstatin) and digested with the chosen endoglycosidase (peptide:*N*-glycosidase F (New England Biolabs) or endoglycosidase H or D (Roche Applied Science)) in a small volume of the appropriate buffer, according to the manufacturer's instructions. These cell extracts were then resolved by SDS-PAGE and analyzed in Western blots.

Immunoprecipitation Assays—Transfected COS7 cells were washed twice with PBS and scraped off of the plates in 150 mM NaCl, 50 mM Tris-HCl (pH 7.4), 0.4 mM PMSF, and 4 μM pepstatin, and the desired amount of protein (Bradford method, Bio-Rad) was solubilized for 30 min at 22 °C in lysis buffer with 0.2% Nonidet P-40. After a 15-min centrifugation at 10,000 × *g*, an aliquot of the lysate was retained to measure the total protein content, and the remainder was precleared by adding 20 μl of 50% protein A or G Sepharose (Sigma) in lysis buffer for 30 min at 4 °C with rotation. After centrifugation, the supernatants were incubated overnight at 4 °C with 2 μg of the desired primary antibody, whereas controls with no antibody were also included. Subsequently, 20 μl of protein A or G-Sepharose beads were added to the samples, and after incubating for 1 h at 4 °C, the beads were washed twice for 5 min with 500 μl of 1× lysis buffer. The bound proteins were then dissociated from the beads by heating at 75 °C for 15 min, resolved by SDS-PAGE, and analyzed in Western blots. Sequential immunoprecipitations were performed as described elsewhere (24). Beads containing anti-CNX immunoprecipitated proteins were incubated with 150 μl of 1% SDS in HEPES-buffered saline at 75 °C for 30 min and centrifuged. The supernatant was then diluted with 1.35 ml of 1% CHAPS in HEPES-buffered saline (final SDS concentration, 0.1%), transferred to a new tube, and incubated with an anti-GlyT2 antibody (1.5 μg) overnight at 4 °C. The immunocomplexes formed were again recovered with fresh beads, eluted, and analyzed as above.

Pulse-Chase Experiments—Cells cultured to 80–90% confluence in p60 or p100 plates were maintained in methionine-free medium for 1 h prior to performing the pulse-chase experiments (24). The cells were then pulse-labeled for 15 min with 0.25 mCi/ml [^{35}S]methionine/cysteine (Redivue Promix, Amersham Biosciences) and chased for varying periods in DMEM + 10% fetal calf serum (FCS) containing 1 mM cycloheximide to quickly stop the elongation of nascent polypeptide chains. Labeling was quenched by the addition of ice-cold PBS containing 20 mM freshly prepared *N*-ethylmaleimide to prevent the oxidation of free sulfhydryl groups. The proteins were immunoprecipitated from the cell lysates with a GlyT2 antibody (35) or sequentially with anti-CNX (Stressgen) and anti-GlyT2 antibodies as described above. The samples were resolved by SDS-PAGE, fixed, and treated with Amplify fluorography reagent (Amersham Biosciences). The gels were dried and exposed for 4–12 days at −70 °C, and the protein bands were quantified by densitometry.

Primary Cultures of Cerebral Cortex—Primary cultures of embryonic cortical neurons were prepared as described previously (37). Briefly, the cortex of Wistar rat fetuses was obtained on the 18th day of gestation, and the tissue was mechanically disaggregated in Hanks' balanced salt solution (Invitrogen) containing 0.25% trypsin (Invitrogen) and 4 mg/ml DNase (Sigma). Cells were plated at a density of 500,000 cells/well in 6-well plates (Falcon), and they were incubated for 4 h in DMEM + 10% FCS, containing glucose (10 mM), sodium pyruvate (10 mM), glutamine (0.5 mM), gentamicin (0.05 mg/ml), streptomycin (0.1 mg/ml), and penicillin G (6×10^{-5} mg/ml). After 4 h, the buffer was replaced with Neurobasal/B27 culture medium containing glutamine (0.5 mM, 50:1 by volume; Invitrogen), and 3 days later, cytosine arabinoside ($2.5–5 \times 10^{-3}$ mM) was added to inhibit further glial growth. For transfection, neurons that had been maintained *in vitro* for 7 days were incubated with 2 μg of total DNA mixed with 4 μl of Lipofectamine 2000 reagent (Invitrogen). GlyT2 glycine transport and membrane expression were measured after 48 h in culture.

Densitometry and Data Analysis—The protein bands visualized by ECL (Amersham Biosciences) or fluorography were quantified in a GS-800 calibrated imaging densitometer using the Bio-Rad Quantity One software, with film exposures in the linear range. Non-linear regression fits of experimental transport data were performed using ORIGIN software (Microcal Software, Northampton, MA). The *error bars* represent the S.E. of at least triplicate samples, and the representative experiments shown were repeated no fewer than three times with comparable results.

RESULTS

S512R Exerts a Dominant Negative Effect on the Wild-type GlyT2—Scanning the 16 coding exons of the human GlyT2 gene (*SLC6A5*) in a cohort of hyperekplexia patients recently revealed a missense mutation in exon 10 associated with dominant autosomic inheritance (10). This mutation yields a protein with a serine to arginine substitution in transmembrane domain 7 (S512R), for which a dominant negative role on GlyT2 trafficking was proposed. To characterize this effect, we expressed the recombinant S512R mutant together with the wild-type GlyT2 in eukaryotic cells, and we measured the mutant's effect on GlyT2 membrane expression and on glycine transport (Fig. 1). We employed an optimized co-transfection protocol that makes use of low amounts of cDNA to avoid saturating the cell's translation machinery (see "Experimental Procedures"). Accordingly, only specific effects were observed that allowed us to characterize the dominant negative behavior of the mutant.

As we reported previously (24), when expressed in heterologous cells, GlyT2 appears as a doublet of two protein bands in Western blots; the mature transport-competent form that is present at the plasma membrane migrated as a 100 kDa band, and the immature hypoglycosylated transporter appeared as a 75-kDa protein band. When the S512R mutant was expressed heterologously, no 100 kDa band was evident in Western blots, and the molecular weight of the sole protein band detected was compatible with that of the 75-kDa immature form (Fig. 1*A*). Thus, it was not surprising that the S512R transporter was inactive. Indeed, when the mutant was co-expressed with the wild-type GlyT2, the amount of the 100 kDa band and glycine transport were both reduced to 42.1 ± 4.5 and 51.0 ± 5.3% (mean ± S.E.) of the original values, respectively. Furthermore, the surface mature wild-type transporter available for biotinylation was reduced in a dose-dependent manner when co-expressed with increasing amounts of S512R mutant. Thus, equal amounts of wild-type and mutant DNA (1:1 condition) caused the wild-type surface expression to decrease to 43.1 ± 2.2% (biotinylated GlyT2) and glycine transport to decrease to 37.1 ± 2.2% of their original values (Fig. 1, *B* and *C*), whereas 2- and 3-fold increases in the concentration of co-expressed mutant (1:2 and 1:3 conditions) produced further reductions in membrane expression (to 24.5 ± 2.3 and 18.6 ± 1.6%, respectively) and in transport activity (to 21.5 ± 1.8 and 14.8 ± 1.7%, respectively). By contrast, when wild-type GlyT2 was expressed together with increasing amounts of another inactive GlyT2 mutant (G485C) that reached the plasma membrane normally, glycine transport was unaltered (Fig. 1, *B* and *D*). Likewise, when increasing concentrations of S512R were co-expressed with the non-related GLT1 (glutamate transporter 1), neither GLT1 plasma membrane expression nor the transport of glutamate was affected (Fig. 1, *B* and *E*). These results confirm a dominant negative role of S512R on wild-type GlyT2 and indicate that the mutant acts specifically on the wild-type GlyT2. Besides, this behavior is not a general feature of GlyT2 mutants but rather a particular property of S512R.

The ability of S512R to reduce the amount of wild-type GlyT2 at the cell surface was also monitored in MDCK cells through its co-localization with the plasma membrane marker E-cadherin (Fig. 1*F*). For this purpose, we used constructs of wild-type and mutant fused to N-terminal tags. The tags did not interfere with either glycine uptake or with the plasma membrane expression of the fusion proteins (see Fig. 5*A*). We co-expressed the wild-type and mutant GlyT2 fused to GFP or RFP, and we analyzed the cells by immunofluorescence to detect E-cadherin. The images show that the RFP-S512R fusion protein was clearly absent from the plasma membrane, and the presence of the mutant strongly diminished the surface expression of the wild-type GFP-GlyT2. Thus, the co-localization of GFP-GlyT2 with E-cadherin was reduced to 50.4 ± 2.5% when it was co-expressed with RFP-S512R rather than with RFP-GlyT2 (*right histogram*). Therefore, the GFP- or RFP-tagged (or HA-tagged) transporter constructs reproduced the dominant negative behavior of the mutant transporter as well as replicating the properties of the wild-type transporter.

S512R Characterization—The failure to detect a mature S512R transporter suggests that the missense mutation prevents the progression along the secretory pathway. To determine whether the removal of the serine or the introduction of the arginine impeded post-translational processing of the transporter, we evaluated multiple amino acid substitutions at position 512 (Fig. 2*A*). Surface biotinylation of the mutants expressed in COS7 cells led us to conclude that the lack of a mature transporter at the cell surface was due to the introduction of the arginine. Indeed, this feature was also observed for a similar substitution at the contiguous position 511, where the presence of an arginine residue also impaired the production of

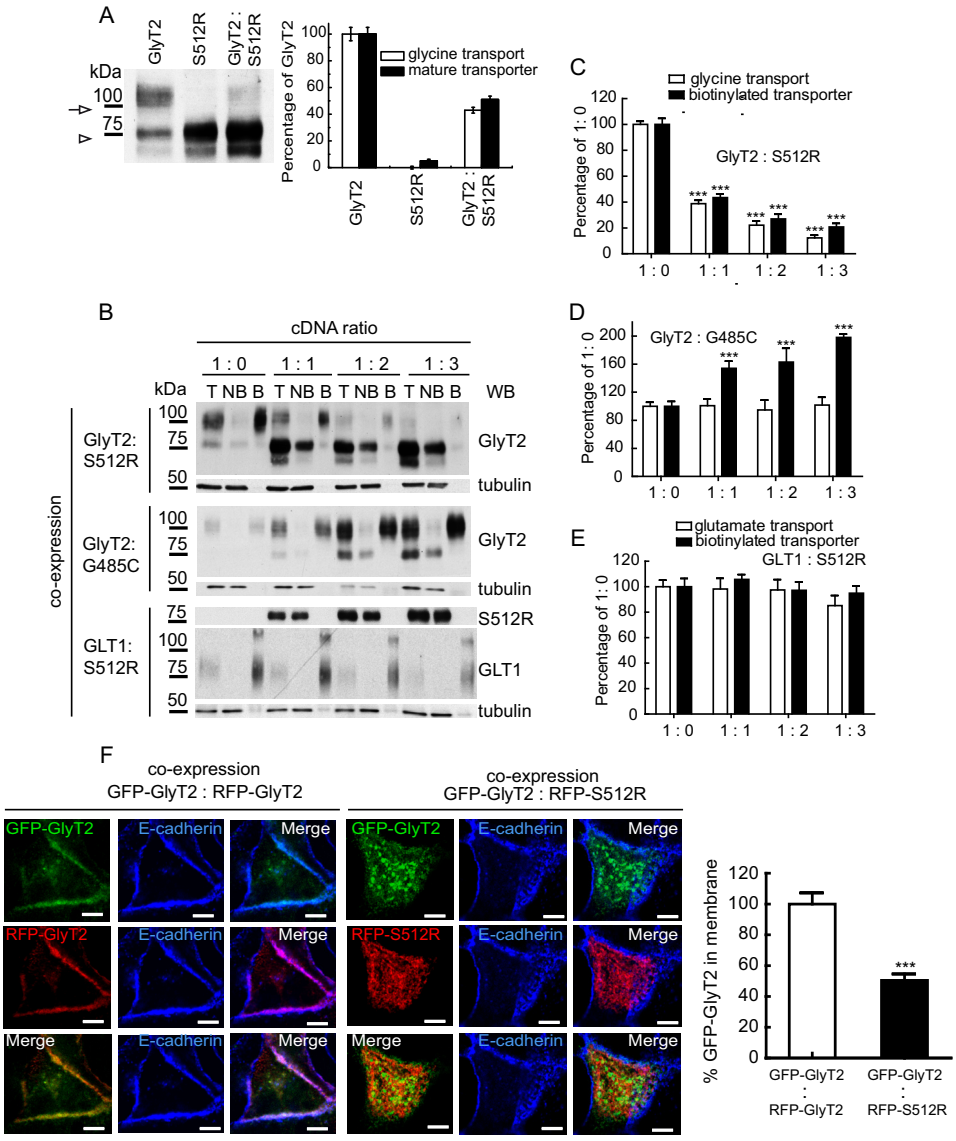

FIGURE 1. **S512R mutant has a dominant negative effect on GLYT2 trafficking.** *A*, COS7 cells expressing GlyT2, S512R, or both (1:1 cDNA ratio, by weight) were assayed in Western blots (*left*) and for glycine transport (*right*). The 100-kDa mature transporter in the Western blot (*arrow*) was densitometered and is represented together with the measured transport activity (*right*). The 75 kDa immature band is labeled with an *arrowhead*. 100% GlyT2 glycine transport was 3.3 ± 0.6 nmol/mg of protein/10 min (mean ± S.E.). *B–E*, COS7 cells were transfected with the wild-type GlyT2 cDNA alone or co-transfected with increasing amounts of S512R cDNA to reach the indicated GlyT2/S512R cDNA ratios (by weight) and then assayed by biotinylation (*B*) and for glycine transport. *T*, total transporter; *B*, biotinylated transporter; *NB*, non-biotinylated transporter. Western blots (*WB*) were reprobed for tubulin as a loading control. *C–E*, 100% glycine and glutamate transport (in nmol/mg of protein/10 min): 3.7 ± 0.5 and 1.2 ± 0.1, respectively (means ± S.E.); ***, $p < 0.001$ with respect to wild-type (ANOVA with Tukey's post hoc test). *F*, MDCK cells expressing the transporters indicated for 48 h were immunolabeled for the plasma membrane marker E-cadherin (*blue*). Three-channel confocal images were obtained (*green* or *red* for transporter and *blue* for E-cadherin), and the regions occupied by E-cadherin were considered as the plasma membrane when using the ImageJ ROI manager, whereas the regions inside the cadherin staining were considered intracellular compartments. After applying an automatic threshold for adjustment, fluorescence intensity was measured separately for membrane and intracellular regions, and the proportion of the transporter at the plasma membrane was calculated (*histogram*). This process was performed in at least 50 cells/condition, representing the means ± S.E. (*error bars*); ***, $p < 0.001$ (Student's *t* test compared with GFP-GlyT2/RFP-GlyT2).

the mature transporter and glycine transport. By contrast, other substitutions were permissive for processing and activity, and although the transport activity of alanine and cysteine mutants was about half that of the wild type, only the serine to threonine mutation restored (and even improved) glycine transport (Fig. 2*A*, *right histogram*). Glycine transport by Ser-512 mutants did not fully correlate with membrane expression, implying that the substitutions affect the activity of surface transporters in addition to their processing. This was predictable because Ser-512 is close to the Na1-coordinating residue, Asn-511. Notably, a serine substitution has been found at this adjacent site associated with hyperekplexia (N511S), yielding a mutant that is almost completely inactive but that reaches the cell surface (10).

We next studied the glycosylation state of the S512R mutant to determine its location in the secretory pathway (Fig. 2*B*). Treating cell lysates expressing wild-type GlyT2 with peptide: *N*-glycosidase F completely removed the *N*-linked glycans from both the 75- and 100-kDa forms, yielding a 60 kDa band. This corresponded to the non-glycosylated protein core because its apparent size coincided with that of the N1234D mutant that lacks the four *N*-glycosylation motifs (24). The mature 100 kDa

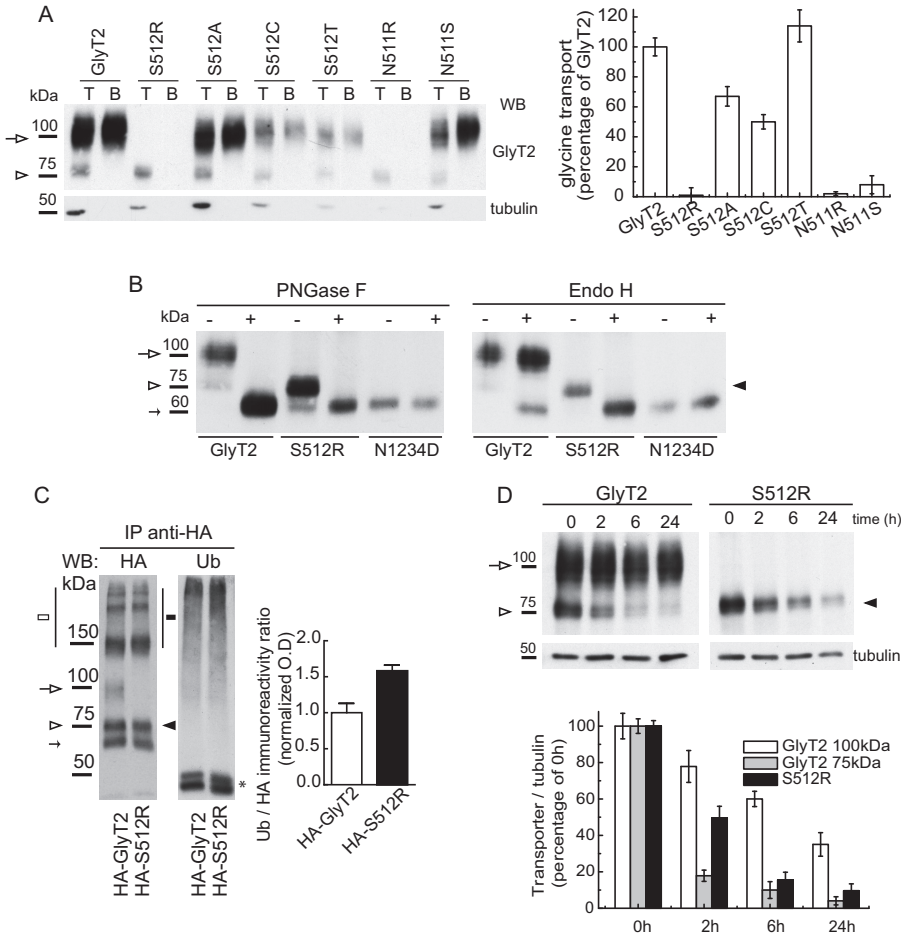

FIGURE 2. **Characterization of the S512R mutant.** *A*, substitution analysis of Ser-512. Shown are biotinylation (*left*) and glycine transport (*right*) of COS7 cells expressing wild-type GlyT2 or mutants with the amino acids indicated at position 512. *T*, total transporter; *B*, biotinylated transporter. Wild-type 100% glycine transport was 3.0 ± 0.6 nmol/mg of protein/10 min (mean ± S.E. (*error bars*)). *B*, carbohydrate modification of S512R. Lysates of COS7 cells expressing the indicated transporters were treated overnight with the vehicle alone (endoglycosidase buffer, −) or with the indicated endoglycosidase (+) in denaturing conditions and then resolved by SDS-PAGE as described under "Experimental Procedures." *C*, the S512R mutant is ubiquitinated. COS7 cells expressing wild-type HA-GlyT2 or HA-S512R mutant were treated with MG132 (10 μM, 4 h), lysed, and immunoprecipitated (*IP*) with the anti-HA monoclonal antibody, and the proteins recovered were probed with an anti-ubiquitin (P4D1) and anti-HA antibody. *White arrow*, GlyT2 (mature); *white arrowhead*, GlyT2 (immature); *black arrowhead*, S512R. *Small arrow*, 60 kDa band (24). High order bands of GlyT2 and S512R are indicated by *white* and *black squares*. *Asterisk*, IgG heavy chain + protein G. Means ± S.E. are shown. *, $p < 0.05$; **, $p < 0.01$, with respect to wild-type GlyT2 (means ± S.E., Student's *t* test). *D*, S512R is more prone to degradation than the wild-type GlyT2. COS7 cells expressing wild-type GlyT2 or S512R mutant were treated with 25 μM cycloheximide to block protein synthesis, and the transporter was monitored by immunoblotting of cell lysates with an anti-GlyT2 antibody at 0, 2, 6, and 24 h. Representative immunoblots (*WB*; *top panels*) and their densitometry (*bottom panels*) are shown. Tubulin immunoreactivity is shown as a loading control (means ± S.E. are shown). *PNGase F*, peptide:*N*-glycosidase F.

band was resistant to endoglycosidase H, indicating that it contained complex oligosaccharides, which would be consistent with a protein that has exited the ER, undergone oligosaccharide processing in the Golgi, and reached the cell surface. By contrast, the immature 75 kDa band was sensitive to Endo-H, indicating that it contained high mannose oligosaccharides borne by proteins in the ER. The glycosidase sensitivity of the S512R mutant paralleled that of the wild-type immature 75 kDa band, indicating that the mutant transporter resides in the ER.

The persistence of the S512R mutant in the ER suggests that this transporter is misfolded. Proteins that are folded incorrectly and are retained in the ER may be sorted for ER-associated degradation (ERAD) (38). Because most ERAD substrates are ubiquitinated by polychain addition prior to their degradation, we assessed the ubiquitination state of the wild-type and mutant transporters. As such, the HA-GlyT2 or HA-mutant transporter (see Fig. 5*A*) was immunoprecipitated from transfected COS7 cells with an anti-HA antibody, and the proteins recovered were analyzed in Western blots probed with an anti-ubiquitin (P4D1) antibody (Fig. 2*C*). Because ubiquitination regulates the endocytosis, recycling, and turnover of the mature GlyT2 (31, 37), it was not surprising that the 100 kDa band detected in the wild-type lysate was strongly ubiquitinated. Nevertheless, the ratio of ubiquitin to HA immunoreactivity was higher for the S512R mutant than the wild type (1.0 ± 0.23 *versus* 1.6 ± 0.19%), suggesting that S512R is modified by ubiquitination to a higher extent than the wild-type GlyT2. This was confirmed by immunoprecipitating the transporter with a KF2 multiubiquitin antibody (data not shown). In agreement with this, the S512R mutant was more prone to degradation. Cells expressing the wild-type or mutant transporter were treated with cycloheximide to block further protein synthesis, and a time course of transporter expression was monitored by immunoblotting at serial time intervals (Fig. 2*D*). Although mature

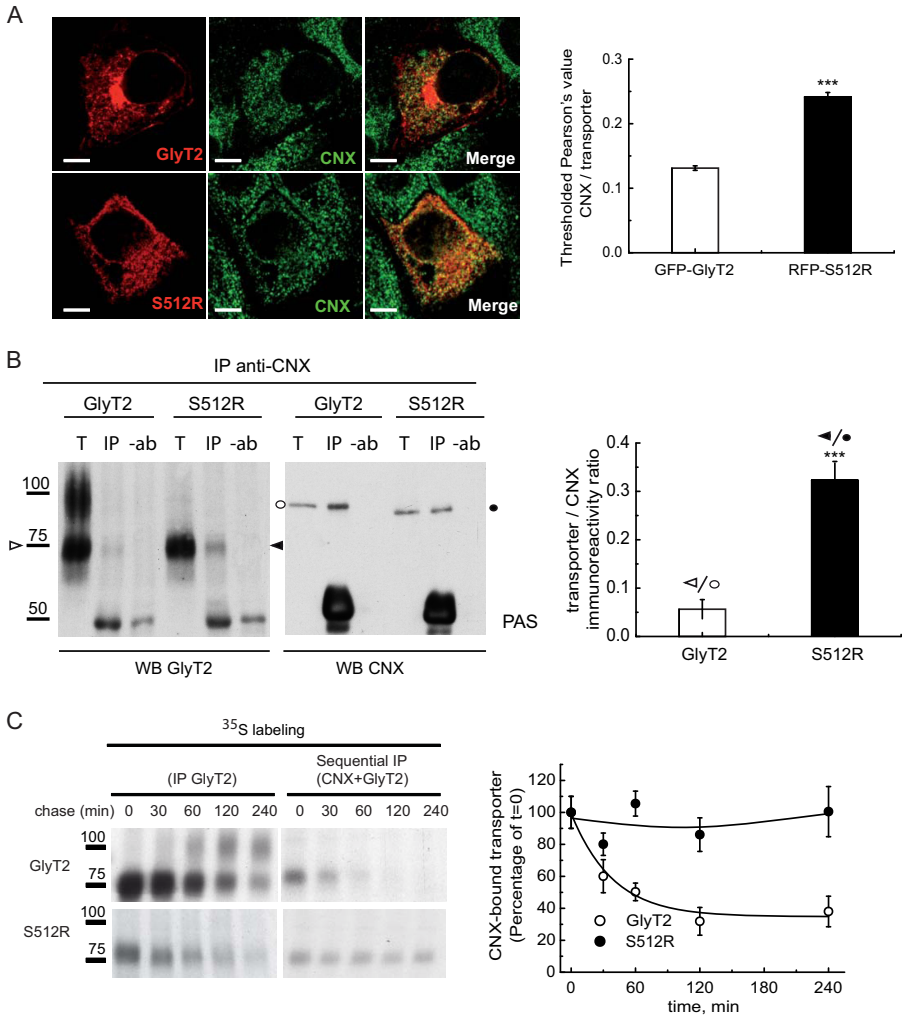

FIGURE 3. **Enhanced association of S512R with calnexin.** *A*, MDCK cells expressing either GFP-GlyT2 or RFP-S512R were immunolabeled for the ER chaperone CNX. For clarity, transporters are shown in *red*, and CNX is shown in *green* rather than in the original colors. Shown is quantification of the co-localization between GFP-GlyT2 and CNX or between RFP-S512R and CNX using Pearson's value of correlation as described under "Experimental Procedures": ***, $p < 0.001$ (Student's *t* test compared with GFP-GlyT2/CNX). *B*, immunoprecipitation of lysates from COS7 cells expressing either untagged GlyT2 or untagged S512R with the anti-CNX antibody. Immunocomplexes were probed in Western blots for GlyT2 (*left*) and CNX (*right*). *T*, total protein (input); *IP*, immunoprecipitated material; −*ab*, control without antibody. 75 kDa (ER) bands are indicated with *arrowheads* (*white*, GlyT2; *black*, S512R), and CNX (97 kDa) is indicated with *circles* (*white* or *black* in cells expressing GlyT2 or S512R). The GlyT2/CNX and S512R/CNX ratios in the immunoprecipitated material were calculated after densitometry of the bands indicated. ***, $p < 0.001$ (Student's *t* test compared with GlyT2/CNX). *C*, COS7 cells expressing the wild-type GlyT2 or S512R were pulse-labeled for 15 min with [^{35}S]methionine/cysteine and chased for the times indicated. The cell lysates were immunoprecipitated with the GlyT2 antibody (*left blot*) or subjected to sequential immunoprecipitation, first with CNX and then with the GlyT2 antibody (*right blot*), as described under "Experimental Procedures." *Right graph*, quantification of the transporter bound to CNX after densitometry of the fluorograms. The CNX-bound transporter was normalized to the total synthesized transporter at each time point and presented as a percentage of $t = 0$ taken as 100% (means ± S.E. (*error bars*) are shown). *WB*, Western blot.

wild-type GlyT2 had a half-life above 20 h (24), the amount of the mutant transporter was reduced by 50% within 2 h (49.7 ± 6.3%). Interestingly, the disappearance of the immature 75-kDa wild-type GlyT2 was faster than that of S512R, suggesting that maturation of GlyT2 was quicker than degradation of S512R. Thus, these results suggest that the S512R mutant is more prone to ERAD than wild-type GlyT2.

The Association of S512R with Calnexin Is Enhanced—The ER is a site where quality control of the glycoproteins synthesized takes place. Elements in the ER, such as molecular chaperones and lectins, recognize folding intermediates and undergo rounds of binding and release to facilitate or rescue folding, suppress aggregation, or mediate the retention and subsequent degradation of aberrant proteins. We recently showed that CNX plays an important role in the quality control of GlyT2 in the ER. The 75-kDa GlyT2 precursor transiently binds to CNX, which facilitates GlyT2 processing (24), and thus, the retention of the mutant in the ER may possibly reflect a more robust or long lasting association with CNX. Therefore, we studied the association of this chaperone to the wild-type or mutant transporter by confocal microscopy. In MDCK cells expressing either GFP-GlyT2 or RFP-S512R and immunostained for CNX, S512R co-localized more strongly with CNX than the wild-type GlyT2, as evident through the almost 2-fold increase in the Pearson value for the mutant (0.24 ± 0.006 *versus* 0.13 ± 0.003; Fig. 3*A*). Although these data suggest enhanced association to CNX of the mutant, the presence of mature and immature transporter forms in the wild type may make it difficult to compare with the co-localized fluorescence of the single-form mutant. Therefore, we assessed the amount

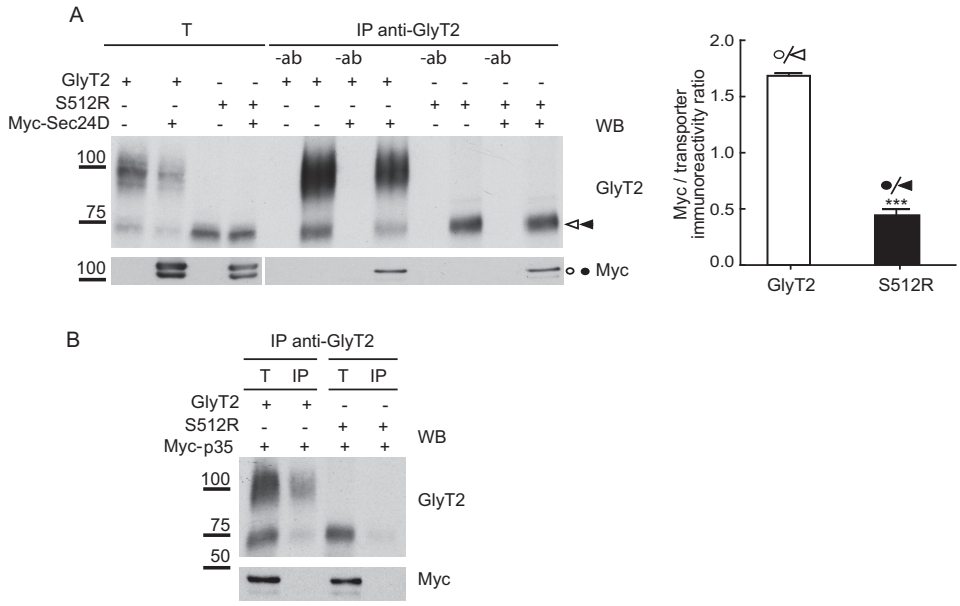

FIGURE 4. **The association of S512R with Sec24D is altered.** Lysates of COS7 cells expressing untagged GlyT2 or S512R in the presence or absence of Myc-Sec24D (A) or Myc-p35 (B) were immunoprecipitated with an anti-GlyT2 antibody, and the immunocomplexes were analyzed in Western blots to detect GlyT2 and Myc. *T*, total protein (input); *IP*, immunoprecipitated material; *−ab*, control without antibody. *Histogram*, Myc-Sec24D/GlyT2 and Myc-Sec24D/S512R ratios were calculated from the densitometry of the Myc bands (*circles*) and ER bands (*arrowheads*; GlyT2 (*white*) and S512R (*black*)): ***, $p < 0.001$ (Student's *t* test compared with Myc-Sec24D/GlyT2). *WB*, Western blot.

of untagged wild-type or mutant transporter recovered when Nonidet P-40 lysates of cells expressing these constructs were immunoprecipitated with an antibody against CNX. The amount of S512R co-precipitated from cells expressing this mutant with the CNX-specific antibody was 6-fold (6.4 ± 0.07) higher than the GlyT2 recovered from cells expressing the wild-type (Fig. 3*B*). This difference in steady-state binding might reflect a stronger or longer lasting association of the mutant transporter with CNX. To assess this possibility, sequential immunoprecipitation of [^{35}S]methionine/cysteine pulse-chased cells expressing the wild-type or mutant transporter was performed, whereby cell lysates were first immunoprecipitated with a CNX-specific antibody after a 15-min labeling pulse and the desired chase, and the immunocomplexes recovered were then immunoprecipitated with a GlyT2 antibody (Fig. 3*C*). In this way, a fraction of the protein bound to CNX in steady state could be isolated, and when the immunoprecipitation was performed after longer chases, we could estimate the half-life of the CNX-transporter complexes. Accordingly, the wild-type GlyT2 75-kDa precursor transiently associated with CNX in a complex with a half-life of around 60 min, at which point the 100-kDa mature transporter was formed (24). By contrast, the complex in which the mutant associated with CNX was much more stable (*right graph*), and this persistent association with CNX might lead to its retention in the ER.

Alterations in the Association of S512R with Sec24D—Cargo transport from the ER to the Golgi is mediated by COPII vesicles that bud off from the ER exit sites. ER export signals are thought to be recognized by the Sec24 subunit of the Sec24-Sec23 protein complex that forms the inner layer of the COPII coat. A binding site for Sec24 resides in the C terminus of several SLC6 transporters, which mostly depend on the Sec24D isoform for ER export (26, 32, 39). One possibility that could explain the slow dissociation of S512R from CNX is a distorted interaction of the mutant with the COPII, such that the delivery from the chaperone is impaired. To test this possibility, we expressed Myc-Sec24D protein in COS7 cells together with either the wild-type GlyT2 or S512R transporter, immunoprecipitated the cell lysates with a GlyT2-specific antibody, and probed the immunocomplexes in Western blots to detect Myc-Sec24D. The amount of Myc-Sec24D co-immunoprecipitated with the 75-kDa wild-type GlyT2 was 4-fold (4.3 ± 0.12) higher than that recovered with the mutant (Fig. 4*A*). This interaction was independent of the Myc tag because a Myc-tagged negative control did not interact with the transporters (Fig. 4*B*). This suggests that the binding of the mutant to Sec24D is somehow altered, and as a consequence, S512R is not exported from the ER.

S512R Forms Oligomers with Wild-type GlyT2—Upon release of the lumenal ER chaperones, most exportable proteins oligomerize, which helps to relieve ER entrapment. However, by forming heteromers with the S512R mutant, it is possible that the wild type could be retained in the ER. To test this hypothesis, we immunoprecipitated lysates of cells expressing differently tagged wild-type and mutant transporters (HA or RFP N-terminal fusions of the transporters that do not interfere with expression or function; Fig. 5*A*), and using a specific antibody against one tag, we monitored the co-precipitation of the other transporter by Western blot. Due to the small size of the HA epitope (less than 1 kDa), the HA-tagged transporters were virtually indistinguishable from the untagged counterparts, so that HA-GlyT2 showed the two bands of about 100 and 75 kDa, and HA-S512R showed the 75 kDa band. By contrast, the pRFP vector used contained a tandem dimer variant of DsRed (27) that increased the size of the bands by ~75 kDa, such that RFP-S512R appeared as a 150 kDa band, and RFP-GlyT2 appeared as a doublet of 175 and 150 kDa. Some additional bands were also observed due to the tendency of the untagged

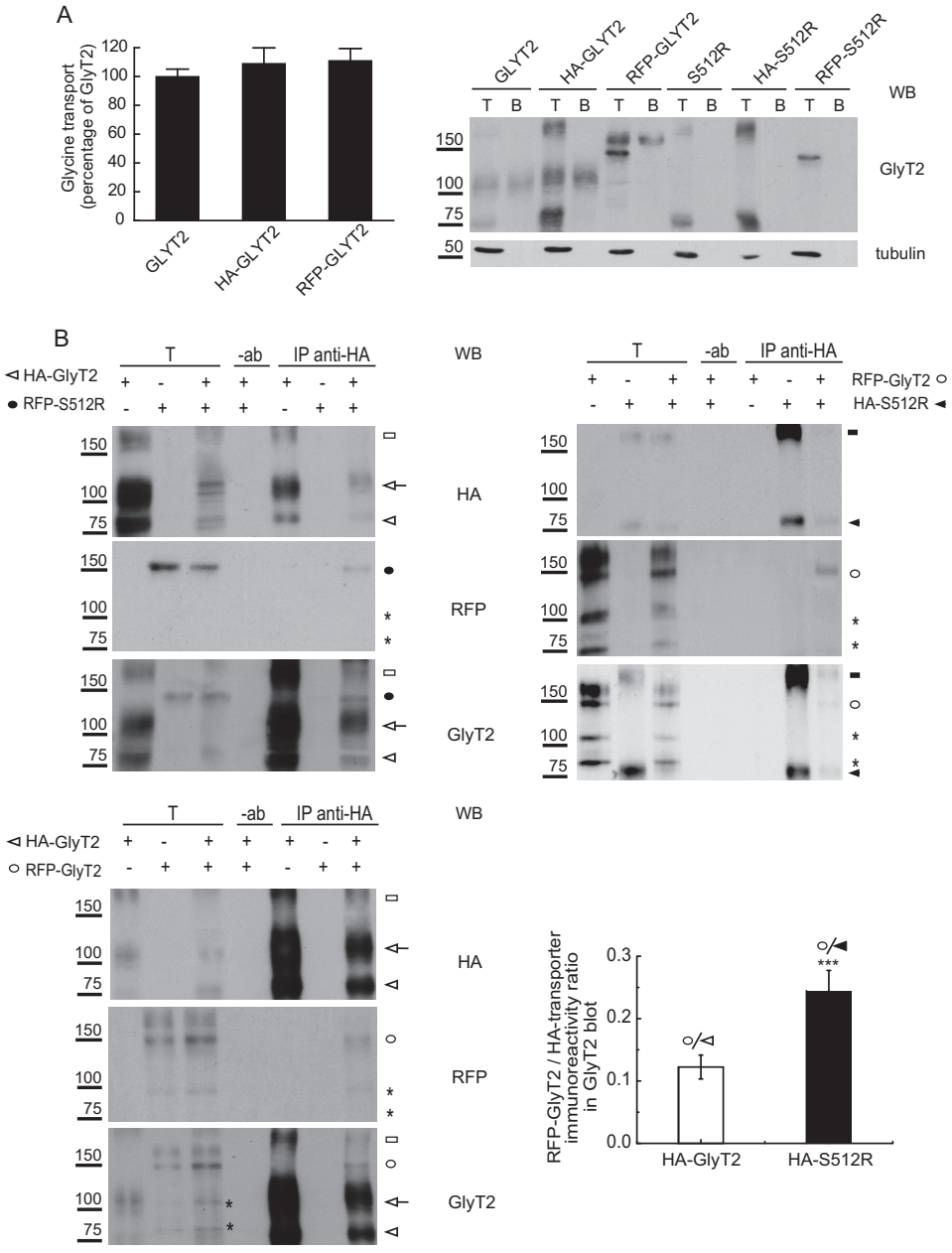

FIGURE 5. **S512R co-immunoprecipitates with wild-type GlyT2.** *A*, glycine transport and surface biotinylation was measured in COS7 cells expressing the indicated untagged or tagged transporters, as described under "Experimental Procedures," and the 100% untagged wild-type GlyT2 transport was 2.8 ± 0.5 nmol/mg protein/10 min (mean ± S.E. (*error bars*)). *T*, total transporter; *B*, biotinylated transporter. *B* and *C*, S512R co-immunoprecipitates with wild-type GlyT2. Lysates of COS7 cells expressing the indicated tagged transporters were immunoprecipitated with anti-HA antibody, and the immunocomplexes were analyzed in Western blots to detect HA, RFP, and GlyT2. *T*, total protein (input); *IP*, immunoprecipitated material; −*ab*, control without antibody. Transporter proteins are indicated as follows. *White arrowhead*, HA-GlyT2 (immature); *white arrow*, HA-GlyT2 (mature); *black circle*, RFP-S512R; *white circle*, RFP-GlyT2 (immature); *black arrowhead*, HA-S512R. High order bands of GlyT2 and S512R are indicated with *white* and *black squares*. *Asterisks* indicate small proteolytic fragments. *Histogram*, the RFP-GlyT2/HA-GlyT2 and RFP-GlyT2/HA-S512R ratios were calculated by densitometry of the indicated ER bands of GlyT2 Western blots (the means ± S.E. are shown): ***, $p < 0.001$ (Student's *t* test compared with HA-GlyT2/CNX). *WB*, Western blot.

or tagged 75-kDa form to generate higher molecular weight forms, clearly recognizable in the GlyT2 Western blots. Also, some small proteolytic products were observed, such as two bands slightly above 100 and 75 kDa. When the anti-HA antibody was used to immunoprecipitate the transporter from cells expressing HA-GlyT2 and RFP-S512R, alone and in combination (a condition that gave clean Western blots when probed for HA, RFP, or GlyT2; Fig. 5*B*, *left*), both tagged proteins were present in the HA immunoprecipitate, indicating that the wild type and mutant interact. This interaction was also detected when we exchanged the tags and co-expressed HA-S512R with RFP-GlyT2 and probed Western blots of the immunocomplexes obtained with anti-HA for RFP-GlyT2 (Fig. 5*B*, *right*). Notably, the 150 kDa RFP-tagged band was that primarily recovered from these cells, suggesting that the wild-type-mutant interaction mainly involves the 75-kDa ER wild-type form. A similar result was obtained when HA was used to immunoprecipitate complexes from cells co-expressing HA-GlyT2 and RFP-GlyT2, indicating that also for the wild-type, the immature forms do interact. The amount of RFP-GlyT2 co-immunopre-

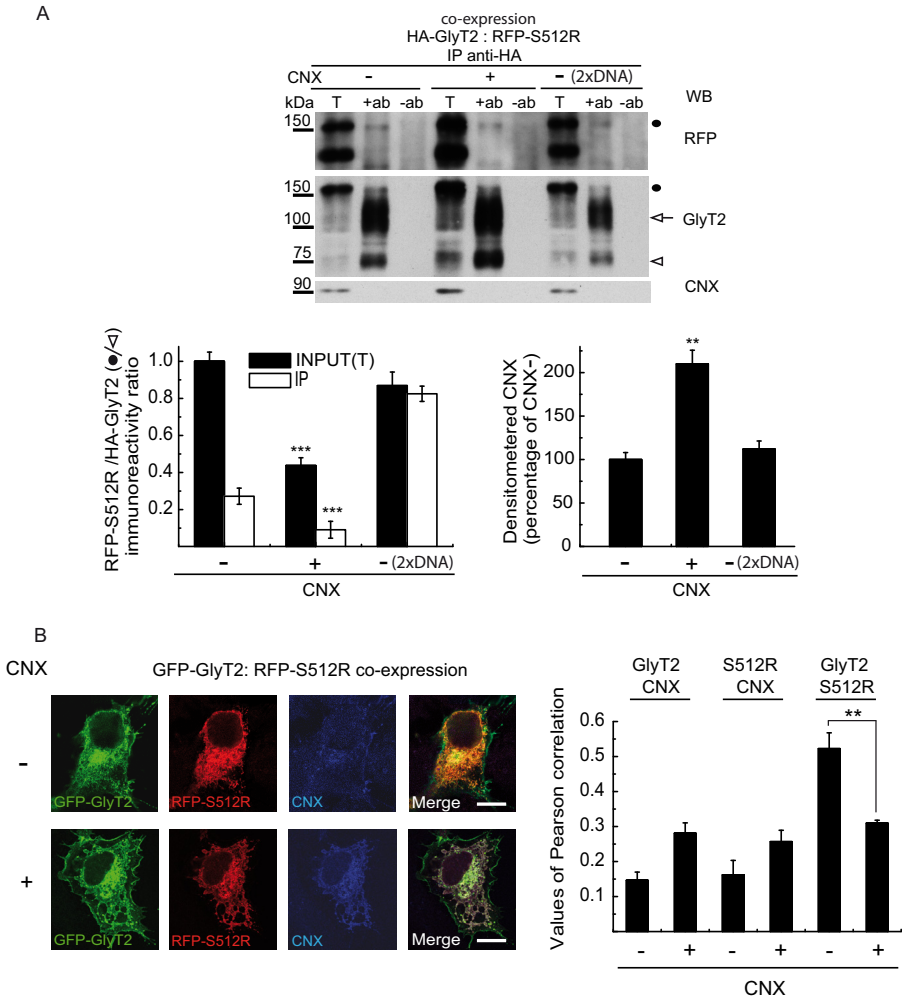

FIGURE 6. **Effect of CNX overexpression on GlyT2-S512R interaction.** *A*, Western blot (*WB*) probed for GlyT2, RFP, and CNX of immunocomplexes obtained with an HA antibody from cells co-expressing HA-GlyT2 and RFP-S512R in the presence or absence of overexpressed recombinant CNX (1:4 cDNA ratio). The control (2× DNA) corresponds to COS7 cells transfected with double the concentration of HA-GlyT2 and RFP-S512R cDNAs. *T*, total protein (input); *IP*, immunoprecipitated material; *−ab*, control without antibody. *Black circle*, RFP-S512R; *white arrow* and *arrowhead*, HA-GlyT2 100 and 75 kDa bands, respectively. The RFP-S512R/HA-GlyT2 immunoreactivity ratios (*left*) and CNX immunoreactivity (*right*) were calculated by densitometry of the corresponding bands: **, $p < 0.01$; ***, $p < 0.001$ (ANOVA with Tukey's post hoc test compared with controls without overexpressed calnexin: *CNX −*). *B*, MDCK cells expressing GFP-GlyT2 and RFP-S512R in the presence (*CNX+*) or absence (*CNX−*) of overexpressed CNX were immunolabeled for CNX. Shown is quantification of the co-localization between GFP-GlyT2/CNX, RFP-S512R/CNX, or GFP-GlyT2/RFP-S512R in the presence (*CNX+*) or absence (*CNX−*) of exogenous CNX, using Pearson's value of correlation as described under "Experimental Procedures" (means ± S.E. (*error bars*) are shown): **, $p < 0.01$ (Student's *t* test compared with control without overexpressed CNX; *CNX−*).

cipitated with HA-S512R was 2-fold (2.0 ± 0.45) higher than that co-immunoprecipitated with HA-GlyT2, suggesting a stronger association of the wild type with the mutant than with other wild-type molecules (Fig. 5*C*, *right histogram*).

CNX Overexpression Rescues Wild-type GlyT2 from the Dominant Negative Effect of S512R—Because the S512R mutant showed enhanced association to CNX (Fig. 3) and it also interacts with wild-type GlyT2 (Fig. 5), we asked whether overexpressing CNX might affect the interaction between the wild-type and mutant transporter. Recombinant CNX was overexpressed in cells co-expressing HA-GlyT2 and RFP-S512R, and the amount of the RFP-mutant transporter co-precipitated with HA-GlyT2 from the cell lysates was quantified by densitometry in Western blots probed for RFP-S512R (Fig. 6*A*). CNX overexpression preferentially favored the accumulation of wild-type GlyT2 in the cells and significantly reduced the mutant/wild-type ratio in the immunocomplexes (*bottom left histogram*). In addition, total transporter expression was increased by the chaperone, consistent with our previous results showing that CNX facilitated GlyT2 biogenesis (24). However, the weaker contribution of RFP-S512R to the complexes was not due to a general increase in transporter expression because enhancing transporter expression by doubling the amount of transporter cDNA used in the transfection did not alter mutant and wild-type co-immunoprecipitation. This was due to the fact that overexpressed CNX increased wild-type transporter expression to a greater extent than mutant expression, which probably reflects the chaperone's ability to discriminate between different conformational states of GlyT2 (24). The overexpression of CNX in COS7 cells co-expressing GFP-GlyT2 and RFP-S512R also provoked a significant decrease in the co-localization of wild-type and mutant immunofluorescence, reflected in the drop in the Pearson value to 59.09 ± 0.12% of its value at endogenous CNX levels (0.44 ± 0.09 *versus*

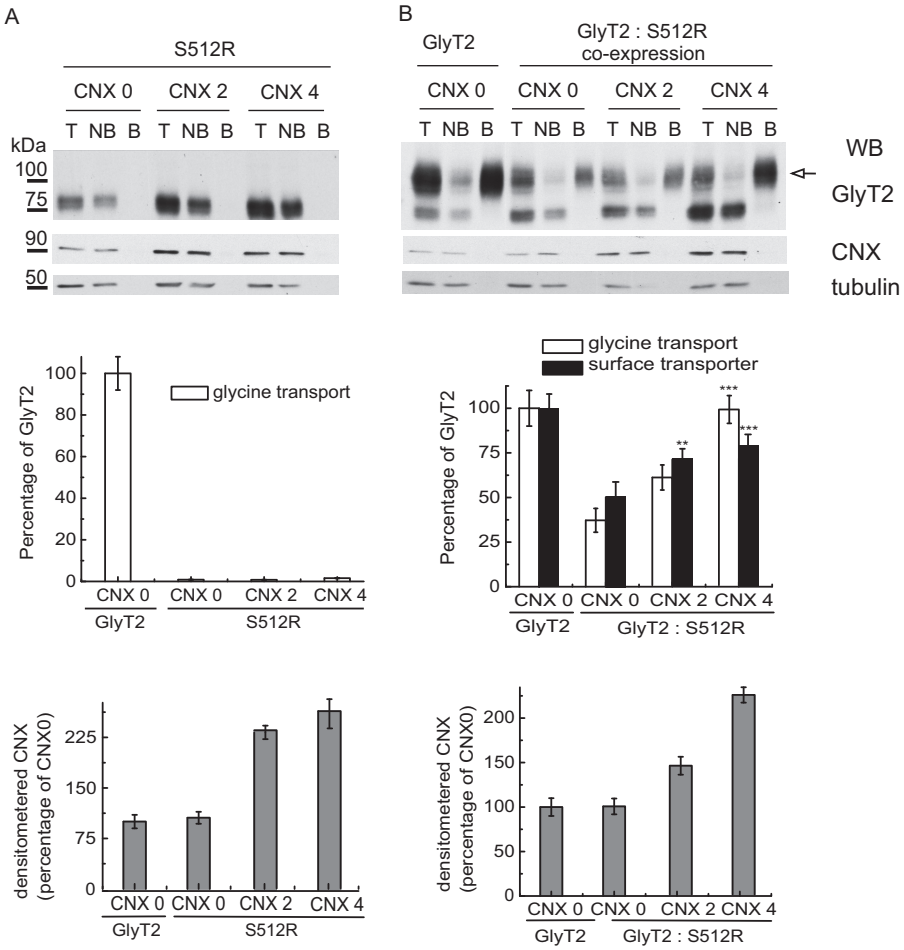

FIGURE 7. **CNX overexpression rescues the function and membrane expression of the wild-type transporter from the dominant negative effect of S512R.** Biotinylation and glycine transport of COS7 cells transfected with untagged S512R cDNA (*A*) or untagged wild-type GlyT2 cDNA, alone or in combination at a 1:1 ratio by weight (*B*), together with increasing concentrations of exogenous CNX cDNA (*0*, *2*, and *4* refer to a 1:0, 1:2, and 1:4 GlyT2/CNX cDNA ratio by weight). *Top panels*, Western blots (*WB*) of streptavidin agarose-bound transporters. *T*, total transporter; *B*, biotinylated transporter; *NB*, non-biotinylated transporter. Biotinylated bands were quantified by densitometry. Tubulin is shown as a non-biotinylated protein control. Surface GlyT2 (100 kDa band, *arrow*) expression is represented in the *middle panel* as *black bars* together with glycine transport (*white bars*). 100% glycine transport was 2.8 ± 0.3 nmol/mg of protein/10 min (mean ± S.E. (*error bars*)). Western blot membranes were reprobed for CNX to verify overexpression, and the CNX bands quantified and normalized to tubulin are shown in the *lower graphs* in *A* and *B*: **, $p < 0.01$; ***, $p < 0.001$ (ANOVA with Tukey's post-hoc test compared with the control with no overexpressed CNX: *CNX 0*).

0.26 ± 0.03; Fig. 6*B*). Remarkably, when the wild-type and mutant transporters were co-expressed, the stronger co-localization of S512R/CNX relative to wild type/CNX that was observed when the transporters were expressed alone with CNX (Fig. 3) was barely or not evident (see "Discussion").

To determine whether CNX overexpression could rescue the function of wild-type GlyT2 from the dominant negative effect of S512R, untagged transporters were expressed alone or together at a 1:1 ratio (which we expect to mimic heterozygosis) in the presence of increasing concentrations of CNX, assessing membrane expression and glycine transport in these cells (Fig. 7). The amount of CNX was monitored by densitometry and normalized to tubulin immunoreactivity (*bottom histograms*). The capacity of the S512R mutant to form a functional transporter with mature glycosylation could not be rescued by CNX despite a 3-fold increase in the amount of 75-kDa S512R that was detected. By contrast, an increase in the concentration of CNX produced partial rescue of the function and membrane expression of wild-type GlyT2 when it was co-transfected with S512R (*right panels*). Interestingly, the recovery of transporter activity was slightly higher than the enhancement of membrane expression, suggesting either more efficient folding of the membrane transporter in the presence of the chaperone (24) or a CNX-induced stimulation of transport activity of unknown nature.

Rescue of Wild-type GlyT2 from the Dominant Negative Effect of the S512R Mutant by Chemical Chaperones—The previous results suggest that treatments increasing the expression or accelerating the processing and membrane translocation of GlyT2 could rescue the dominant negative effect produced by S512R. Folding mutants of some membrane proteins, such as ATP-binding cassette transporters, can be corrected with ligands/substrates (40, 41). Although the pharmacology of GlyT2 is very scarce, we incubated transfected COS7 cells during the protein processing of this transporter (48 h post-transfection) with several glycine analogues known to inhibit GlyT2 transport to some extent (42). Only glycine produced some rescue (27.3 ± 5.1% of transport and 10.1 ± 2.6% of mature transporter; Fig. 8*A*), although a minor effect was also detected with glycine methyl ester. Conversely, neither the specific GlyT2

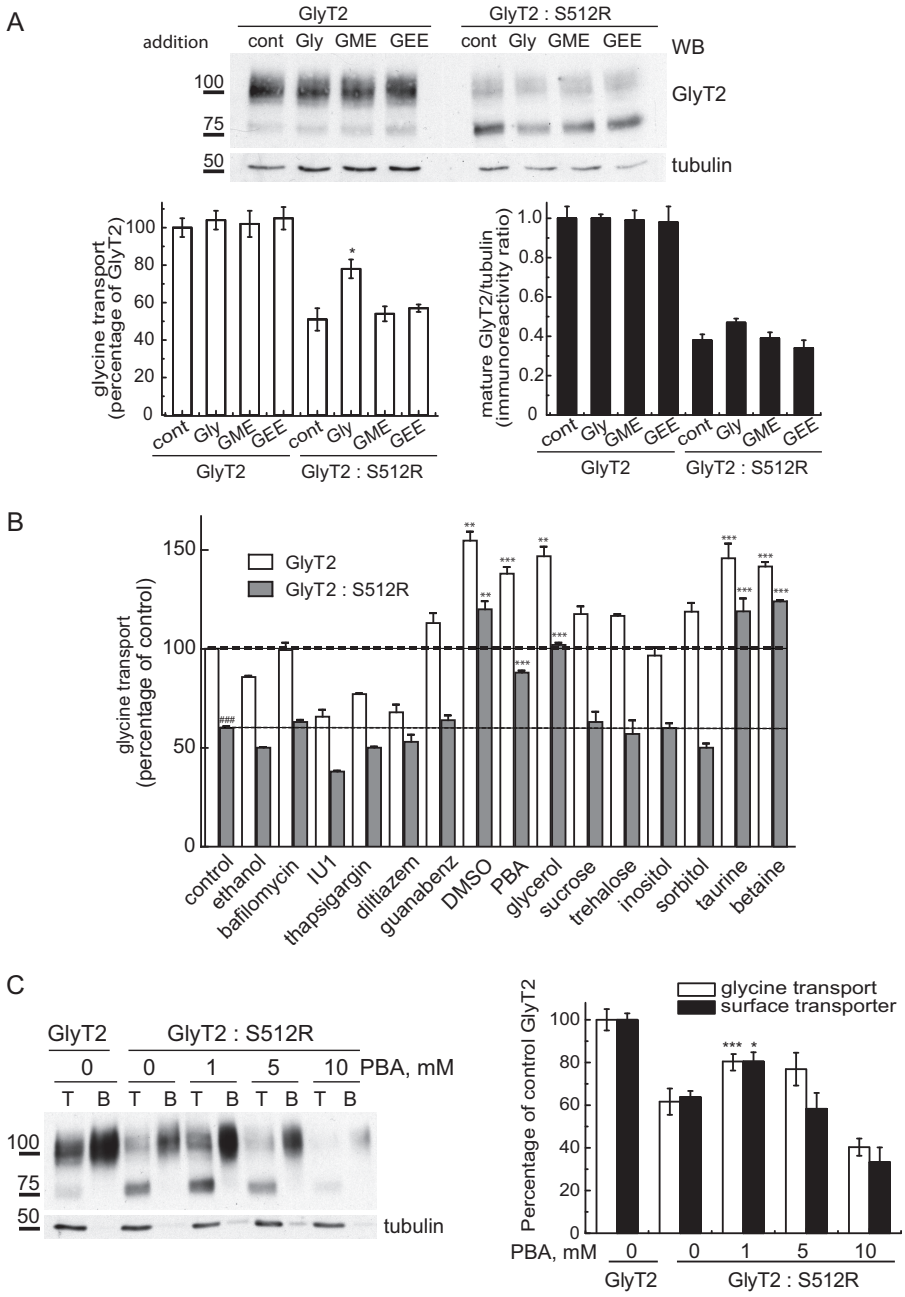

FIGURE 8. **Chemical chaperones rescue the wild-type transporter from the dominant negative effect of S512R.** *A*, COS7 cells expressing wild-type GlyT2 alone or co-expressed with S512R in a 1:1 ratio were incubated for 72 h (before and during transporter biogenesis) with 5 mM glycine (*Gly*), glycine methyl ester (*GME*), or glycine ethyl ester (*GEE*), and 48 h post-transfection, they were analyzed in Western blots (*WB*) and for glycine transport. *Top*, Western blots probed for GlyT2 and tubulin as a loading control. *Bottom right*, densitometry of the 100-kDa mature GlyT2 band normalized to tubulin immunoreactivity. *Bottom left*, glycine transport relative to the control GlyT2 (alone), 100% glycine transport 2.7 ± 0.4 nmol/mg of protein/10 min (mean ± S.E. (*error bars*)): ###, $p < 0.001$ (Student's *t* test compared with GlyT2 alone); **, $p < 0.01$; ***, $p < 0.001$ (ANOVA with Tukey's post hoc test compared with control GlyT2/S512R). *B*, conditions identical to those in *A*, except the cells were incubated with 200 nM bafilomycin, 50 μM IU1, 1 μM thapsigargin dissolved in ethanol (vehicle), 20 μM diltiazem, 5 mM guanabenz, 1% DMSO, 1 mM PBA, 1% glycerol, 100 mM sucrose, trehalose, inositol, sorbitol, taurine, and betaine. *C*, conditions identical to those in *A*, except the cells were incubated with increasing concentrations of PBA and subjected to surface biotinylation. *Left*, Western blot after biotinylation; *right*, glycine transport (relative to GlyT2 alone: 2.1 ± 0.3 nmol/mg of protein/10 min, mean ± S.E.) and surface GlyT2 densitometry (means ± S.E.).

inhibitor ALX1393 nor sarcosine, a GlyT1-specific substrate, could provoke significant rescue (data not shown). We next assessed general chemical chaperones, drugs that can aid the folding of membrane proteins and accelerate their trafficking to the membrane. These compounds belong to three main classes of osmolytes (43): carbohydrates (glycerol, sorbitol, and inositol); amino acids and derivatives (glycine, taurine, alanine, and proline); and methylamines (betaine and trimethylamine *N*-oxide). Hence, we tested several representatives of each class, together with substances that influence cell proteostasis and other more generally accepted chemical chaperones: sodium 4-phenylbutyrate (PBA) (44) and the autophagy inducer trehalose (45). Like CNX, no compound produced any effect on S512R expressed alone; however, the transport activity of wild-type GlyT2 when expressed alone or together with S512R was significantly stimulated (increases of 40–60%) by dimethyl

sulfoxide (DMSO), PBA, glycerol, taurine, and betaine. Thus, the wild-type GlyT2 was rescued from the dominant negative effect of S512R (Fig. 8*B*). Of these compounds, DMSO and glycerol produced some toxicity on the cells (not shown), whereas taurine and betaine were effective at very high concentrations (100 mM). By contrast, the maximal effect of PBA was observed at 1 mM, and it produced an increase in glycine transport (40.6 ± 9.6%, mean ± S.E.) and membrane expression of the active transporter (38.1 ± 9.5%, mean ± S.E.) comparable with CNX (Fig. 8*C*). In addition, no toxic effects on COS7 cells were detected, as would be expected for a compound approved by the United States Food and Drug Administration for use in humans (46).

In light of these data, we assayed this compound in primary cortical neurons, which displayed robust surface co-localization of two differentially tagged wild-type transporters (GFP-GlyT2 and RFP-GlyT2). However, GFP-GlyT2 and RFP-S512 co-expression in these cells reproduced the dominant negative effect observed in non-neural cells, with strong intracellular staining of both transporters and reduced surface expression of the wild-type GlyT2 (Fig. 9*A*). Indeed, when the dominant negative effect detected in neurons was quantified, it was comparable with that observed in COS7 cells (Fig. 9*B*). It is noteworthy that the size of the immature and mature GlyT2 was barely distinguishable in Western blots of neurons, probably due to neuron-specific patterns of glycosylation.[4] Nevertheless, the expression was strong enough to measure robust transport activity in the presence of the GlyT1 inhibitor NFPS (about 5 and 1.3 nmol of glycine/mg of protein/7 min in GlyT2 and mock-transfected neurons, respectively). The expression of the wild-type and mutant transporters at a 1:1 ratio reduced GlyT2 membrane expression to 34.1 ± 5.3 and glycine transport to 42.5 ± 4.1% (mean ± S.E.). Moreover, a further increase in the concentration of the co-expressed mutant provoked an additional decrease in transporter expression and function. Remarkably, PBA (1 mM) promoted significant rescue of this effect and restored both membrane expression (92.6 ± 8.6%) and glycine transport (86.1 ± 8.4%) of the active GlyT2 co-expressed with the mutant in these primary neurons. Thus, for the first time, our results show the possibility of overcoming the dominant negative effect of the S512R mutant in a neuronal preparation.

DISCUSSION

In this report, we have verified and characterized the dominant negative effect of the S512R mutant of GlyT2, whose co-expression with the wild-type transporter provokes a considerable reduction in glycine transport and prevents it from reaching the plasma membrane, both in COS7 cells and in primary cortical neurons.

S512R is a folding-defective mutant that does not produce a mature transporter; rather, the immature transporter is retained in the ER. Its apparent molecular weight and glycosidase sensitivity indicates its processing is arrested after receiving the first preassembled glycans, transferred by the oligosaccharyltransferase to the Asn-*X*-Ser/Thr consensus sites from the lipid dolichol-pyrophosphate donor in the ER membrane. The glycans are then rapidly trimmed in a co-translational manner by the sequential action of glucosidases I and II to generate monoglucosylated side chains that support binding to lectin chaperones like CNX (47). For this reason, S512R is a preferred substrate for CNX, and its association with the chaperone is stronger than that of the wild-type transporter, as witnessed by co-immunoprecipitation and fluorescence co-immunolocalization. This association provokes the ER retention of the mutant transporter. Retention of misfolded proteins in the ER leads to their polychain ubiquitination, a signal for degradation by the 26 S proteasome through ERAD. Our results indicate that CNX-retained S512R is targeted for ERAD because it is more intensely ubiquitinated than the wild-type GlyT2 and it has a much shorter half-life. The fact that CNX overexpression cannot rescue the mutant indicates that chaperone binding precedes degradation and not maturation, as occurs in the wild type.

Misfolding of S512R seems to be due to the introduction of the large positive charged arginine rather than the removal of the serine. Two additional hyperekplexia-associated missense mutations have been identified in the same TM7 region, both predicting clashes or disturbances of crucial residues involved in Na1 and Cl^- coordination (N511S and S515I, rat position numbering) (10, 12). Hence, substitutions in this important region alter the protein's function, although only severe structural alterations may provoke its misfolding. This suggests that Ser-512, which is located at the membrane-exposed surface of the transporter, may expose motifs (hydrophobic patches or unpaired cysteines) involved in chaperone binding when replaced by arginine. In the recently modeled *Drosophila* DAT, the serine homologous to Ser-512 is situated in a groove between TM5 and TM7, where a cholesterol molecule is bound to the transporter. Therefore, Ser-512, although not directly involved in the binding of cholesterol, is shielded by the bound cholesterol molecule, and it may influence the binding site. A modulatory role in maintaining an outward-open state of the transporter has been proposed for the cholesterol-binding site (19). As in DAT, the GlyT2 transport is modulated by cholesterol, and the transporter displays optimal transport activity when included in lipid rafts (31). The modulation of transport by cholesterol suggests a connection between the cholesterol binding site and the substrate binding site. New data from the DAT crystal suggested that the bound cholesterol molecule modulates the movement of TM1a that occurs during the transport cycle. TM1a is connected to internal loop 1, which in turn is hydrogen-bonded to the C-terminal latch of the transporter. In several SLC6 members, this region contains the binding site for the cargo receptor of the COPII complex Sec24 that permits ER export (26, 39), and C-terminal deletion mutants of GlyT2 are retained in the ER (32). We have demonstrated that the interaction of wild-type GlyT2 with Sec24D is altered in the S512R mutant. Although this alteration has to be confirmed with endogenous Sec24D in neural preparations, we hypothesize that the S512R mutation causes structural distortion of the cholesterol modulatory region that is transmitted to the C-terminal latch and that somehow influences the interaction with

[4] E. Arribas-González, J. de Juan-Sanz, C. Aragón, and B. López-Corcuera, unpublished results.

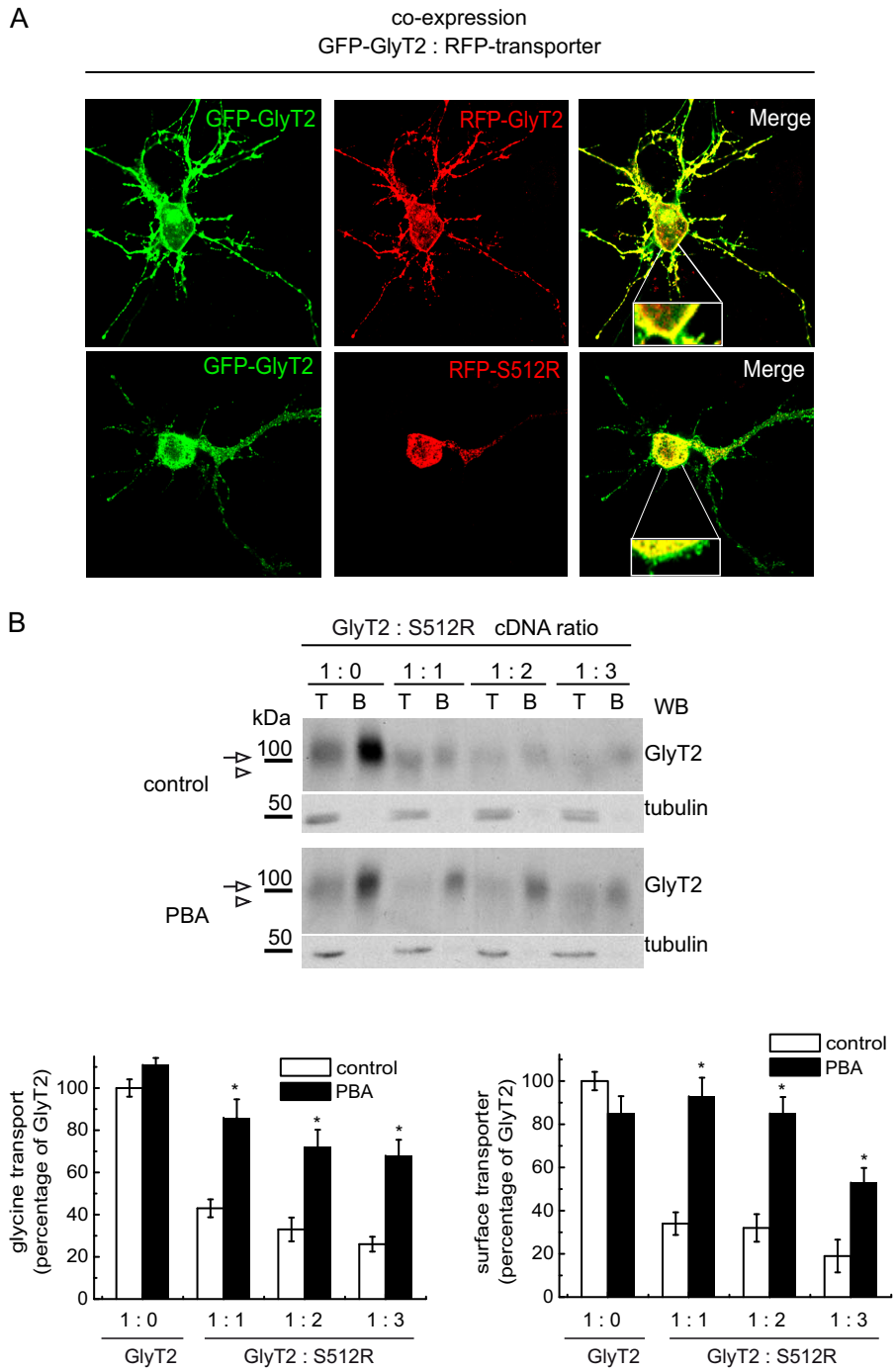

FIGURE 9. **PBA rescues the wild-type transporter from the dominant negative effect of S512R in primary neurons.** *A*, confocal microscopy images of cortical neurons co-expressing the indicated tagged transporters. GFP-GlyT2 or RFP transporters were detected with the corresponding anti-tag antibody and are shown in *green* or *red*, respectively. *B*, cortical neurons maintained *in vitro* for 7 days were transfected with wild-type GlyT2 cDNA alone or with increasing amounts of S512R cDNA to reach the indicated GlyT2/S512R cDNA ratios (by weight). The cells were treated 4 h post-transfection with 1 mM PBA or with the vehicle alone (Neurobasal/B27 culture medium) and subjected to biotinylation and glycine transport determination. *Top*, Western blot after biotinylation. Mature GlyT2 bands are indicated with an *arrow*. An *arrowhead* indicates the position of the immature transporter. *T*, total transporter; *B*, biotinylated transporter. Tubulin immunoreactivity is shown as a non-biotinylated protein control. Bands were quantified by densitometry, and biotinylated GlyT2 is represented in the *right histogram*. *Left histogram*, glycine transport relative to GlyT2 alone (100% glycine transport, 3.2 ± 0.5 nmol/mg protein/10 min; mean ± S.E.): *, $p < 0.05$ (ANOVA with Tukey's post hoc test compared with the absence of PBA). *WB*, Western blot.

COPII to provoke its retention in the ER. It is tempting to speculate that cholesterol binding to the mutant might be impaired, although this could not be proven in our hands due to the effects of altering cholesterol concentrations on the proteostasis of the cells (data not shown) (50).

In this study, we have also shown that wild-type GlyT2 forms oligomers with the S512R mutant and that this interaction is more stable than its binding to other wild-type molecules. This interaction mainly takes place in the ER, such that ER retention of the wild-type/mutant oligomers prevents the progression of

GlyT2 through the secretory pathway and explains the dominant negative behavior of the mutant. CNX overexpression rescues this effect, suggesting that the wild-type and mutant isoforms compete for binding to the chaperone, which may facilitate the selective transport of the wild-type folded transporter to the plasma membrane (24). The fact that the association of S512R with the wild-type GlyT2 is diminished in the presence of overexpressed CNX, despite its more persistent binding to CNX and its enhanced association with the wild-type isoform, sustains the selective role of the chaperone. GlyT2 oligomerization was previously shown after transporter cross-linking (49). Our data confirm that oligomer formation is required for ER export, as demonstrated for other SLC6 transporters (26). Therefore, the immature GlyT2 forms appear to bind to CNX prior to the formation of oligomers, and they are subsequently exported from the ER to continue transporter maturation.

Chemical chaperones are non-selective small molecules that stabilize mutant proteins and accelerate their membrane trafficking, reminiscent of the chaperoning function of intracellular molecular chaperones (43). Due to this activity, chemical chaperones may potentially have therapeutic value to improve ER stress-related pathologies (41). Most chemical chaperones are osmotically active, such that they equilibrate cellular osmotic pressure during ER crowding. Here, the effect of chemical chaperones in the rescue of GlyT2 was analyzed in cultured cells and transfected cortical neurons. According to CNX action, no effect of any of these compounds was seen on S512R expressed alone. However, the influence of these molecules on the dominant negative effect of the mutant allows us to speculate on the conditions that might favor correct GlyT2 folding. The calcium concentration seems not to be critical for GlyT2 folding because no significant effect was observed in the presence of compounds that reduce (thapsigargin) or increase (diltiazem) ER calcium levels. Conversely, substantial rescue was detected with the antioxidant molecule DMSO, in agreement with the high number of cysteines present in GlyT2. The osmotically active compounds glycerol, taurine, and betaine promote significant rescue, suggesting that some ER crowding takes place. Moreover, although we found no protein kinase-like endoplasmic reticulum kinase phosphorylation, we did detect some increase in BiP expression (2.3 $\pm$ 0.4-fold), suggesting some enhancement of the unfolded protein response (50) when the mutant was expressed or co-expressed with the wild type. However, no effect was observed for activators of the proteasome (IU1) (44) or autophagy (trehalose) (45) or inhibitors of bulk aggregation (guanabenz) (44). Still, our data did indicate that PBA produces significant rescue in mild conditions that produce no toxic effects, both in COS7 cells and in cultured neurons. PBA increases GlyT2 transport activity and plasma membrane expression by fulfilling chaperone-like activity, as proven for other misfolded pathogenic proteins (44, 51). PBA is an interesting compound because not only is it a chemical chaperone approved by the Food and Drug Administration for use in humans, but it can also pass across the blood-brain barrier, and it has been implicated as a protective agent in neurodegenerative diseases involving ER stress (52). Therefore, PBA may potentially rescue the dominant negative effect of GlyT2 mutants inherited in heterozygosis, positively affecting glycinergic neural transmission by accelerating membrane trafficking of GlyT2. Our results support the possibility that selective pharmacoperones (17) that may enter cells and may bind specifically to misfolded mutant GlyT2, correct its folding, and allow correct routing have potential therapeutic effects in hyperekplexia. However, further work along these lines must be carried out to confirm this hypothesis.

Acknowledgments—We thank Francisco Zafra, Jose Antonio Esteban, José María Requena, and Pablo Alonso-Torres (Centro de Biología Molecular Severo Ochoa) for generously providing the Myc-Sec24D, Myc-p35, and HA-GlyT2 constructs in pcDNA3, the pRFP vector, the in-house RFP antibody, and S512R in pcDNA3, respectively. The expert technical assistance of Enrique Núñez is also acknowledged. We are grateful to the confocal microscopy facility at the Centro de Biología Molecular Severo Ochoa for valuable and expert help with the confocal microscopy work.

REFERENCES

1. Aragón, C., and López-Corcuera, B. (2003) Structure, function and regulation of glycine neurotransporters. *Eur. J. Pharmacol.* **479,** 249–262
2. Gomeza, J., Ohno, K., Hülsmann, S., Armsen, W., Eulenburg, V., Richter, D. W., Laube, B., and Betz, H. (2003) Deletion of the mouse glycine transporter 2 results in a hyperekplexia phenotype and postnatal lethality. *Neuron* **40,** 797–806
3. Aragón, C., and López-Corcuera, B. (2005) Glycine transporters: crucial roles of pharmacological interest revealed by gene deletion. *Trends Pharmacol. Sci.* **26,** 283–286
4. Rousseau, F., Aubrey, K. R., and Supplisson, S. (2008) The glycine transporter GlyT2 controls the dynamics of synaptic vesicle refilling in inhibitory spinal cord neurons. *J. Neurosci.* **28,** 9755–9768
5. Apostolides, P. F., and Trussell, L. O. (2013) Rapid, activity-independent turnover of vesicular transmitter content at a mixed glycine/GABA synapse. *J. Neurosci.* **33,** 4768–4781
6. Bakker, M. J., van Dijk, J. G., van den Maagdenberg, A. M., and Tijssen, M. A. (2006) Startle syndromes. *Lancet Neurol.* **5,** 513–524
7. Bakker, M. J., van Dijk, J. G., van den Maagdenberg, A. M., and Tijssen, M. A. (2006) Startle syndromes. *Lancet Neurol.* **5,** 513–524
8. Harvey, R. J., Topf, M., Harvey, K., and Rees, M. I. (2008) The genetics of hyperekplexia: more than startle!. *Trends Genet.* **24,** 439–447
9. Harvey, R. J., and Yee, B. K. (2013) Glycine transporters as novel therapeutic targets in schizophrenia, alcohol dependence and pain. *Nat. Rev. Drug Discov.* **12,** 866–885
10. Rees, M. I., Harvey, K., Pearce, B. R., Chung, S. K., Duguid, I. C., Thomas, P., Beatty, S., Graham, G. E., Armstrong, L., Shiang, R., Abbott, K. J., Zuberi, S. M., Stephenson, J. B., Owen, M. J., Tijssen, M. A., van den Maagdenberg, A. M., Smart, T. G., Supplisson, S., and Harvey, R. J. (2006) Mutations in the gene encoding GlyT2 (SLC6A5) define a presynaptic component of human startle disease. *Nat. Genet.* **38,** 801–806
11. Eulenburg, V., Becker, K., Gomeza, J., Schmitt, B., Becker, C. M., and Betz, H. (2006) Mutations within the human GLYT2 (SLC6A5) gene associated with hyperekplexia. *Biochem. Biophys. Res. Commun.* **348,** 400–405
12. Carta, E., Chung, S. K., James, V. M., Robinson, A., Gill, J. L., Remy, N., Vanbellinghen, J. F., Drew, C. J., Cagdas, S., Cameron, D., Cowan, F. M., Del Toro, M., Graham, G. E., Manzur, A. Y., Masri, A., Rivera, S., Scalais, E., Shiang, R., Sinclair, K., Stuart, C. A., Tijssen, M. A., Wise, G., Zuberi, S. M., Harvey, K., Pearce, B. R., Topf, M., Thomas, R. H., Supplisson, S., Rees, M. I., and Harvey, R. J. (2012) Mutations in the GlyT2 gene (*SLC6A5*) are a second major cause of startle disease. *J. Biol. Chem.* **287,** 28975–28985
13. Giménez, C., Pérez-Siles, G., Martínez-Villarreal, J., Arribas-González, E., Jiménez, E., Núñez, E., de Juan-Sanz, J., Fernández-Sánchez, E., García-Tardón, N., Ibáñez, I., Romanelli, V., Nevado, J., James, V. M., Topf, M.,

Chung, S. K., Thomas, R. H., Desviat, L. R., Aragón, C., Zafra, F., Rees, M. I., Lapunzina, P., Harvey, R. J., and López-Corcuera, B. (2012) A novel dominant hyperekplexia mutation Y705C alters trafficking and biochemical properties of the presynaptic glycine transporter GlyT2. *J. Biol. Chem.* **287,** 28986–29002
14. Kanner, B. I., and Zomot, E. (2008) Sodium-coupled neurotransmitter transporters. *Chem. Rev.* **108,** 1654–1668
15. Rudnick, G., Krämer, R., Blakely, R. D., Murphy, D. L., and Verrey, F. (2014) The SLC6 transporters: perspectives on structure, functions, regulation, and models for transporter dysfunction. *Pflugers Arch.* **466,** 25–42
16. Pérez-Siles, G., Núñez, E., Morreale, A., Jiménez, E., Leo-Macías, A., Pita, G., Cherubino, F., Sangaletti, R., Bossi, E., Ortíz, A. R., Aragón, C., and López-Corcuera, B. (2012) An aspartate residue in the external vestibule of GLYT2 (glycine transporter 2) controls cation access and transport coupling. *Biochem. J.* **442,** 323–334
17. Conn, P. M., and Janovick, J. A. (2009) Drug development and the cellular quality control system. *Trends Pharmacol. Sci.* **30,** 228–233
18. Yamashita, A., Singh, S. K., Kawate, T., Jin, Y., and Gouaux, E. (2005) Crystal structure of a bacterial homologue of Na^+/Cl^--dependent neurotransmitter transporters. *Nature* **437,** 215–223
19. Penmatsa, A., Wang, K. H., and Gouaux, E. (2013) X-ray structure of dopamine transporter elucidates antidepressant mechanism. *Nature* **503,** 85–90
20. Núñez, E., Alonso-Torres, P., Fornés, A., Aragón, C., and López-Corcuera, B. (2008) The neuronal glycine transporter GLYT2 associates with membrane rafts: functional modulation by lipid environment. *J. Neurochem.* **105,** 2080–2090
21. Park, E., and Rapoport, T. A. (2012) Mechanisms of Sec61/SecY-mediated protein translocation across membranes. *Annu. Rev. Biophys.* **41,** 21–40
22. Rutkevich, L. A., and Williams, D. B. (2011) Participation of lectin chaperones and thiol oxidoreductases in protein folding within the endoplasmic reticulum. *Curr. Opin. Cell Biol.* **23,** 157–166
23. Martinez-Maza, R., Poyatos, I., Lopez-Corcuera, B., Núñez, E., Giménez, C., Zafra, F., and Aragón, C. (2001) The role of *N*-glycosylation in transport to the plasma membrane and sorting of the neuronal glycine transporter GLYT2. *J. Biol. Chem.* **276,** 2168–2173
24. Arribas-González, E., Alonso-Torres, P., Aragón, C., and López-Corcuera, B. (2013) Calnexin-assisted biogenesis of the neuronal glycine transporter 2 (GlyT2). *PLoS One* **8,** e63230
25. Farhan, H., Freissmuth, M., and Sitte, H. H. (2006) Oligomerization of neurotransmitter transporters: a ticket from the endoplasmic reticulum to the plasma membrane. *Handb. Exp. Pharmacol.* 233–249
26. Chiba, P., Freissmuth, M., and Stockner, T. (2014) Defining the blanks: pharmacochaperoning of SLC6 transporters and ABC transporters. *Pharmacol. Res.* **83,** 63–73
27. Brown, T. C., Correia, S. S., Petrok, C. N., and Esteban, J. A. (2007) Functional compartmentalization of endosomal trafficking for the synaptic delivery of AMPA receptors during long-term potentiation. *J. Neurosci.* **27,** 13311–13315
28. Liu, Q. R., López-Corcuera, B., Mandiyan, S., Nelson, H., and Nelson, N. (1993) Cloning and expression of a spinal cord- and brain-specific glycine transporter with novel structural features. *J. Biol. Chem.* **268,** 22802–22808
29. Jimenez, E., Zafra, F., Perez-Sen, R., Delicado, E. G., Miras-Portugal, M. T., Aragon, C., and Lopez-Corcuera, B. (2011) P2Y purinergic regulation of the glycine neurotransmitter transporters *J. Biol. Chem.* **286,** 10712–10724
30. Geerlings, A., Núñez, E., Rodenstein, L., López-Corcuera, B., and Aragón, C. (2002) Glycine transporter isoforms show differential subcellular localization in PC12 cells. *J. Neurochem.* **82,** 58–65
31. de Juan-Sanz, J., Zafra, F., López-Corcuera, B., and Aragón, C. (2011) Endocytosis of the neuronal glycine transporter GLYT2: role of membrane rafts and protein kinase C-dependent ubiquitination. *Traffic* **12,** 1850–1867
32. Fernández-Sánchez, E., Díez-Guerra, F. J., Cubelos, B., Giménez, C., and Zafra, F. (2008) Mechanisms of endoplasmic-reticulum export of glycine transporter-1 (GLYT1). *Biochem. J.* **409,** 669–681
33. de Juan-Sanz, J., Núñez, E., Villarejo-López, L., Pérez-Hernández, D., Rodriguez-Fraticelli, A. E., López-Corcuera, B., Vázquez, J., and Aragón, C. (2013) Na^+/K^+-ATPase is a new interacting partner for the neuronal glycine transporter GlyT2 that downregulates its expression *in vitro* and *in vivo*. *J. Neurosci.* **33,** 14269–14281
34. Bolte, S., and Cordelières, F. P. (2006) A guided tour into subcellular colocalization analysis in light microscopy. *J. Microsc.* **224,** 213–232
35. Zafra, F., Gomeza, J., Olivares, L., Aragón, C., and Giménez, C. (1995) Regional distribution and developmental variation of the glycine transporters GLYT1 and GLYT2 in the rat CNS. *Eur. J. Neurosci.* **7,** 1342–1352
36. Núñez, E., Pérez-Siles, G., Rodenstein, L., Alonso-Torres, P., Zafra, F., Jiménez, E., Aragón, C., and López-Corcuera, B. (2009) Subcellular localization of the neuronal glycine transporter GLYT2 in brainstem. *Traffic* **10,** 829–843
37. de Juan-Sanz, J., Núñez, E., López-Corcuera, B., and Aragón, C. (2013) Constitutive endocytosis and turnover of the neuronal glycine transporter GlyT2 is dependent on ubiquitination of a C-terminal lysine cluster. *PLoS One* **8,** e58863
38. Nakatsukasa, K., and Brodsky, J. L. (2008) The recognition and retrotranslocation of misfolded proteins from the endoplasmic reticulum. *Traffic* **9,** 861–870
39. Sucic, S., Koban, F., El-Kasaby, A., Kudlacek, O., Stockner, T., Sitte, H. H., and Freissmuth, M. (2013) Switching the clientele: a lysine residing in the C terminus of the serotonin transporter specifies its preference for the coat protein complex II component SEC24C. *J. Biol. Chem.* **288,** 5330–5341
40. Pettit, R. S. (2012) Cystic fibrosis transmembrane conductance regulator-modifying medications: the future of cystic fibrosis treatment. *Ann. Pharmacother.* **46,** 1065–1075
41. Leidenheimer, N. J., and Ryder, K. G. (2014) Pharmacological chaperoning: a primer on mechanism and pharmacology. *Pharmacol. Res.* **83,** 10–19
42. López-Corcuera, B., Vázquez, J., and Aragón, C. (1991) Purification of the sodium- and chloride-coupled glycine transporter from central nervous system. *J. Biol. Chem.* **266,** 24809–24814
43. Engin, F., and Hotamisligil, G. S. (2010) Restoring endoplasmic reticulum function by chemical chaperones: an emerging therapeutic approach for metabolic diseases. *Diabetes Obes. Metab.* **12,** 108–115
44. Lindquist, S. L., and Kelly, J. W. (2011) Chemical and biological approaches for adapting proteostasis to ameliorate protein misfolding and aggregation diseases: progress and prognosis. *Cold Spring Harb. Perspect. Biol.* 10.1101/cshperspect.a004507
45. Ghavami, S., Shojaei, S., Yeganeh, B., Ande, S. R., Jangamreddy, J. R., Mehrpour, M., Christoffersson, J., Chaabane, W., Moghadam, A. R., Kashani, H. H., Hashemi, M., Owji, A. A., and Łos, M. J. (2014) Autophagy and apoptosis dysfunction in neurodegenerative disorders. *Prog. Neurobiol.* **112,** 24–49
46. Iannitti, T., and Palmieri, B. (2011) Clinical and experimental applications of sodium phenylbutyrate. *Drugs R. D.* **11,** 227–249
47. Merulla, J., Fasana, E., Soldà, T., and Molinari, M. (2013) Specificity and regulation of the endoplasmic reticulum-associated degradation machinery. *Traffic* **14,** 767–777
48. Deleted in proof
49. Bartholomäus, I., Milan-Lobo, L., Nicke, A., Dutertre, S., Hastrup, H., Jha, A., Gether, U., Sitte, H. H., Betz, H., and Eulenburg, V. (2008) Glycine transporter dimers: evidence for occurrence in the plasma membrane. *J. Biol. Chem.* **283,** 10978–10991
50. Ron, D., and Walter, P. (2007) Signal integration in the endoplasmic reticulum unfolded protein response. *Nat. Rev. Mol. Cell Biol.* **8,** 519–529
51. Fujiwara, M., Yamamoto, H., Miyagi, T., Seki, T., Tanaka, S., Hide, I., and Sakai, N. (2013) Effects of the chemical chaperone 4-phenylbutylate on the function of the serotonin transporter (SERT) expressed in COS-7 cells. *J. Pharmacol. Sci.* **122,** 71–83
52. Ozcan, L., Ergin, A. S., Lu, A., Chung, J., Sarkar, S., Nie, D., Myers, M. G., Jr., and Ozcan, U. (2009) Endoplasmic reticulum stress plays a central role in development of leptin resistance. *Cell Metab.* **9,** 35–51

Artículo #3

de Juan-Sanz J, Núñez E, Zafra F, Berrocal M, Corbacho I, Ibáñez I, **Arribas-González E**, Marcos D, López-Corcuera B, Mata A.M. and Aragón C (2014)

Presynaptic control of glycine transporter 2 (GlyT2) by physical and functional association with plasma membrane Ca2+-ATPase (PMCA) and Na+-Ca2+ exchanger (NCX)

J Biol Chem 289(49):34308-24

THE JOURNAL OF BIOLOGICAL CHEMISTRY VOL. 289, NO. 49, pp. 34308–34324, December 5, 2014

Presynaptic Control of Glycine Transporter 2 (GlyT2) by Physical and Functional Association with Plasma Membrane Ca^{2+}-ATPase (PMCA) and Na^{+}-Ca^{2+} Exchanger (NCX)*

Received for publication, June 5, 2014, and in revised form, September 29, 2014 Published, JBC Papers in Press, October 14, 2014, DOI 10.1074/jbc.M114.586966

Jaime de Juan-Sanz[‡], Enrique Núñez[§¶‖], Francisco Zafra[§¶‖], María Berrocal[**], Isaac Corbacho[**], Ignacio Ibáñez[§¶‖], Esther Arribas-González[§¶‖], Daniel Marcos[**], Beatriz López-Corcuera[§¶‖], Ana M. Mata[**], and Carmen Aragón[§¶‖1]

From the [‡]Department of Biochemistry, Weill Cornell Medical College, New York, New York 10065, the [§]Centro de Biología Molecular "Severo Ochoa," Universidad Autónoma de Madrid, Consejo Superior de Investigaciones Científicas, 28049-Madrid, Spain, the [¶]Centro de Investigación Biomédica en Red de Enfermedades Raras, ISCIII, 46009-Valencia, Spain, the [‖]IdiPAZ-Hospital, Universitario La Paz, 28046-Madrid, Spain, and the [**]Departamento de Bioquímica y Biología Molecular y Genética, Facultad de Ciencias, Universidad de Extremadura, 06006-Badajoz, Spain

Background: GlyT2 is crucial for glycinergic neurotransmission, but only a few interacting partners for this protein are known.
Results: PMCA2/3 and NCX1 interact with GlyT2 and modulate its activity in lipid raft subdomains.
Conclusion: Functional interaction of GlyT2 with PMCA2/3 and NCX1 helps Na^{+} and Ca^{2+} local homeostasis in glycinergic terminals.
Significance: Learning how GlyT2 is regulated might help with developing new therapies for hyperekplexia or neuropathic pain.

Fast inhibitory glycinergic transmission occurs in spinal cord, brainstem, and retina to modulate the processing of motor and sensory information. After synaptic vesicle fusion, glycine is recovered back to the presynaptic terminal by the neuronal glycine transporter 2 (GlyT2) to maintain quantal glycine content in synaptic vesicles. The loss of presynaptic GlyT2 drastically impairs the refilling of glycinergic synaptic vesicles and severely disrupts neurotransmission. Indeed, mutations in the gene encoding GlyT2 are the main presynaptic cause of hyperekplexia in humans. Here, we show a novel endogenous regulatory mechanism that can modulate GlyT2 activity based on a compartmentalized interaction between GlyT2, neuronal plasma membrane Ca^{2+}-ATPase (PMCA) isoforms 2 and 3, and Na^{+}/Ca^{2+}-exchanger 1 (NCX1). This GlyT2·PMCA2,3·NCX1 complex is found in lipid raft subdomains where GlyT2 has been previously found to be fully active. We show that endogenous PMCA and NCX activities are necessary for GlyT2 activity and that this modulation depends on lipid raft integrity. Besides, we propose a model in which GlyT2·PMCA2–3·NCX complex would help Na^{+}/K^{+}-ATPase in controlling local Na^{+} increases derived from GlyT2 activity after neurotransmitter release.

Glycine is a major inhibitory neurotransmitter of the CNS that acts in neuronal circuits of the central auditory pathway, receptive fields in the retina, and spinal cord-sensitive pathways. Glycinergic synaptic inhibition is terminated by two sodium- and chloride-coupled transporters, GlyT1[2] and GlyT2, located in the glial plasma membrane and presynaptic terminals, respectively (1, 2). Additionally, GlyT2 transport activity supplies glycine for presynaptic vesicle refilling, a process that is absolutely necessary to preserve quantal glycine content in synaptic vesicles (3–5). GlyT2 activity dysfunctions reduce presynaptic glycine release and cause significant lacking of inhibitory glycinergic neurotransmission. In humans, this situation causes hyperekplexia or startle disease, a rare disease that is characterized by an exaggerated startle response, usually evoked by tactile or auditory stimuli, leading to hypertonia and apnea episodes that in some cases produce sudden infant death (6–8). GlyT2 has a crucial role in the pathophysiology of inhibitory glycinergic neurotransmission, and studying modulatory factors that regulate its activity might help the success of future therapies. Indeed, studies of endogenous GlyT2 regulatory mechanisms have revealed that GlyT2 activity is regulated by PKC activation (9, 10), lipid raft environment (10, 11), P2Y purinergic receptors (12), ubiquitination (13), calnexin function (14), or Na^{+}/K^{+}-ATPase interaction (15). In addition, we have also described that GlyT2 exocytosis is regulated by syntaxin-1A and calcium (Ca^{2+}) increases (16). Ca^{2+} ions are widely known essential regulators of synaptic function because of the following: (*a*) synaptic neurotransmitter release is driven by Ca^{2+} influxes through voltage-gated calcium channels (17, 18), and (*b*) Ca^{2+} ions have an important role as secondary

* This work was supported by Spanish Dirección General de Investigación Científica y Técnica Grants SAF2008-05436 and SAF2011-28674, Fondo de Investigaciones Sanitarias (Centro de Investigación Biomédica en Red de Enfermedades Raras) and Fundación Ramón Areces (to C. A. and B. L. C.), and Ministerio de Economía y Competitividad, Junta de Extremadura, and Fondo Europeo de Desarrollo Regional Grants BFU2011-23313 from (to A. M. M.).
[1] To whom correspondence should be addressed: Centro de Biología Molecular "Severo Ochoa," Universidad Autónoma de Madrid, 28049-Madrid, Spain. Tel.: 34-91-1964632; Fax: 34-91-1964420; E-mail: caragon@cbm.csic.es.

[2] The abbreviations used are: GlyT1, glycine transporter 1; GlyT2, glycine transporter 2; PMCA, plasma membrane Ca^{2+}-ATPase; NCX, Na^{+}-Ca^{2+} exchanger; NKA, Na^{+}/K^{+}-ATPase; SERCA, sarco(endo)plasmic reticulum; SPCA, secretory pathway; DRM, detergent-resistant membrane; ANOVA, analysis of variance; BAPTA, 1,2-bis(2-aminophenoxy)ethane-*N*,*N*,*N*′,*N*′-tetraacetic acid tetrakis(acetoxymethyl ester); KB-mes, KB-R7943 mesylate; MβCD, methyl-β-cyclodextrin.

messengers in numerous signal transduction processes (19–21). Thus, neurons invest large amounts of energy in controlling and maintaining an abrupt gradient between intracellular (~0.1-μM) and extracellular (~1.4-mM) Ca^{2+} concentrations. Plasma membrane calcium ATPases (PMCAs) have the key biochemical function of extruding cytosolic Ca^{2+} out of the cell (by the spent of ATP) in a calmodulin-stimulated manner (22–24). These Ca^{2+} pumps belong to the P-type ATPase superfamily that also encompasses, for example, the Na^+/K^+-ATPase (NKA) or the Ca^{2+}-ATPases of the sarco(endo)plasmic reticulum (SERCA) (25) and the secretory pathway (SPCA) (26). Four different genes have been described (*ATP2B1–4*) that encode four PMCA isoforms (PMCA1–4), and the average amino acid sequence identity amounts to only about 80% (27, 28). The four PMCA isoforms show differential patterns of expression, with PMCAs 1 and 4 being ubiquitously expressed and PMCAs 2 and 3 being expressed predominantly in the CNS (29, 30). The distribution of PMCA isoforms in isolated DRMs (or lipid rafts) is a point of controversy because in synaptic plasma membranes (SPMs) from pig cerebellum PMCA4 seems to be the only isoform located in raft domains (31), although in primary cortical neurons (32) or hippocampus membranes[3] all isoforms appear to be raft-associated. Recently, Jiang *et al.* (33) have described by quantitative mass spectrometry that the four isoforms are associated with rafts in synaptic plasma membranes from whole rat brain, representing about 60% of the total PMCA. This DRM-associated PMCA pool has been shown to have higher specific activity (32–35) according to the initial proposition that PMCAs are more active when included in these membrane subdomains (36). Similarly, we have described that GlyT2 can be found in DRMs where it displays the highest transport activity (11) suggesting that GlyT2 presence/absence in lipid rafts could be a versatile regulatory mechanism for the transporter (9, 10).

In this study, we have identified neuronal PMCA isoforms 2 and 3 and the Na^+/Ca^{2+} exchanger (NCX1) as new interacting and regulatory partners of GlyT2. We found that GlyT2, PMCA2/3, and NCX1 are co-enriched in neuronal lipid raft membrane clusters. Pharmacological inhibition of PMCA activity by the specific inhibitor caloxin 2a1, as well as specific inhibition of the reverse mode of NCX by KB-R7943 mesylate (KB-mes), led to a marked reduction in GlyT2 activity suggesting that proper Ca^{2+} extrusion in presynaptic terminals is somehow necessary for optimal GlyT2 activity. This PMCA/NCX regulation of GlyT2 depends on lipid raft integrity because lipid raft disruption by methyl-β-cyclodextrin (MβCD) blocks caloxin 2a1 and KB-mes effects and reduces co-localization of NCX and PMCAs with GlyT2. Here, we suggest that the local functional coupling between GlyT2, PMCA2/3, and NCX1 occurs in lipid raft domains and that this association may help in correcting the local imbalance of Na^+ produced during high activity periods of 1glycine-3Na^+ co-transport by GlyT2 after neurotransmitter release. These local increases in cytosolic Na^+ could not be entirely covered by the Na^+/K^+-ATPase activity due to its slow Na^+-extruding rate (200 s^{-1}) (37) forcing NCX to extrude Na^+ at its normal higher speed (5000 s^{-1}) (38, 39) and producing local Ca^{2+} increases that will be amended by PMCA activity.

[3] D. Marcos and A. M. Mata, unpublished data.

EXPERIMENTAL PROCEDURES

Materials

Male Wistar rats were bred under standard conditions at the Centro de Biología Molecular Severo Ochoa in accordance with the current guidelines for the use of animals in research. All animal procedures were approved by the institutional animal care committee and performed according to European Union guidelines (Council Directive 2010/63/EU). Antibodies against GlyT2 were obtained in-house (rabbit and rat (1, 40)), although the other primary antibodies used were as follows: anti-PMCA2, anti-PMCA3, anti-PMCA4, and anti-PMCA (clone 5F10) from Thermo Scientific; anti-Thy-1 (Pharmingen); anti-flotillin1 (BD Biosciences); anti-clathrin heavy chain (BD Transduction Laboratories); PSD95 (Neuromab); and anti-NCX1 (Swant). Fluorophore-coupled secondary antibodies were from Molecular Probes. All chemicals used were from Sigma unless otherwise noted, and Neurobasal medium and B-27 supplement were purchased from Invitrogen. Caloxin 2a1 (VSNSNWPSFPSSGGG-NH_2) (41) was custom-synthesized by the proteomics service of the Centro de Biología Molecular Severo Ochoa (Madrid, Spain).

Immunoprecipitation

Synaptosomes or primary neurons from the brainstem or spinal cord (100 μg) were lysed for 30 min at room temperature at a concentration of 1.5 mg of protein/ml in TN buffer (25 mM Tris-HCl and 150 mM NaCl (pH 7.4)) containing 0.25% Nonidet P-40 and protease inhibitors (0.4 mM phenylmethylsulfonyl fluoride (PMSF) + Sigma mixture). After 15 min of centrifugation in a microcentrifuge to remove the cell debris, 4 μg of protein were separated to quantify total protein, and 5 μl of the primary antibody were added and left overnight at 4 °C using the following antibodies for immunoprecipitation: rat anti-GlyT2, anti-PMCA (clone 5F10), or anti-NCX1. A negative control was also run in parallel in which an irrelevant antibody was added, denoted as IgG. Subsequently, 50 μl of 50% protein G-agarose beads (ABT Beads) were added and incubated for 45 min at 4 °C. The beads were collected by mild centrifugation and washed twice for 7 min with lysis buffer at room temperature. Finally, the beads were pelleted, and the immunoprecipitated proteins were eluted in Laemmli buffer at 75 °C for 10 min, resolved in SDS-polyacrylamide gels (7.5%), detected in Western blots by ECL, and quantified on a GS-810 imaging densitometer (Bio-Rad). The amount loaded was always 4 μg of total protein and 96 μg of immunoprecipitated sample or IgG immunoprecipitation controls. This ratio allows having both samples in the same linear range of exposure.

Primary Cultures of Brainstem and Spinal Cord Neurons

Primary cultures of brainstem and spinal cord neurons were prepared as described previously (13, 15).

Immunofluorescence of Primary Neurons and Synaptosomes from Rat Brainstem and Spinal Cord

Primary neurons or purified synaptosomes were analyzed by immunofluorescence as reported previously (15). The primary antibodies used in this work were incubated overnight at 4 °C using the following dilutions: GlyT2 (1:500); PSD95 (1:500); PMCA2 (1:250); PMCA3 (1:150); NCX1 (1:200); and Thy-1 (1:500). The cells were visualized by confocal microscopy on an inverted microscope Axiovert200 (Zeiss).

Immunohistochemistry of Rat Brainstem Slices

Immunohistochemistry experiments from rat brainstem slices were performed as described previously (42). The sections shown in this work correspond to the ventral cochlear nucleus of the brainstem.

[^{3}H]Glycine Transport Assays in Brainstem and Spinal Cord Synaptosomes

Uptake assays in brainstem and spinal cord synaptosomes were performed in constant mild shaking at 37 °C in PBS containing 2 μCi/ml [^{3}H]glycine (1.6 TBq/mmol; PerkinElmer Life Sciences), cold glycine (1 μM final concentration), plus 10 μM *N*[3-(4′-fluorophenyl)-3-(4′-phenylphenoxy)propyl]sarcosine to inhibit glycine transport by GlyT1 (IC_{50} = 16 nM) with or without the specific GlyT2 inhibitor ALX1393 (0.5 μM, IC_{50} = 50 nM) to measure background glycine accumulation. After incubating 20 μg of synaptosomes for 7 min with radioactive medium, synaptosomes were recovered using 0.45-μm nitrocellulose filters (Millipore), washed three times, and prepared for scintillation counting. All assays were performed at least in triplicate and expressed as mean ± S.E.

Ca^{2+}-ATPase Activity Measurement in Brainstem and Spinal Cord Synaptosomes

The Ca^{2+}-ATPase activity was measured using a coupled assay in different conditions to measure the contribution of PMCA and the intracellular SERCA and SPCA ATPases as described in Sepúlveda *et al.* (43).

Immunofluorescence Quantification, Generation of Color Maps, and Generation of Pixel Fluorescence Intensity Profiles

At least 45 images for each condition were quantified using ImageJ software (National Institutes of Health). Images were processed with a 2.0-pixel median filter, and the threshold used was automatically determined by the JACoP plugin (44). The Pearson's value was obtained with JACoP by comparing the two thresholded channels and measuring the correlation between them. The value can range from −1 to 1, with 1 representing the maximal co-localization possible (two identical images), whereas values ≥0.5 can usually be considered as valid co-localization (45). Co-localization color maps were generated in ImageJ using the co-localization color map plugin (46). Pixel fluorescence intensity profiles were also generated using ImageJ software. The linear region of interest was manually drawn to cross several GlyT2-PMCA/NCX-Thy-1 clusters, and the fluorescence intensity profiles were obtained from each individual color channel using the RGB_profiler plugin. Intensity profile plots were generated in Origin 8.0 (Figs. 5 and 8, *green*, PMCAs/NCX1; *red*, GlyT2; *blue*, Thy-1), and triple co-localization spots were considered valid only when intensity values of the three proteins were higher than 65% of the maximum at the same region.

Mass Spectrometry Assays

In-Gel Digestion—In-gel digestion was performed as described previously (47, 48).

Reverse Phase-Liquid Chromatography RP-LC-MS/MS Analysis (Dynamic Exclusion Mode)—The desalted protein digest was dried, resuspended in 10 μl of 0.1% formic acid, and analyzed by RP-LC-MS/MS in an Easy-nLC II system coupled to an ion trap LTQ-Orbitrap-Velos-Pro mass spectrometer (Thermo Scientific). The peptides were concentrated by reverse phase chromatography using a 0.1 × 20-mm C18 RP precolumn (Proxeon) and then separated using a 0.075 × 100-mm C18 RP column (Proxeon) operating at 0.3 μl/min. Peptides were eluted using a 90-min gradient from 5 to 40% solvent B (solvent A: 0.1% formic acid in water, and solvent B: 0.1% formic acid, 80% acetonitrile in water). ESI ionization was done using a Nano-bore emitter stainless steel inner diameter of 30 μm (Proxeon) interface. The Orbitrap resolution was set at 30,000.

Peptides were detected in survey scans from 400 to 1600 atomic mass units (1 microscan), followed by 15 data-dependent MS/MS scans (top 15), using an isolation width of 2 units (in mass-to-charge ratio units), normalized collision energy of 35%, and dynamic exclusion applied during 30-s periods. Peptide identification from raw data was carried out using the SEQUEST algorithm (Proteome Discoverer 1.3, Thermo Scientific). Database search was performed against uniprot-rattus.fasta. The following constraints were used for the searches: tryptic cleavage after Arg and Lys, up to two missed cleavage sites, and tolerances of 10 ppm for precursor ions and 0.8 Da for MS/MS fragment ions, and the searches were performed allowing optional Met oxidation and Cys carbamidomethylation. Search against decoy database (integrated decoy approach) was performed using a false discovery rate of <0.01.

Lipid Raft Isolation

Membrane rafts were biochemically isolated from brainstem and spinal cord synaptosomes as described previously (10). Quantification of the relative distribution in lipid rafts of the different proteins was performed as shown in Equation 1,

$$\text{raft} = \frac{R}{R + NR} \cdot 100;\ \text{non-raft} = \frac{NR}{R + NR} \cdot 100 \qquad \text{(Eq. 1)}$$

where *R* is the raft optical density/μg of protein, and *NR* is the non-raft optical density/μg of protein. Densitometric analyses were performed on at least three independent Western blots representing the means ± S.E.

Data Analysis

All statistical analyses were performed using Origin 8.0 (OriginLab Corp.). One-way analysis of variance (ANOVA) was

A

Short name	Accession	Description	# AAs	MW [kDa]	Score	IPGlyT2	IgG
GlyT2	P58295-2	Sodium- and chloride-dependent glycine transporter 2 [SC6A5_RAT]	791	86,99	60,10	20	0
PMCA1	P11505-1	Plasma membrane calcium-transporting ATPase 1 [AT2B1_RAT]	1,258	138,72	0,00	0	0
PMCA2	P11506-5	Plasma membrane calcium-transporting ATPase 2 [AT2B2_RAT]	1154	127,28	19,64	7	0
PMCA3	Q64568-12	Plasma membrane calcium-transporting ATPase 3 [AT2B3_RAT]	1115	122,79	18,93	6	0
PMCA4	Q64542-1	Plasma membrane calcium-transporting ATPase 4 [AT2B4_RAT]	1203	133,09	0,00	0	0
SERCA	Q71UZ2	Sarco/endoplasmic reticulum Ca2+-ATPase [Q71UZ2_RAT]	869	95,19	8,89	3	0
Calmodulin	P62161	Calmodulin [CALM_RAT]	149	16,83	6,93	2	0
CamKIIα	P11275	Calcium/calmodulin-dependent protein kinase type II subunit alpha [KCC2A_RAT]	478	54,08	4,70	2	0
CADPS1	F1LLX6	Calcium-dependent secretion activator 1 [F1LLX6_RAT]	1148	129,60	7,32	2	0
SCaM2	Q8K3P6	Calcium-binding mitochondrial carrier protein SCaMC-2 [SCMC2_RAT]	469	52,66	4,80	2	0
UqCrC2	P32551	Cytochrome b-c1 complex subunit 2, mitochondrial [QCR2_RAT]	452	48,37	57,94	13	13

B PMCA3; Unique peptide: IQEAYGDVSGLCR. XCorr:3.21

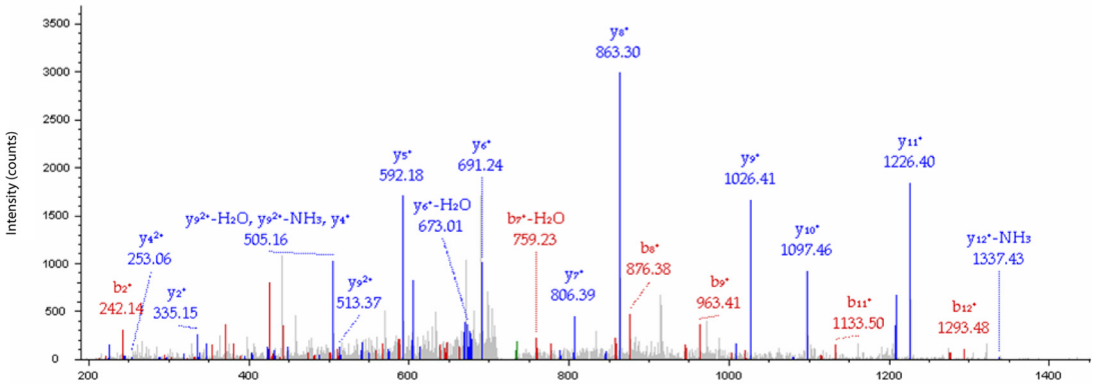

C PMCA2; Unique peptide: TSPVEGLPGTAPDLEK. XCorr:2.92

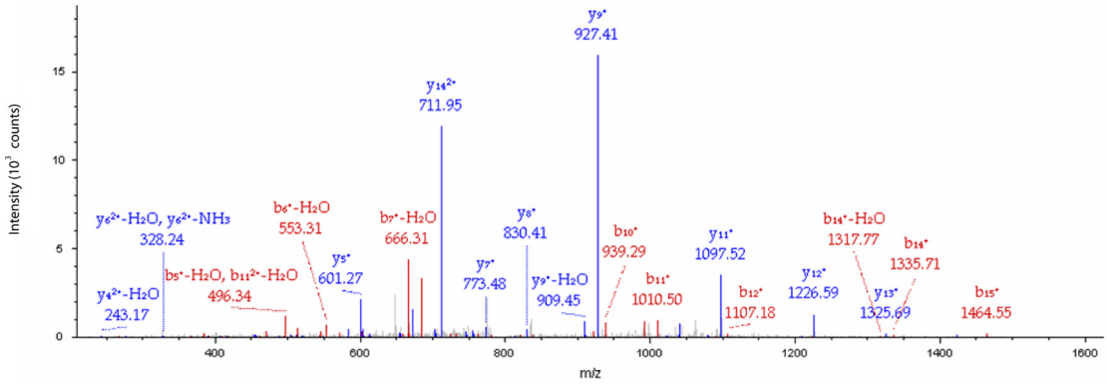

FIGURE 1. **Proteomic identification of PMCA2 and PMCA3 as putative interacting partners of GlyT2.** *A, table* represents the number of peptides obtained from mass spectrometry from GlyT2 immunoprecipitates (IPGlyT2) or control IgG immunoprecipitates (IgG). GlyT2 is shown as an auto-immunoprecipitated positive control, and cytochrome *b*-c_1 complex is shown as an example of a nonspecific interaction that was identified equally in controls and GlyT2 immunoprecipitations. Note the significant number of PMCA2 and PMCA3 peptides identified in GlyT2 immunoprecipitations. *B* and *C,* MS/MS spectra from the double charged ions at *m/z* 734.35, corresponding to the IQEAYGDVSGLCR peptide of PMCA3 (*B*), and 805.92, corresponding to TSPVEGLPGTAPDLEK peptide of PMCA2 (*C*).

used to compare multiple groups, with subsequent Tukey's post hoc test to determine the significant differences between samples. The Student's *t* test was used to compare two separate groups. *p* values are denoted through the text as follows: *, $p < 0.05$; **, $p < 0.01$; ***, $p < 0.001$; and $p < 0.05$ or lower values were considered significantly different when compared by one-way ANOVA (Tukey's post hoc test) or Student's *t* test. When shown, box whisker plots represent the following: median (line); mean (point); 25th to 75th percentile (box); 10th to 90th percentile (whisker); 1st to 99th percentile (×); and minimum to maximum (−) ranges.

RESULTS

Given the pathophysiological important role of GlyT2 (6) and considering the small number of proteins currently known to interact with this transporter, we carried out a proteomic study to identify new molecular partners involved in the functional regulation of GlyT2. Thus, the native transporter was immunoprecipitated from brainstem and spinal cord synaptosomes using a specific GlyT2 antibody (40), and co-purified proteins were identified by high throughput mass spectrometry. GlyT2 immunoprecipitates were found to selectively enhance the detection of several proteins, including some of the

previously described GlyT2 interacting partners such as syntaxin-1 (16) or Na^+/K^+-ATPase (15). We also found other molecules that are known to be implicated in GlyT2 trafficking, such as clathrin heavy chain (10).

Surprisingly, mass spectrometry also revealed other proteins, the main function of which is related to intracellular calcium homeostasis. In this last group, the highest number of specific peptides detected corresponded to the neuron-specific PMCA isoforms 2 and 3 (Fig. 1*A*, highlighted in *red*), which are responsible for extruding calcium out of cells at the expense of ATP and thus regulating cytosolic calcium concentration at nerve terminals (representative tandem mass spectra of PMCA2- and PMCA3-specific peptides obtained in these assays are shown in Fig. 1, *B* and *C*). PMCA2 and PMCA3 have been shown to be richly expressed in synapses (49–52), where they are proposed to control neurotransmission dynamics (via controlling Ca^{2+}-mediated synaptic vesicle fusion) and/or regulate local Ca^{2+} signaling (53, 54).

GlyT2 Interacts with PMCA2 and PMCA3 in Brainstem and Spinal Cord Synaptosomes and in Heterologous Systems—To confirm the interaction between GlyT2 and PMCA2 and 3, we performed reverse immunoprecipitations from brainstem and spinal cord synaptosomal lysates using an antibody that recognizes the four PMCA isoforms (PMCA1–4, clone 5F10) (Fig. 2*A*). Western blotting showed that the antibody selectively immunoprecipitated the respective target protein and that GlyT2 specifically co-purified in PMCA immunoprecipitates (Fig. 2*A*), indicating that native GlyT2 and PMCA proteins interact specifically under physiological conditions. However, proteomic data only pointed out the neuron-specific PMCA isoforms 2 and 3 as putative interacting partners of GlyT2 (Fig. 1), and consequently, we performed further GlyT2 immunoprecipitations and detected PMCA2 and PMCA3 using isoform-specific antibodies (Fig. 2, *B–D*). Western blotting showed a specific co-purification of PMCA2 and PMCA3, yet no signal was observed when an irrelevant antibody was added (denoted as IgG). Furthermore, PMCA4 is not found co-purifying in these conditions (Fig. 2*D*), in agreement with proteomic data.

The interaction between GlyT2 and PMCA2 or PMCA3 was also detected in a heterologous COS7 cell line overexpressing each isoform together with the wild type transporter or with a GlyT2 mutant lacking the C-terminal region, which contains a PDZ (95/Disc large/Zonula occludens-1) ligand motif that could potentially interact with the PDZ binding domain of the pumps, as reported for some PMCA-interacting partners (55–57). Western blot assays (Fig. 2, *E* and *F*) showed that both PMCA2 and PMCA3 clearly maintained their association with the transporter despite the lack of its PDZ-containing C-terminal region, indicating that the PMCA2- and PMCA3-GlyT2 interactions are not PDZ domain-based interactions and suggesting that other regions of GlyT2 are implicated in the physical coupling between both proteins.

To further confirm the interaction between GlyT2 and PMCA2 or PMCA3 in the native system, their co-localization was examined by immunohistochemistry in rat brainstem slices. As shown in Fig. 3, double labeling for GlyT2 and PMCA2 or PMCA3 indicates that GlyT2 clearly co-localizes

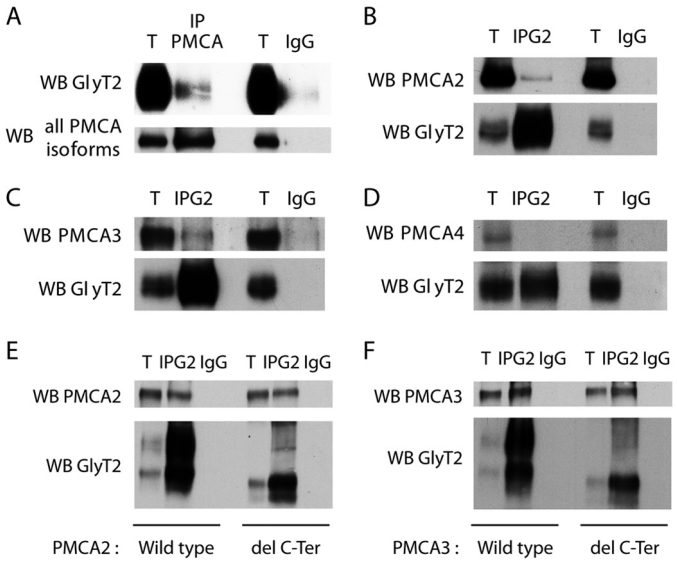

FIGURE 2. **GlyT2 interacts with PMCA2 and PMCA3 in CNS preparations and heterologous cells.** *A–D,* synaptosomes from rat brainstem and spinal cord were lysed and incubated with antibodies against GlyT2 (*B–D*), PMCA (against all isoforms, clone 5F10) (*A*), or the equivalent IgGs as control (*A–D*). Precipitated protein complexes were analyzed by Western blots (*WB*) probed with anti-GlyT2, anti-PMCA (all isoforms), anti-PMCA2, anti-PMCA3, or anti-PMCA4 antibodies. *T,* total protein; *IP,* immunoprecipitated sample; *IgG,* IgG immunoprecipitation controls. Note that an interaction can be detected between GlyT2 and PMCA isoforms 2 and 3, yet no signal is observed in PMCA4 Western blots or in the IgG controls. *E* and *F,* COS7 cells were transfected to express wild type GlyT2 or GlyT2 lacking the C-terminal region (amino acids from 737–799; denoted as *del C-Ter*) and PMCA isoforms 2 or 3. Lysed cells were incubated with antibodies against GlyT2 or the equivalent IgGs as control and protein complexes were precipitated using protein-agarose beads and analyzed in Western blots probed with anti-GlyT2 (*E* and *F*) and anti-PMCA2 (*E*) or anti-PMCA3 (*F*) antibodies. Two bands of wild type GlyT2 are detected when expressed in COS cells as reported previously (14). *T,* total protein; *IP,* immunoprecipitated sample; *IgG,* IgG immunoprecipitation controls. Note that the interaction can still be detected between GlyT2 lacking the C-terminal region and the PMCA isoforms, indicating that the PDZ domain of GlyT2 is not necessary for this interaction.

with PMCA2 (Fig. 3*A*) and PMCA3 (Fig. 3*B*), especially in presynaptic structures (Fig. 3, *A* and *B, detail*). In addition, we performed immunocytochemistry in synaptosomes from brainstem and spinal cord (Fig. 4). Double labeling for GlyT2 and PMCA2 or PMCA3 (Fig. 4, *B* and *C*) indicates that most GlyT2 overlaps with both isoforms, whereas no co-localization is observed with a postsynaptic marker, PSD-95 (Fig. 4*A*). These differences can be quantified using the Pearson's value of correlation, obtaining a significant co-localization between PMCAs and GlyT2 (Fig. 4*D*, PMCA2 Pearson's value: 0.635 ± 0.013 S.E., $p = 1.98 \times 10^{-23}$; PMCA3 Pearson's value: 0.596 ± 0.009 S.E.; $p = 7.97 \times 10^{-22}$). Together, these immunoprecipitation, immunohistochemical, and immunocytochemical results indicate a specific interaction between GlyT2 and the neuronal PMCA2 and PMCA3 isoforms.

GlyT2 and PMCA Isoforms 2 and 3 Are Co-enriched in Neuronal Lipid Raft Membrane Clusters—DRMs or lipid rafts are small (10–200 nm), heterogeneous, highly dynamic, and sterol- and sphingolipid-enriched domains that compartmentalize cellular processes (58–60). GlyT2 displays optimal transport activity when it is associated with these subdomains at the cell surface, where most of the transporter resides in primary neurons and synaptosomes from the rat brainstem (11, 15). Considering that PMCA isoforms are also localized in lipid rafts,

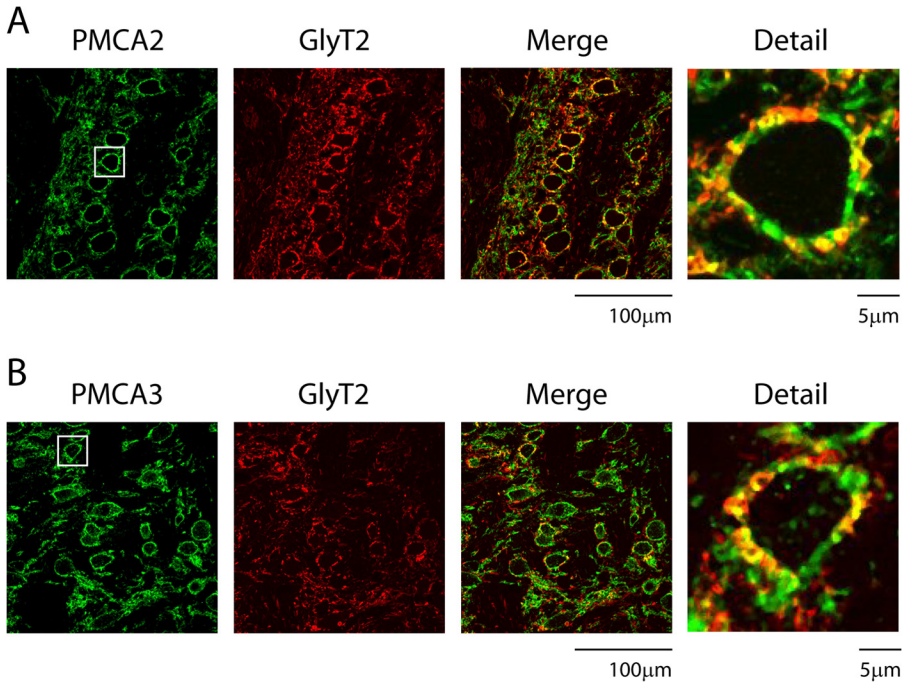

FIGURE 3. **GlyT2 co-localizes with PMCA2 and PMCA3 in brainstem slices.** *A* and *B,* adult rat brainstem slices were fixed and incubated with antibodies against GlyT2 and PMCA2 (*A*) or PMCA3 (*B*). After incubation with the secondary antibodies, the slices were visualized by confocal microscopy, showing GlyT2 in *red* and PMCAs in *green*. Note the co-localization of both proteins, especially in presynaptic structures (ventral cochlear nucleus slices are shown). *Scale bar,* 100 μm. *Scale bar* of detailed images, 5 μm.

where they are known to be optimally active (32–35), we investigated whether the coupling shown here between PMCAs and GlyT2 could be facilitated by membrane subdomain compartmentalization of these proteins. As a first approach, we sought to determine the distribution of GlyT2, PMCA2, and PMCA3 in raft subdomains using sucrose gradient centrifugation. As shown in Fig. 5, the three proteins are distributed among raft and non-raft fractions (Fig. 5, *A* and *B*). In agreement with previously reported results, GlyT2 is enriched in raft fractions (9, 15), showing here a relative distribution in rafts of 77.26 ± 4.46% S.E., whereas PMCA2 and PMCA3 distributions are 51.09 ± 6.25% and 49.46 ± 7.57% S.E., respectively (Fig. 5*B*). Correct biochemical isolation of raft fractions was confirmed by Western blotting of raft and non-raft markers, flotillin1 and clathrin heavy chain, respectively.

To find out whether GlyT2 and PMCA2 or PMCA3 are present in the same raft clusters, we performed immunocytochemical assays in primary neurons using specific antibodies against GlyT2, PMCA2 or PMCA3, and Thy-1, a marker of neuronal rafts (Fig. 5, *C–H*) (61). We observed a clear co-localization between GlyT2 and Thy-1, as reported previously (15). Interestingly, these GlyT2-Thy-1 clusters extensively co-localized with PMCA2 or PMCA3, leading to a high degree of triple co-localization as shown by the white color in the overlay image (denoted as *Merge* in Fig. 5, *D* and *G*). To clearly visualize triple co-localization, we generated color maps that highlight pixels of co-localization (Fig. 5, *D* and *G*) (46) and pixel fluorescence intensity profiles of each individual color staining that show a substantial overlap among the plots of each color staining (Fig. 5, *E* and *H*) (62). In this case, triple co-localization spots are highlighted by inverted arrows. Taken together, these biochemical and immunocytochemical results suggest that GlyT2 and PMCA pumps are associated in lipid raft subdomains, where both proteins have been shown to be optimally active (11, 32–35).

PMCA Function Regulates Presynaptic Glycine Transport by GlyT2—Given that GlyT2 and PMCAs are co-enriched in raft membrane subdomains, where they have been proposed to be fully functional, we next analyzed the possible regulatory interplay between these proteins. As a first approach, we measured GlyT2 and PMCA activities in brainstem and spinal cord synaptosomes in the presence of ALX1393, a specific GlyT2 inhibitor (63). As expected, ALX1393 reduced about 90% of the transporter activity (Fig. 6*A*) but did not affect PMCA activity (Fig. 6*B*), suggesting that PMCA function is independent of GlyT2 activity. We also tested the reverse hypothesis measuring GlyT2 transport in the presence of the PMCA inhibitor caloxin 2a1, which specifically impairs PMCA function in a dose-dependent manner (Fig. 6, *C* and *D*) while not affecting other Ca^{2+}-ATPases such as SERCA or SPCA (Fig. 6*C*) (64, 65). Fig. 7*A* shows that incubation with 400 μM caloxin 2a1 for 10 min produced a significant down-regulation of GlyT2 transport, with the remaining activity of 66.38 ± 2.26% S.E. compared with the control ($p = 1.36 \times 10^{-7}$, *green box plot*). However, the same protocol did not produce any differences when we measured the activity of the highly related glycine transporter GlyT1 (Fig. 7*B*; $p = 0.152$) (1). This suggests a specific regulation of GlyT2 by PMCA activity, indicating that somehow Ca^{2+} extrusion by PMCAs is necessary for optimal GlyT2 glycine recapture. PMCA function is tightly related to the function of the plasma membrane sodium/calcium exchanger (NCX) (66). In virtually all cells, NCX mainly operates in its "forward" mode harnessing the electrochemical gradient of Na^+ to extrude Ca^{2+} with a known stoichiometry of $3Na^+$:

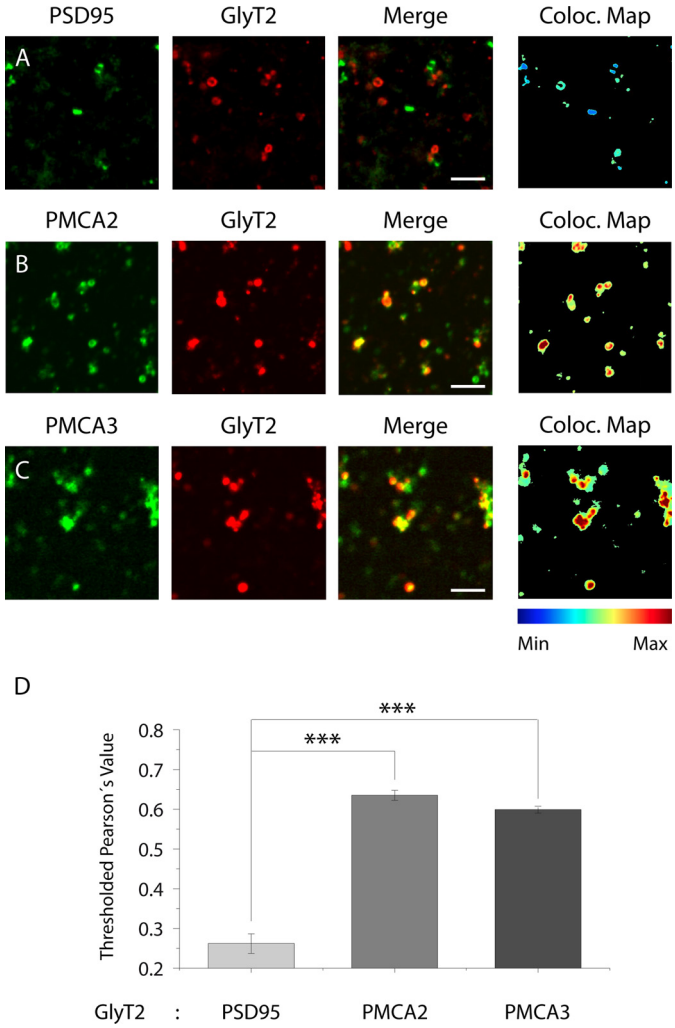

FIGURE 4. **GlyT2 co-localizes with PMCA2 and PMCA3 in synaptosomes from adult rat brainstem and spinal cord.** *A–D,* synaptosomes isolated from the adult rat brainstem and spinal cord were deposited on glass coverslips, fixed, and incubated with antibodies against GlyT2 and PSD95, PMCA2, or PMCA3. Synaptosomes were visualized by confocal microscopy, showing GlyT2 in *red* and PSD95/PMCAs in *green*. *D,* quantification of the co-localization using Pearson's value was performed as described under "Experimental Procedures." The histogram represents the mean ± S.E. ($n = 3$; on average, 30 images per condition were analyzed in each experiment): ***, significantly different, $p < 0.001$ by ANOVA with Tukey's post hoc test. PSD95 is shown as a negative control of no co-localization. *Scale bar,* 3 μm.

$1Ca^{2+}$ (67), helping PMCA proteins in the cytosolic calcium clearance (68, 69). However, during high frequency action potentials in presynaptic terminals, the activity-mediated increase in cytosolic Na^+ can switch NCX direction of flux exchange extruding Na^+ and allowing Ca^{2+} entry (70–72). In this mode, NCX produces local increases in Ca^{2+} concentration that are thought to be corrected by PMCA activity. Based on these data, we hypothesized that PMCA-mediated modulation of GlyT2 transport could be based on NCX locally acting in the reverse mode to correct Na^+ entry mediated by GlyT2 transport, which is known to introduce $3Na^+$ ions per glycine recaptured (73). NCX reverse mode can be pharmacologically inhibited by the isothiourea derivative KB-mes (74–77). Brainstem and spinal cord synaptosomes incubated with KB-mes showed a significant down-regulation of GlyT2 transport (42.99 ± 5.71% S.E.; $p = 1.53 \times 10^{-9}$) in a similar level to that observed in the presence of caloxin 2a1 (66.38 ± 2.26% S.E.; $p = 1.36 \times 10^{-7}$) (Fig. 7*A*, *purple box plot*), indicating that NCX function is also needed for optimal GlyT2 activity and suggesting a PMCA/NCX cooperative effect in regulating GlyT2 transport. Moreover, simultaneous treatment with caloxin 2a1 and KB-mes produced a reduction in GlyT2 activity (49.88 ± 6.17% S.E.) that is not significantly different from KB-mes ($p = 0.9627$) or caloxin 2a1 ($p = 0.17$) treatments alone, further supporting the hypothesis that both proteins are acting in the same pathway (Fig. 7*A*, *light blue box plot*). In addition, to confirm that Ca^{2+} extrusion by PMCAs is necessary for optimal GlyT2 glycine recapture, we used BAPTA-AM, a cell-permeant ion chelator that is a highly selective for Ca^{2+}. Incubation of synaptosomes with BAPTA-AM reduces the availability of cytosolic Ca^{2+} affecting PMCA activity and interfering on the NCX functional shift toward the reverse mode (71). In these conditions, GlyT2 activity appears to be significantly reduced (71.80 ± 6.10% S.E.; $p = 0.00043$), suggesting that cytosolic concentration of Ca^{2+} could affect glycine recapture by affecting NCX/PMCA proteins.

GlyT2 Interacts with NCX1, and Both Proteins Are Present in the Same Neuronal Membrane Raft Clusters—Results from Fig. 7 indicate that NCX functions contribute to GlyT2-mediated glycine recapture in the presynaptic terminal. A working hypothesis of this work is that NCX could act by correcting the local imbalance of Na^+ produced during high activity periods of glycine-Na^+ co-transport by GlyT2 after neurotransmitter release that could not be covered by Na^+/K^+-ATPase due to its slow rate (200^{-1} s) (37). This localized process should be facilitated by the proximity of both proteins, and therefore we sought to determine whether GlyT2 and NCX physically interact and/or are compartmentalized in the same membrane clusters. NCX was not detected in the initial proteomic studies (Fig. 1), not even increasing the false discovery rate to 5% (data not shown). However, some proteins are particularly difficult to detect by mass spectrometry or they can be present in amounts below the detection limit of this technique. Therefore, not finding unique peptides of a protein in immunoprecipitation experiments does not exclude the possibility of a real interaction. To test this putative interaction between GlyT2 and NCX, we performed reverse immunoprecipitations from brainstem and spinal cord synaptosomal lysates using antibodies that recognize NCX1 or GlyT2 (Fig. 8, *A* and *B*). Western blot assays showed that each antibody selectively immunoprecipitated the respective target protein, that GlyT2 was specifically co-purified in NCX1 immunoprecipitates (Fig. 8*A*), and that NCX1 was specifically co-purified in GlyT2 immunoprecipitates (Fig. 8*B*), indicating indeed a physical interaction.

In addition, to find out whether GlyT2 and NCX1 are present in the same raft clusters, immunocytochemical assays were performed in primary neurons using specific antibodies against GlyT2, NCX1, and Thy-1 as done in Fig. 5 for PMCAs (Fig. 8, *C* and *D*). In this case, GlyT2-Thy-1 clusters also extensively co-localized with NCX1, visualized by triple co-localization color maps or pixel fluorescence intensity profiles from each individual protein. Taken together, results from Fig. 8 indicate that NCX1 is physically interacting with

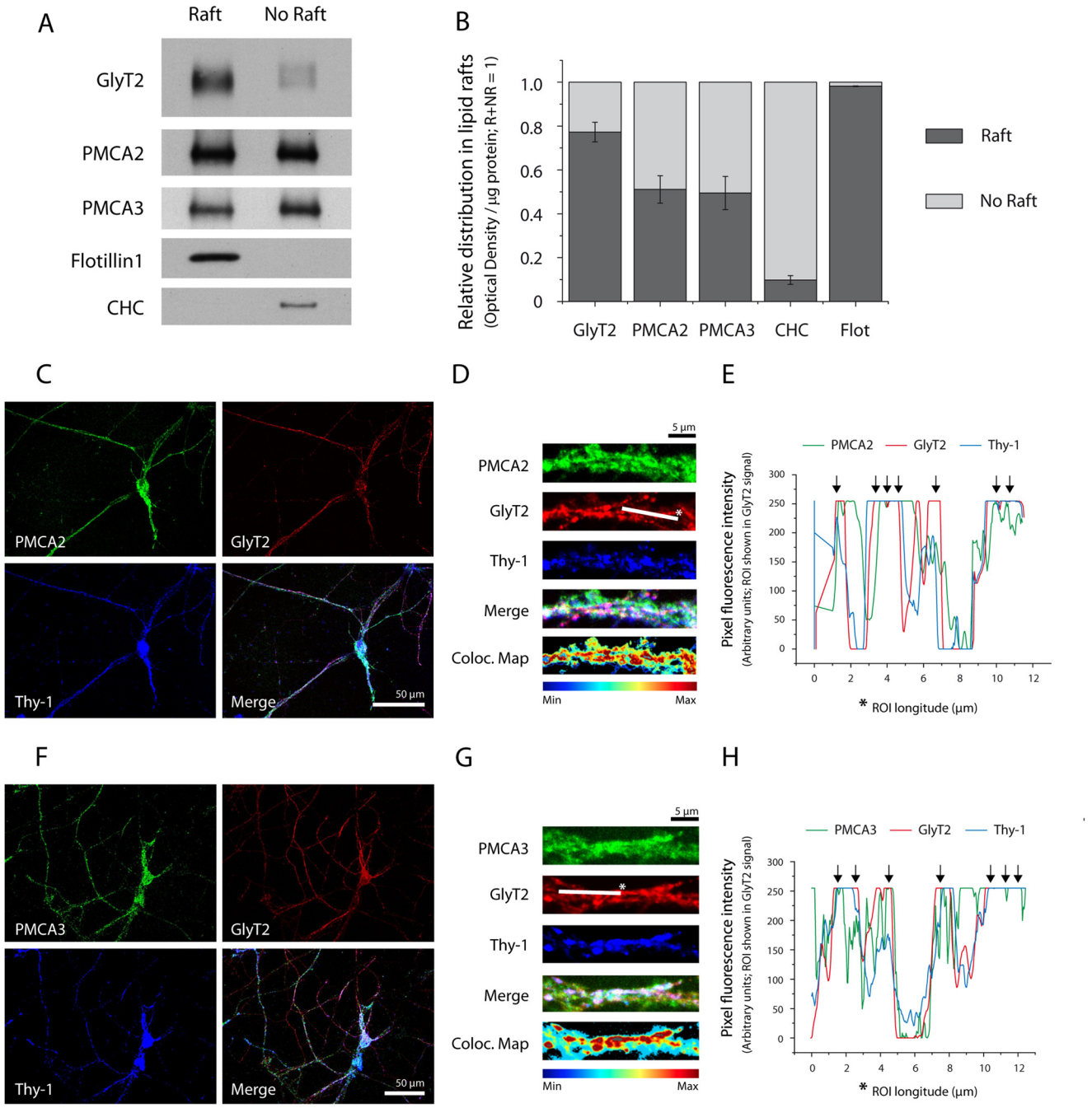

FIGURE 5. **GlyT2 is present in neuronal lipid rafts containing PMCA2 or PMCA3.** *A* and *B*, lipid raft fractions (denoted as *Raft*) were isolated from brainstem and spinal cord synaptosomal lysates and analyzed by Western blot to determine GlyT2, PMCA2, and PMCA3 distribution in lipid rafts. The purity of the isolation was determined probing anti-flotillin1 (raft marker) and anti-clathrin heavy chain (*CHC*, non-raft marker). *B*, histogram shows the quantification of the relative distribution of each protein representing the means ± S.E. from three different experiments as shown in *A*. *C–H*, primary cultures of spinal cord and brainstem neurons were fixed and incubated with primary and secondary antibodies against PMCA2 or PMCA3 (*green*), GlyT2 (*red*), and the lipid raft marker Thy-1 (*blue*). Cells were visualized by confocal microscopy, and amplified high definition images of axonal regions were taken to generate triple co-localization maps (*Coloc. Map*) (*D* and *G*). *E* and *H*, pixel fluorescence intensity profiles were generated to visualize co-distribution of GlyT2 and PMCA2/3 in Thy-1-positive clusters. The linear region of interest was manually drawn from left to right, and fluorescence intensity profiles were obtained from each individual color channel. Triple co-localization spots are highlighted by *inverted arrows*. *Scale bar* in *C* and *F*, 50 µm. *Scale bar* in *D* and *G*, 5 µm.

GlyT2 and suggest that both proteins are present in the same membrane clusters. Therefore, we suggest that GlyT2 is coupled to NCX1 and PMCAs in lipid raft subdomains where both proteins coordinately act in regulating glycine recapture by correcting local Na^+ and Ca^{2+} variations after neurotransmitter release.

PMCA/NCX1 Regulation of GlyT2 Activity Depends on Lipid Raft Integrity—PMCA pumps are optimally active when they are present in lipid raft subdomains (32–35). In addition, GlyT2 is more active when it is raft-associated (11). In this work, we show that PMCA, NCX, and GlyT2 are together in the same raft clusters; therefore, we next sought to assess whether the

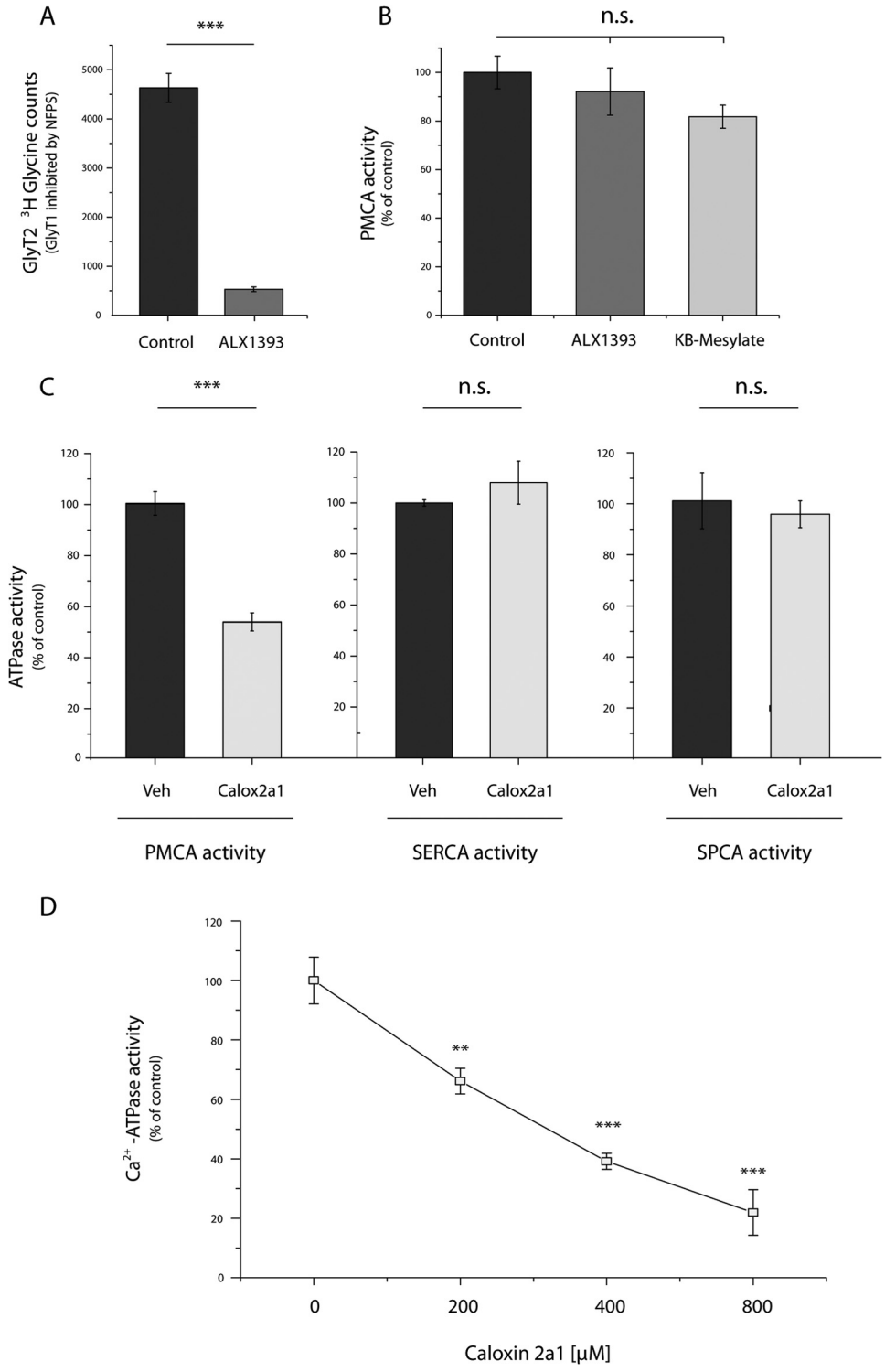

FIGURE 6. **Effects of ALX1393 in PMCA and GlyT2 activities and effects of caloxin 2a1 in Ca^{2+}-ATPase activities in brainstem and spinal cord synaptosomes.** *A–D,* synaptosomes from the rat brainstem and spinal cord were isolated and incubated with the compounds indicated for 10 min at 37 °C and PMCA-, SERCA-, SPCA-, or GlyT2-specific activities were measured as detailed under "Experimental Procedures." ALX1393 concentrations in *A* and *B* were 1 μM; KB-mes concentration in *B* was 10 μM, and caloxin 2a1 concentration in *C* was 400 μM. GlyT2 transport in *A* is shown as total [^{3}H]glycine counts in a 10-min assay in the presence of *N*[3-(4′-fluorophenyl)-3-(4′-phenylphenoxy)propyl]sarcosine (GlyT1 inhibitor). *Bars* represent S.E. of triplicates from at least three different experiments. **, significantly different from control, $p < 0.01$; ***, significantly different from control, $p < 0.001$; *n.s.*, not significantly different from control by ANOVA using Tukey's post hoc test. *Veh,* vehicle.

PMCA/NCX1-mediated regulation of GlyT2 was dependent on lipid raft integrity. A common approach used to disrupt raft structures is based on the use of methyl-β-cyclodextrin (MβCD), a cholesterol chelator that extracts cholesterol from the plasma membrane disassembling raft structures (58, 78–80). Brainstem and spinal cord synaptosomes were incubated with different concentrations of MβCD (0–2 and 5 mM) with or without caloxin 2a1 (Fig. 9, *A* and *B*) or KB-mes (Fig. 9,

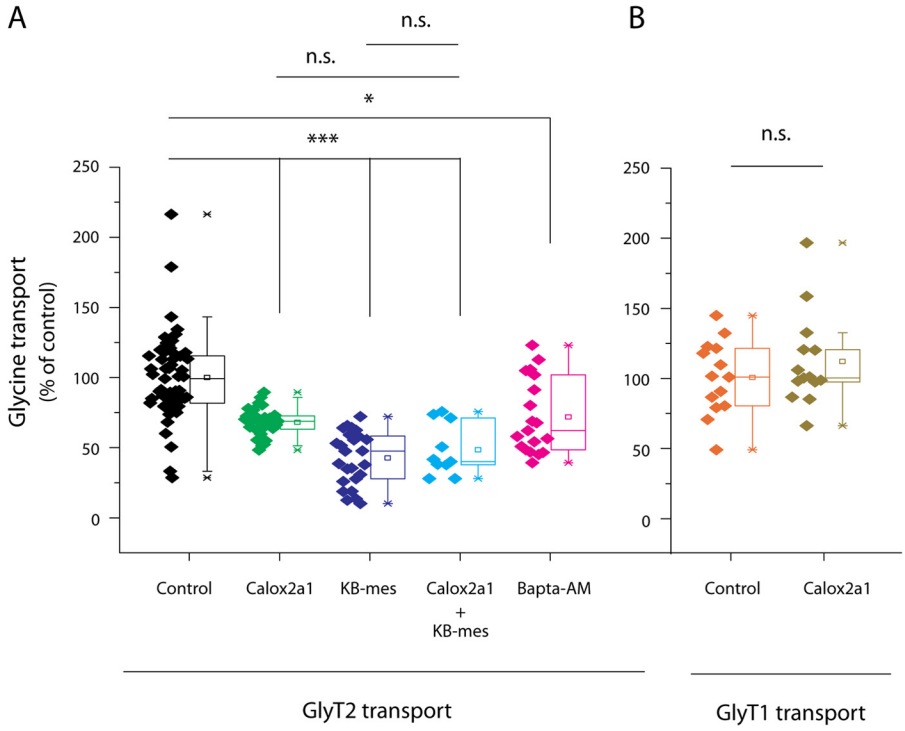

FIGURE 7. **PMCA and NCX activities modulate GlyT2 transport of glycine.** *A,* synaptosomes from the rat brainstem and spinal cord were incubated with vehicle (*control, n* = 60, *black*) or 400 μM caloxin 2a1 (*calox2a1*, *n* = 31, *green*), 10 μM KB-mes (*n* = 25, *purple*), both compounds at those concentrations (*n* = 11, *blue*) or 20 μM BAPTA-AM (*n* = 19, *pink*). The glycine uptake by GlyT2 was then measured. 100% glycine transport by GlyT2 was 51.30 ± 1.97 pmol of Gly/mg of protein/min. *B,* synaptosomes from the rat cortex were incubated in presence of vehicle (*control*, *n* = 14, *orange*) or 400 μM caloxin 2a1 (*calox2a1*, *n* = 14, *brown*). The glycine uptake by GlyT1 was then measured. 100% of activity was 4.07 ± 0.24 pmol of Gly/mg of protein/min. *, significantly different from control, $p < 0.05$; ***, significantly different from control, $p < 0.001$; *n.s.*, not significantly different. Comparisons of the means were performed using ANOVA by Tukey's post hoc test.

C and *D*). Inhibition of GlyT2 activity by caloxin 2a1 or KB-mes was blocked in a dose-dependent manner (Fig. 9, *A* and *C*), showing a complete blockage of the inhibition with 5 mM MβCD treatments (Fig. 9*B*, caloxin2a1 + MβCD remaining transport 97.74 ± 14.39% S.E., $p = 0.9998$; Fig. 9*D*, KB-mes + MβCD remaining transport 91.15 ± 17.45% S.E., $p = 0.9986$), which points out the importance of raft structures for the GlyT2/NCX/PMCA interplay. To further support these results, we studied the effect of MβCD on the co-localization of GlyT2/PMCA/NCX in primary neurons. The treatment used in this work (5 mM, 30 min) has been previously shown to reorganize GlyT2 in primary neurons, showing a specific punctae redistribution that is not observed in other neuronal markers such as MAP2 and that is independent of cellular toxicity (11). We measured Pearson's values on MβCD-treated and -untreated cells and observed a significant reduction in the co-localization of GlyT2 with PMCA2 (*B*, $p = 0.00167$), PMCA3 (*D*, $p = 0.00109$), and NCX (*F*, $p = 6.33 \times 10^{-5}$), suggesting a reduction in the local compartmentalization of these proteins (Fig. 10, *A–F*).

Together, these results show that caloxin2a1 and KB-mes-mediated inhibitions of GlyT2 need lipid raft integrity, and they suggest that spatial compartmentalization of these proteins favors the functional coupling between them.

DISCUSSION

In this study, we have used high throughput mass spectrometry to identify proteins that interact with GlyT2 in CNS preparations to unravel new mechanisms that might modulate GlyT2 function. In this way, we have identified PMCA isoforms 2 and 3 as new protein partners of GlyT2. Reciprocal co-immunoprecipitation, immunohistochemical studies, and immunocytochemical experiments further confirmed proteomic data and indicated that GlyT2 associates and co-localizes with PMCA2 and PMCA3, whereas the interaction with the ubiquitously expressed PMCA4 isoform could not be found. Both PMCAs 2 and 3 are mainly expressed in the CNS and localize pre- and post-synaptically where they are proposed to function as calcium controllers for Ca^{2+}-driven vesicle exocytosis and neuronal Ca^{2+}-dependent regulatory mechanisms (52–54, 81). Besides this important role, PMCA2 also appears to be crucial for the survival of spinal cord cells, in particular motor neurons, under pathological conditions (82). In addition, PMCA2 genetic alterations have been described as a cause of human deafness (83, 84), and recently, a genetic alteration of isoform 3 of PMCAs was identified in a family with X-linked congenital cerebellar ataxia (54).

One important finding of this work is that GlyT2 not only interacts with PMCA2/3 isoforms but also with NCX1, an exchanger ubiquitously distributed through the CNS with a crucial role for intracellular calcium homeostasis (66, 85). These protein interactions are probably enriched in lipid raft membrane subdomains, as suggested both by triple co-localization between GlyT2, PMCA2/PMCA3/NCX1, and the neuronal raft marker Thy-1 and through the dependence on lipid raft

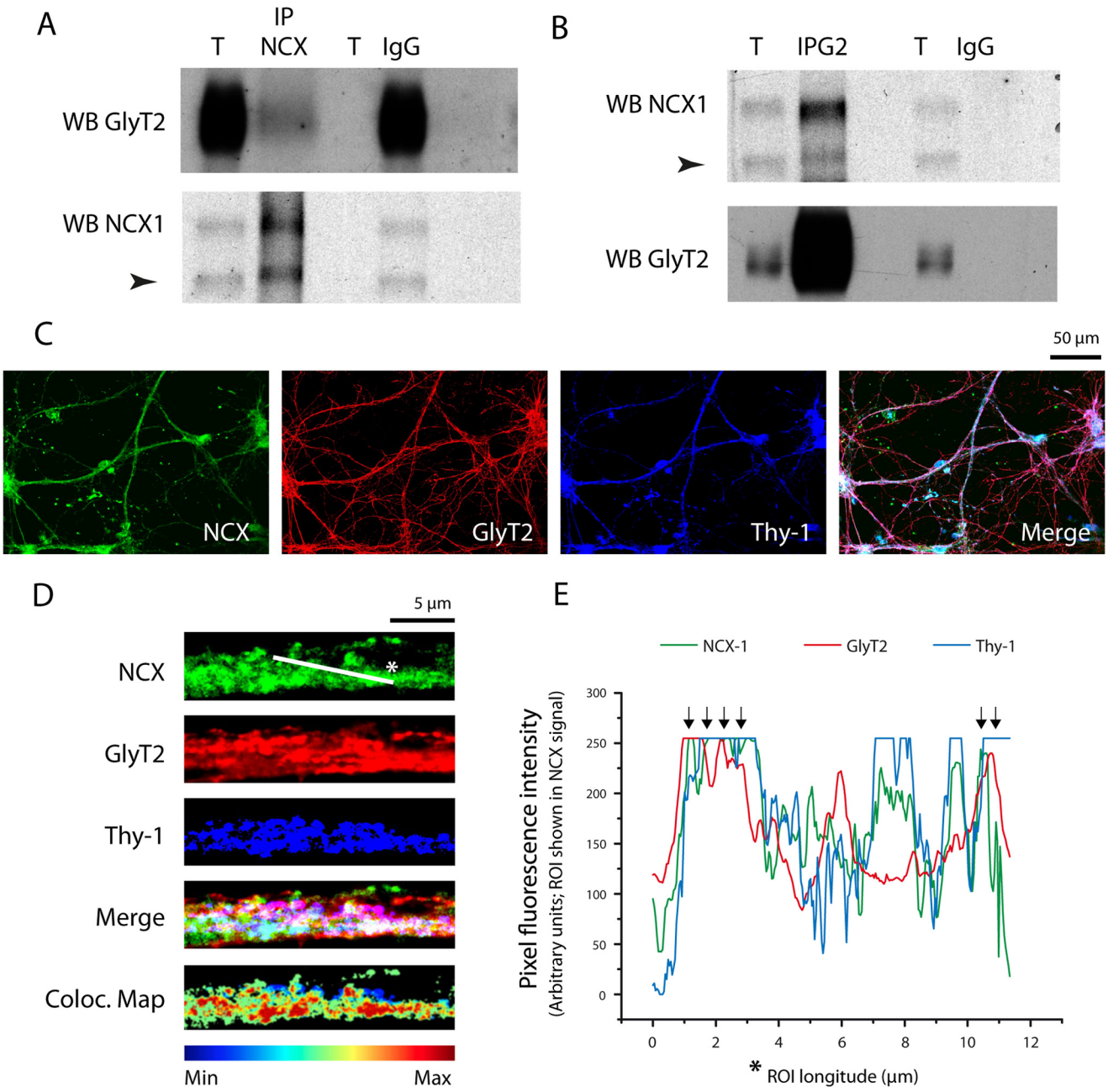

FIGURE 8. **GlyT2 interacts with the Na^+/Ca^{2+} exchanger (NCX) and both proteins are present in the same neuronal membrane raft clusters.** *A* and *B*, synaptosomes from the rat brainstem and spinal cord were lysed and incubated with antibodies against NCX1 (*A*) or GlyT2 (*B*) or the equivalent IgGs as control (*A* and *B*). Precipitated protein complexes were analyzed in Western blots (*WB*) probed with anti-GlyT2 or anti-NCX1 antibodies. *T*, total protein; *IP*, immunoprecipitated sample; *IgG*, IgG immunoprecipitation controls. Note that two bands are observed in NCX1 Western blots that correspond to the full-length protein (highlighted by an *arrowhead*, 100 kDa) and the nonreduced protein around 160 kDa (96). *C–E*, primary cultures of spinal cord and brainstem neurons were fixed and incubated with primary and secondary antibodies against NCX1 (*green*), GlyT2 (*red*), and the lipid raft marker Thy-1 (*blue*). Cells were visualized by confocal microscopy, and amplified high definition images of axonal regions were taken to generate triple co-localization maps. Top panel indicated ROI longitude that is represented in the *abscissa* of *E*. *E*, pixel fluorescence intensity profiles were generated to visualize co-distribution of GlyT2 and NCX1 in Thy-1-positive clusters. The linear region of interest (*ROI*) was manually drawn from right to left, and fluorescence intensity profiles were obtained from each individual color channel. Triple co-localization spots are highlighted by *inverted arrows*. *Scale bar, C,* 50 µm. *Scale bar, D,* 5 µm.

integrity for GlyT2 inhibition during PMCA or NCX1 blockage. This membrane compartmentalization would favor the interaction between active populations of GlyT2, PMCA2/3, and NCX1, facilitating local presynaptic sodium/calcium homeostasis during glycine recapture while functioning in an ionic microdomain in which Na^+ and Ca^{2+} concentrations differ from those in the bulk cytosol (86, 87). At synapses, NCX and PMCA are the two only plasma membrane proteins responsible for Ca^{2+} extrusion and work together to control the recovery of Ca^{2+} basal levels in the small compartment of axon terminals. They have complementary functional characteristics, whereas the PMCA has high Ca^{2+} affinity and low transport capacity, NCX has low Ca^{2+} affinity but high capacity for Ca^{2+} transport (88). NCX is highly expressed in presynaptic terminals where it is very active (89). Under basal conditions, NCX transports $3Na^+$ into the cell and extrudes $1Ca^{2+}$ from the cytoplasm

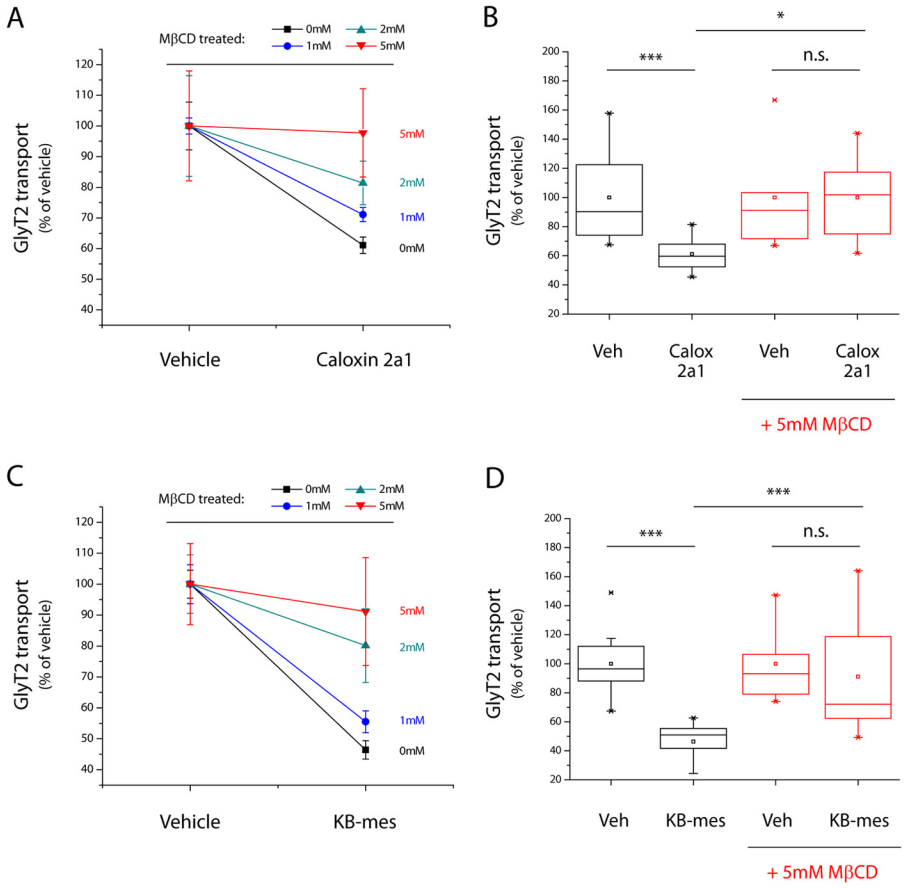

FIGURE 9. **PMCA and NCX regulation of GlyT2 activity depends on lipid raft integrity.** *A–D* synaptosomes from the rat brainstem and spinal cord were incubated in the presence of vehicle (*Veh*), caloxin 2a1 (*Calox 2A1*) (*A* and *B*), or KB-mes (*C* and *D*) with or without increasing concentrations of MβCD (1, 2, and 5 mM). The glycine uptake by GlyT2 was then measured. Each vehicle condition (0, 1, 2, and 5 mM MβCD) was normalized to 100%, having vehicle GlyT2 activities of 51.30 ± 1.97, 45.32 ± 1.19, 21.47 ± 3.53, and 5.30 ± 0.95 pmol of Gly/mg of protein/min, respectively, accordingly to published results (11). *Bars* represent S.E. of triplicates from at least three different experiments in *A* and *C*. *B,* box whisker plot showing differences in GlyT2 transport in vehicle (*veh*) and caloxin 2a1 compared with vehicle and caloxin 2a1 in the presence of 5 mM MβCD. Note that inhibition produced by caloxin 2a1 (*black*) is reversed in the presence of 5 mM MβCD, reaching a 97.74% ± 14.40 of vehicle activity. *D,* box whisker plot showing differences in GlyT2 transport in vehicle (*veh*) and KB-mes compared with vehicle and KB-mes in the presence of 5 mM MβCD. Note that inhibition produced by KB-mes (*black*) is reversed in the presence of 5 mM MβCD, reaching a 91.15 ± 17.45% of vehicle activity. *, significantly different from control, $p < 0.05$; ***, significantly different from control, $p < 0.001$; *n.s.*, not significantly different. Comparisons of the means were performed using ANOVA by Tukey's post hoc test.

functioning in the "forward mode." However, under certain physiological conditions such as neuronal activity, intracellular Na^+ increases can switch NCX to function in the "reverse mode" to expel Na^+ excess (Ca^{2+} influx, Na^+ efflux) (71, 72). Thus, it is conceivable that local increases in intracellular Na^+ in similar conditions could switch NCX from its forward mode to its reverse mode of action.

The results presented in this paper lead us to propose the existence of a functional complex where GlyT2 would be tightly coupled to PMCA and NCX to promote Na^+ and Ca^{2+} homeostasis in specific microdomains of the presynaptic glycinergic membranes (Fig. 11*A*). In this regard, the decrease in GlyT2 transport activity caused by caloxin 2a1 and KB-mes (selective inhibitors of PMCA and reversed NCX, respectively) suggests that when PMCA and NCX are inhibited, GlyT2 activity could be directly affected by local changes in Na^+/Ca^{2+} gradients due to a decrease in the Na^+ driving force necessary for glycine transport and/or be inactivated by an unknown Na^+- and/or Ca^{2+}-mediated signaling mechanism that would block glycine recapture. Independently of the molecular mechanism, similar homeostatic regulation has been proposed for other proteins, as the interplay between AMPA receptors and the Na^+/Ca^{2+} exchanger in neocortical interneurons (90), and the interaction between PMCA2 and nicotinic acetylcholine receptors in hippocampal interneurons (91).

It has been previously shown that PMCA isoforms participate in multiprotein complexes at the cell membrane (27). PMCA2 interacts presynaptically with syntaxin-1A, a member of the SNARE complex, and postsynaptically with the scaffolding protein PSD95 (52). Given its fast Ca^{2+} activation kinetics, PMCA2 is especially suited for rapid clearance of presynaptic Ca^{2+} in fast-spiking inhibitory nerve terminals (51). Therefore, its association with syntaxin-1A may provide PMCA2 a docking place close to the site of neurotransmitter release where precise and rapid control of presynaptic Ca^{2+} levels is crucial for neurotransmission (18). It should be noted that some years ago we reported an interaction between GlyT2 and syntaxin-1A that is involved in a calcium-dependent rapid increase of the amount of GlyT2 in the presynaptic membrane during neuronal activity. The GlyT2/syntaxin-1A interaction favors the rapid reuptake and recycling of glycine into the nerve terminal (16). Thus GlyT2, syntaxin-1A, and PMCA2 could be forming a

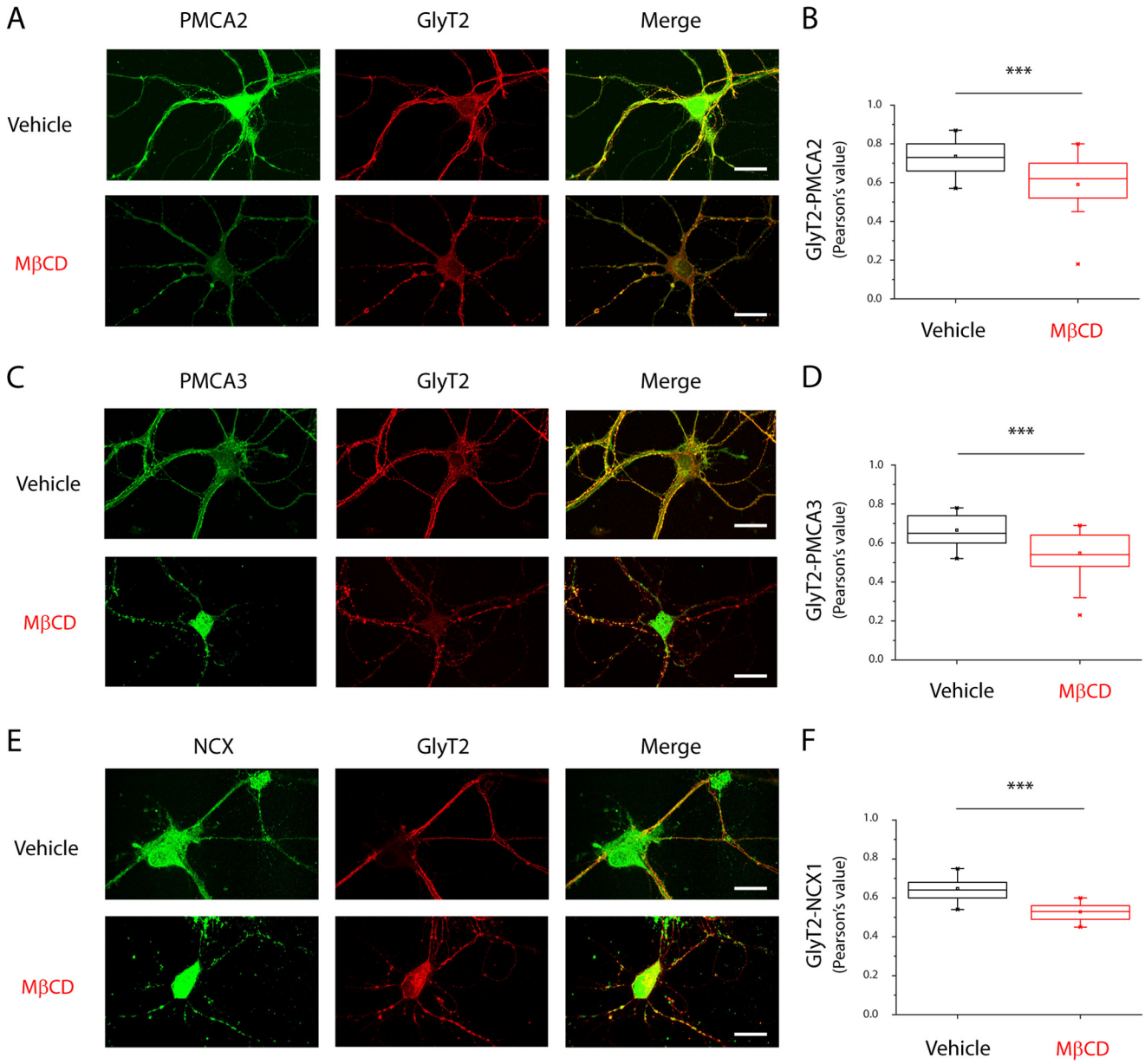

FIGURE 10. **Disruption of lipid raft integrity reduces co-localization of GlyT2 with NCX, PMCA2, and PMCA3 in primary cultures of neurons.** *A–F*, primary cultures of spinal cord and brainstem neurons were treated with 5 mM MβCD during 30 min, fixed, and incubated with primary and secondary antibodies against GlyT2 and PMCA2 (*A*), PMCA3 (*C*), or NCX (*E*). Cells were visualized by confocal microscopy, and images of primary neurons were taken. *Scale bar*, 50 μm. *B, C,* and *F,* quantification of the co-localization using Pearson's value was performed as described under "Experimental Procedures." The box whisker plots show differences on the co-localization between GlyT2 and PMCA2 (*B*), PMCA3 (*D*), and NCX (*F*). ***, significantly different from control, $p < 0.001$. Comparisons of the means were performed using ANOVA by Tukey's post hoc test ($n = 3$; on average, 20 images per condition were analyzed in each experiment).

presynaptic protein complex that would regulate GlyT2 via controlling both activity and surface expression of the transporter during neurotransmitter release.

Considering our recent identification of NKA as a partner for GlyT2 that modulates endocytosis and expression of the transporter (15), the above discussion raises the exciting possibility that GlyT2 interactions described so far with syntaxin-1A, NKA, PMCA, and NCX could occur within the same presynaptic surface complex. In agreement with this hypothesis, an interaction between NCX and NKA has also been reported (92–95). Moreover, NCX-NKA coupling has been proposed to facilitate local intracellular calcium regulation in specific and dynamic calcium signaling microdomains where lipid composition and lipid/protein interactions play an important role (87). As a compendium of these protein-protein couplings, a scheme of the physical and functional interplay between NKA, NCX, PMCA, STX1A, and GlyT2 is shown in Fig. 11*B*.

In summary, as proposed in Fig. 11*A*, binding of GlyT2 to PMCA isoforms 2 and 3 and to the NCX1 in lipid raft subdomains is postulated to help in the local homeostasis of Na^+ and Ca^{2+} during high rates of GlyT2-mediated recapture of glycine in presynaptic terminals. After neurotransmitter release, active raft-associated GlyT2 reuptakes large amounts of glycine back to the terminal producing Na^+ imbalances that must be restored. In normal conditions, this recovery is performed by Na^+/K^+-ATPase, but the pump can be saturated in

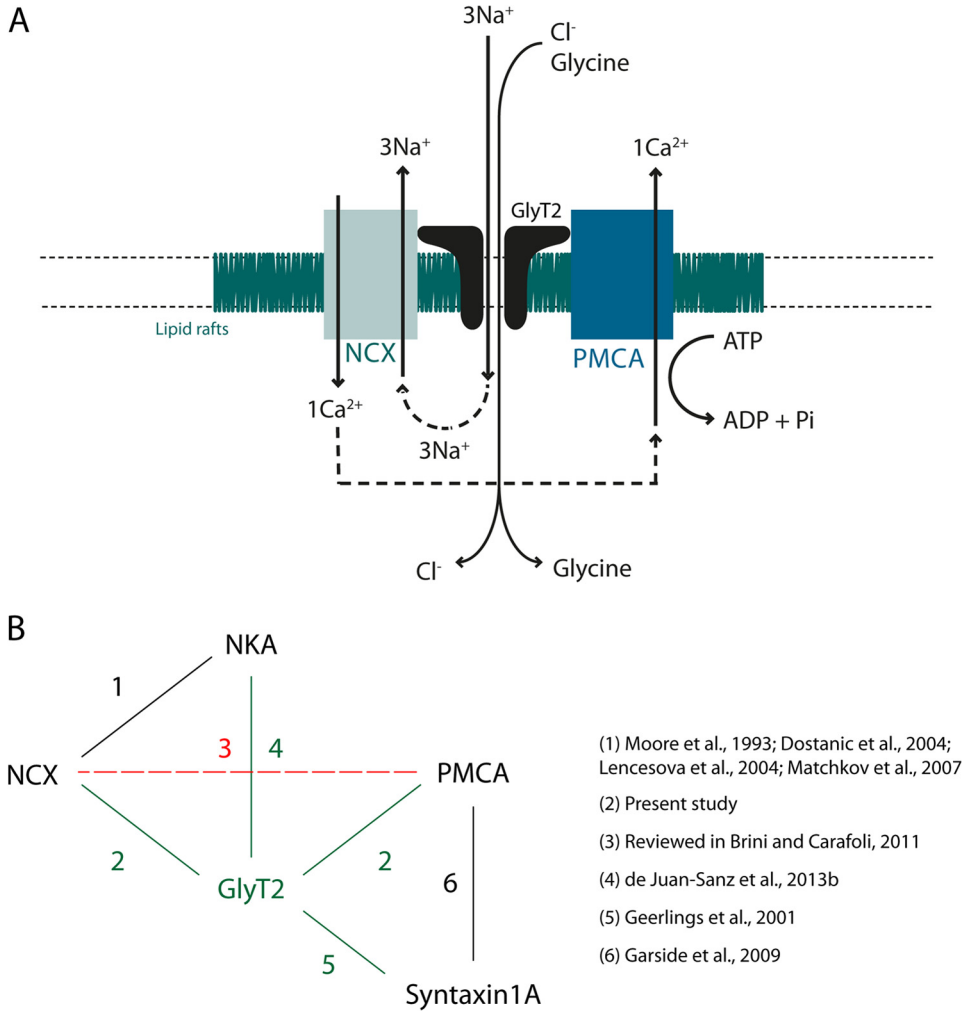

FIGURE 11. **Proposed functional relationship between GlyT2, NCX, and PMCAs in glycinergic terminals and functional interplay between NKA, NCX, PMCA, STX1A, and GlyT2.** *A,* putative model of a glycinergic terminal showing the GlyT2·NCX·PMCA complex (*black/green/blue*, respectively). *Arrows* indicate the movement of neurotransmitter and ions. The *hatched area* represent lipid rafts subdomains in the plasma membrane. *B,* scheme of physical and functional interplay between GlyT2 interacting proteins. GlyT2 interactions are denoted by *green lines* (*2, 4* and *5*). Interactions between GlyT2 interacting proteins are denoted by *black lines* (1, 6). NCX and PMCA have not been shown to physically interact, but they are highly related functionally, and this is denoted by a *dashed line* in *red* (3). Legend at *right* shows the references where these interactions are described.

situations of strong demand due to its low rates of transport (200 Hz) (37). We propose that under these conditions of saturation, Na^+ is extruded out of the terminal by NCX (a much faster Na^+-transporting protein, 2000–5000 Hz) (88). This protein would work locally in the reverse mode introducing $1Ca^{2+}$ ion while extruding $3Na^+$ ions per cycle from the terminal. The local compartmentalization of PMCAs in these membrane raft domains would facilitate the extrusion of the Ca^{2+} ion introduced by NCX, locally balancing Ca^{2+} concentration in these situations of high glycine recapture.

Acknowledgments—We thank Dr. Ana Isabel Marina and Carlos García from the Proteomic Service of Centro de Biología Molecular Severo Ochoa for their valuable and expert assistance in the proteomic analysis; Dr. Jesús Vazquez from the Centro Nacional de Investigaciones Cardiovasculares for helpful suggestions, and Dr. Michael B. Hoppa (Dartmouth University) for valuable discussions and comments on the manuscript.

REFERENCES

1. Zafra, F., Aragón, C., Olivares, L., Danbolt, N. C., Giménez, C., and Storm-Mathisen, J. (1995) Glycine transporters are differentially expressed among CNS cells. *J. Neurosci.* **15,** 3952–3969
2. Aragón, C., and López-Corcuera, B. (2005) Glycine transporters: crucial roles of pharmacological interest revealed by gene deletion. *Trends Pharmacol. Sci.* **26,** 283–286
3. Gomeza, J., Ohno, K., Hülsmann, S., Armsen, W., Eulenburg, V., Richter, D. W., Laube, B., and Betz, H. (2003) Deletion of the mouse glycine transporter 2 results in a hyperekplexia phenotype and postnatal lethality. *Neuron* **40,** 797–806
4. Rousseau, F., Aubrey, K. R., and Supplisson, S. (2008) The glycine transporter GlyT2 controls the dynamics of synaptic vesicle refilling in inhibitory spinal cord neurons. *J. Neurosci.* **28,** 9755–9768
5. Apostolides, P. F., and Trussell, L. O. (2013) Rapid, activity-independent turnover of vesicular transmitter content at a mixed glycine/GABA synapse. *J. Neurosci.* **33,** 4768–4781
6. Rees, M. I., Harvey, K., Pearce, B. R., Chung, S.-K., Duguid, I. C., Thomas, P., Beatty, S., Graham, G. E., Armstrong, L., Shiang, R., Abbott, K. J., Zuberi, S. M., Stephenson, J. B., Owen, M. J., Tijssen, M. A., van den Maagdenberg, A. M., Smart, T. G., Supplisson, S., and Harvey, R. J. (2006) Mutations in the gene encoding GlyT2 (SLC6A5) define a presynaptic

component of human startle disease. *Nat. Genet.* **38,** 801–806
7. Carta, E., Chung, S.-K., James, V. M., Robinson, A., Gill, J. L., Remy, N., Vanbellinghen, J.-F., Drew, C. J., Cagdas, S., Cameron, D., Cowan, F. M., Del Toro, M., Graham, G. E., Manzur, A. Y., Masri, A., Rivera, S., Scalais, E., Shiang, R., Sinclair, K., Stuart, C. A., Tijssen, M. A., Wise, G., Zuberi, S. M., Harvey, K., Pearce, B. R., Topf, M., Thomas, R. H., Supplisson, S., Rees, M. I., and Harvey, R. J. (2012) Mutations in the GlyT2 gene (SLC6A5) are a second major cause of startle disease. *J. Biol. Chem.* **287,** 28975–28985
8. Giménez, C., Pérez-Siles, G., Martínez-Villarreal, J., Arribas-González, E., Jiménez, E., Núñez, E., de Juan-Sanz, J., Fernández-Sánchez, E., García-Tardón, N., Ibáñez, I., Romanelli, V., Nevado, J., James, V. M., Topf, M., Chung, S.-K., Thomas, R. H., Desviat, L. R., Aragón, C., Zafra, F., Rees, M. I., Lapunzina, P., Harvey, R. J., and López-Corcuera, B. (2012) A novel dominant hyperekplexia mutation Y705C alters trafficking and biochemical properties of the presynaptic glycine transporter GlyT2. *J. Biol. Chem.* **287,** 28986–29002
9. Fornés, A., Núñez, E., Alonso-Torres, P., Aragón, C., and López-Corcuera, B. (2008) Trafficking properties and activity regulation of the neuronal glycine transporter GLYT2 by protein kinase C. *Biochem. J.* **412,** 495–506
10. de Juan-Sanz, J., Zafra, F., López-Corcuera, B., and Aragón, C. (2011) Endocytosis of the neuronal glycine transporter GLYT2: role of membrane rafts and protein kinase C-dependent ubiquitination. *Traffic* **12,** 1850–1867
11. Núñez, E., Alonso-Torres, P., Fornés, A., Aragón, C., and López-Corcuera, B. (2008) The neuronal glycine transporter GLYT2 associates with membrane rafts: functional modulation by lipid environment. *J. Neurochem.* **105,** 2080–2090
12. Jiménez, E., Zafra, F., Pérez-Sen, R., Delicado, E. G., Miras-Portugal, M. T., Aragón, C., and López-Corcuera, B. (2011) P2Y purinergic regulation of the glycine neurotransmitter transporters. *J. Biol. Chem.* **286,** 10712–10724
13. de Juan-Sanz, J., Núñez, E., López-Corcuera, B., and Aragón, C. (2013) Constitutive endocytosis and turnover of the neuronal glycine transporter GlyT2 is dependent on ubiquitination of a C-terminal lysine cluster. *PLoS One* **8,** e58863
14. Arribas-González, E., Alonso-Torres, P., Aragón, C., and López-Corcuera, B. (2013) Calnexin-assisted biogenesis of the neuronal glycine transporter 2 (GlyT2). *PLoS One* **8,** e63230
15. de Juan-Sanz, J., Núñez, E., Villarejo-López, L., Pérez-Hernández, D., Rodriguez-Fraticelli, A. E., López-Corcuera, B., Vázquez, J., and Aragón, C. (2013) Na^+/K^+-ATPase is a new interacting partner for the neuronal glycine transporter GlyT2 that downregulates its expression *in vitro* and *in vivo*. *J. Neurosci.* **33,** 14269–14281
16. Geerlings, A., Núñez, E., López-Corcuera, B., and Aragón, C. (2001) Calcium- and syntaxin 1-mediated trafficking of the neuronal glycine transporter GLYT2. *J. Biol. Chem.* **276,** 17584–17590
17. Dittman, J., and Ryan, T. A. (2009) Molecular circuitry of endocytosis at nerve terminals. *Annu. Rev. Cell Dev. Biol.* **25,** 133–160
18. Ariel, P., and Ryan, T. A. (2012) New insights into molecular players involved in neurotransmitter release. *Physiology* **27,** 15–24
19. Berridge, M. J., Lipp, P., and Bootman, M. D. (2000) The versatility and universality of calcium signalling. *Nat. Rev. Mol. Cell Biol.* **1,** 11–21
20. Augustine, G. J., Santamaria, F., and Tanaka, K. (2003) Local calcium signaling in neurons. *Neuron* **40,** 331–346
21. Bading, H. (2013) Nuclear calcium signalling in the regulation of brain function. *Nat. Rev. Neurosci.* **14,** 593–608
22. Mata, A. M., Berrocal, M., and Sepúlveda, M. R. (2011) Impairment of the activity of the plasma membrane Ca^{2+}-ATPase in Alzheimer's disease. *Biochem. Soc. Trans.* **39,** 819–822
23. Berrocal, M., Sepulveda, M. R., Vazquez-Hernandez, M., and Mata, A. M. (2012) Calmodulin antagonizes amyloid-β peptides-mediated inhibition of brain plasma membrane Ca^{2+}-ATPase. *Biochim. Biophys. Acta* **1822,** 961–969
24. Tidow, H., Poulsen, L. R., Andreeva, A., Knudsen, M., Hein, K. L., Wiuf, C., Palmgren, M. G., and Nissen, P. (2012) A bimodular mechanism of calcium control in eukaryotes. *Nature* **491,** 468–472
25. Bublitz, M., Musgaard, M., Poulsen, H., Thøgersen, L., Olesen, C., Schiøtt, B., Morth, J. P., Møller, J. V., and Nissen, P. (2013) Ion pathways in the sarcoplasmic reticulum Ca^{2+}-ATPase. *J. Biol. Chem.* **288,** 10759–10765
26. Vandecaetsbeek, I., Vangheluwe, P., Raeymaekers, L., Wuytack, F., and Vanoevelen, J. (2011) The Ca^{2+} pumps of the endoplasmic reticulum and Golgi apparatus. *Cold Spring Harb. Perspect. Biol.* **3,** a004184
27. Strehler, E. E., Caride, A. J., Filoteo, A. G., Xiong, Y., Penniston, J. T., and Enyedi, A. (2007) Plasma membrane Ca^{2+}-ATPases as dynamic regulators of cellular calcium handling. *Ann. N.Y. Acad. Sci.* **1099,** 226–236
28. Strehler, E. E., Filoteo, A. G., Penniston, J. T., and Caride, A. J. (2007) Plasma-membrane Ca^{2+} pumps: structural diversity as the basis for functional versatility. *Biochem. Soc. Trans.* **35,** 919–922
29. Strehler, E. E., and Zacharias, D. A. (2001) Role of alternative splicing in generating isoform diversity among plasma membrane calcium pumps. *Physiol. Rev.* **81,** 21–50
30. Mata, A. M., and Sepúlveda, M. R. (2005) Calcium pumps in the central nervous system. *Brain Res. Brain Res. Rev.* **49,** 398–405
31. Sepúlveda, M. R., Berrocal-Carrillo, M., Gasset, M., and Mata, A. M. (2006) The plasma membrane Ca^{2+}-ATPase isoform 4 is localized in lipid rafts of cerebellum synaptic plasma membranes. *J. Biol. Chem.* **281,** 447–453
32. Jiang, L., Fernandes, D., Mehta, N., Bean, J. L., Michaelis, M. L., and Zaidi, A. (2007) Partitioning of the plasma membrane Ca^{2+}-ATPase into lipid rafts in primary neurons: effects of cholesterol depletion. *J. Neurochem.* **102,** 378–388
33. Jiang, L., Bechtel, M. D., Galeva, N. A., Williams, T. D., Michaelis, E. K., and Michaelis, M. L. (2012) Decreases in plasma membrane Ca^{2+}-ATPase in brain synaptic membrane rafts from aged rats. *J. Neurochem.* **123,** 689–699
34. Tortelote, G. G., Valverde, R. H., Lemos, T., Guilherme, A., Einicker-Lamas, M., and Vieyra, A. (2004) The plasma membrane Ca^{2+} pump from proximal kidney tubules is exclusively localized and active in caveolae. *FEBS Lett.* **576,** 31–35
35. Zhang, J., Xiao, P., and Zhang, X. (2009) Phosphatidylserine externalization in caveolae inhibits Ca^{2+} efflux through plasma membrane Ca^{2+}-ATPase in ECV304. *Cell Calcium* **45,** 177–184
36. Fujimoto, T. (1993) Calcium pump of the plasma membrane is localized in caveolae. *J. Cell Biol.* **120,** 1147–1157
37. Skou, J. C. (1990) The energy coupled exchange of Na^+ for K^+ across the cell membrane. *FEBS Lett.* **268,** 314–324
38. Hilgemann, D. W., Nicoll, D. A., and Philipson, K. D. (1991) Charge movement during Na^+ translocation by native and cloned cardiac Na^+/Ca^{2+} exchanger. *Nature* **352,** 715–718
39. Hilgemann, D. W. (1996) Unitary cardiac Na^+, Ca^{2+} exchange current magnitudes determined from channel-like noise and charge movements of ion transport. *Biophys. J.* **71,** 759–768
40. Núñez, E., Pérez-Siles, G., Rodenstein, L., Alonso-Torres, P., Zafra, F., Jiménez, E., Aragón, C., and López-Corcuera, B. (2009) Subcellular localization of the neuronal glycine transporter GLYT2 in brainstem. *Traffic* **10,** 829–843
41. Chaudhary, J., Walia, M., Matharu, J., Escher, E., and Grover, A. K. (2001) Caloxin: a novel plasma membrane Ca^{2+} pump inhibitor. *Am. J. Physiol. Cell Physiol.* **280,** C1027–C1030
42. Cubelos, B., Leite, C., Giménez, C., and Zafra, F. (2014) Localization of the glycine transporter GLYT1 in glutamatergic synaptic vesicles. *Neurochem. Int.* **73,** 204–210
43. Sepúlveda, M. R., Berrocal, M., Marcos, D., Wuytack, F., and Mata, A. M. (2007) Functional and immunocytochemical evidence for the expression and localization of the secretory pathway Ca^{2+}-ATPase isoform 1 (SPCA1) in cerebellum relative to other Ca^{2+} pumps. *J. Neurochem.* **103,** 1009–1018
44. Bolte, S., and Cordelières, F. P. (2006) A guided tour into subcellular colocalization analysis in light microscopy. *J. Microsc.* **224,** 213–232
45. Zinchuk, V., and Grossenbacher-Zinchuk, O. (2011) Quantitative colocalization analysis of confocal fluorescence microscopy images. *Curr. Protoc. Cell Biol.* 2011 Chapter 4, Unit 4.19
46. Jaskolski, F., Mulle, C., and Manzoni, O. J. (2005) An automated method to quantify and visualize colocalized fluorescent signals. *J. Neurosci. Methods* **146,** 42–49

47. Shevchenko, A., Wilm, M., Vorm, O., and Mann, M. (1996) Mass spectrometric sequencing of proteins from silver-stained polyacrylamide gels. *Anal. Chem.* **68,** 850–858
48. Bonzon-Kulichenko, E., Pérez-Hernández, D., Núñez, E., Martínez-Acedo, P., Navarro, P., Trevisan-Herraz, M., Ramos, M. del C., Sierra, S., Martínez-Martínez, S., Ruiz-Meana, M., Miró-Casas, E., García-Dorado, D., Redondo, J. M., Burgos, J. S., and Vázquez, J. (2011) A robust method for quantitative high-throughput analysis of proteomes by ^{18}O labeling. *Mol. Cell. Proteomics* **10,** M110.003335
49. Burette, A., and Weinberg, R. J. (2007) Perisynaptic organization of plasma membrane calcium pumps in cerebellar cortex. *J. Comp. Neurol.* **500,** 1127–1135
50. Jensen, T. P., Filoteo, A. G., Knopfel, T., and Empson, R. M. (2007) Presynaptic plasma membrane Ca^{2+} ATPase isoform 2a regulates excitatory synaptic transmission in rat hippocampal CA3. *J. Physiol.* **579,** 85–99
51. Burette, A. C., Strehler, E. E., and Weinberg, R. J. (2009) "Fast" plasma membrane calcium pump PMCA2a concentrates in GABAergic terminals in the adult rat brain. *J. Comp. Neurol.* **512,** 500–513
52. Garside, M. L., Turner, P. R., Austen, B., Strehler, E. E., Beesley, P. W., and Empson, R. M. (2009) Molecular interactions of the plasma membrane calcium ATPase 2 at pre- and post-synaptic sites in rat cerebellum. *Neuroscience* **162,** 383–395
53. Boczek, T., Lisek, M., Kowalski, A., Pikula, S., Niewiarowska, J., Wiktorska, M., and Zylinska, L. (2012) Downregulation of PMCA2 or PMCA3 reorganizes Ca^{2+} handling systems in differentiating PC12 cells. *Cell Calcium* **52,** 433–444
54. Zanni, G., Calì, T., Kalscheuer, V. M., Ottolini, D., Barresi, S., Lebrun, N., Montecchi-Palazzi, L., Hu, H., Chelly, J., Bertini, E., Brini, M., and Carafoli, E. (2012) Mutation of plasma membrane Ca^{2+} ATPase isoform 3 in a family with X-linked congenital cerebellar ataxia impairs Ca^{2+} homeostasis. *Proc. Natl. Acad. Sci. U.S.A.* **109,** 14514–14519
55. DeMarco, S. J., and Strehler, E. E. (2001) Plasma membrane Ca^{2+}-ATPase isoforms 2b and 4b interact promiscuously and selectively with members of the membrane-associated guanylate kinase family of PDZ (PSD95/Dlg/ZO-1) domain-containing proteins. *J. Biol. Chem.* **276,** 21594–21600
56. Di Leva, F., Domi, T., Fedrizzi, L., Lim, D., and Carafoli, E. (2008) The plasma membrane Ca^{2+} ATPase of animal cells: structure, function and regulation. *Arch. Biochem. Biophys.* **476,** 65–74
57. Enyedi, A., and Strehler, E. E. (2011) Regulation of apical membrane enrichment and retention of plasma membrane Ca ATPase splice variants by the PDZ-domain protein NHERF2. *Commun. Integr. Biol.* **4,** 340–343
58. Allen, J. A., Halverson-Tamboli, R. A., and Rasenick, M. M. (2007) Lipid raft microdomains and neurotransmitter signalling. *Nat. Rev. Neurosci.* **8,** 128–140
59. Pike, L. J. (2009) The challenge of lipid rafts. *J. Lipid Res.* **50,** S323–S328
60. Simons, K., and Sampaio, J. L. (2011) Membrane organization and lipid rafts. *Cold Spring Harb. Perspect. Biol.* **3,** a004697
61. Madore, N., Smith, K. L., Graham, C. H., Jen, A., Brady, K., Hall, S., and Morris, R. (1999) Functionally different GPI proteins are organized in different domains on the neuronal surface. *EMBO J.* **18,** 6917–6926
62. Shi, F., and Sottile, J. (2008) Caveolin-1-dependent beta1 integrin endocytosis is a critical regulator of fibronectin turnover. *J. Cell Sci.* **121,** 2360–2371
63. Dohi, T., Morita, K., Kitayama, T., Motoyama, N., and Morioka, N. (2009) Glycine transporter inhibitors as a novel drug discovery strategy for neuropathic pain. *Pharmacol. Ther.* **123,** 54–79
64. Szewczyk, M. M., Pande, J., and Grover, A. K. (2008) Caloxins: a novel class of selective plasma membrane Ca^{2+} pump inhibitors obtained using biotechnology. *Pflugers Arch.* **456,** 255–266
65. Pande, J., Szewczyk, M. M., and Grover, A. K. (2011) Allosteric inhibitors of plasma membrane Ca^{2+} pumps: Invention and applications of caloxins. *World J. Biol. Chem.* **2,** 39–47
66. Brini, M., and Carafoli, E. (2011) The plasma membrane Ca^{2+} ATPase and the plasma membrane sodium calcium exchanger cooperate in the regulation of cell calcium. *Cold Spring Harb. Perspect. Biol.* **3,** a004168
67. Liao, J., Li, H., Zeng, W., Sauer, D. B., Belmares, R., and Jiang, Y. (2012) Structural insight into the ion-exchange mechanism of the sodium/calcium exchanger. *Science* **335,** 686–690
68. Blaustein, M. P., and Lederer, W. J. (1999) Sodium/calcium exchange: its physiological implications. *Physiol. Rev.* **79,** 763–854
69. Duman, J. G., Chen, L., and Hille, B. (2008) Calcium transport mechanisms of PC12 cells. *J. Gen. Physiol.* **131,** 307–323
70. Zhong, N., Beaumont, V., and Zucker, R. S. (2001) Roles for mitochondrial and reverse mode Na^+/ Ca^{2+} exchange and the plasmalemma Ca^{2+} ATPase in post-tetanic potentiation at crayfish neuromuscular junctions. *J. Neurosci.* **21,** 9598–9607
71. Roome, C. J., Power, E. M., and Empson, R. M. (2013) Transient reversal of the sodium/calcium exchanger boosts presynaptic calcium and synaptic transmission at a cerebellar synapse. *J. Neurophysiol.* **109,** 1669–1680
72. Roome, C. J., and Empson, R. M. (2013) The contribution of the sodium-calcium exchanger (NCX) and plasma membrane Ca^{2+} ATPase (PMCA) to cerebellar synapse function. *Adv. Exp. Med. Biol.* **961,** 251–263
73. Roux, M. J., and Supplisson, S. (2000) Neuronal and glial glycine transporters have different stoichiometries. *Neuron* **25,** 373–383
74. Watano, T., Kimura, J., Morita, T., and Nakanishi, H. (1996) A novel antagonist, No. 7943, of the Na^+/Ca^{2+} exchange current in guinea-pig cardiac ventricular cells. *Br. J. Pharmacol.* **119,** 555–563
75. Iwamoto, T., Watano, T., and Shigekawa, M. (1996) A novel isothiourea derivative selectively inhibits the reverse mode of Na^+/Ca^{2+} exchange in cells expressing NCX1. *J. Biol. Chem.* **271,** 22391–22397
76. Elias, C. L., Lukas, A., Shurraw, S., Scott, J., Omelchenko, A., Gross, G. J., Hnatowich, M., and Hryshko, L. V. (2001) Inhibition of Na^+/Ca^{2+} exchange by KB-R7943: transport mode selectivity and antiarrhythmic consequences. *Am. J. Physiol. Heart Circ. Physiol.* **281,** H1334–H1345
77. Iwamoto, T., Watanabe, Y., Kita, S., and Blaustein, M. P. (2007) Na^+/Ca^{2+} exchange inhibitors: a new class of calcium regulators. *Cardiovasc. Hematol. Disord. Drug Targets* **7,** 188–198
78. Eckert, G. P. (2010) Manipulation of lipid rafts in neuronal cells. *Open Biol. J.* **3,** 32–38
79. Nothdurfter, C., Tanasic, S., Di Benedetto, B., Rammes, G., Wagner, E.-M., Kirmeier, T., Ganal, V., Kessler, J. S., Rein, T., Holsboer, F., and Rupprecht, R. (2010) Impact of lipid raft integrity on 5-HT3 receptor function and its modulation by antidepressants. *Neuropsychopharmacology* **35,** 1510–1519
80. Roh, S.-E., Hong, Y. H., Jang, D. C., Kim, J., and Kim, S. J. (2014) Lipid rafts serve as signaling platforms for mGlu1 receptor-mediated calcium signaling in association with caveolin. *Mol. Brain* **7,** 9
81. Bublitz, M., Morth, J. P., and Nissen, P. (2011) P-type ATPases at a glance. *J. Cell Sci.* **124,** 2515–2519
82. Kurnellas, M. P., Li, H., Jain, M. R., Giraud, S. N., Nicot, A. B., Ratnayake, A., Heary, R. F., and Elkabes, S. (2010) Reduced expression of plasma membrane calcium ATPase 2 and collapsin response mediator protein 1 promotes death of spinal cord neurons. *Cell Death Differ.* **17,** 1501–1510
83. Schultz, J. M., Yang, Y., Caride, A. J., Filoteo, A. G., Penheiter, A. R., Lagziel, A., Morell, R. J., Mohiddin, S. A., Fananapazir, L., Madeo, A. C., Penniston, J. T., and Griffith, A. J. (2005) Modification of human hearing loss by plasma-membrane calcium pump PMCA2. *N. Engl. J. Med.* **352,** 1557–1564
84. Ficarella, R., Di Leva, F., Bortolozzi, M., Ortolano, S., Donaudy, F., Petrillo, M., Melchionda, S., Lelli, A., Domi, T., Fedrizzi, L., Lim, D., Shull, G. E., Gasparini, P., Brini, M., Mammano, F., and Carafoli, E. (2007) A functional study of plasma-membrane calcium-pump isoform 2 mutants causing digenic deafness. *Proc. Natl. Acad. Sci. U.S.A.* **104,** 1516–1521
85. Yu, L., and Colvin, R. A. (1997) Regional differences in expression of transcripts for Na^+/Ca^{2+} exchanger isoforms in rat brain. *Mol. Brain Res.* **50,** 285–292
86. Llinás, R., Sugimori, M., and Silver, R. B. (1992) Microdomains of high calcium concentration in a presynaptic terminal. *Science* **256,** 677–679
87. Tian, J., and Xie, Z. (2008) The Na-K-ATPase and calcium-signaling microdomains. *Physiology* **23,** 205–211
88. Blaustein, M. P., Juhaszova, M., Golovina, V. A., Church, P. J., and Stanley, E. F. (2002) Na/Ca exchanger and PMCA localization in neurons and astrocytes. *Ann. N.Y. Acad. Sci.* **976,** 356–366
89. Reuter, H., and Porzig, H. (1995) Localization and functional significance of the Na^+/Ca^{2+} exchanger in presynaptic boutons of hippocampal cells in culture. *Neuron* **15,** 1077–1084

90. Goldberg, J. H., Tamas, G., Aronov, D., and Yuste, R. (2003) Calcium microdomains in aspiny dendrites. *Neuron* **40,** 807–821
91. Gómez-Varela, D., Schmidt, M., Schoellerman, J., Peters, E. C., and Berg, D. K. (2012) PMCA2 via PSD-95 controls calcium signaling by α7-containing nicotinic acetylcholine receptors on aspiny interneurons. *J. Neurosci.* **32,** 6894–6905
92. Moore, E. D., Etter, E. F., Philipson, K. D., Carrington, W. A., Fogarty, K. E., Lifshitz, L. M., and Fay, F. S. (1993) Coupling of the Na^+/Ca^{2+} exchanger, Na^+/K^+ pump and sarcoplasmic reticulum in smooth muscle. *Nature* **365,** 657–660
93. Dostanic, I., Schultz Jel, J., Lorenz, J. N., and Lingrel, J. B. (2004) The α1 isoform of Na,K-ATPase regulates cardiac contractility and functionally interacts and co-localizes with the Na/Ca exchanger in heart. *J. Biol. Chem.* **279,** 54053–54061
94. Lencesova, L., O'Neill, A., Resneck, W. G., Bloch, R. J., and Blaustein, M. P. (2004) Plasma membrane-cytoskeleton-endoplasmic reticulum complexes in neurons and astrocytes. *J. Biol. Chem.* **279,** 2885–2893
95. Matchkov, V. V., Gustafsson, H., Rahman, A., Briggs Boedtkjer, D. M., Gorintin, S., Hansen, A. K., Bouzinova, E. V., Praetorius, H. A., Aalkjaer, C., and Nilsson, H. (2007) Interaction between Na^+/K^+-pump and Na^+/Ca^{2+}-exchanger modulates intercellular communication. *Circ. Res.* **100,** 1026–1035
96. Philipson, K. D., Longoni, S., and Ward, R. (1988) Purification of the cardiac Na^+- Ca^{2+} exchange protein. *Biochim. Biophys. Acta* **945,** 298–306

Artículo #4

Giménez C, Pérez-Siles G, Martínez-Villarreal J, **Arribas-González E**, Jiménez E, Núñez E, de Juan-Sanz J, Fernández-Sánchez E, García-Tardón N, Ibáñez I, Romanelli V, Nevado J, James VM, Topf M, Chung SK, Thomas RH, Desviat LR, Aragón C, Zafra F, Rees MI, Lapunzina P, Harvey RJ, López-Corcuera B (2012)

A novel dominant hyperekplexia mutation Y705C alters trafficking and biochemical properties of the presynaptic glycine transporter GlyT2

J Biol Chem. 287(34):28986-9002

THE JOURNAL OF BIOLOGICAL CHEMISTRY VOL. 287, NO. 34, pp. 28986–29002, August 17, 2012

A Novel Dominant Hyperekplexia Mutation Y705C Alters Trafficking and Biochemical Properties of the Presynaptic Glycine Transporter GlyT2*

Received for publication, October 31, 2011, and in revised form, June 18, 2012 Published, JBC Papers in Press, June 29, 2012, DOI 10.1074/jbc.M111.319244

Cecilio Giménez[‡§¶], Gonzalo Pérez-Siles[‡§], Jaime Martínez-Villarreal[‡§¶], Esther Arribas-González[‡¶], Esperanza Jiménez[‡§¶], Enrique Núñez[‡§¶], Jaime de Juan-Sanz[‡§¶], Enrique Fernández-Sánchez[‡], Noemí García-Tardón[‡§¶], Ignacio Ibáñez[‡], Valeria Romanelli[§‖], Julián Nevado[§‖], Victoria M. James[**], Maya Topf[‡‡], Seo-Kyung Chung[§§], Rhys H. Thomas[§§], Lourdes R. Desviat[‡], Carmen Aragón[‡§¶], Francisco Zafra[‡§¶], Mark I. Rees[§§], Pablo Lapunzina[§‖], Robert J. Harvey[**], and Beatriz López-Corcuera[‡§¶1]

From the [‡]Departamento de Biología Molecular and Centro de Biología Molecular "Severo Ochoa," (Consejo Superior de Investigaciones Científicas-Universidad Autónoma de Madrid), Madrid 28049, Spain, the [§]Centro de Investigación Biomédica en Red de Enfermedades Raras, Instituto de Salud Carlos III, Madrid 28029, Spain, the [¶]IdiPAZ-Hospital Universitario La Paz, the [‖]Instituto de Genética Médica y Molecular, IdiPAZ-Hospital Universitario La Paz, Universidad Autónoma de Madrid, Madrid 28046, Spain, the [**]Department of Pharmacology, University College London School of Pharmacy, London WC1N 1AX, United Kingdom, the [‡‡]Institute of Structural and Molecular Biology, Crystallography, Birkbeck College, London WC1E 7HX, United Kingdom, and the [§§]Institute of Life Science, College of Medicine, Swansea University, Swansea SA2 8PP, United Kingdom

Background: Hyperekplexia or startle disease is caused by defects in glycinergic transmission.
Results: A new mutation pY705C in the glycine transporter GlyT2 alters protein trafficking and H^+ and Zn^{2+} transport modulation.
Conclusion: Multiple pathogenic mechanisms may contribute to the complex phenotype of individuals with the Y705C mutation.
Significance: This is the first common dominant mutation associated with hyperekplexia affecting the presynaptic glycine transporter GlyT2.

Hyperekplexia or startle disease is characterized by an exaggerated startle response, evoked by tactile or auditory stimuli, producing hypertonia and apnea episodes. Although rare, this orphan disorder can have serious consequences, including sudden infant death. Dominant and recessive mutations in the human glycine receptor (GlyR) α1 gene (*GLRA1*) are the major cause of this disorder. However, recessive mutations in the presynaptic Na^+/Cl^--dependent glycine transporter GlyT2 gene (*SLC6A5*) are rapidly emerging as a second major cause of startle disease. In this study, systematic DNA sequencing of *SLC6A5* revealed a new dominant GlyT2 mutation: pY705C (c.2114A→G) in transmembrane domain 11, in eight individuals from Spain and the United Kingdom. Curiously, individuals harboring this mutation show significant variation in clinical presentation. In addition to classical hyperekplexia symptoms, some individuals had abnormal respiration, facial dysmorphism, delayed motor development, or intellectual disability. We functionally characterized this mutation using molecular modeling, electrophysiology, [^{3}H]glycine transport, cell surface expression, and cysteine labeling assays. We found that the introduced cysteine interacts with the cysteine pair Cys-311–Cys-320 in the second external loop of GlyT2. This interaction impairs transporter maturation through the secretory pathway, reduces surface expression, and inhibits transport function. Additionally, Y705C presents altered H^+ and Zn^{2+} dependence of glycine transport that may affect the function of glycinergic neurotransmission *in vivo*.

The extracellular concentration of synaptic glycine is regulated by Na^+/Cl^--dependent glycine transporters. These proteins mediate reuptake of glycine into presynaptic terminals (GlyT2)[2] and glial cells adjacent to glycinergic inhibitory neurons (GlyT1) (1). Mouse knock-out studies have revealed that glial GlyT1 is the main regulator of the extracellular glycine concentrations (2). By contrast, neuronal GlyT2 is involved in the removal and recycling of synaptic glycine generating a vectorial flow from the synaptic cleft into the terminal, supplying substrate to the low affinity vesicular inhibitory amino acid transporter (2, 3). Inactivation of the GlyT2 gene (*Slc6a5*) pre-

* This work was supported by Spanish Dirección General de Enseñanza Superior e Investigación Científica Grants BFU2005-05931/BMC and BIO2005-05786, Ministerio de Ciencia e Innovación Grant SAF2008-05436, Comunidad Autónoma de Madrid Grants 11/BCB/010 and S-SAL-0253/2006, Ministerio de Economia y Competitividad Grant SAF2011-28674, Centro de Investigación Biomédica en Red de Enfermedades Raras Intramural Project U-751/U-753, an institutional grant from the Fundación Ramón Areces, Medical Research Council Grant G0601585, and Action Medical Research Grant 1966. The group is member of the European Regional Development Fund Grant BFU2007-30688-E/BFI.

[1] To whom correspondence should be addressed: Dept. de Biología Molecular, Centro de Biología Molecular "Severo Ochoa," Universidad Autónoma de Madrid, 28049 Madrid, Spain. Tel.: 34-91-1964631; Fax: 34-91-1964420; E-mail: blopez@cbm.uam.es.

[2] The abbreviations used are: GlyT, glycine transporter; GlyR, glycine receptor; GLR, glycine receptor subunit; HBS, Hepes-buffered saline; $LeuT_{Aa}$, leucine transporter from *A. aeolicus*; MesNa, sodium methanethiosulfonate; MTSEA, 2 aminoethyl methanethiosulfonate; SLC, solute carrier; TCEP, tris(2-carboxyethyl) phosphine; TM, transmembrane domain; HBS, Hepes-buffered saline; MDCK, Madin-Darby canine kidney.

vents glycine loading into synaptic vesicles, impairing inhibitory glycinergic neurotransmission (4). GlyT2 knock-out mice have a complex motor phenotype (4, 5) that mimics clinical signs of hyperekplexia or startle disease (OMIM 149400). This rare human disorder is characterized by an exaggerated startle response to acoustic or tactile stimuli (6). Startle disease can have serious consequences for neonates, including brain damage and/or sudden death caused by apnea episodes. The abnormal startle response, which can provoke unprotected falls resulting in injury, can persist throughout development and into adulthood (7). However, unlike rodent, cattle, and canine defects (6), humans with *SLC6A5* mutations survive, and clinical signs often resolve after the neonatal and infantile risk period (8).

Genetic analysis of individuals with human hyperekplexia has revealed mutations in genes for postsynaptic proteins involved in glycinergic neurotransmission. These include the GlyR α1 and β subunits (*GLRA1* and *GLRB*) and proteins that assist receptor trafficking to the synaptic membrane (9–11). Sequencing the 16 exons of the human GlyT2 gene (*SLC6A5*) also revealed that missense, nonsense, and frameshift mutations affecting presynaptic glycine transport can cause hyperekplexia (8, 12). The structure of a prokaryotic homologue ($LeuT_{Aa}$) of the SLC6 family (13) has provided a useful model for explaining the effects of selected missense mutations on Na^+ and glycine-binding residues crucial for transport activity (6, 8, 12). It is also noteworthy that the majority of GlyT2 mutations were recessive, producing bi-allelic loss of function caused by the absence of protein in the plasma membrane or by production of an inactive transporter (6). In the present study, we report the identification of a novel dominant mutation (c.2114A→G, pY705C) in exon 15 of *SLC6A5*. This change was found in eight individuals from three families in two cohorts of hyperekplexia patients that were devoid of GlyR gene mutations. Functional characterization of this GlyT2 substitution revealed the introduced cysteine impacts on transporter protein maturation through the secretory pathway and alters the H^+ and Zn^{2+} dependence of glycine transport. The biochemical features of the mutant transporter may produce detrimental effects on glycinergic inhibition *in vivo*.

EXPERIMENTAL PROCEDURES

Molecular Genetic Analysis of the Human GlyT2 Gene (SLC6A5)—Informed consent was obtained from all individuals using guidelines approved by the local ethical committees. Patients of both sexes were studied. Patient genomic DNA was amplified using primers for the 16 exons of the *SLC6A5* gene as previously described (8). 60 ng of genomic DNA were amplified using an Expand high fidelity PCR system (Roche Applied Science) in 25-μl reactions containing 10 pmol of each primer, 1× buffer with 1.5 mM $MgCl_2$, 200 μM dNTPs, and 1 unit of Taq polymerase (Roche Applied Science). PCR conditions were 94 °C for 5 min followed by 35 cycles of 30 s at 94 °C, 30 s at 60 °C, and 30 s at 72 °C. Amplification products were analyzed on 2% agarose gels, extracted with a QIAQuick gel extraction kit (Qiagen), and sequenced employing BigDye Terminator v.3.1 mix (Applied Biosystems Foster City, CA). Genomic DNA from 200 commercially available controls was obtained from the European Collection of Cell Cultures, human random control. Population analysis was conducted by DNA sequencing of control amplicons or using the artificially created restriction site method (14), where an NdeI site is introduced into control but not mutated amplicons during PCR. Electropherograms were analyzed using Sequencher (Gene Codes Corp., Ann Arbor, MI). Analysis of copy number variations in hyperekplexia genes was assessed by multiplex ligation-dependent probe amplification. Briefly, DNA (250 μg) was tested using the SALSA multiplex ligation-dependent probe amplification kit P274 (MRC Holland), which evaluates several regions of *GLRA1*, *GLRB*, and *SLC6A5*. No abnormalities (deletions nor duplications) were observed in any of the samples evaluated, ruling out copy number variations as a cause of hyperekplexia in these cases.

In Silico Analysis—Conservation of the mutated residues was assessed by alignment of orthologous and human protein sequences using ClustalW software (15). The putatively damaging effects of the predicted amino acid substitution was assessed using the PolyPhen-2 program (16) that gives the results as "benign," "possibly damaging," "probably damaging," or "unknown." A GlyT2 homology model was obtained using MODELLER (17) as previously reported (6, 18), based on the crystal structure of $LeuT_{Aa}$ from the bacterium *Aquifex aeolicus* (Protein Data Bank code 2A65) (13).

Mutagenesis and Expression of Human GlyT2 cDNA in Mammalian Cells—The human GlyT2 cDNA was cloned into the vectors pRC-CMV (Invitrogen) and pEGFP-C1 (Clontech) as previously described (8). Missense mutations were generated in pRC-CMV GlyT2 by site-directed mutagenesis using the QuikChange kit (Stratagene). Two independent *Escherichia coli* colonies carrying the mutant plasmids were characterized by DNA sequencing and [^{3}H]glycine transport activity. We sequenced the full coding region of each construct to verify that only the desired mutation had been introduced. Transient expression in COS7 cells was performed as described (18) using Lipofectamine Plus (Invitrogen) or Neofectin™ (MidAtlantic Biolabs). The cells were incubated for 48 h at 37 °C, unless otherwise indicated in the figure legends. For electrophysiological recordings, the human GlyT2 cDNA was subcloned into the vector pSP64T, generously provided by Dr. Carmen Montiel (Universidad Autónoma of Madrid, Madrid, Spain).

Glycine Transport Assays—Transport assays in COS7 cells were performed at 37 °C in 0.25 ml of Hepes-buffered saline (HBS: 150 mM NaCl, 10 mM Hepes-Tris, pH 7.4, 1 mM $CaCl_2$, 5 mM KCl, 1 mM $MgSO_4$, 10 mM glucose). 2 μCi/ml [^{3}H]glycine (1.6 TBq/mmol; PerkinElmer Life Sciences) isotopically diluted at 10 μM final glycine concentration was used (19), unless a different concentration is specified. The reactions were terminated after 10 min by aspiration followed by washing with HBS. Transport was measured by subtracting the glycine accumulation by mock-transfected COS7 cells from that of GlyT2 transfected cells and normalizing to the protein concentration. Kinetic analysis was performed by varying glycine concentration in the uptake medium between 10 and 1000 μM.

Expression of the Human GlyT2 cDNA in Xenopus Oocytes—Wild-type and mutant GlyT2 cDNAs were cloned in the vector pSP64T, which contains a β1-globin promoter. Constructs

were linearized with XbaI, and cRNA was transcribed with SP6 polymerase and capped with 5′7-methylguanosine using the mMESSAGE mMACHINE SP6 RNA kit (Ambion Inc.). *Xenopus laevis* females were obtained from *Xenopus* Express (France). The oocytes were harvested from *X. laevis* anesthetized in tricaine methasulfonate 0.10% (w/v) solution in tap water. All of the procedures were in accordance with the Spanish and European guidelines for the prevention of cruelty to animals. The follicular membrane was removed by incubation in a medium (90 mM NaCl, 1 mM KCl, 1 mM $MgCl_2$, 5 mM Hepes, pH 7.4) containing 300 units/ml collagenase (Type 1; Sigma) for 1 h. Wild-type or mutant mRNAs (50 ng) were injected into defolliculated stage V and VI *X. laevis* oocytes. The oocytes were maintained in Barth's medium (88 mM NaCl, 1 mM KCl, 0.33 mM $Ca(NO_3)_2$, 0.41 mM $CaCl_2$, 0.82 mM $MgSO_4$, 2.4 mM $NaHCO_3$, and 10 mM Hepes, pH 7.4), and transport or electrophysiological experiments were assayed 5 days post-injection.

Two-microelectrode Voltage-Clamp Recordings from Xenopus Oocytes—Electrophysiological recordings were obtained after incubation of the injected oocytes at 18 °C in standard oocyte solution (100 mM NaCl, 2 mM KCl, 1 mM $CaCl_2$, 1 mM $MgCl_2$, 10 mM Hepes, pH adjusted to pH 7.5 with HCl). Two-electrode voltage clamp was used to measure and control the membrane potential and to monitor the capacitative currents using Axoclamp 900A (Axon Instruments), digitized using a Digidata 1440 (Axon Instruments). Both instruments were controlled by pCLAMP software (Axon Instruments), and the results were analyzed using Clampfit 10.2 software (Axon Instruments). Recordings were performed at room temperature using standard micropipettes filled with 3 M KCl (resistance varied between 0.5 and 2 MΩ). The oocytes were held at −40 mV, and to obtain current-voltage (I-V) relations, the pulse protocol consisted of 350-ms voltage steps between −130 and +50 mV in 20 mV steps. The currents were subjected to low pass filtering at 100 Hz.

Cell Surface Labeling—Thiol-specific biotinylation and total surface biotinylation was performed with MTSEA-biotin (Toronto Research Chemicals Inc., Toronto, Canada) and sulfo-NHS-SS-biotin (Pierce) on transfected COS7 cells as described (20, 21). 0.5 mM MTSEA-biotin or 1.5 mg/ml sulfo-NHS-SS-biotin and a 3-h incubation with streptavidin-agarose beads (Sigma) were used. Biotinylated proteins (B) were eluted from the beads with Laemmli buffer (40 mM Tris, pH 6.8, 2% SDS, 10% glycerol, 0.1 M DTT, 0.01% bromphenol blue) for 10 min at 70 °C and then analyzed in Western blots (7.5% SDS-PAGE) with anti-GlyT2 antibody (Santa Cruz). Protein bands were visualized by ECL and quantified on a GS-710 calibrated imaging densitometer from Bio-Rad with Quantity One software, using film exposures in the linear range. Loading controls were performed by reprobing Western blot membranes using an anti-calnexin antibody. Standard errors were calculated from at least three separate experiments.

GlyT2 Subcellular Localization—Wild-type or mutant GlyT2 in pEGFP-C1 were transfected in MDCK cells and 48 h later were subjected to immunofluorescence as described previously (22) using the antibody against the indicated marker protein. Secondary antibodies were coupled to Alexa Fluor® 555. Alternatively, the cells were transfected with pEGFP-C1 GlyT2 (23) and were fixed with 4% paraformaldehyde in PBS. The cells were visualized by confocal microscopy on a LSM510 confocal microscope (Zeiss) using a vertical microscope Axio Imager.Z1 M (Zeiss).

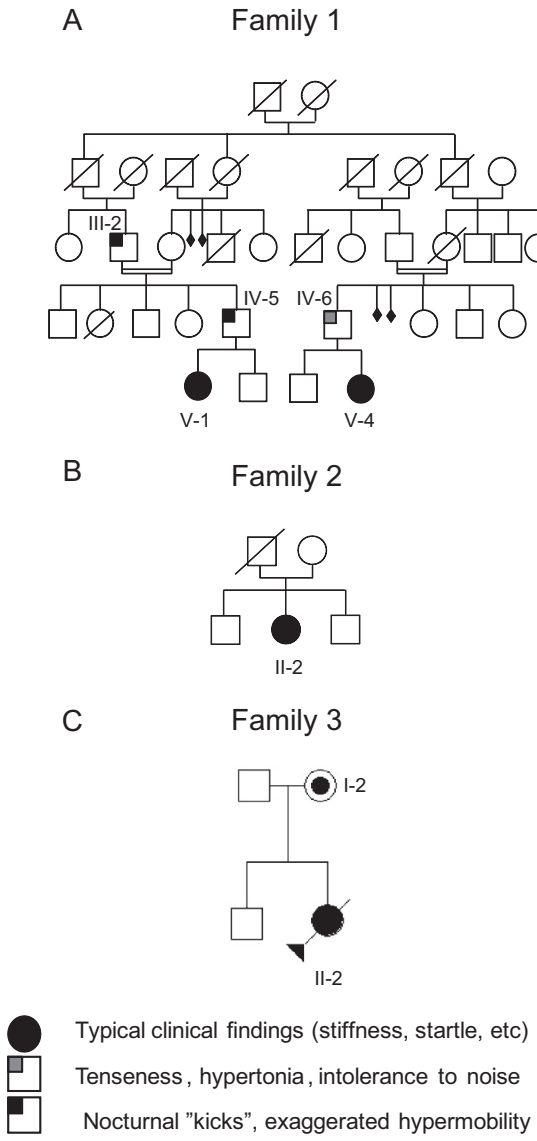

FIGURE 1. **Pedigree of families 1 (*A*), 2 (*B*), and 3 (*C*).** Individuals are numbered according to their position in the pedigree lines as I, II, III, and IV, and then each individual from left to right as 1, 2, 3, etc. Males and females are represented by *squares* and *circles*, respectively. *Shaded symbols* represent individuals with the Y705C mutation or who are/were affected, with clinical signs observed.

RESULTS

Patient Information—A total of 16 probands from Spain and 188 from the UK with clinical diagnosis of hyperekplexia, all of which had proved gene-negative in screens of *GLRA1* and *GLRB*, were provided from neurological units. Genomic DNA samples from the patients were screened for *SLC6A5* mutations. Clinical features of patients carrying the novel mutation in the *SLC6A5* gene are summarized below. Fig. 1 shows the pedigrees of the patient families.

The first patient from family 1, V-1, displayed perinatal onset persistent crying and hypertonia. This was ameliorated when she was removed from the neonatal intensive care unit and was placed in a quiet, low stimuli environment. Physical examination at day 7 revealed an exaggerated startle reaction and prominent head retraction. She had delayed motor development and showed a severe degree of intellectual disability. With the second patient from family 1, V-4, concern was raised when the child was 1 month old because of hypertonia and abnormal crying. Neurological evaluation demonstrated abnormal head retraction and hypertonia, which improved during sleep. Patient IV-5 from family 1 had similar neonatal behavior to V-1; he "kicked" and had exaggerated movements during rest at bed, mainly when sleeping. Patient IV-6 in family 1 showed some intolerance to noise and crowded places, and when he was a boy suffered from attacks of stiffness precipitated by surprise or school tests.

Patient II-2 in family 2 was a girl who presented with stiffness and frequent falling and was intellectually intact. Patient II-2 in family 3 had perinatal hypertonia with clonus (variable, partially resolving in sleep) and triggered startle episodes (paroxysmal clonic movements). In addition she had abnormal respiration with prominent apnea episodes. Physically she had several dysmorphic features: tongue protrusion, striking excess neck skin folds, large atrial-septal defect, short palpebral fissures, small carp-like mouth, subtly low set ears, single palmar crease, contractures at the knees, and overlapping clenched fingers and hands. Cranial calcification was also seen. Her MRI demonstrated small focal areas of signal change in the deep, subcortical white matter of both cerebral hemispheres and possible gyral swelling. She died aged 21 weeks having spent the majority of her life in pediatric intensive care. The mother is apparently asymptomatic. She was physically examined at the age of thirty-one and no abnormality or excessive startle was detected.

Genetic Analysis—Genomic DNA samples from 204 individuals with hyperekplexia who had tested negative for disease-causing mutations in *GLRA1* (5q33.1) and *GLRB* (4q32.1) were scanned on all 16 coding exons and extended flanking intronic regions of *SLC6A5* (11p15.1), encoding human GlyT2. Several single-nucleotide polymorphisms present in patients and controls were found. In addition, DNA sequence analysis revealed a heterozygous nonsynonymous change (c.2114A→G) in exon 15 in four of the patients analyzed (patients V-1 and V-2 of family 1, patient II-2 of family 2, and patient II-2 of family 3). Familial analysis revealed the presence of this sequence variant in four more individuals (Fig. 1). This change was not detected in 600 unrelated, normal control chromosomes (data from the United Kingdom; not detected in 400 normal control chromosomes, Caucasian samples), as assessed using two different techniques (see "Experimental Procedures"). This mutation resulted in a tyrosine (T*A*T) to cysteine (T*G*T) substitution at position 705 (pY705C) in transmembrane domain 11 (TM11; Fig. 2). Homology modeling of GlyT2 using the crystal structure of the $LeuT_{Aa}$ (13) located Tyr-705 at the carboxyl-terminal portion of the TM11, near the extracellular face of the transporter (Fig. 2*B*). A loss of a hydrogen bond with the side chain of Glu-701 is predicted. Phylogenetic comparisons of the TM11 region of GlyT2 show high evolutionary conservation of Tyr-705 (Fig. 2*C*). Alignment of GlyT2 with other Na^+/Cl^--dependent neurotransmitter transporters of the SLC6 family demonstrates that a tyrosine is found at the equivalent position in most human neurotransmitter transporters from the GABA, amino acid, and monoamine subfamilies (norepinephrine transporter and dopamine transporter) with the exception of GABA transporter 1 and serotonin transporter (Fig. 2*D*). This suggests that Tyr-705 has a relevant role for transporter function within this superfamily and accordingly, the Y705C substitution was predicted to be "probably damaging" in PolyPhen-2 analysis, with a score of 1.000.

Mutagenesis and Functional Characterization—Functional consequences of the Y705C mutation were initially assessed by assaying [^{3}H]glycine uptake of recombinant wild-type and mutant GlyT2 after transient expression in COS7 cells (Fig. 3*A*). The V_{max} of glycine transport by the Y705C mutant was reduced to ~60% as compared with wild-type GlyT2 (23 ± 2.5 for the Y705C *versus* 38 ± 3.2 nmol of Gly/mg of protein/5 min for wild type). The co-expression of wild-type and Y705C transporters resulted in a V_{max} of 30 ± 3.1 nmol of Gly/mg of protein/5 min, representing 79% of wild-type GlyT2. This value is close to the predicted average value of the activity of each transporter population. A slight but significant increase of the K_m for glycine was observed in the Y705C mutant when expressed alone. Investigation of other features of glycine transport by GlyT2 indicated that sensitivity to Na^+ and Cl^-, the ions required for transport, was unaffected in Y705C mutant, and the sensitivity of the mutant transporter to the inhibition by the selective GlyT2 inhibitor ALX1393 was unchanged as compared with wild-type GlyT2 (data not shown).

Additional functional characterization was performed by overexpressing wild-type and mutant GlyT2 in *Xenopus* oocytes to examine the electrophysiological properties of both proteins. As shown in Fig. 3*B*, glycine-induced inward currents were observed in oocytes expressing either wild-type GlyT2 or the Y705C mutant. In agreement with the reduced V_{max} for glycine transport observed in COS cells, maximal currents recorded from oocytes were ~35% lower than observed for wild-type GlyT2. We also studied the voltage dependence of the observed currents by employing a voltage-clamp protocol consisting of long square pulses from −130 to +50 mV. The current triggered by glycine showed inward rectification for both transporters (Fig. 3*C*). The *I-V* relationships were similar in shape, suggesting no alteration of the voltage dependence of glycine transport. However, at each voltage examined, the current mediated by wild-type GlyT2 was larger than that of the Y705C mutant.

Plasma Membrane Expression—One possible explanation for the reduction in V_{max} for glycine transport of the Y705C mutant could be impaired plasma membrane expression. We determined the levels of transporters present in the plasma membrane using two different approaches. First, we expressed EGFP-tagged wild-type GlyT2 or the Y705C mutant in MDCK cells (Fig. 4*A*), immunolabeling the cells for the plasma membrane marker protein E-cadherin (22, 24). The percentage of Y705C co-localization with the plasma membrane marker was

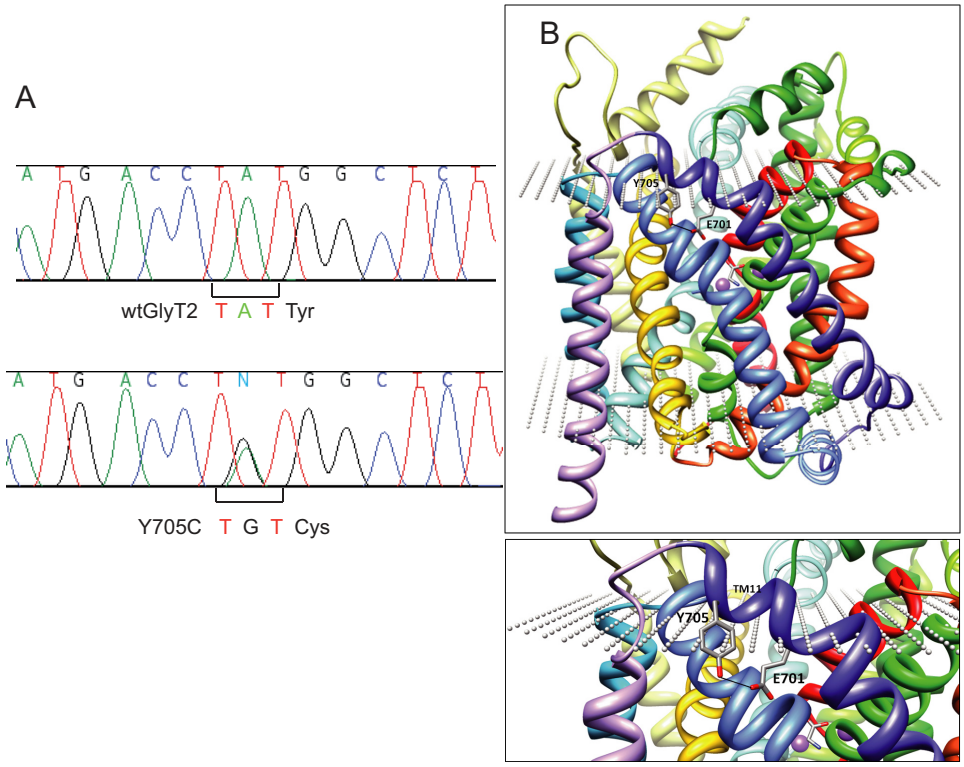

C

Homo sapiens	VCWAFVTPTILTFILCFSFYQWEPMTYGSYRYPNWSMVLGWLMLACSVIWIP
Mus musculus	VCWAFVTPTILTFILCFSFYQWEPMTYGSYRYPNWSMVLGWLMLACSVIWIP
Rattus norvegicus	VCWAFVTPTILTFILCFSFYQWEPMTYGSYRYPNWSMVLGWLMLACSVIWIP
Canis familiaris	VCWAFVTPTILTFILCFSFYQWEPMTYGSYRYPNWSMVLGWLMLACSVIWIP
Monodelphis domestica	VCWAFVTPTILTFILCFSFYQWEPMTYGSYRYPNWSMVLGWLMLACSVIWIP
Gallus gallus	VCWAFVTPTILTFILCFSFYQWEPMTYGAYHYPGWSMVLGWLMLACSVIWIP
Danio rerio	VCWAFVTPTILTFILALSLYQWKVMTYEDYTYPNWSMVLGWLMVICSVIWIP
Strongylocentrotus p.	VNWSAFTPGLMVFVLFFNWLQWVEPSYNG-PFPTWAVIIGWLMTTMSLIWIP

D

hGlyT2	SLC6A5	CWAFVTPTILTFILCFSFYQWEPMTYGS-YRYPNWSMVLGWLMLACSVIWIP
hGlyT1	SLC6A9	CWRFVSPAIIFFILVFTVIQYQPITYNH-YQYPGWAVAIGFLMALSSVLCIP
hPROT	SLC6A7	CWLFLSPATLLALMVYSIVKYQPSEYGS-YRFPPWAELLGILMGLLSCLMIP
hTAUT	SLC6A6	SWAVITPVLCVGCFIFSLVKYVPLTYNKTYVYPNWAIGLGWSLALSSMLCVP
hGAT1	SLC6A1	CWSFFTPIIVAGVFIFSAVQMTPLTMGN-YVFPKWGQGVGWLMALSSMVLIP
hGAT2	SLC6A13	CWLFLTPAVCTATFLFSLIKYTPLTYNKKYTYPWWGDALGWLLALSSMVCIP
hGAT3	SLC6A11	CWMIMTPGICAGIFIFFLIKYKPLKYNNIYTYPAWGYGIGWLMALSSMLCIP
hBGT1	SLC6A12	SWLFLTPGLCLATFLFSLSKYTPLKYNNVYVYPPWGYSIGWFLALSSMVCVP
hCRTR	SLC6A8	CWSFFTPLVCMGIFIFNVVYYEPLVYNNTYVYPWWGEAMGWAFALSSMLCVP
hNET	SLC6A2	CWKFVSPAFLLFVVVVSIINFKPLTYDD-YIFPPWANWVGWGIALSSMVLVP
hDAT	SLC6A3	CWKLVSPCFLLFVVVVSIVTFRPPHYGA-YIFPDWANALGWVIATSSMAMVP
hSERT	SLC6A4	CWVAISPLFLLFIICSFLMSPPQLRLFQ-YNYPYWSIILGYCIGTSSFICIP

FIGURE 2. **Genetic and structural analysis of the Y705C mutant.** *A*, partial sequences of exon 15 from control and patient 1 DNAs, respectively. Note the heterozygous single-nucleotide polymorphism c.2114A→G changes the codon TAT to TGT, resulting in a pY705C substitution in GlyT2. *B*, molecular model of GlyT2 showing the localization of Tyr-705 in TM11. *C*, phylogenetic comparison of TM11 regions of GlyT2 containing the amino acid Tyr-705 (in *red*). *D*, sequence alignment of GlyT2 TM11 region in human SLC6 family members. Sequences were obtained from NCBI (www.ncbi.nlm.nih.gov) and were aligned using ClustalW software and MUSCLE alignment server.

76.8 ± 2.3% compared with wild-type GlyT2. In addition, surface labeling with the nonpermeant reagent Sulfo-NHS-SS-biotin of the proteins expressed in the plasma membrane of COS7 cells allowed the isolation and quantification of the surface-resident transporters. In agreement with this finding, the Y705C mutant amounted for 68.9 ± 5.7% of wild-type GlyT2 levels (Fig. 4*B*). GlyT2 protein expressed in cultured cells appears as a mature 100-kDa protein band, which is the form present on the plasma membrane, and a 75-kDa underglycosylated immature transporter (25). As shown in Fig. 4*B*, the Y705C mutant showed a higher proportion of immature precursor compared with wild-type GlyT2, so that the mature/immature protein ratio was 50% reduced for the mutant. This is highly suggestive of a deficiency in the biogenesis and processing of the Y705C mutant along the secretory pathway, slowing the transformation of the immature precursor into the mature protein. However, we did not observe clear co-localization of the transporter mutant with the endoplasmic reticulum marker (calnexin), nor with other cellular markers such as TGN38, Rab5, or the early endosome marker EEA1 as compared with wild-type GlyT2 (Fig. 4*C*). This suggests that the mutant protein is not arrested in a precise compartment of the secretory pathway but perhaps progresses slowly along the endomembrane system. In addition, no alteration of the typical GlyT2

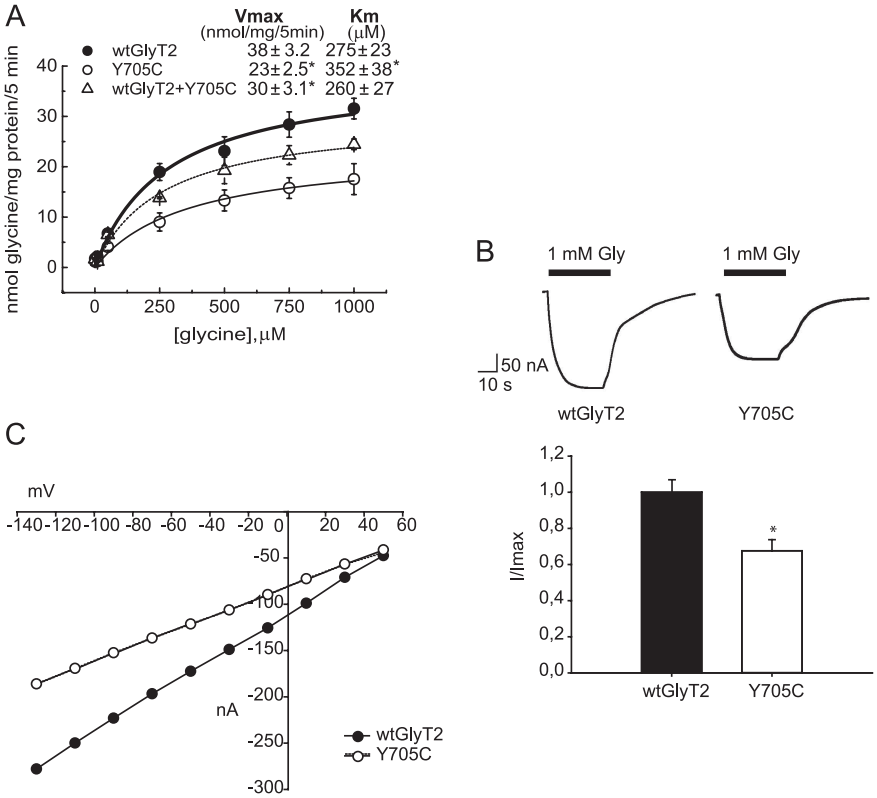

FIGURE 3. **Glycine transport and electrophysiological characterization of wild-type GlyT2 and the Y705C mutant.** *A*, COS7 cells expressing the indicated transporters were assayed for ^{3}[H]glycine transport during 10 min in HBS containing 150 mM NaCl in the presence of increasing glycine concentrations from 0.5 to 1 mM. Experimental data were fitted to hyperbolae. Kinetic parameters are indicated on the graph. *, significantly different from wild-type GlyT2, $p < 0.05$ in Student's *t* test. *B*, inward currents evoked by glycine in representative oocytes expressing wild-type GlyT2 or the Y705C mutant. The cells were voltage-clamped at −40 mV, and 1 mM glycine was superfused for the period indicated by the *solid bar*. Histogram represents arithmetic means ± S.E. ($n = 5$–10 oocytes) of normalized inward currents for wild-type GlyT2 and the Y705C mutant. *, significantly different from wild-type GlyT2, $p < 0.05$ in Student's *t* test. *C*, current-voltage plots of the glycine-mediated inward currents of wild-type GlyT2 and Y705C mutant determined by subtracting, in each case, the currents observed in the absence of glycine.

apical sorting (26) was observed in polarized MDCK cells growing in Transwells (Fig. 4*D*), because the asymmetric distribution of the Y705C mutant was coincident with that of wild-type GlyT2.

Substitution Analysis of Tyr-705—Multiple amino acid substitutions at Tyr-705 showed a comparable, although smaller impairment of plasma membrane localization than that observed for Y705C (Fig. 5*A*). This suggests that the defect in transporter biogenesis is not only due to the introduction of Cys-705 but also due to Tyr-705 removal. Moreover, different Tyr-705 substitutions had heterogeneous effects on glycine transport (Fig. 5*B*). Y705F or Y705A had no or low impact, showing 100 ± 12 and 80 ± 10% of wild-type transport, respectively. By contrast, Y705K and Y705S surpassed wild-type activity by 108 ± 11 and 135 ± 10%, respectively. Remarkably, substitution by glutamic acid (Y705E) profoundly impaired function resulting in 37 ± 4% of wild-type transport. Because transport activity of these mutants does not correlate with membrane expression, Tyr-705 substitutions affect the activity of surface transporters in addition to membrane trafficking.

To further investigate the effect of the cysteine substitution found in the hyperekplexia patients and taking into account that this residue can potentially form disulfide bonds with other cysteines, we performed DTT treatment on cells expressing Tyr-705 mutants. Interestingly, DTT rescued the transport activity of the Y705C mutant from 61 ± 6 to 100 ± 7% of wild-type transport (Fig. 5*B*). As expected, this effect was specific for the Y705C mutant, suggesting that glycine transport activity was restored by reduction of a disulfide bond involving Cys-705. DTT can readily cross the plasma membrane and may affect both transporter trafficking and transport activity. To distinguish between these two possibilities, we used the non-permeant reducing agents MesNa (27) and TCEP (28) (Fig. 5, *C* and *D*). Both reagents consistently produced lower recovery of Y705C function than DTT. This suggests the internal access of the reagent is important for the activation. The small activation produced by the negatively charged MesNa might be due to its decreased reactivity compared with the uncharged TCEP. However, none of the nonpermeant reagents reached the activation produced by DTT. We therefore assumed that DTT can improve a defect in the processing/folding of the transporter during biogenesis, whereas MesNa or TCEP can only "activate" plasma membrane-localized Y705C. Consistent with this theory, Fig. 5*D* shows that MesNa and TCEP promoted higher activation of the Y705C mutant than wild-type GlyT2 or the Y705A mutant.

DTT Increases Plasma Membrane Expression of the Y705C Mutant—Next, we wished to know whether DTT activation targets the intracellular Y705C transporter and increases

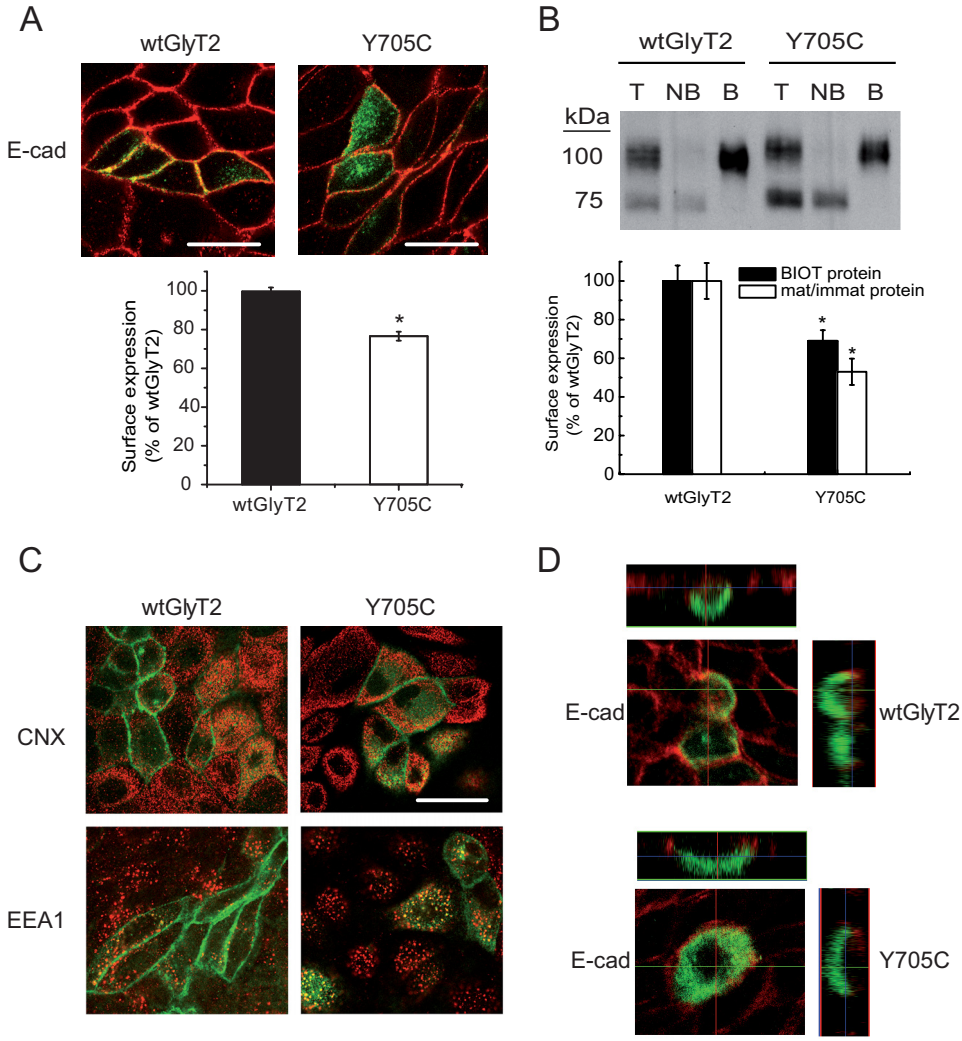

FIGURE 4. **Cell and plasma membrane expression of wild-type GlyT2 and Y705C.** *A*, immunofluorescence quantification of plasma membrane transporters. Wild-type EGFP-tagged GlyT2 or Y705C expressed in MDCK cells for 48 h were immunolabeled for the plasma membrane marker E-cadherin (*E-cad*). Two channel confocal images were obtained (*green* for GlyT2 and *red* for E-cadherin), and regions occupied by E-cadherin were taken as plasma membrane and regions inside the cadherin staining were taken as intracellular, using the Image J ROI manager. After applying an automatic threshold to adjust images, the fluorescence intensity was measured separately for membrane and intracellular regions, and the percentage of transporter in plasma membrane was calculated (histogram). This process was performed at least in 150 cells/condition. *, $p < 0.05$ values calculated using Student's *t* test by comparing wild-type GlyT2 with the Y705C mutant. *B*, COS7 cells expressing wild-type GlyT2 or Y705C mutant were subjected to biotinylation as described under "Experimental Procedures." 8 μg of total (*lanes T*) and nonbiotinylated proteins (*lanes NB*) and 24 μg of biotinylated proteins (*lanes B*) were subjected to Western blotting for GlyT2 detection, and the membranes were reprobed for calnexin immunoreactivity as a loading control. *Lower panel*, densitometric analysis. *Black bars*, total transporter that was biotin-labeled (*B* as a % of *T*) as percentage of that of wild-type GlyT2. *Open bars*, mature/immature transporter ratio (100 kDa/75 kDa) as a percentage of the ratio (100 kDa/75 kDa) for wild-type GlyT2. *, $p < 0.05$ in Student's *t* test. *C*, MDCK cells expressing wild-type EGFP-tagged GlyT2 or Y705C were immunolabeled for calnexin (*CNX*, endoplasmic reticulum marker) or early endosome antigen 1 (*EEA1*, early endosome marker). No significantly difference in co-localization was observed. *D*, MDCK cells transfected with wild-type EGFP-tagged GlyT2 or Y705C were plated on cell culture filter inserts and grown to confluence. Samples were examined by laser scanning confocal microscopy. *Left panel*, en face views. *Right panel*, *x-z* cross-sections. The *x-z* cross-sections are derived from the indicated transept lines.

plasma membrane levels sufficiently to restore the wild-type levels of surface-active GlyT2. For this purpose, we treated COS7 cells expressing wild-type GlyT2 or the Y705C mutant with DTT for increasing periods of time up to 30 min and measured [^{3}H]glycine transport and surface biotinylation in parallel (Fig. 6, *A* and *B*). As shown above, glycine transport by the Y705C mutant was rapidly increased by DTT, reaching wild-type levels of activity in 3–4 min and continuing up to 10 min before reaching a plateau (Fig. 6*A*). A 10-min period has been shown to be sufficient for trafficking to the Golgi of polytopic proteins expressed in mammalian cells (29). We have measured comparable time courses of plasma membrane expression for GlyT2.[3] In fact, extended time periods in DTT increased the amount of surface mutant transporter with a slightly delayed time course. This indicates a fast activation of surface-inserted transporter (5 min) followed by a slower increase in the amount of plasma membrane protein (10–30 min; Fig. 6*B*, *left histogram*). A decrease in the levels of the immature protein was also observed (Fig. 6*B*, *right histogram*). By contrast, the quantity of wild-type GlyT2 present in the plasma membrane was slightly diminished by DTT, and the transport activity was only slightly

[3] E. Arribas-González, P. Alonso-Torres, C. Aragón, and B. López-Corcuera, manuscript in preparation.

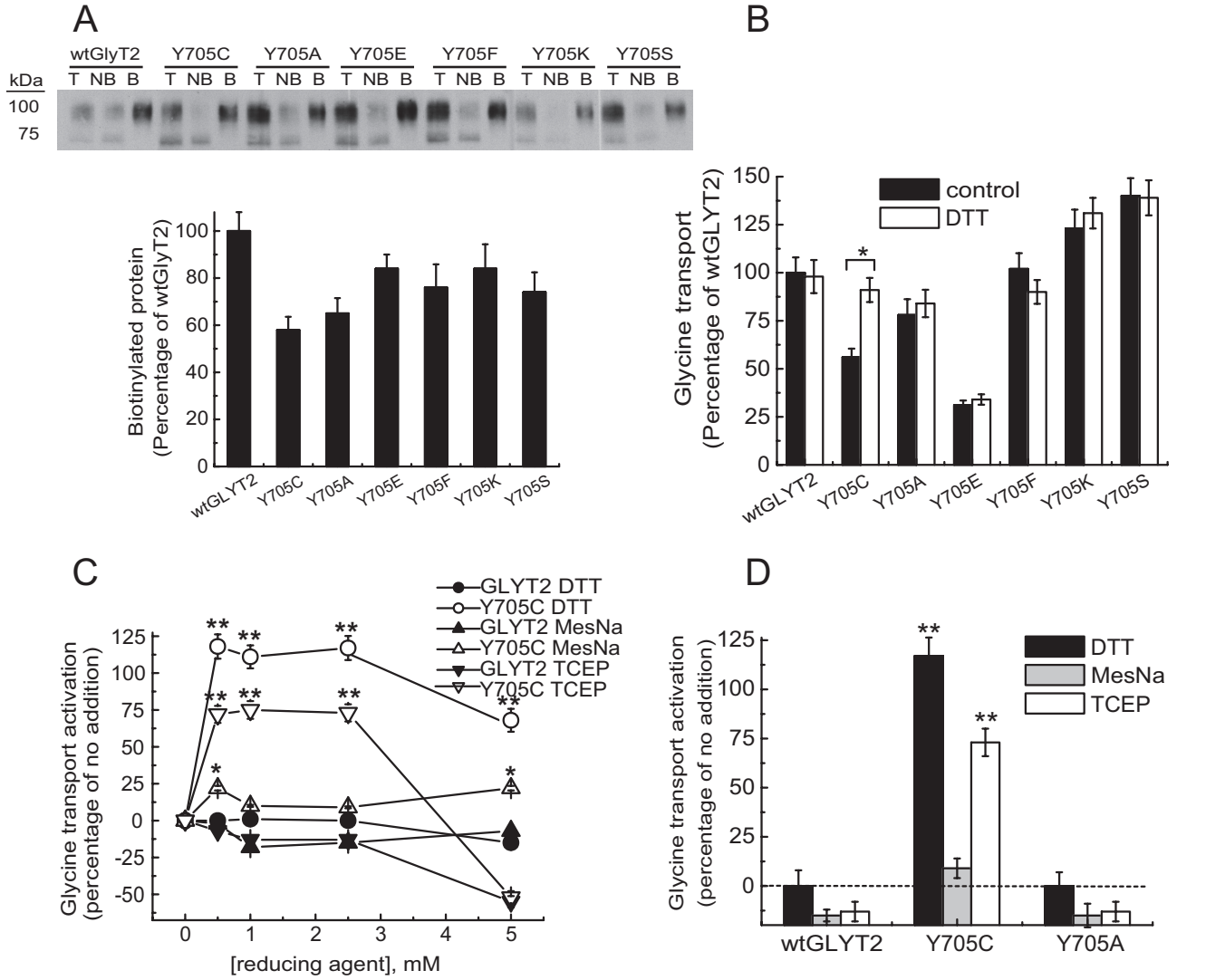

FIGURE 5. **Substitution analysis of Tyr-705 and effect of DTT on glycine transport.** Transiently transfected COS7 cells expressing wild-type GlyT2 or mutants with the indicated amino acids at position 705, were subjected to biotinylation as described in Fig. 4 to determine plasma membrane expression (*A*) or treated with vehicle or 12 mM DTT (*B*) or 2.5 mM DTT (*D*) or the specified concentrations of the indicated reducing agents (*C*) and then assayed for [^{3}H]glycine transport. In *B*, * indicates significantly different from wild-type GlyT2, $p < 0.05$ in Student's *t* test. In *C* and *D*, ** indicates $p < 0.01$, and * indicates $p < 0.05$ by analysis of variance. *Lanes T*, total proteins; *lanes NB*, nonbiotinylated proteins; *lanes B*, biotinylated proteins.

increased. To confirm that DTT can induce Y705C exocytosis, we treated MDCK cells expressing EGFP-tagged transporters with DTT and monitored co-localization with the plasma membrane marker E-cadherin (Fig. 6, *C* and *D*). As shown in Fig. 4*A*, the percentage of Y705C co-localization with the plasma membrane marker was ~65% compared with wild-type GlyT2, and the co-localization was increased by 40% by DTT (Fig. 6*D*).

Y705C Forms an Aberrant Disulfide Bond Interfering with the Cys-311–Cys-320 Pair—One possible explanation of the recovery of Y705C function with DTT could be that Cys-705 forms a disulfide bond with one of the 23 endogenous cysteines present in GlyT2 (Fig. 7*B*). Such a covalent bond could impair glycine transport and/or transporter trafficking. Cleavage of this bond by DTT could restore mutant membrane expression and transport activity. To test this possibility, we took advantage of the predicted external accessibility of Cys-705 and labeled the cells expressing the transporters with the nonpermeable SH-specific reagent MTSEA-biotin (Fig. 7, *A*, *E*, and *F*). This probe reacts with externally accessible free thiol groups in an aqueous environment. In control conditions, the fraction of SH-labeled Y705C mutant was higher than that of wild-type GlyT2 (~2 ± 0.5-fold; Fig. 7, *A* and *E*). Taking into account that the membrane expression of Y705C is ~65% of wild-type GlyT2 (Fig. 4), this means the cysteine specific label is ~3-fold higher in the Y705C mutant than in wild-type GlyT2. In fact, pretreatment with DTT, which increases mutant membrane expression to wild-type levels (Fig. 6), yielded ~3-fold higher labeling for Y705C compared with wild-type GlyT2 (Fig. 7, *A*, *E*, and *F*). This suggests that the Y705C mutation involves structural effects that increase cysteine availability. When the cells were pretreated with *N*-ethylmaleimide in the absence of DTT to prevent SH reagent reaction with the free cysteines, both transporters showed reduced labeling (Fig. 7*A*). Under this condition, the Y705C labeling was ~65% of that of wild-type GlyT2, reflecting lower membrane expression. Moreover, if *N*-ethyl-

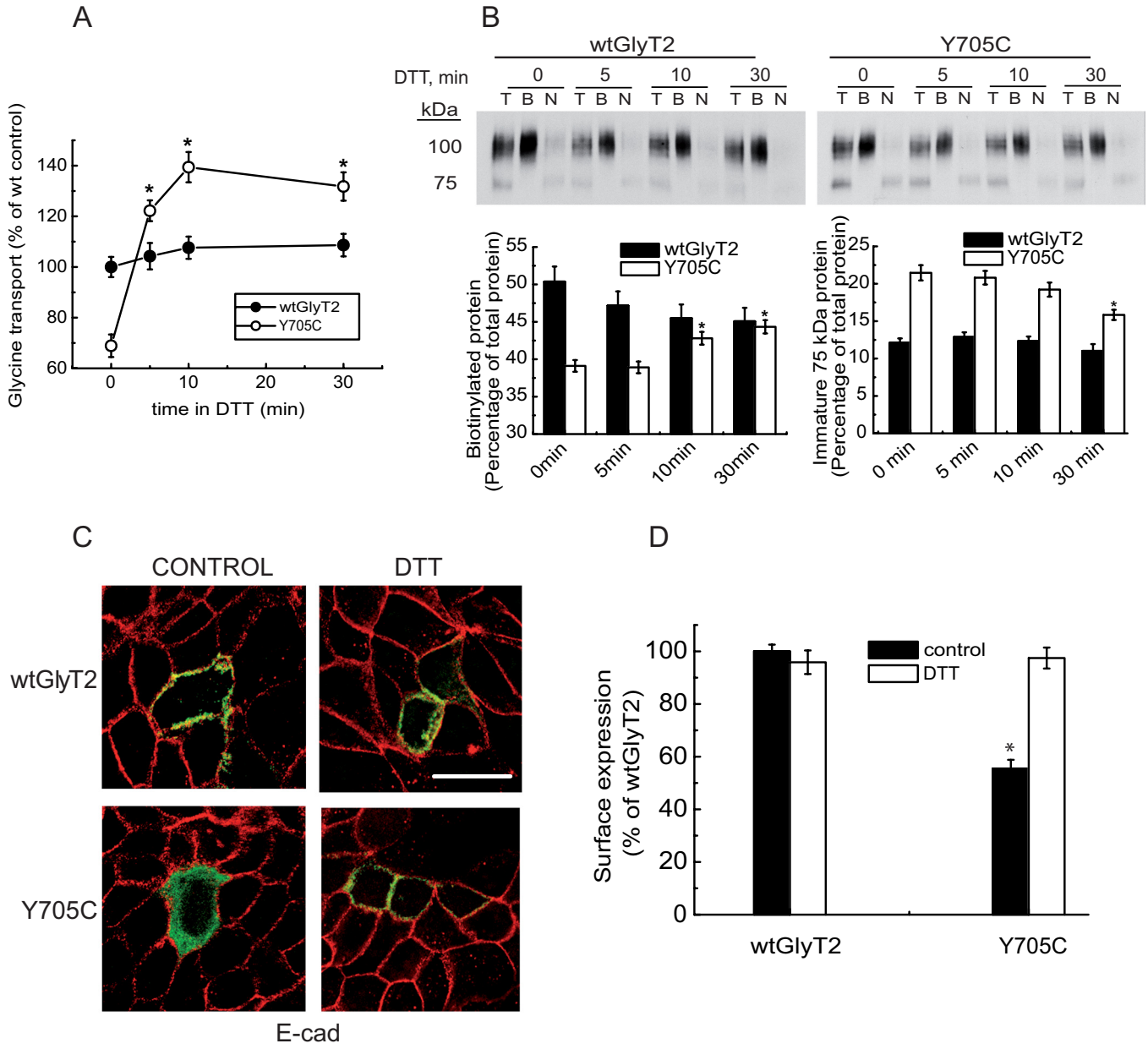

FIGURE 6. **Effect of DTT on Y705C plasma membrane expression.** COS7 cells expressing wild-type GlyT2 or Y705C were treated with 12 mM DTT at 22 °C for the indicated times and then assayed for [^{3}H]glycine transport for 10 min (*A*) or subjected to sulfo-NHS-SS-biotinylation as described under "Experimental Procedures" (*B*). *A*, transport data are expressed as percentages of wild-type GlyT2 transport activity, which was 2.8 ± 0.3 nmol of Gly/mg of protein/10 min. *, significantly different from no DTT, $p < 0.05$ in Student's *t* test. *B*, *upper panel*, Western blot for GlyT2 detection of a SDS-PAGE loaded with 8 μg of total (*lanes T*) and nonbiotinylated proteins (*lanes N*) and 24 μg of biotinylated proteins (*lanes B*). *Lower panel*, densitometric analysis. *, significantly different from no DTT, $p < 0.05$ in Student's *t* test. *C*, MDCK cells expressing wild-type EGFP-tagged GlyT2 or Y705C were treated for 30 min with 12 mM DTT, placed on ice to stop trafficking, and immunolabeled for the plasma membrane marker E-cadherin (*E-cad*). *D*, co-localization of transporter and marker was performed as described for Fig. 4. *, $p < 0.05$ values calculated using Student's *t* test by comparing wild-type GlyT2 with the Y705C mutant.

maleimide pretreatment was performed, and then DTT was added to release cysteines from disulfides, the DTT-induced increase in SH-specific label of the Y705C mutant was higher than that of wild-type GlyT2 (Fig. 7*A*). This result suggests the presence of an additional disulfide bond in the Y705C mutant. To identify the binding partner for Cys-705, we inspected the three-dimensional structure of GlyT2 and selected several cysteine residues based on location that might permit the formation of an intra- or intermolecular disulfide bond with Cys-705 (Fig. 7*B*). Selected cysteines were individually substituted to serine to form Cys → Ser mutants. Single substitutions were introduced into the Cys-705 background to generate double mutants (*CXS/Y705C*), which were tested for DTT activation of glycine transport (Fig. 7, *C* and *D*). Two of the mutants (C311S/Y705C and C320S/Y705C) were activated to a smaller extent than the other mutants (Fig. 7*D*). This result supports a potential interaction between a cysteine at position 705 and cysteines at positions 311 and 320. Accordingly, C311S/Y705C or C320S/Y705C double mutants display a significantly reduced MTSEA-biotin labeling compared with the Y705C mutant, indicating that Cys-705 can interact with either Cys-311 or Cys-320 (Fig. 7, *E* and *F*). Cysteines 311 and 320 are located in the second

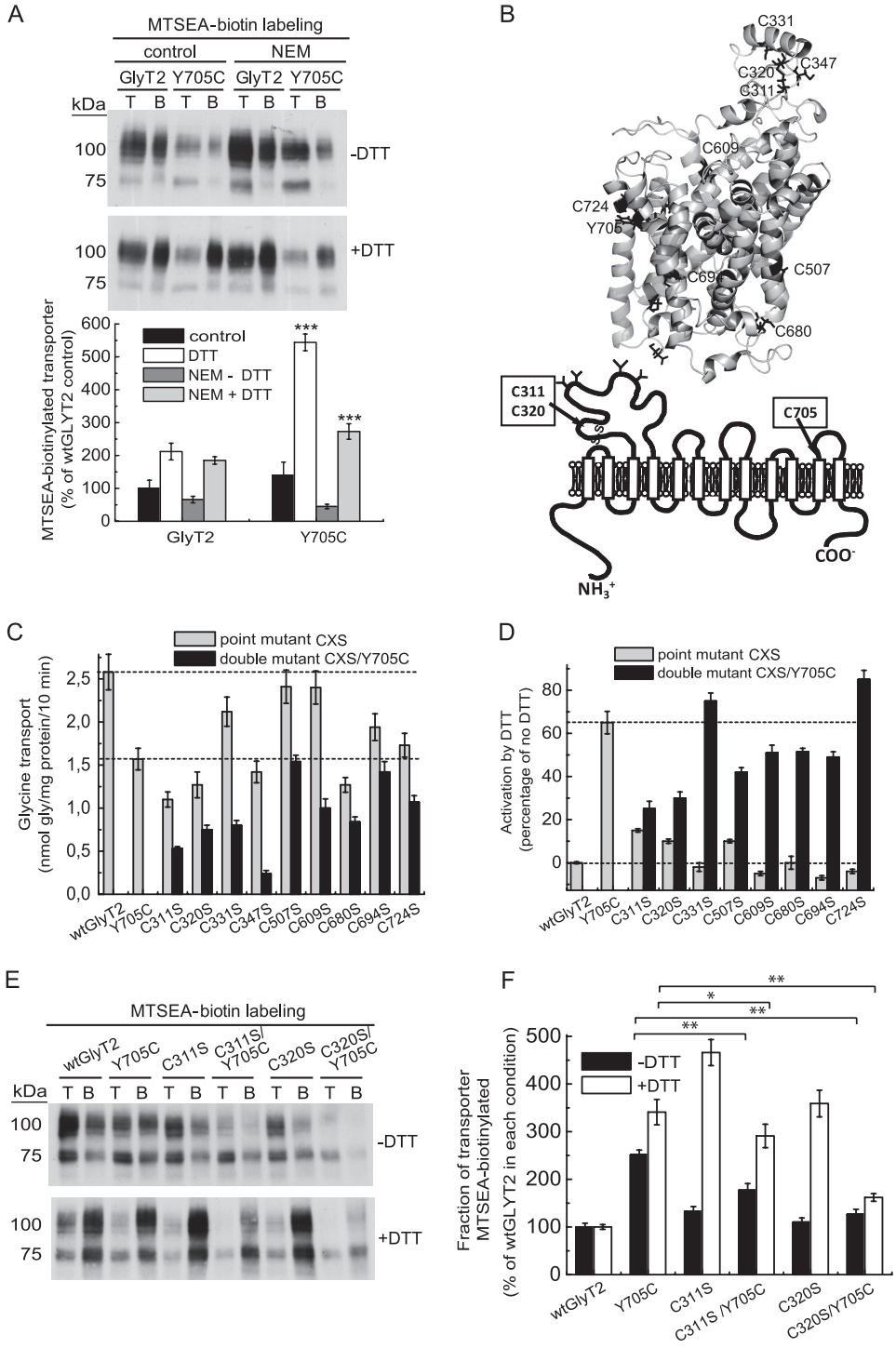

FIGURE 7. **MTSEA-biotin labeling and transport activity of Y705C and GlyT2 cysteine mutants.** *A*, COS7 cells expressing wild-type GlyT2 or Y705C were treated with vehicle or 50 mM *N*-ethylmaleimide (*NEM*) for 10 min, washed, and treated with HBS or 12 mM DTT in HBS for 30 min, washed, and subjected to MTSEA-biotinylation as described under "Experimental Procedures." *Upper panel*, Western blot for GlyT2 detection of a SDS-PAGE loaded with 10 μg of total (*lanes T*) and 100 μg of biotinylated proteins (*lanes B*). *Lower panel*, densitometric analysis of the percentage of total transporter (*B* as a % of *T*) that was MTSEA-biotin-labeled in each condition as percentage of control wild-type GlyT2. ***, Significantly different from wild-type GlyT2, $p < 0.001$ in Student's *t* test. *B*, *upper panel*, molecular model of GlyT2 showing the localization of Tyr-705 and some of the endogenous cysteines (*black*). *Lower panel*, location of the Cys-311–Cys-320 pair in the second external loop as compared with Cys-705 on schematic GlyT2 secondary structure. *C* and *D*, effect of DTT on glycine transport by cysteine to serine mutants in the background of wild-type GlyT2 or the Y705C mutant. COS7 cells expressing wild-type GlyT2, Y705C, cysteine to serine mutants (*CXS*), or Y705C/cysteine to serine double mutants (*CXS/Y705C*) for 48 h were assayed for [^{3}H]glycine transport for 10 min after being treated with vehicle (*C*) or with 12 mM DTT at 22 °C for 5 min (*D*). *E*, COS7 cells expressing the indicated transporters were treated with vehicle (−DTT) or DTT (+DTT) for 30 min, washed, and MTSEA-biotin-labeled; streptavidin-agarose bound proteins were run in nonreducing (−*DTT*) or reducing (+*DTT*) SDS-PAGE and subjected to Western blotting as above. *F*, densitometric analysis of the percentage of total transporter that was MTSEA-biotin-labeled in each condition. For clarity, this was expressed as percentage of the respective wild-type GlyT2 in each condition. Significantly different from the Y705C single mutant: *, $p < 0.05$; **, $p < 0.01$ in Student's *t* test.

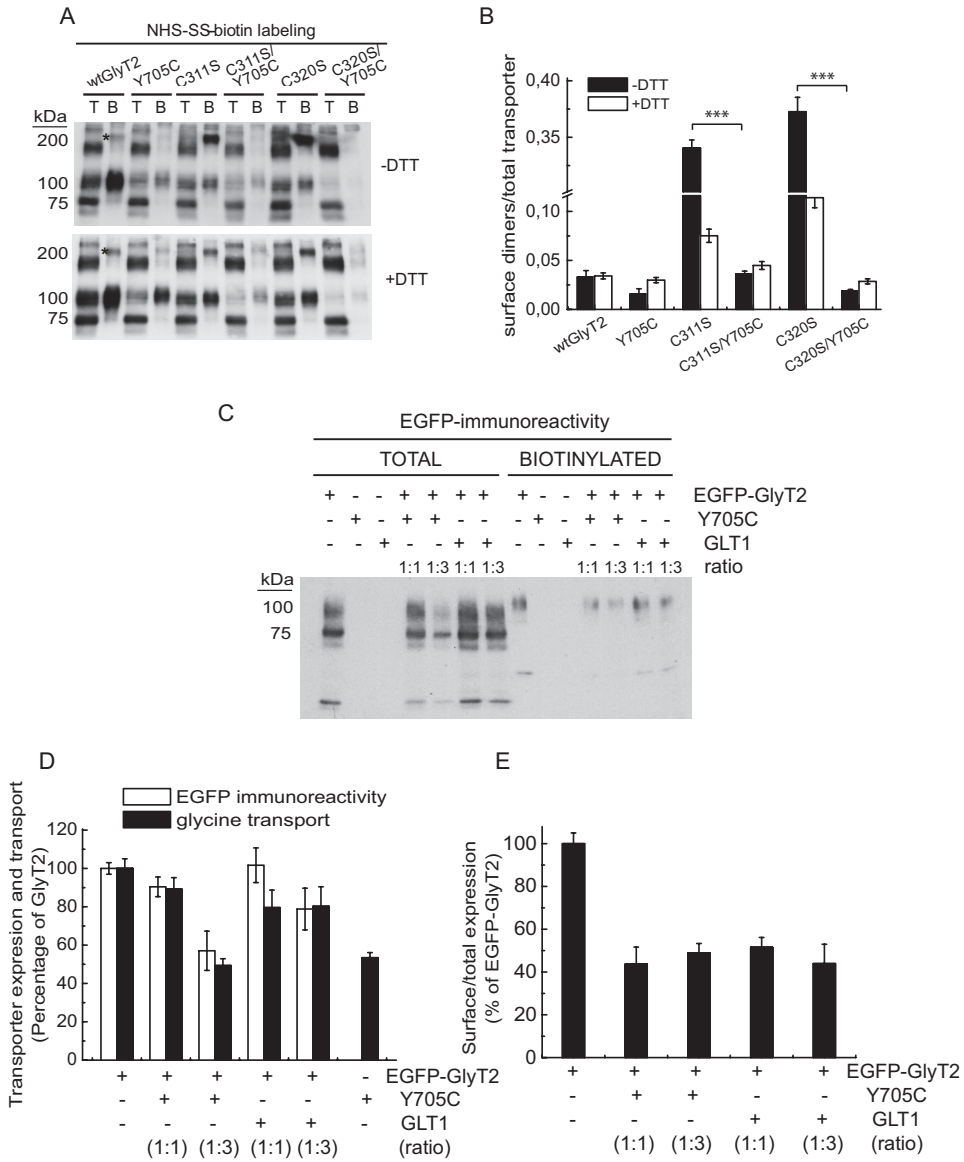

FIGURE 8. **Surface labeling and co-expression of Y705C and GlyT2 cysteine mutants.** *A*, COS7 cells expressing the indicated transporters were treated with vehicle (−*DTT*) or DTT (+*DTT*) for 30 min, washed, and subjected to NHS-SS-biotinylation as in Fig. 4*B*. *Lanes T*, total proteins; *lanes B*, biotinylated proteins. *B*, densitometric analysis of three blots as in *A* showing the immunoreactivity of 200-kDa dimers (*band* marked with *asterisk* in *A*) normalized by the total transporter immunoreactivity. ***, significantly different from the respective single mutant, $p < 0.01$ in Student's *t* test. *C*, effect of wild-type GlyT2 and Y705C on transporter expression. COS7 cells expressing wild-type GlyT2 or Y705C tagged with EGFP as described in Ref. 24 at the indicated ratios (increasing mutant cDNA) were assayed for [^{3}H]glycine transport and in parallel subjected to NHS-SS-biotinylation as described under "Experimental Procedures" except anti-EGFP antibody was used for the Western blots. *D*, effect of the expression of Y705C on EGFP-GlyT2 expression (densitometric analysis of blots as in *C*) and transport activity. *E*, effect of the expression of Y705C on EGFP-GlyT2 surface expression.

external loop (EL2) of GlyT2 (Fig. 7*B*). This region cannot currently be accurately modeled because of significant divergence in sequence and length compared with $LeuT_{Aa}$ (18, 21). However, equivalent conserved cysteines have been shown to form a disulfide bond in other members of the SLC6 family (30, 31). Unexpectedly, although C311S and C320S mutants should both have a single unpaired extracellular cysteine like Y705C, they have much lower cysteine labeling in the absence of DTT. In addition, they display very high MTSEA-biotin label after DTT treatment (Fig. 7, *E* and *F*). This unexpected result made us consider the possibility that the unpaired cysteine from the Cys-311–Cys-320 disulfide might form a disulfide bond with another monomer, creating disulfide-linked dimers. Fig. 8*A* shows that C311S and C320S mutants form disulfide-mediated dimers on the cell surface (band indicated by an *asterisk*), which are cleaved to monomers in the double C311S/Y705C or C320S/Y705C mutants. This reinforces the evidence that Cys-705 interacts with Cys-311 and Cys-320 (Fig. 8*B*).

A further relevant question is whether the trafficking defect of Y705C affects the expression of wild-type GlyT2. To answer this, we co-expressed wild-type and mutant GlyT2 differentially tagged with EGFP (Fig. 8*C*). The Y705C mutant reduces total wild-type GlyT2 expression by 10–20% when expressed at 1:1 ratio. This is comparable with the effect of a nonrelevant protein, the glutamate transporter GLT1 (Fig. 8*D*). At a higher GlyT2-Y705C ratio (1:3), a slight reduction of GlyT2 expression by the Y705C mutant was observed, although this effect was not due to a reduced delivery to the plasma membrane (Fig. 8*E*). Moreover, wild-type GlyT2 co-

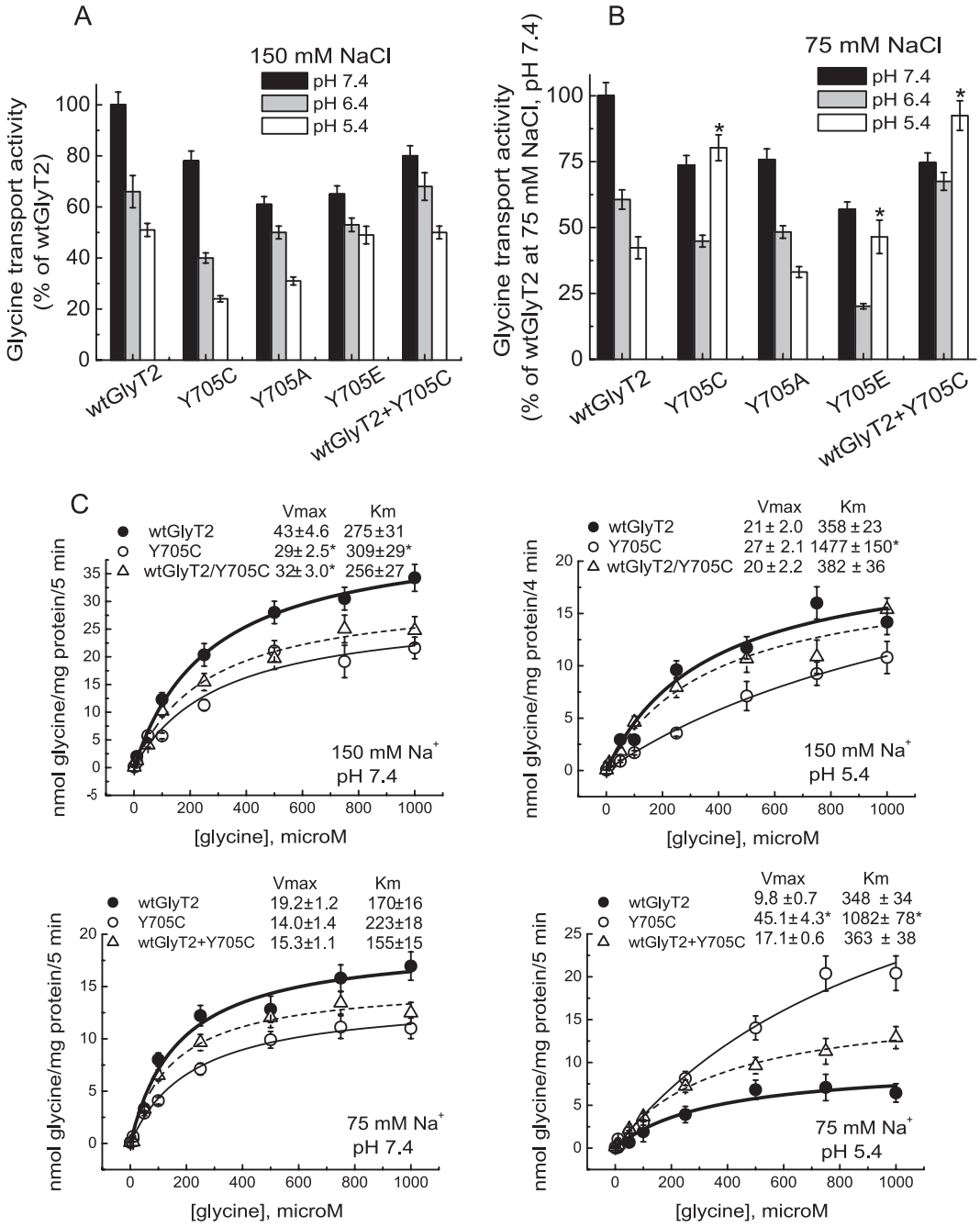

FIGURE 9. **Effect of pH on glycine transport by wild-type GlyT2 and the Tyr-705 mutant.** Transiently transfected COS7 cells expressing wild-type GlyT2 or mutants with the indicated amino acid substitutions at position 705 were assayed for [^{3}H]glycine transport for 5 min in HBS containing 150 (*A* and *C*) or 75 (*B* and *C*) mM NaCl at 10 μM or the indicated final glycine concentration and pH. Control GlyT2 transport values at pH 7.4 were 1.4 $\pm$ 0.2 and 0.73 $\pm$ 0.1 nmol of Gly/mg of protein/5 min at 150 and 75 mM NaCl, respectively. Mean pH change was significantly different from wild-type GlyT2. *, $p < 0.05$ by analysis of variance with Dunnett's post hoc test. *C*, kinetics of glycine transport at low pH. COS7 cells expressing wild-type GlyT2, the Y705C mutant, or the indicated combination of the respective cDNAs were assayed for [^{3}H]glycine transport at pH 7.4 or 5.4 for 5 min in HBS containing 150 or 75 mM NaCl and glycine concentrations increasing from 0.5 μM to 1 mM. Experimental data were fitted to hyperbolae. The kinetic parameters are indicated on the graphs. Mean pH change significantly different from wild-type GlyT2. *, $p < 0.05$ in Student's *t* test.

expressed with Y705C reduces the expression of the mutant by ~10–20% (data not shown). These results indicate that the traffic defect of the Y705C mutant is not dominant when it is co-expressed at the same dose as wild-type GlyT2.

H^+ Dependence of Glycine Transport Is Inverted in the Y705C Mutant—According to the above data, DTT is likely to disrupt an aberrant disulfide bond in the Y705C mutant. This facilitates exocytosis and induces the emergence of the mutant transporter on the cell surface. In addition, the Y705C substitution predicts the introduction of a local negative charge on the surface of the transporter because of the more acidic nature of the cysteine side chain (pK_a of 8.3 *versus* 10.3 for tyrosine). Because the protonation state of protein ionizable groups is dependent on pH, we tested the pH dependence of Tyr-705 mutants containing titratable side chains (Fig. 9). In agreement with published data on GABA transporters (32, 33), wild-type GlyT2 is

inhibited at low pH, showing ~50–60% transport activity at pH 5.4. The inhibition was even higher when assayed in low external sodium (Fig. 9, *A* and *B*). This is in agreement with the proposed competition of the two cations in the external transporter vestibule (32, 33). When the assay was performed at the physiological NaCl concentration (150 mM), the wild-type response to low pH was also observed for the Y705C, Y705E, and Y705A mutants (Fig. 9*A*). However, lowering the external pH in the presence of low NaCl concentrations (75 mM) produced a differential response in the Y705C and Y705E mutants. They became activated at pH 5.4 instead of inhibited, indicating an altered proton dependence of transport in these Tyr-705 substitutions (Fig. 9*B*). Furthermore, the pH dependence of wild-type GlyT2 co-transfected at a 1:1 cDNA ratio with the Y705C mutant resembled that of the mutant rather than wild-type GlyT2. This suggests a dominant phenotype for Y705C (Fig. 9, *A* and *B*). Therefore, we characterized the transport kinetics at acidic pH (Fig. 9*C*). The Y705C mutant had increased V_{max} at pH 5.4 when expressed alone and in co-expression with wild-type, especially at low sodium. This is in contrast to wild-type GlyT2 that showed a ~50% reduction in V_{max} value at acidic *versus* neutral pH. In addition, a general increase in K_m at low pH was observed for all the transporters. This was more pronounced for Y705C and the co-expression, especially at low sodium (~2-, 5-, and 2.5-fold for wild-type GlyT2, Y705C, and Y705C+wild-type GlyT2, respectively). Taken together, these data indicate that the Y705C mutation in GlyT2 induces an altered response to proton modulation of glycine transport.

Y705C Mutant Is Partially Resistant to Zn^{2+} Inhibition of Glycine Transport—Protons and metal transition dications are competitive inhibitors of several crucial mediators of glycinergic neurotransmission, such as the glycine receptor (34–36) and the glycine transporter GlyT1 (37, 38). Because H^+ and Zn^{2+} frequently bind to overlapping intersubunit sites (39–41), and the binding of transition dications can induce cysteine deprotonation (42), we tested the effect of Y705C substitution on the sensitivity of GlyT2 to Zn^{2+}. Although GlyT2 is not very sensitive to this cation (38), we observed a low but significant inhibition of GlyT2 transport by Zn^{2+} (Fig. 10). As expected, we found that Zn^{2+} sensitivity of wild-type transport was pH-dependent, being higher at pH 7.4 than 5.4, in agreement with the competitive nature of H^+ and Zn^{2+} inhibition (35, 38, 39). By contrast, the inhibition by Zn^{2+} of the Y705C mutant was much less sensitive to the presence of protons and slightly more pronounced at acidic pH. As expected from the proton response shown above, the co-expression of wild-type GlyT2 and the Y705C mutant also resulted in Y705C behavior, confirming a dominant phenotype (Fig. 10*A*). Fig. 10*B* shows that the IC_{50} for Zn^{2+} inhibition of wild-type GlyT2 was significantly increased at acidic pH from 63 ± 10 at pH 7.4 to 466 ± 42 μM at pH 5.4. By contrast, the Y705C mutant had IC_{50} values of 100 ± 15 and 189 ± 19 μM at these same pH values. The co-expressed wild-type GlyT2 and Y705C mutant displayed IC_{50} values of 99 ± 10 and 198 ± 22 μM, which are close to those of Y705C mutants. Further kinetic analysis of glycine transport in the presence of Zn^{2+} showed a significantly lower decrease in the V_{max} of transport by the Y705C-containing transporters than for wild-type GlyT2. In addition, a higher increase in K_m was observed. These data confirm the reduced sensitivity of Y705C-containing glycine transporters to Zn^{2+} inhibition (Fig. 10*C*).

DISCUSSION

We have identified a novel missense mutation in *SLC6A5*, encoding GlyT2, present in eight individuals from three families in two cohorts of hyperekplexia patients from Spain and the United Kingdom. The mutation results in a tyrosine to cysteine substitution at residue 705 (Y705C) in transmembrane domain 11 (TM11). This change was found in the heterozygous state in all positive cases suggesting a dominant mode of inheritance. This contrasts with the majority of the previously characterized GlyT2 mutations that were inherited in a recessive or compound heterozygous state (11). Y705C-harboring patients show significant variability in clinical presentation. As well as classical hyperekplexia symptoms, certain individuals exhibited abnormal respiration, facial dysmorphism, delayed motor development, or intellectual disability. This may be due to a complex phenotype caused by the mutation or to the presence of additional unknown mutations or modifiers. However, no other potential disease-causing mutations were detected in *SLC6A5*. Study of the biochemical properties of the mutant transporter in cultured cells revealed that the introduced cysteine affects several aspects of transporter biochemistry. These include impaired transporter protein maturation through the secretory pathway and an alteration of H^+ and Zn^{2+} dependence of glycine transport. The latter feature constitutes a dominant effect, because it is observed when the mutant is expressed alone and also when mutant and wild-type transporters are co-expressed.

The Y705C substitution introduces a free thiol in the place of a hydroxyl-containing side chain. Thiol labeling with impermeant cysteine MTS reagents confirmed that Cys-705 is accessible from the exterior of the plasma membrane, as predicted by molecular modeling. Therefore, the Y705C mutant exposes the introduced cysteine to the lumen of the secretory pathway cisternae during trafficking. This seems to be detrimental for transporter biogenesis, because Y705C has reduced expression at the plasma membrane, together with a higher proportion of immature precursor compared with wild-type GlyT2. This is in agreement with recent reports indicating that polymorphisms containing an uneven number of cysteine residues in extracellular loops impair the expression of G-protein-coupled receptors and other plasma membrane proteins. This feature has frequently been associated with disease states (29, 43–45). Restoration of Y705C membrane expression to wild-type levels with the permeable thiol reagent DTT and experiments using SH-specific and surface labeling of cells expressing the transporters suggest that Cys-705 is involved in aberrant disulfide bond formation. Cys-705 binding partners are either of two EL2 cysteines that are likely to form a disulfide bond in wild-type GlyT2 (C311-C320 pair) (30, 31). This interference is probably conformation-dependent, because EL2 may approach TM11 during the inward-facing conformation (46). Disruption of this aberrant bond with reducing agents may facilitate plasma membrane arrival and/or the conformational movements needed for transport in the surface-resident transporter. How-

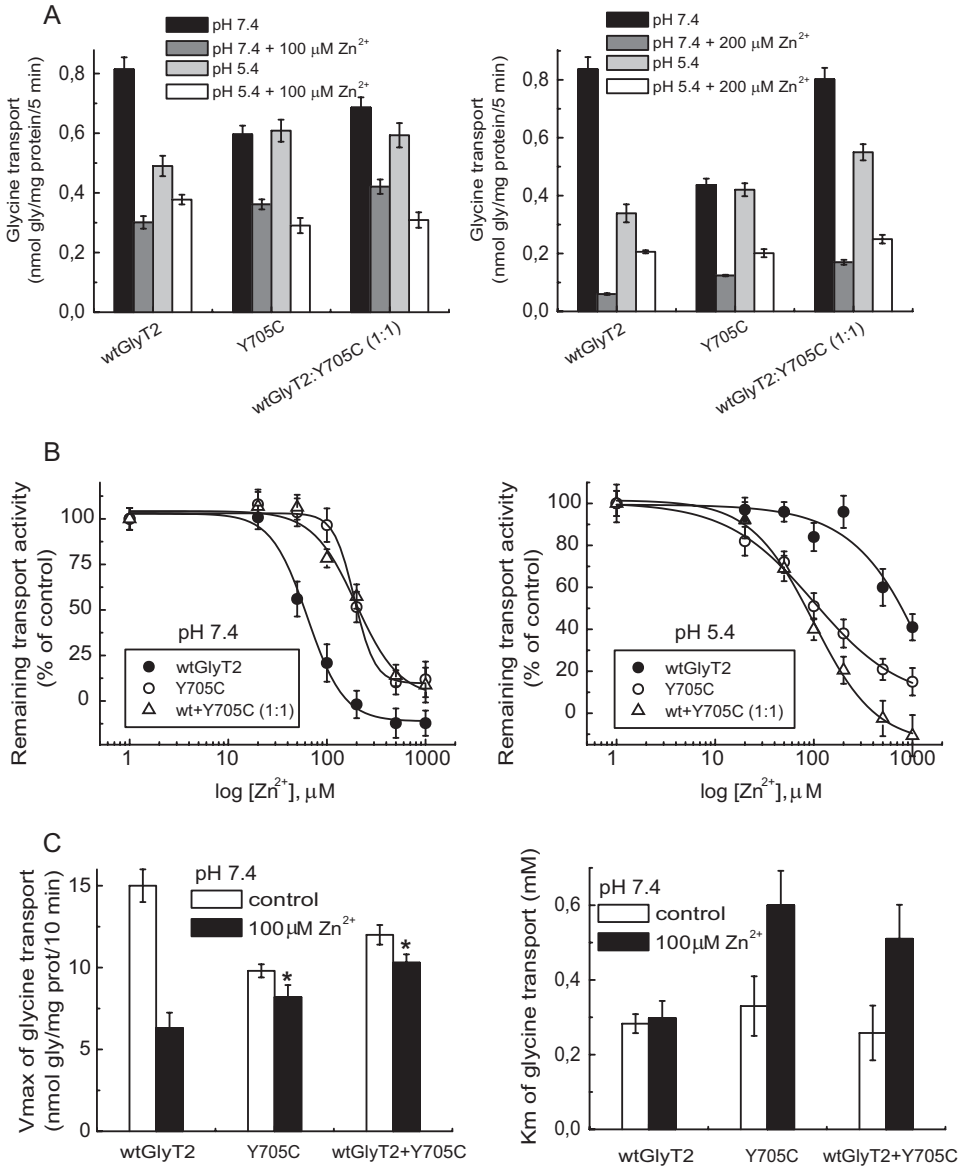

FIGURE 10. **Effect of Zn^{2+} on glycine transport by wild-type GlyT2 and the Y705C mutant.** Transiently transfected COS7 cells expressing wild-type GlyT2, the Y705C mutant, or the indicated combinations of the respective cDNAs were assayed for [^{3}H]glycine transport for 5 min in HBS containing 75 mM NaCl at the indicated pH and 10 μM final glycine concentration (*A* and *B*) or increasing glycine concentrations (*C*) in the presence of the indicated ZnCl concentrations (*A–C*). NaCl was isotonically substituted by choline chloride. *B*, dose-response data were fit to logistic curves. *C*, transport data were fitted to hyperbolae, and kinetic parameters were obtained from the best fit. Mean change significantly different from wild-type GlyT2. *, $p < 0.05$ in Student's *t* test.

ever, it is not clear whether Y705C expression is lower because a proper disulfide bridge cannot be formed or because the aberrant disulfide bond distorts the protein structure, because both conditions are present in Y705C. The single C311S and C320S mutants show approximately half the membrane expression of wild-type GlyT2, suggesting that the lack of the endogenous disulfide bond is detrimental for surface expression. However, the unusual behavior of these mutants prevents us from drawing clear conclusions. The fact that Y705C and wild-type GlyT2 are differentially sensitive to low concentrations of reducing agents but are inhibited by higher concentrations (Fig. 5*C* and data not shown) suggests that the aberrant disulfide bond involving Cys-705 is more sensitive to cleavage than the Cys-311–Cys-320 disulfide bond. The recovery of the expression in the Y705C mutant might be due to the cleavage of aberrant disulfide bonds without affecting the Cys-311–Cys-320 pairing. It is also possible that GlyT2 requires disulfide-mediated dimerization for plasma membrane expression as has been suggested for other SLC6 transporters (31) and that this process is disrupted by the Y705C mutation. Because GlyT2 multimerization has been proposed to be required for plasma membrane localization (47), this is an issue that will require further study.

The Y705C substitution is also predicted to introduce a local negative charge at the transporter surface. The endogenous Tyr-705 residue with a typical pK_a value of ~10.3 would be mostly protonated at physiological pH. By contrast, the side chain of Cys-705 would, in theory, be also protonated, but the more acidic pK_a value (close to 8.3) makes the probability of ionization higher than for the tyrosine side chain. In addition, a high dielectric medium favors cysteine deprotonation, whereas

a low dielectric medium favors the protonated state (42). Because Cys-705 is extracellular, it is therefore likely to be in a high dielectric environment. Deprotonation is also favored by the presence of transition metal dications, which may perform a metal-assisted deprotonation of cysteine side chains, especially if bound to polarizable ligands (42). Other factors such as the possible hydrogen-bonding network including the cysteine may affect the pK_a (48). All of these factors may drive Cys-705 to be deprotonated at physiological pH. By contrast, acidic pH may displace the equilibrium toward the protonated form. GlyT2 transport activity seems to be sensitive to the protonation state of Cys-705, and protonation may activate the mutant transporter. Therefore, although glycine transport by wild-type GlyT2 is inhibited at low pH, the Y705C mutant is resistant to this inhibition.

Functional analysis of the Y705C mutant has revealed the existence of an unexpected fine-tuning mechanism of glycine transport by external H^+, with Tyr-705 playing a central role. Interestingly, the GlyR is also inhibited by protons and the proton-binding site also involves a hydroxyl-containing residue (Thr-112), which when substituted by a tyrosine (but not by a neutral amino acid) preserves the H^+ sensitivity of the receptor (49). Both Tyr-705 in GlyT2 and Thr-112 in GlyRs are highly conserved. A threonine is found at the equivalent position in all pH-sensitive GlyR, $GABA_A$, and $GABA_C$ receptors. Equally, a Tyr-705 equivalent is found in many SLC6 family members, suggesting that this tyrosine might have a general role in pH sensitivity of Na^+-and Cl^--dependent neurotransmitter transporters. The location of Tyr-705 in an extracellular accessible region of the transporter would fulfill one of the prerequisites for H^+-binding sites, which are usually located outside the membrane electric field (49, 50). Proton and transition dication binding sites are usually overlapping in pH- and Zn^{2+}-sensitive proteins (34–36, 38). In the GlyR, Thr-112 also forms part of the group of crucial residues involved in regulation by Zn^{2+} (35). In several plasma membrane proteins present in inhibitory synapses, H^+/Zn^{2+}-binding sites are contributed by several adjacent subunits (35, 49, 51, 52). This structural requirement might also hold true for GlyT2 and would sustain the dominant nature of the aberrant pH sensitivity and Zn^{2+} dependence of the Y705C mutant co-expressed with wild-type GlyT2.

In summary, we have identified a novel missense mutation in GlyT2 associated with hyperekplexia and described altered biochemical properties of the mutant transporter. The Y705C mutation affects several aspects of transporter biochemistry including impaired transporter protein maturation through the secretory pathway and an alteration of H^+ and Zn^{2+} dependence of glycine transport. Any of these features may contribute to the etiology of the disease. In addition to effects in pathophysiological conditions such as inflammation and ischemia, transient changes in extracellular pH occur under physiological conditions. For example, in synaptic transmission, the acidic contents of transmitter vesicles cause an extracellular acid shift within the synaptic cleft (53, 54) and may reduce the local Na^+ concentration. Different sources of protons have been suggested in the synapse: acidic contents after vesicle fusion, incorporation of the vesicular ATPase to the plasma membrane, or extrasynaptic sources such as H^+ ion exchangers and voltage-gated H^+ conductances (51). These pH changes are especially relevant during repetitive electrical stimulation that may produce acid shifts of ~30 s in duration (53). Acidification reduces the duration of glycinergic synaptic currents and accelerates desensitization of the receptor significantly affecting the kinetics of glycinergic neurotransmission (54). Increased external pH potentiated, whereas decrease inhibited both the amplitude and frequency of glycinergic miniature inhibitory postsynaptic potential currents, suggesting the involvement of both presynaptic and postsynaptic mechanisms (54). In addition, Zn^{2+} is highly enriched in synaptic vesicles, from which it can be co-released with glutamate in an activity-dependent manner (36). Zn^{2+} modulates both current responses mediated by excitatory and inhibitory neurotransmitter receptors and the efficacy of transporter-driven neurotransmitter reuptake (55). We hypothesize that Y705C mutant may alter the kinetics of glycinergic inhibition by taking up glycine when the transporter is supposed to be inhibited by synaptic H^+ or Zn^{2+}. This may disrupt the coordination of neurotransmitter release and subsequent reuptake, leading to a damaging effect, mainly during repetitive firing. In addition, the mutant transport activity, which is resistant to two "natural" synaptic inhibitors, may prevent or dampen the interaction of glycine with GlyRs by simple competition. Finally, defective trafficking of the mutant may reduce the uptake of glycine at neutral pH, thus reducing the availability of transmitter in the terminal for synaptic vesicle loading. Future work performed in neuronal preparations will reveal to what extent glycinergic neurotransmission is impaired by the Y705C mutation.

Acknowledgments—We acknowledge the expert technical assistance of the confocal microscopy facility at the Centro de Biología Molecular "Severo Ochoa" (Madrid, Spain). Carlos Ernesto Fernández García is also acknowledged.

REFERENCES

1. Aragón, C., and López-Corcuera, B. (2003) Structure, function and regulation of glycine neurotransporters. *Eur. J. Pharmacol.* **479,** 249–262
2. Gomeza, J., Hülsmann, S., Ohno, K., Eulenburg, V., Szöke, K., Richter, D., and Betz, H. (2003) Inactivation of the glycine transporter 1 gene discloses vital role of glial glycine uptake in glycinergic inhibition. *Neuron* **40,** 785–796
3. Aragón, C., and López-Corcuera, B. (2005) Glycine transporters. Crucial roles of pharmacological interest revealed by gene deletion. *Trends Pharmacol. Sci.* **26,** 283–286
4. Gomeza, J., Ohno, K., Hülsmann, S., Armsen, W., Eulenburg, V., Richter, D. W., Laube, B., and Betz, H. (2003) Deletion of the mouse glycine transporter 2 results in a hyperekplexia phenotype and postnatal lethality. *Neuron* **40,** 797–806
5. Gomeza, J., Ohno, K., and Betz, H. (2003) Glycine transporter isoforms in the mammalian central nervous system. Structures, functions and therapeutic promises. *Curr. Opin. Drug Discov. Devel.* **6,** 675–682
6. Harvey, R. J., Topf, M., Harvey, K., and Rees, M. I. (2008) The genetics of hyperekplexia. More than startle!. *Trends Genet.* **24,** 439–447
7. Andermann, F., Keene, D. L., Andermann, E., and Quesney, L. F. (1980) Startle disease or hyperekplexia. Further delineation of the syndrome. *Brain* **103,** 985–997
8. Rees, M. I., Harvey, K., Pearce, B. R., Chung, S. K., Duguid, I. C., Thomas, P., Beatty, S., Graham, G. E., Armstrong, L., Shiang, R., Abbott, K. J., Zuberi, S. M., Stephenson, J. B., Owen, M. J., Tijssen, M. A., van den Maagdenberg, A. M., Smart, T. G., Supplisson, S., and Harvey, R. J. (2006) Mutations in the gene encoding GlyT2 (*SLC6A5*) define a presynaptic

component of human startle disease. *Nat. Genet.* **38,** 801–806
9. Rees, M. I., Harvey, K., Ward, H., White, J. H., Evans, L., Duguid, I. C., Hsu, C. C., Coleman, S. L., Miller, J., Baer, K., Waldvogel, H. J., Gibbon, F., Smart, T. G., Owen, M. J., Harvey, R. J., and Snell, R. G. (2003) Isoform heterogeneity of the human gephyrin gene (*GPHN*), binding domains to the glycine receptor, and mutation analysis in hyperekplexia. *J. Biol. Chem.* **278,** 24688–24696
10. Harvey, R. J., Depner, U. B., Wässle, H., Ahmadi, S., Heindl, C., Reinold, H., Smart, T. G., Harvey, K., Schütz, B., Abo-Salem, O. M., Zimmer, A., Poisbeau, P., Welzl, H., Wolfer, D. P., Betz, H., Zeilhofer, H. U., and Müller, U. (2004) GlyR α3. An essential target for spinal PGE_2-mediated inflammatory pain sensitization. *Science* **304,** 884–887
11. Chung, S. K., Vanbellinghen, J. F., Mullins, J. G., Robinson, A., Hantke, J., Hammond, C. L., Gilbert, D. F., Freilinger, M., Ryan, M., Kruer, M. C., Masri, A., Gurses, C., Ferrie, C., Harvey, K., Shiang, R., Christodoulou, J., Andermann, F., Andermann, E., Thomas, R. H., Harvey, R. J., Lynch, J. W., and Rees, M. I. (2010) Pathophysiological mechanisms of dominant and recessive *GLRA1* mutations in hyperekplexia. *J. Neurosci.* **30,** 9612–9620
12. Eulenburg, V., Becker, K., Gomeza, J., Schmitt, B., Becker, C. M., and Betz, H. (2006) Mutations within the human GLYT2 (*SLC6A5*) gene associated with hyperekplexia. *Biochem. Biophys. Res. Commun.* **348,** 400–405
13. Yamashita, A., Singh, S. K., Kawate, T., Jin, Y., and Gouaux, E. (2005) Crystal structure of a bacterial homologue of Na^+/Cl^--dependent neurotransmitter transporters. *Nature* **437,** 215–223
14. Haliassos, A., Chomel, J. C., Tesson, L., Baudis, M., Kruh, J., Kaplan, J. C., and Kitzis, A. (1989) Modification of enzymatically amplified DNA for the detection of point mutations. *Nucleic Acids Res.* **17,** 3606
15. Larkin, M. A., Blackshields, G., Brown, N. P., Chenna, R., McGettigan, P. A., McWilliam, H., Valentin, F., Wallace, I. M., Wilm, A., Lopez, R., Thompson, J. D., Gibson, T. J., and Higgins, D. G. (2007) Clustal W and Clustal X version 2.0. *Bioinformatics* **23,** 2947–2948
16. Ramensky, V., Bork, P., and Sunyaev, S. (2002) Human non-synonymous SNPs. Server and survey. *Nucleic Acids Res.* **30,** 3894–3900
17. Sali, A., and Blundell, T. L. (1993) Comparative protein modelling by satisfaction of spatial restraints. *J. Mol. Biol.* **234,** 779–815
18. Pérez-Siles, G., Morreale, A., Leo-Macías, A., Pita, G., Ortíz, A. R., Aragón, C., and López-Corcuera, B. (2011) Molecular basis of the differential interaction with lithium of glycine transporters GLYT1 and GLYT2. *J. Neurochem.* **118,** 195–204
19. Fornés, A., Núñez, E., Aragón, C., and López-Corcuera, B. (2004) The second intracellular loop of the glycine transporter 2 contains crucial residues for glycine transport and phorbol ester-induced regulation. *J. Biol. Chem.* **279,** 22934–22943
20. Pérez-Siles, G., Núñez, E., Morreale, A., Jiménez, E., Leo-Macías, A., Pita, G., Cherubino, F., Sangaletti, R., Bossi, E., Ortíz, A. R., Aragón, C., and López-Corcuera, B. (2012) An aspartate residue in the external vestibule of GLYT2 (glycine transporter 2) controls cation access and transport coupling. *Biochem. J.* **442,** 323–334
21. Jiménez, E., Zafra, F., Pérez-Sen, R., Delicado, E. G., Miras-Portugal, M. T., Aragón, C., and López-Corcuera, B. (2011) P2Y purinergic regulation of the glycine neurotransmitter transporters. *J. Biol. Chem.* **286,** 10712–10724
22. Núñez, E., Pérez-Siles, G., Rodenstein, L., Alonso-Torres, P., Zafra, F., Jiménez, E., Aragón, C., and López-Corcuera, B. (2009) Subcellular localization of the neuronal glycine transporter GLYT2 in brainstem. *Traffic* **10,** 829–843
23. Fornés, A., Núñez, E., Alonso-Torres, P., Aragón, C., and López-Corcuera, B. (2008) Trafficking properties and activity regulation of the neuronal glycine transporter GLYT2 by protein kinase C. *Biochem. J.* **412,** 495–506
24. de Juan-Sanz, J., Zafra, F., López-Corcuera, B., and Aragón, C. (2011) Endocytosis of the neuronal glycine transporter GLYT2. Role of membrane rafts and protein kinase C-dependent ubiquitination. *Traffic* **12,** 1850–1867
25. López-Corcuera, B., Martínez-Maza, R., Núñez, E., Roux, M., Supplisson, S., and Aragón, C. (1998) Differential properties of two stably expressed brain-specific glycine transporters. *J. Neurochem.* **71,** 2211–2219
26. Martínez-Maza, R., Poyatos, I., López-Corcuera, B., Núñez, E., Giménez, C., Zafra, F., and Aragón, C. (2001) The role of *N*-glycosylation in transport to the plasma membrane and sorting of the neuronal glycine transporter GLYT2. *J. Biol. Chem.* **276,** 2168–2173
27. Dunn, S. M., Conti-Tronconi, B. M., and Raftery, M. A. (1986) Acetylcholine receptor dimers are stabilized by extracellular disulfide bonding. *Biochem. Biophys. Res. Commun.* **139,** 830–837
28. Hepojoki, J., Strandin, T., Vaheri, A., and Lankinen, H. (2010) Interactions and oligomerization of hantavirus glycoproteins. *J. Virol.* **84,** 227–242
29. Petäjä-Repo, U. E., Hogue, M., Bhalla, S., Laperrière, A., Morello, J. P., and Bouvier, M. (2002) Ligands act as pharmacological chaperones and increase the efficiency of delta opioid receptor maturation. *EMBO J.* **21,** 1628–1637
30. Chen, J. G., Liu-Chen, S., and Rudnick, G. (1997) External cysteine residues in the serotonin transporter. *Biochemistry* **36,** 1479–1486
31. Chen, R., Wei, H., Hill, E. R., Chen, L., Jiang, L., Han, D. D., and Gu, H. H. (2007) Direct evidence that two cysteines in the dopamine transporter form a disulfide bond. *Mol. Cell Biochem.* **298,** 41–48
32. Forlani, G., Bossi, E., Ghirardelli, R., Giovannardi, S., Binda, F., Bonadiman, L., Ielmini, L., and Peres, A. (2001) Mutation K448E in the external loop 5 of rat GABA transporter rGAT1 induces pH sensitivity and alters substrate interactions. *J. Physiol.* **536,** 479–494
33. Grossman, T. R., and Nelson, N. (2003) Effect of sodium lithium and proton concentrations on the electrophysiological properties of the four mouse GABA transporters expressed in *Xenopus* oocytes. *Neurochem. Int.* **43,** 431–443
34. Lynch, J. W., Jacques, P., Pierce, K. D., and Schofield, P. R. (1998) Zinc potentiation of the glycine receptor chloride channel is mediated by allosteric pathways. *J. Neurochem.* **71,** 2159–2168
35. Hirzel, K., Müller, U., Latal, A. T., Hülsmann, S., Grudzinska, J., Seeliger, M. W., Betz, H., and Laube, B. (2006) Hyperekplexia phenotype of glycine receptor α1 subunit mutant mice identifies Zn^{2+} as an essential endogenous modulator of glycinergic neurotransmission. *Neuron* **52,** 679–690
36. Tóth, K. (2011) Zinc in neurotransmission. *Annu. Rev. Nutr.* **31,** 139–153
37. Laube, B. (2002) Potentiation of inhibitory glycinergic neurotransmission by Zn^{2+}. A synergistic interplay between presynaptic $P2X_2$ and postsynaptic glycine receptors. *Eur. J. Neurosci.* **16,** 1025–1036
38. Ju, P., Aubrey, K. R., and Vandenberg, R. J. (2004) Zn^{2+} inhibits glycine transport by glycine transporter subtype 1b. *J. Biol. Chem.* **279,** 22983–22991
39. Chu, X. P., Wemmie, J. A., Wang, W. Z., Zhu, X. M., Saugstad, J. A., Price, M. P., Simon, R. P., and Xiong, Z. G. (2004) Subunit-dependent high-affinity zinc inhibition of acid-sensing ion channels. *J. Neurosci.* **24,** 8678–8689
40. Baron, A., Voilley, N., Lazdunski, M., and Lingueglia, E. (2008) Acid sensing ion channels in dorsal spinal cord neurons. *J. Neurosci.* **28,** 1498–1508
41. Chen, J., Myerburg, M. M., Passero, C. J., Winarski, K. L., and Sheng, S. (2011) External Cu^{2+} inhibits human epithelial Na^+ channels by binding at a subunit interface of extracellular domains. *J. Biol. Chem.* **286,** 27436–27446
42. Dudev, T., and Lim, C. (2002) Factors governing the protonation state of cysteines in proteins. An *ab initio*/CDM study. *J. Am. Chem. Soc.* **124,** 6759–6766
43. Leskelä, T. T., Markkanen, P. M., Alahuhta, I. A., Tuusa, J. T., and Petäjä-Repo, U. E. (2009) Phe27Cys polymorphism alters the maturation and subcellular localization of the human delta opioid receptor. *Traffic* **10,** 116–129
44. Schülein, R., Zühlke, K., Krause, G., and Rosenthal, W. (2001) Functional rescue of the nephrogenic diabetes insipidus-causing vasopressin V2 receptor mutants G185C and R202C by a second site suppressor mutation. *J. Biol. Chem.* **276,** 8384–8392
45. Williams, S. E., Reed, A. A., Galvanovskis, J., Antignac, C., Goodship, T., Karet, F. E., Kotanko, P., Lhotta, K., Morinière, V., Williams, P., Wong, W., Rorsman, P., and Thakker, R. V. (2009) Uromodulin mutations causing familial juvenile hyperuricaemic nephropathy lead to protein maturation defects and retention in the endoplasmic reticulum. *Hum. Mol. Genet.* **18,** 2963–2974
46. Krishnamurthy, H., and Gouaux, E. (2012) X-ray structures of LeuT in substrate-free outward-open and apo inward-open states. *Nature* **481,** 469–474

47. Bartholomäus, I., Milan-Lobo, L., Nicke, A., Dutertre, S., Hastrup, H., Jha, A., Gether, U., Sitte, H. H., Betz, H., and Eulenburg, V. (2008) Glycine transporter dimers. Evidence for occurrence in the plasma membrane. *J. Biol. Chem.* **283,** 10978–10991
48. Pace, C. N., Grimsley, G. R., and Scholtz, J. M. (2009) Protein ionizable groups. pK values and their contribution to protein stability and solubility. *J. Biol. Chem.* **284,** 13285–13289
49. Chen, Z., Dillon, G. H., and Huang, R. (2004) Molecular determinants of proton modulation of glycine receptors. *J. Biol. Chem.* **279,** 876–883
50. Aubrey, K. R., Mitrovic, A. D., and Vandenberg, R. J. (2000) Molecular basis for proton regulation of glycine transport by glycine transporter subtype 1b. *Mol. Pharmacol.* **58,** 129–135
51. Krishtal, O. (2003) The ASICs. Signaling molecules? Modulators? *Trends Neurosci.* **26,** 477–483
52. Jasti, J., Furukawa, H., Gonzales, E. B., and Gouaux, E. (2007) Structure of acid-sensing ion channel 1 at 1.9 Å resolution and low pH. *Nature* **449,** 316–323
53. Krishtal, O. A., Osipchuk, Y. V., Shelest, T. N., and Smirnoff, S. V. (1987) Rapid extracellular pH transients related to synaptic transmission in rat hippocampal slices. *Brain Res.* **436,** 352–356
54. Li, Y. F., Wu, L. J., Li, Y., Xu, L., and Xu, T. L. (2003) Mechanisms of H^+ modulation of glycinergic response in rat sacral dorsal commissural neurons. *J. Physiol.* **552,** 73–87
55. Smart, T. G., Hosie, A. M., and Miller, P. S. (2004) Zn^{2+} ions. Modulators of excitatory and inhibitory synaptic activity. *Neuroscientist* **10,** 432–442

Anexo Artículo #5

Arribas-González E, Núñez E, Benito-Muñoz C, Dos Santos HG, Perona A, Aragón C and López-Corcuera B (En preparación, 2017)

Oligomer assembly of the neuronal glycine transporter GlyT2

Oligomer assembly of the neuronal glycine transporter GlyT2

Esther Arribas-González[1,2,3,4], Enrique Núñez[2,3,4], Cristina Benito-Muñoz[1,2], Helena Gomes Dos Santos[2,6], Almudena Perona[5], Carmen Aragón[1,2,3,4] and Beatriz López-Corcuera[1,2,3,4]*

[1]*Departamento de Biología Molecular and* [2]*Centro de Biología Molecular "Severo Ochoa," Consejo Superior de Investigaciones Científicas-Universidad Autónoma de Madrid, Madrid 28049, Spain.*
[3]*Centro de Investigación Biomédica en Red de Enfermedades Raras, Instituto de Salud Carlos III, Madrid 28029, Spain.*
[4]*IdiPAZ-Hospital Universitario La Paz, Universidad Autónoma de Madrid, Madrid 28046, Spain.*
[5]*Smartligs, Parque Científico de Madrid, Campus de Cantoblanco, Madrid 28049, Spain.*
[6]*Present address: Department of Biological Sciences, Biomolecular Sciences Institute, Florida International University, 11200 SW 8th St, Miami, FL 33199, USA*

***Corresponding author:** Beatriz López-Corcuera, Departamento de Biología Molecular, Centro de Biología Molecular "Severo Ochoa", Universidad Autónoma de Madrid, 28049 Madrid, Spain. Tel.: 34-91-1964631; Fax: 34-91-1964420; E-mail: blopez@cbm.csic.es

Keywords: neurotransmitter: sodium symporters; glycine, transport, hyperekplexia, structure, oligomer

Running title: GlyT2 oligomeric structure

ABSTRACT

Glycine is an inhibitory neurotransmitter in the central nervous system of vertebrates. The neuronal glycine transporter GlyT2 is involved in the removal and recycling of synaptic glycine, supplying substrate for synaptic vesicle refilling at glycinergic synapses. Loss of function mutations in the human GlyT2 gene (*SLC6A5*; solute carrier 6A5) are the most common cause of presynaptic hyperekplexia (OMIM 149400), and are due to the generation of inactive transporters or trafficking defects. Oligomer assembly is a prerequisite to export GlyT2 from the endoplasmic reticulum and for its subsequent delivery to the plasma membrane. While most studies have focused on GlyT2 structure/function, much less information is available regarding the interactions that stabilize the assembly of this protein and its role in trafficking. In this study, we analyze GlyT2 native state under non-denaturing conditions. Combination of native and denaturing electrophoresis reveals oligomeric and monomeric GlyT2. Native GlyT2 forms oligomers sensitive to reducing agents, suggesting a role of disulfide bonds in multimer stabilization. We generated a model of the three-dimensional structure of GlyT2 dimer, which permitted studying the oligomerization interface and to search for possible cysteines involved in oligomer stability. Cysteines 611, 612, 614, 726 and 696 are candidate crucial residues in the dimerization interface.

INTRODUCTION

Glycine is the major inhibitory neurotransmitter in the posterior areas of the vertebrate central nervous system such as the brainstem and spinal cord. Glycinergic transmission participates in the motor and sensory functions involved in movement, vision and audition (Lynch 2004; Hirzel, Muller et al. 2006) and contributes to nociceptive signal modulation (Harvey, Depner et al. 2004) and rhythmic breathing (Manzke, Niebert et al. 2010). Depolarization produced by the arrival of an action potential to the glycinergic terminal triggers the release of glycine-containing vesicles by calcium-dependent exocytosis. In the synaptic space, glycine interacts and activates strychnine-sensitive glycine receptors (GlyRs) that hyperpolarize, and therefore inhibit, the postsynaptic neuron (Legendre 2001). The action of glycine ends by Na^+-and Cl^--dependent glycine reuptake by specific glycine transporters (GlyTs) that decrease glycine synaptic concentrations to the level before stimulation (Aragon and Lopez-Corcuera 2003).

The neuronal glycine transporter GlyT2 is involved in the removal and recycling of glycine from inhibitory synapses and supplies substrate to the low-affinity vesicular inhibitory amino acid transporter VIAAT/VGAT, in charge of glycine packing in synaptic vesicles (McIntire, Reimer et al. 1997; Gomeza, Ohno et al. 2003; Aragon and Lopez-Corcuera 2005). The synaptic glycine taken up by GlyT2 is the main source of the releasable transmitter at glycinergic synapses (Rousseau, Aubrey et al. 2008; Apostolides and Trussell 2013). Accordingly, inactivation of the mouse GlyT2 gene generates a complex postnatal neuromotor phenotype that mimics clinical signs of human hyperekplexia (Gomeza, Ohno et al. 2003), a rare clinical syndrome characterized by an alteration of the brainstem startle reflex controlled by glycinergic neurons. The most severe consequences of the disease include brain damage and even sudden infant death from lapses in cardiorespiratory function (Thomas, Chung et al. 2013).

Hyperekplexia or startle disease (OMIM 149400) is a glycinergic synaptopathy affecting proteins necessary for the proper functioning of glycine neurotransmission. The most frequent cause of the disease are mutations preventing the function of the GlyRs (Harvey and Yee 2013). The second most common cause are mutations in the *SLC6A5* gene, encoding GlyT2 that generate inactive transporters or trafficking defects. Most GlyT2 mutations are recessive, although two dominant missense mutations have been described. One is Y705C, where the introduced cysteine aberrantly interacts with the cysteine pair Cys-311/Cys-320 in the second external loop of GlyT2 impairing transporter maturation through the secretory pathway in a recessive manner. In addition, the mutation alters the H^+ and Zn^{2+} sensitivity of wild type GlyT2 in a dominant negative manner, thereby affecting the function of the GlyT2 heteromers carrying wild type and mutant subunits (Gimenez, Perez-Siles et al. 2012). Even though GlyT2 oligomerization was previously reported under nonnative conditions after transporter cross-linking (Bartholomaus, Milan-Lobo et al. 2008), the dominance of Y705C mutation was the first in vivo evidence of the quaternary structure of GlyT2 at the plasma membrane. Another piece of evidence came from the second dominant mutation found in hyperekplexia patients that further confirmed the oligomeric state of GlyT2. S510R mutant affects GlyT2 intracellular trafficking and blocks the arrival of the wild-type transporter to the plasma membrane exerting a dominant-negative effect (Rees, Harvey et al. 2006). The inclusion of an arginine rather than a serine in a crucial region provokes GlyT2 misfolding, enhances its association to the endoplasmic reticulum (ER) chaperone calnexin, alters the association with the COPII component Sec24D and, as a consequence, impedes exit of the transporter from the ER (Arribas-Gonzalez, de Juan-Sanz et al. 2015). Thus, the ER-arrested mutant included into heteromers together with the wild-type GlyT2 causes its retention and therefore the dominant negative effect.

GlyT2 is a polytopic glycoprotein of the SLC6 family (Rudnick, Kramer et al. 2014) with twelve transmembrane domains (TM) connected by external and internal loops (EL, IL). The synthesis of the transporter begins with the co-translational translocation of the nascent protein to the endoplasmic reticulum (ER) where it receives preassembled glycan chains in four asparagines located in the second external loop (EL2)(Martinez-Maza, Poyatos et al. 2001). Correct folding of the transporter requires the interaction with several ER chaperones such as calnexin (Arribas-Gonzalez, Alonso-Torres et al. 2013). The ER quality control is very efficient so that only properly folded and oligomerized GlyT2 will be packed into COPII vesicles to reach the Golgi. Oligomerization has been clearly proven as a requirement for the exit from the ER both for GlyT1 (Fernandez-Sanchez, Diez-Guerra et al. 2008) and GlyT2 (Arribas-Gonzalez, de Juan-Sanz et al. 2015), and the above dominant mutations rely in the existence of heteromers carrying wild type and mutant protomers. However, the structural domains involved in the oligomerization of GlyTs, remain to be defined. Since the recently solved crystals of Drosophila melanogaster dopamine transporter (dDAT) (Penmatsa, Wang et al. 2013) and human serotonin transporter (hSERT)(Coleman, Green et al. 2016) point out to oligomerization interfaces different from that suggested by the prokaryotic homolog LeuTAa (Yamashita, Singh et al. 2005), we have developed GlyTs oligomerization models based on LeuTAa and dDAT and selected possible residues involved in oligomer assembly. In this report we study the quaternary structure of GlyT2 and the structural basis of the oligomerization interface.

EXPERIMENTAL PROCEDURES

Cell growth and protein expression

COS7 cells (American Type Culture Collection) were grown at 37°C and 5% CO_2 in Dulbecco's modified Eagle's medium supplemented with 10% fetal bovine serum. Transient expression was achieved using Turbofect (Thermo Scientific), according to the manufacturer's protocol, and the cells were then incubated for 48 h at 37°C. Reproducible results were obtained with 50-60% confluent cells on 60 mm or 6 well plates, using 5 μg and 2 μg of total DNA, respectively. In co-transfection experiments every co-transfected cDNA was 25% of the total DNA. The transfection efficiency was determined by co-transfecting the cDNAs with the pSV-β-galactosidase plasmid (Promega) and measuring β-galactosidase activity 24 h later, as described elsewhere (Arribas-Gonzalez, Alonso-Torres et al. 2013).

Plasmid constructs

The pRFP vector was a generous gift of José Antonio Esteban (Centro de Biología Molecular Severo Ochoa, Madrid, Spain). GlyT2 (Liu, Lopez-Corcuera et al. 1993) was subcloned into pcDNA3 and the GlyT2 mutants were constructed by site-directed mutagenesis using the QuikChange kit (Stratagene) (Jimenez, Zafra et al. 2011). Plasmids from two independent Escherichia coli colonies were transfected into eukaryotic cells and [^{3}H]glycine transport was measured in the cells for verification. The GFP-GlyT2 plasmid was constructed and characterized as described previously (Geerlings, Nunez et al. 2002; de Juan-Sanz, Zafra et al. 2011). The RFP and GFP tags were fused in frame with GlyT2 at the N-terminus and they did not interfere either with the uptake capacity in [^{3}H]glycine uptake assays or its expression at the plasma membrane as assessed by biotinylation(Arribas-Gonzalez, de Juan-Sanz et al. 2015).

Transport assays

Glycine transport assays on COS7 cells were performed at 37°C in phosphate-buffered saline (PBS) containing 10 mM glucose and 2 μCi/ml [2-3H]-labeled glycine (1.6 TBq/mmol; PerkinElmer), diluted to a final concentration of 10 μM as described previously (Perez-Siles, Nunez et al. 2012). For glutamate transport assays the radiolabeled glycine was substituted with the same amount of [^{3}H]-labeled glutamate. These reactions were run for 10 min and then terminated by aspiration. The protein concentration was determined in aliquots taken from each

well (Bradford) and the uptake of [2-^{3}H]-glycine was measured by liquid scintillation (LKB 1219 Rackbeta). Transport was quantified by subtracting the glycine accumulated in mock-transfected COS7 cells (or in the presence of the specific GlyT2 inhibitor, ALX1393) from that of the transporter-transfected cells, and normalized to the protein concentration. Assays were performed in triplicate or quadruplicate.

Surface biotinylation

COS7 cells expressing the transporters were grown in 6 well plates (Nunc), washed, labeled at 4°C with 1.0 mg/ml Sulfo-NHS-Biotin in PBS (Pierce), quenched with 100 mM L-lysine to inactivate the free biotin and lysed with 1x lysis buffer as described elsewhere (Arribas-Gonzalez, Alonso-Torres et al. 2013). A portion of the lysate was saved (total protein) and the remainder was incubated with streptavidin-agarose beads for 2 h at room temperature with rotary shaking. After low speed centrifugation, the supernatant (non-biotinylated fraction) was removed, and the agarose beads recovered were washed 3 times with 1x lysis buffer and the bound proteins (biotinylated) were eluted with Laemmli buffer (65 mM Tris, 10% glycerol, 2.3% SDS, 100 mM DTT, 0.01% bromophenol blue) for 10 minutes at 75 ºC. The samples were then analyzed in Western blots.

Primary cultures of cerebral cortex and transfection

Primary cultures of embryonic cortical neurons were prepared as described (de Juan-Sanz, Nunez et al. 2013). Briefly, the cortices of Wistar rat fetuses were obtained at the 18th day of gestation (E18) and the tissue was then mechanically disaggregated in Hanks' balanced salt solution (HBSS, Invitrogen) containing 0.25% trypsin (Invitrogen) and 4 mg/ml DNase (Sigma). Cells were plated at a density of 2.10^{6} cells/well in p60 plates (Falcon) and they were incubated for 4 h in 10% fetal calf serum-Dulbecco's modified Eagle's medium containing in mM: glucose, 10; sodium pyruvate 10; glutamine, 0.5; in mg/mL: gentamicin, 0.05; streptomycin, 0.1 and penicillin G, $6x10^{-5}$. After 4 hours the buffer was replaced with Neurobasal/B27 culture medium containing 0.5 mM glutamine (50:1 by volume: Invitrogen) and 3 days later cytosine arabinoside (2.5-5 x 10^{-3} mM) was added to inhibit further glial growth. For transfection, neurons which had been maintained in vitro for 7 days growing in each plate, were incubated with 5 µg of total DNA mixed with 10 µl of Lipofectamine 2000 reagent (Invitrogen) and after five hours the medium was replaced with Neurobasal/B27. GlyT2 expression were measured after 48h in culture.

Obtention of synaptosomes

Synaptosomes were purified from rat (3 months old, male) brainstem and spinal cord as described (Nagy and Delgado-Escueta 1984), and resuspended in ice-cold HBM buffer (Hepes-buffered medium, composition in mM: NaCl 140, KCl 5, $MgCl_2$ 1, Na_2HPO_4 1.2, $NaHCO_3$ 5, glucose 10, and HEPES-NaOH 20, pH 7.4). This buffer was used as a Ca^{2+}-free medium.

Lentivirus production and infection of primary cortical neurons

Lentiviral particles were produced using reagents and protocols from Didier Trono (The Swiss Federal Institute of Technology Lausanne (EPFL), Switzerland) with the following modifications. HEK293T cells were transiently co-transfected using Turbofect reagent following instructions of the supplier (Thermofisher Scientific, R0532) with 8 µg of the corresponding lentivector plasmid (pLoxSyn-hGlyT2-Syn-GFP), 4 µg of the packaging plasmid pCMVdR8.74 (Addgene plasmid 22036) and 2 µg of the VSV G envelope protein plasmid pMD2G (Addgene plasmid 12259) expressing the gag/pol genes. The supernatants containing the viral particles were collected 48–60 h after transfection and filtered to remove cellular debris (Pall Corporation, Life Sciences Acrodis 25mm, 0.45µm Supor membrane). pLoxSyn-hGlyT2-Syn-GFP lentivector plasmid encoding for wild-type hGlyT2 was constructed in the dual

expression vector pLOX-Syn-DSRED-Syn-GFP donated by Francisco Gómez-Scholl (University of Sevilla) between the BglII and Not I sites.

Primary neuronal cultures were transduced at DIV1 by adding concentrated lentivirus at a multiplicity of infection (m.o.i.) of 0.5 to the growing media and incubated overnight. The following morning the culture medium was replaced by fresh medium and analyzed between DIV10-DIV14.

One-dimensional gel electrophoresis: blue native BN-PAGE

Most BN–PAGE experiments were performed with gels poured in-house. The most frequently used native gel was the 3-7.5% or 3-9% acrylamide gradient gel (8 × 8 cm, 1.5 mm thick and fifteen slots); protein samples from synaptosomes, cellular derived lysates of transfected cortical neurons or COS7 cells were collected and protein concentration was measured. 50µg of this collection was separated and reduced with 50mM DTT for 25 minutes at 4ºC and free sulfydryl groups were quenched with 20 mM N-ethylmaleimide (NEM). For solubilization, in preliminary experiments we tested Triton X-100 and digitonin at least at three detergent/protein ratios (data not shown). Digitonin was selected at a 10:1 detergent:protein ratio and incubated for 30 min at 4ºC. After solubilization, the samples were ultracentrifuged at 30000 rpm for 30 min (Beckman TL-100 ultracentrifuge, TLA100.1 rotor). The supernatant was transferred to a new tube and mixed with 2× NativePAGE loading buffer containing 500 mM aminocaproic acid (SERVA) at a volume ratio of 1:1. To each lane of a native gel, 8–10 µg of protein were loaded and subjected to electrophoresis in a 3–7.5% polyacrylamide gradient gel at 50 V for 30 min and then for 2 h at 120 V at RT, cathode buffer (50 mM Tricine, 15 mM BisTris (pH 7.0) and anode buffer (50 mM BisTris, pH 7.0). The gel was transferred to methanol-activated polyvinylidene fluoride (PVDF) membranes by semi-dry electrotransfer (Life Technologies Inc.: 1.2 mA/cm2 for 2 h) and the membranes were destained using 10% acetic acid and 25% methanol for 30 minutes. Then membranes were dried, blue background dye reduced with pure methanol and then blocked with 5% milk in PBS overnight at 4°C (Schagger and von Jagow 1991; Wittig, Braun et al. 2006).

Two-dimensional gel electrophoresis: BN/SDS-PAGE

Two-dimensional (2D) native/SDS-PAGE was performed as described (Reisinger and Eichacker 2007). Briefly, single-lane first-dimension (BN-PAGE) strips were excised from native gels and denatured with Laemmli buffer (40 mM Tris, pH 6.8, 2.5% SDS, 10% glycerol, 0.1 M DTT, 0.01% bromphenol blue) for 60 min at 80°C and subsequently placed onto 4% stacking and a 7.5% resolving SDS-PAGE gels. Electrophoresis was carried out at room temperature at 30mA for each minigel. Samples were analyzed by Western blot with anti-GlyT2 antibodies against N-teminal or C-terminal of the transporter.

Densitometric quantitation and data analysis

Protein bands visualized by enhanced chemiluminescence (Amersham) were quantified in a GS-800 Calibrated Imaging Densitometer using the BioRad Quantity One program with film exposures in the linear range. Non-linear regression fits of experimental transport data were performed using ORIGIN software (Microcal Software, Northampton, MA). The bars represent the S.E.M. of at least triplicate samples and the representative experiments shown were repeated no less than 3 times with comparable results.

Computational methods

A *h*GlyT2 model was obtained using MODELLER version 9.13 (Sali 1993) taking the crystallized dopamine transporter from *Drosophila melanogaster* (*d*DAT) (PDB code 4M48)(Penmatsa, Wang et al. 2013) as a template. Sequence alignments between of *d*DAT and GlyT2 were performed with the program Muscle (Edgar 2004). Multiple sequence alignment

(MSA), were obtained with the program MAFFT (Katoh, Misawa et al. 2002) using sequences with an e-value below 1e-15 in the program blastp (Altschul, Gish et al. 1990) against the NCBI's nr database. The modelled region for GlyT2 was from Lys-191 to Trp-760, excluding the loop between Leu-329 and Ala-365, which is not present at *d*DAT. Models were further refined by means of molecular dynamics simulations. Using the Membrane Builder module (Jo, Kim et al. 2007; Jo, Lim et al. 2009) in CHARMM-GUI (www.charmm-gui.org)(Jo, Kim et al. 2008).

RESULTS and DISCUSSION

The oligomeric state of GlyT2 is mediated by disulfide bonds

The identification and analysis of two GlyT2 dominant mutations in hyperekplexia patients sustained that GlyT2 oligomers formed in the ER are constitutively maintained both at the cell surface and during trafficking. In such a way, mutations present in heterozygosis could affect the neurochemical properties of the GlyT2 heterooligomers carrying wild type and mutant subunits (Gimenez, Perez-Siles et al. 2012; Arribas-Gonzalez, de Juan-Sanz et al. 2015). In addition, in one of these mutations, Y705C, the cysteine introduced in the external portion of TM11 aberrantly interacts with an extracellular cysteine pair of GlyT2 impairing transporter maturation through the secretory pathway in a recessive manner (Gimenez, Perez-Siles et al. 2012). This disulfide bond is conserved within the SLC6 transporter family and, together with the N-linked glycans, is present in the largest second external loop (EL2) (Figure 1). These co/postraductional modifications have critical roles in the proper transporter trafficking to the plasma membrane (Olivares, Aragon et al. 1995; Chen, Liu-Chen et al. 1997). During the analysis of the Y705C mutation, we realized that substitution mutants of the cysteines forming the EL2 pair Cys-311/Cys-320 (or the equivalent in the rat sequence Cys-313/Cys-322) that prevented the formation of the disulfide bond, generated a huge increase in the intensity of a high molecular weight band when subjected to biotinylation and Western blot (Figure 1B). This band was present, although very much reduced, in the double mutant (C313S/C322S) and in the wild-type suggesting the mutants favored intermolecular disulfide bonds between neighbor transporters. The apparent molecular weight of this band was consistent with oligomeric structures under denaturing conditions (SDS-PAGE), but the protein assembly could not be established. For this reason, we implemented the resolution in non-denaturing conditions using blue native-PAGE (BN-PAGE) to analyze the quaternary structure of GlyT2 (Figure 1C).

Blue native gel electrophoresis is a popular method for the determination of the oligomeric state of membrane proteins (Schagger, Cramer et al. 1994; Wittig, Braun et al. 2006). Oligomeric species are only observed under poor solubilization conditions, which permit association of the protein subunits. The kind and concentration of the detergent used and the time of solubilization are crucial parameters (Heuberger, Veenhoff et al. 2002; Swamy, Siegers et al. 2006). For example, yeast ATP synthase might be dimeric using low concentrations of Triton X-100 but monomeric using high Triton X-100/protein ratio (Wittig, Carrozzo et al. 2006). After testing several detergent/protein ratios for Triton X-100 and digitonin (data not shown) we selected 1:1 for Triton X-100 and 10:1 for digitonin and solubilized for 30 min at 4ºC (Figure 1C). Although digitonin exerts a moderate delipidating effect and the digitonin/protein ratio is not too critical, we chose a 10:1 ratio for the following experiments, initially in 3-12% acrylamide gels. Both solubilization conditions, showed two main high molecular weight forms that migrated exactly as the bands observed in the C313S and C322S mutants, which were compatible with oligomeric states of GlyT2. According to the native molecular weight markers, the molecular weight of these bands could correspond to the dimer (**) and the tetramer (****) of the transporter, respectively. One interesting feature of these native bands is that the form showing slower mobility was sensitive to the reducing agent DTT and disappeared after reduction, suggesting the protein assembly is mediated by disulfide bonds (Figure 1C).

GlyT2 tetramers are supported by disulfide bonds and dimers by hydrophobic interactions

In order to check whether the high molecular weight bands detected in blue native gels from the heterologous system could be reproduced in the endogenous neuronal system, the same type of experiment was performed in primary spinal neurons, primary cortical neurons and a preparation enriched in synaptic terminals, synaptosomes. In the optimized native gels performed at 3-9% acrylamide, all expression systems depicted similar quaternary structure pattern of the transporter, confirming that this is a property of GlyT2 in the native state (Figure 2A). Remarkably, the oligomeric forms represented the main species of the native transporter since we could not detect a band corresponding to the monomeric form. Only when the sample was pretreated with the denaturing agent SDS, and the transporter was resolved on BN-PAGE, a lower band was detected. The appearance of this low mobility band was dependent on the SDS concentration but could not be detected after treatments with urea or increasing DTT concentration. This demonstrates the existence of the monomeric form of GlyT2 as a consequence of the previous loss of the quaternary structure (Figure 2B). Interestingly, the different sensitivity of both forms to the denaturing and reducing agents in synaptosomes, suggests that tetramer stabilization is mediated by disulfide bonds and the dimer is linked by other types of hydrophobic interactions dissociated after denaturation (Figure 2C). It is worthy to note the smaller amount of oligomer obtained from the primary culture of spinal cord neurons relative to synaptosomes which is a preparation from adult rat. This suggests that the GlyT2 oligomerization state appears to be related to neuronal maturation.

The GlyT2 C-terminal domain is not involved in oligomerization of the transporter

The usual Western blot detection used for GlyT2 in our laboratory consists in an antibody against the N-terminal domain of the transporter (Zafra, Gomeza et al. 1995) that allows us identifying mature and immature forms in heterologous systems, but only mature forms in the native system (primary neurons and synaptosomes) (Figure 3A). Curiously, the antibody against the C-terminal domain of the transporter (Arribas-Gonzalez, Alonso-Torres et al. 2013) is able to detect the immature form in this adult rat preparation suggesting that in the other samples the epitope could be masked. One possibility that may explain this observation is that the C-terminus is involved in oligomer stabilization and it is masked due to interaction with neighbor subunits. To test this hypothesis, we analyzed GlyT2 C-terminal deletion mutants in native gels and found that the progressive GlyT2 C-terminal deletion does not abolish the assembly of the carrier (Figure 3B). However, the amount of dimeric forms, especially in the reduced conditions, was progressively decreased. Since in the neuronal samples the immature band is not detected by the GlyT2 antibody against the N-terminus (Figure 3A), the different size cannot be due to the protein maturation stage. Besides, the analysis of the mutant in which we have removed 64aa from the C-terminus in denaturing SDS gels indicated it does not produce mature transporter but only immature forms (Figure 3C). This further evidences that in our BN-PAGE conditions we only detect mature forms in neural samples supporting the idea that mature oligomers are present on the plasma membrane. This agrees with oligomer detection in the biotinylated fraction in Figure 1B.

An interesting feature produced by the treatment with DTT is the increase in the apparent molecular weight of the reduced dimer, indicating that the untreated tetramer but also the untreated dimer are sensitive to DTT. This could be due to a reduction and cleavage of some other intermolecular disulfides that alters the conformation of the proteins. Indeed, there are two cysteines in GlyT2 structure that in our 3D models are located within disulfide bond distance (less than 2Å) which are Cys294 in the TM3 and Cys401 in the TM4. The substitution mutants of these cysteines would probably give an answer in BN-PAGE. Another possibility is that DTT

treatment provokes the binding of GlyT2 subunits to any other molecule (palmitoyl chain or any other lipid). If this link is mediated or affected by the C-terminus, this could explain the observed progressive reduction in the amount of reduced dimer in the C-terminus mutants of progressively higher deletions (Figure 3B). The study of these postranslational modifications is presently in course in our laboratory.

Combination of native and denaturing electrophoresis reveals immature y mature forms in oligomeric forms of GlyT2

Since oligomerization of GlyT2 seems to be a prerequisite for ER export (Chiba, Freissmuth et al. 2014; Arribas-Gonzalez, de Juan-Sanz et al. 2015), and the species present in the ER are the immature forms, oligomers containing the immature transporter should appear in BN-PAGE. A strategy to know the composition of the bands results from the combination of native and denaturing conditions that allow the dissociation of the complexes (Sapp, Valencia et al. 2012).

BN-PAGE in combination with second dimension SDS-PAGE has been the method of choice for the investigation of the respiratory protein complexes of the electron transfer chains of a range of organisms, including bacteria, yeasts, animals and plants (Eubel, Braun et al. 2005; Wittig, Carrozzo et al. 2006). This technique allows the separation in two dimensions extremely hydrophobic protein sets for analysis and also provides information on their native interactions. The used combination of non-denaturing (BN-PAGE) and denaturing (SDS-PAGE) conditions allowed us concluding that both mature and immature transporter molecules are present in oligomeric forms in transfected cortical neurons and synaptosomes, despite only immature forms of GlyT2 were attributed to oligomerization in previous studies (Horiuchi, Nicke et al. 2001). The evidence of this conclusion came from the fact that every band obtained from BN-PAGE and run in a second dimension in SDS-PAGE gives two bands in SDS-PAGE of the size expected for a mature (100kDa) and immature (75kDa) monomer (Figure 4). As indicated above, the immature bands could only be detected using the antibody against the C-terminal domain of the transporter at long exposures but not with the antibody against the N-terminal epitope, further confirmation of the maturation state of the bands.

The oligomeric forms of GlyT2 are intracellular and plasma membrane

As a second approach to confirm that GlyT2 exists as an oligomer and to determine its cellular location, we used a membrane-permeable crosslinker disuccinimidyl suberate (DSS) and its homobifunctional membrane-impermeable analogous reagent, N-hydroxysuccinimide ester cross-linker (BS3). Both NHS-esters have 11.4Å distance spacer arm with identical reactivity toward primary amines present in the side chain of lysine residues and the N-terminus of each polypeptide (Okuda, Osawa et al. 2012). In this way, transfected cortical neurons expressing the transporter were treated with the reagents. After chemical crosslinking, neurons were collected and subjected under control or DTT conditions and analyzed by BN-PAGE and SDS-PAGE and immunoblotted with an anti-GlyT2 antibody. Due to BS3 crosslinking reagent's water solubility, conjugation reactions can conveniently take place at physiological conditions. After crosslinking, the tetramer was partially resistant to DTT reduction in both cases, although the degree of resistance was greater with DSS that reacts with surface and intracellular GlyT2 than with BS3 that only reaches surface transporter. The presence of tetramers resistant to the impermeable agent BS3 proves that these structures are present at the plasma membrane where the transporter is functional. The analysis in denaturing gels reproduced the same result on the faint oligomer bands present in these conditions confirming the irreversible nature of the crosslinkers (Figure 5A).

Chemical crosslinking offers a direct method to identify both transient and stable interactions because it involves the formation of covalent bonds between two proteins. One of the questions derived from this study is whether the high molecular weight species are GlyT2 homooligomers or are heteromers including GlyT2 and another protein subunit. One approach to answer this question is to use GlyT2 subunits labeled with different tags and visualize the samples under native conditions. If GlyT2 forms homooligomers, a common band with mixed oligomers containing both tags should be visible. We tried to perform this experiment in transfected cortical neurons but the tags were not detected in native conditions. Therefore, we used COS7 cells for this experiment in which we did detect them. We observed that both RFP and GFP tagged transporter sized up but retain the tetramer and dimer pattern as the unlabeled transporter. A common band detected with both antibodies suggested the presence of mixed GlyT2 oligomers in the sample thus confirming the quaternary structure of the transporter (Figure 5B). However, we did not detect all possible mixed oligomers containing both tags and it is difficult to establish whether they are dimers or tetramers. As described elsewhere (Anderluh, Hofmaier et al. 2017), the oligomerization is a dynamic process along the secretory pathway that it may be fixed in the plasma membrane but the transient assemblies would be reinforced using a crosslinking. For this reason, these preliminary results have to be re-addressed by combining the use of tagged transporters with crosslinker treatment that may freeze all the mixed oligomers.

Possible GlyT2 oligomerization interface

Previous studies in the NSS transporter family have considered regions that could be involved in oligomerization. Dimer structures of the bacterial NSS homologue, LeuTAa reveals that dimerization is mediated by TM12 and TM9a, as well as residues from the second extracellular loop (Yamashita, Singh et al. 2005). However, there is no evidence as yet that LeuTAa functions as an oligomer. In the recently solved SERT crystal, TM12 is proposed to be involved in the formation of a crystallographic dimer (Coleman, Green et al. 2016). However, the dDAT crystal gave additional information about TM12, since a kink in the center at Pro572 causing the second half of the helix to turn away from the transporter, indicated that the dimerization interface of LeuTAa could be different from the oligomerization interfaces of eukaryotic NSSs. Although previous studies indicate that NSSs oligomerize, dDAT crystal is monomeric in detergent micelles and in the crystal lattice thus suggesting that a membrane bilayer or additional molecules may be required for NSS assembly. Therefore, neurons represent the best system to study this process where these components are preserved intact. In fact, a current study is being conducted to find out the influence of the lipid environment on this oligomeric assembly since GlyT2 shows optimum activity when included in lipid rafts (data not shown). In addition, it is interesting that although there is substantial evidence for oligomerization of both DAT and SERT (Anderluh, Klotzsch et al. 2014), the crystal structures, to date, failed to capture the oligomeric forms (Penmatsa, Wang et al. 2013; Penmatsa, Wang et al. 2015; Coleman, Green et al. 2016). This might be due to the formation of relatively weakly associated oligomers unable to withstand the rigors of the extraction and isolation processes required for structural studies. This issue has also been highlighted for the recent structure of the monomeric form of an SLC26 family member, where loss of the oligomeric form was assumed to be a result of the harsh nature of the detergent treatment (Geertsma, Chang et al. 2015). However, the oligomeric structure seems to be preserved in our experimental conditions retaining native protein.

To analyze the possible oligomerization interface of GlyT2 we have proposed a disulfide bond model at the TM9-TM12 interface as was proposed for LeuTAa crystallized as a dimer but based on the DAT crystal. The three-dimensional model generated from GlyT2 using dDAT as a template shows a perfect fit between the TM12 and TM9 of each monomer (Figure 6) therefore, the carrier could oligomerize by clashing TM12-TM12 and TM9-TM9 between

monomers. Due to the ability of DTT to cleave the GlyT2 tetramers, we selected several cysteine residues located in the transporter surface that could account for the disulfide bonds stabilizing the dimers. According to this selection, we generated different combinations of cysteine mutants of TM9 (C611S, C612S and C614S) and TM12 (C664S, C696S, C726S) in order to analyzed them on BN-PAGE (Figure 7C). The substitution of one, two or three cysteines in single, double or triple mutants yielded active transporters with transport activities ranging from 100% to 70% of wild-type transport. The substitution of up to four cysteines as in mutant 4CS (C611S, C612S, C614S and C726S) was still compatible with the glycine transport and this mutant retained about 60% wild-type activity (Figure 7A) and between 50-70% membrane expression (Figure 7B). However, mutation of more than four cysteines (4CS) caused detriment in transport activity, so, mutant 5CSbis was about 30% active and mutants 5CS (4CS+C664S) and 6CS (C611S, C612S, C614S, C726S, C696S and C664S) were totally inactive. The analysis of the mutants using BN-PAGE under control or DTT treatment revealed that the sensitivity to DTT was partially loss in the double, triple and especially the 4CS mutant. However, the inactive mutants containing more than four substitutions, although apparently loss completely the DTT sensitivity, displayed a smeared pattern suggesting the transporter lost its correct folding and consequently its functionality as shown in the transport activity assay (Figure 7A).

In accordance to our model, regardless of the location of the monomers in the tetramer, reduction by DTT would always generate dimers sustained by hydrophobic interactions. Indeed, except the 6CS mutant, which apparently loss the ability to get dissociated, probably due to some aggregation problem, the rest of the mutants exhibited a robust band corresponding to the dimer. However, it is remarkable that the size of the dimer became progressively higher as more cysteines were substituted, and this did not take place when cysteines out the predicted dimerization interface were mutated (Figure 7C, D and E). This increase initiates even in the C611S and C612S single mutants and it was maximal in the double, triple and 4CS mutants (Figure 7C). Since in this study we detected an increase in the apparent molecular weight of the dimer after DTT treatment (Figure 3), the loss of this increase may absence of disulfide bonds clevable by DTT in the untreated tetramer (or the reduced dimer). Mutations of four cysteines or more (mutants 4CS, 5CSbis and 6Cs, induced the loss of this increase, suggesting either the tetramer or the reduced dimer are not DTT sensitive.

This makes us to revisit the hypothesis of the transporter binding to a molecule that increases the molecular weight of the dimer although the role of the mutated cysteines in this possible association is presently unknown. The study of GlyT2 palmitoylation is presently an ongoing research in our group, and there are candidate cysteines in TM9. It is possible that GlyT2 oligomerization is controlled by palmitoylation or other lipid modification (PIP2) and any alteration of the dimerization interface disrupts the equilibrium binding to the transporter. Further work is needed to answer this and other questions as the functional character of the oligomers that remains to be clarified.

REFERENCES

Altschul, S. F., W. Gish, et al. (1990). "Basic local alignment search tool." J Mol Biol **215**(3): 403-10.

Anderluh, A., T. Hofmaier, et al. (2017). "Direct PIP(2) binding mediates stable oligomer formation of the serotonin transporter." Nature Communications **8**: 14089.

Anderluh, A., E. Klotzsch, et al. (2014). "Single molecule analysis reveals coexistence of stable serotonin transporter monomers and oligomers in the live cell plasma membrane." J Biol Chem **289**(7): 4387-94.

Apostolides, P. F. and L. O. Trussell (2013). "Rapid, activity-independent turnover of vesicular transmitter content at a mixed glycine/GABA synapse." J Neurosci **33**(11): 4768-81.

Aragon, C. and B. Lopez-Corcuera (2003). "Structure, function and regulation of glycine neurotransporters." Eur J Pharmacol **479**(1-3): 249-62.

Aragon, C. and B. Lopez-Corcuera (2005). "Glycine transporters: crucial roles of pharmacological interest revealed by gene deletion." Trends Pharmacol Sci **26**(6): 283-6.

Arribas-Gonzalez, E., P. Alonso-Torres, et al. (2013). "Calnexin-assisted biogenesis of the neuronal glycine transporter 2 (GlyT2)." PLoS One **8**(5): e63230.

Arribas-Gonzalez, E., J. de Juan-Sanz, et al. (2015). "Molecular basis of the dominant negative effect of a glycine transporter 2 mutation associated with hyperekplexia." J Biol Chem **290**(4): 2150-65.

Bartholomaus, I., L. Milan-Lobo, et al. (2008). "Glycine transporter dimers: evidence for occurrence in the plasma membrane." J Biol Chem **283**(16): 10978-91.

Coleman, J. A., E. M. Green, et al. (2016). "X-ray structures and mechanism of the human serotonin transporter." Nature **532**(7599): 334-9.

Chen, J. G., S. Liu-Chen, et al. (1997). "External cysteine residues in the serotonin transporter." Biochemistry **36**(6): 1479-86.

Chiba, P., M. Freissmuth, et al. (2014). "Defining the blanks - Pharmacochaperoning of SLC6 transporters and ABC transporters." Pharmacol Res **83**: 63-73.

de Juan-Sanz, J., E. Nunez, et al. (2013). "Constitutive endocytosis and turnover of the neuronal glycine transporter GlyT2 is dependent on ubiquitination of a C-terminal lysine cluster." PLoS One **8**(3): e58863.

de Juan-Sanz, J., F. Zafra, et al. (2011). "Endocytosis of the neuronal glycine transporter GLYT2: role of membrane rafts and protein kinase C-dependent ubiquitination." Traffic **12**(12): 1850-67.

Edgar, R. C. (2004). "MUSCLE: multiple sequence alignment with high accuracy and high throughput." Nucleic Acids Res **32**(5): 1792-7.

Eubel, H., H.-P. Braun, et al. (2005). "Blue-native PAGE in plants: a tool in analysis of protein-protein interactions." Plant Methods **1**: 11-11.

Fernandez-Sanchez, E., F. J. Diez-Guerra, et al. (2008). "Mechanisms of endoplasmic-reticulum export of glycine transporter-1 (GLYT1)." Biochem J **409**(3): 669-81.

Geerlings, A., E. Nunez, et al. (2002). "Glycine transporter isoforms show differential subcellular localization in PC12 cells." J Neurochem **82**(1): 58-65.

Geertsma, E. R., Y. N. Chang, et al. (2015). "Structure of a prokaryotic fumarate transporter reveals the architecture of the SLC26 family." Nat Struct Mol Biol **22**(10): 803-8.

Gimenez, C., G. Perez-Siles, et al. (2012). "A novel dominant hyperekplexia mutation Y705C alters trafficking and biochemical properties of the presynaptic glycine transporter GlyT2." J Biol Chem **287**(34): 28986-9002.

Gomeza, J., K. Ohno, et al. (2003). "Deletion of the mouse glycine transporter 2 results in a hyperekplexia phenotype and postnatal lethality." Neuron **40**(4): 797-806.

Harvey, R. J., U. B. Depner, et al. (2004). "GlyR alpha3: an essential target for spinal PGE2-mediated inflammatory pain sensitization." Science **304**(5672): 884-7.

Harvey, R. J. and B. K. Yee (2013). "Glycine transporters as novel therapeutic targets in schizophrenia, alcohol dependence and pain." Nat Rev Drug Discov **12**(11): 866-85.

Heuberger, E. H., L. M. Veenhoff, et al. (2002). "Oligomeric state of membrane transport proteins analyzed with blue native electrophoresis and analytical ultracentrifugation." J Mol Biol **317**(4): 591-600.

Hirzel, K., U. Muller, et al. (2006). "Hyperekplexia phenotype of glycine receptor alpha1 subunit mutant mice identifies Zn(2+) as an essential endogenous modulator of glycinergic neurotransmission." Neuron **52**(4): 679-90.

Horiuchi, M., A. Nicke, et al. (2001). "Surface-localized glycine transporters 1 and 2 function as monomeric proteins in Xenopus oocytes." Proceedings of the National Academy of Sciences of the United States of America **98**(4): 1448-1453.

Jimenez, E., F. Zafra, et al. (2011). "P2Y purinergic regulation of the glycine neurotransmitter transporters." J Biol Chem **286**(12): 10712-24.

Jo, S., T. Kim, et al. (2007). "Automated builder and database of protein/membrane complexes for molecular dynamics simulations." PLoS One **2**(9): e880.

Jo, S., T. Kim, et al. (2008). "CHARMM-GUI: a web-based graphical user interface for CHARMM." J Comput Chem **29**(11): 1859-65.

Jo, S., J. B. Lim, et al. (2009). "CHARMM-GUI Membrane Builder for mixed bilayers and its application to yeast membranes." Biophys J **97**(1): 50-8.

Katoh, K., K. Misawa, et al. (2002). "MAFFT: a novel method for rapid multiple sequence alignment based on fast Fourier transform." Nucleic Acids Res **30**(14): 3059-66.

Legendre, P. (2001). "The glycinergic inhibitory synapse." Cell Mol Life Sci **58**(5-6): 760-93.

Liu, Q. R., B. Lopez-Corcuera, et al. (1993). "Cloning and expression of a spinal cord- and brain-specific glycine transporter with novel structural features." J Biol Chem **268**(30): 22802-8.

Lynch, J. W. (2004). "Molecular structure and function of the glycine receptor chloride channel." Physiol Rev **84**(4): 1051-95.

Manzke, T., M. Niebert, et al. (2010). "Serotonin receptor 1A-modulated phosphorylation of glycine receptor alpha3 controls breathing in mice." J Clin Invest **120**(11): 4118-28.

Martinez-Maza, R., I. Poyatos, et al. (2001). "The role of N-glycosylation in transport to the plasma membrane and sorting of the neuronal glycine transporter GLYT2." J Biol Chem **276**(3): 2168-73.

McIntire, S. L., R. J. Reimer, et al. (1997). "Identification and characterization of the vesicular GABA transporter." Nature **389**(6653): 870-6.

Nagy, A. and A. V. Delgado-Escueta (1984). "Rapid Preparation of Synaptosomes from Mammalian Brain Using Nontoxic Isoosmotic Gradient Material (Percoll)." Journal of Neurochemistry **43**(4): 1114-1123.

Okuda, T., C. Osawa, et al. (2012). "Transmembrane topology and oligomeric structure of the high-affinity choline transporter." J Biol Chem **287**(51): 42826-34.

Olivares, L., C. Aragon, et al. (1995). "The role of N-glycosylation in the targeting and activity of the GLYT1 glycine transporter." J Biol Chem **270**(16): 9437-42.

Penmatsa, A., K. H. Wang, et al. (2013). "X-ray structure of dopamine transporter elucidates antidepressant mechanism." Nature **503**(7474): 85-90.

Penmatsa, A., K. H. Wang, et al. (2015). "X-ray structures of Drosophila dopamine transporter in complex with nisoxetine and reboxetine." Nat Struct Mol Biol **22**(6): 506-508.

Perez-Siles, G., E. Nunez, et al. (2012). "An aspartate residue in the external vestibule of GLYT2 (glycine transporter 2) controls cation access and transport coupling." Biochem J **442**(2): 323-34.

Rees, M. I., K. Harvey, et al. (2006). "Mutations in the gene encoding GlyT2 (SLC6A5) define a presynaptic component of human startle disease." Nat Genet **38**(7): 801-6.

Reisinger, V. and L. A. Eichacker (2007). "How to Analyze Protein Complexes by 2D Blue Native SDS-PAGE." PROTEOMICS **7**(S1): 6-16.

Rousseau, F., K. R. Aubrey, et al. (2008). "The glycine transporter GlyT2 controls the dynamics of synaptic vesicle refilling in inhibitory spinal cord neurons." J Neurosci **28**(39): 9755-68.

Rudnick, G., R. Kramer, et al. (2014). "The SLC6 transporters: perspectives on structure, functions, regulation, and models for transporter dysfunction." Pflugers Arch **466**(1): 25-42.

Sali, A., Blundell, T. L. (1993). "Comparative protein modelling by satisfaction of spatial restraints." J Mol Biol **234**(3): 779-815.

Sapp, E., A. Valencia, et al. (2012). "Native mutant huntingtin in human brain: evidence for prevalence of full-length monomer." J Biol Chem **287**(16): 13487-99.

Schagger, H., W. A. Cramer, et al. (1994). "Analysis of molecular masses and oligomeric states of protein complexes by blue native electrophoresis and isolation of membrane protein complexes by two-dimensional native electrophoresis." Anal Biochem **217**(2): 220-30.

Schagger, H. and G. von Jagow (1991). "Blue native electrophoresis for isolation of membrane protein complexes in enzymatically active form." Anal Biochem **199**(2): 223-31.

Swamy, M., G. M. Siegers, et al. (2006). "Blue native polyacrylamide gel electrophoresis (BN-PAGE) for the identification and analysis of multiprotein complexes." Sci STKE **2006**(345): pl4.

Thomas, R. H., S.-K. Chung, et al. (2013). "Genotype-phenotype correlations in hyperekplexia: apnoeas, learning difficulties and speech delay." Brain **136**(10): 3085-3095.

Wittig, I., H. P. Braun, et al. (2006). "Blue native PAGE." Nat Protoc **1**(1): 418-28.

Wittig, I., R. Carrozzo, et al. (2006). "Supercomplexes and subcomplexes of mitochondrial oxidative phosphorylation." Biochim Biophys Acta **1757**(9-10): 1066-72.

Yamashita, A., S. K. Singh, et al. (2005). "Crystal structure of a bacterial homologue of Na+/Cl--dependent neurotransmitter transporters." Nature **437**(7056): 215-23.

Zafra, F., J. Gomeza, et al. (1995). "Regional distribution and developmental variation of the glycine transporters GLYT1 and GLYT2 in the rat CNS." Eur J Neurosci **7**(6): 1342-52.

Acknowledgments: The authors wish to thank Francisco Zafra and Vega García-Escudero (Centro de Biología Molecular Severo Ochoa, Madrid) for help with the constructs in the lentivector plasmid and with the lentivirus production, respectively. Jose Antonio Esteban and José María Requena (Centro de Biología Molecular Severo Ochoa, Madrid) are recognized for generously providing the pRFP vector and the in-house RFP antibody, respectively. Francisco Gómez-Scholl (University of Sevilla) is acknowledged for generous supply of the pLOX-Syn-DSRED-Syn-GFP vector. The authors are grateful to Fulvio Santacatterina (Centro de Biología Molecular Severo Ochoa, Madrid) for help with the BN-PAGE optimization.

Footnotes: *This work was supported by the Spanish 'Ministerio de Economia y Competitividad' (SAF2011-28674 and SAF2014-58045-R), CIBERER, and by an institutional grant from the 'Fundación Ramón Areces'. E.A-G is a recipient of a grant BES-2012-053800 from the Spanish Ministerio de Economia y Competitividad.

The abbreviations used are: BS3, N-hydroxysuccinimideester; COPII, coatomer protein II; DAT, dopamine transporter; DSS, disuccinimidyl suberate; DTT, dithiothreitol; IL, internal loop; EL, external loop; ER, endoplasmic reticulum; GFP, green fluorescent protein; GlyT, glycine transporter; HBS, HEPES-buffered saline; LeuTAa, leucine transporter from Aequifex aeolicus; NSS, neurotransmitter sodium symporters; PBS, phosphate-buffered saline; RFP, red fluorescent protein; SERT, serotonin transporter; SLC, solute carrier; TM, transmembrane domain; VIAAT(VGAT), vesicular inhibitory amino acid transporter.

FIGURE LEGENDS

Figure 1. Structural analysis of the disulfide bond preserved in EL2 and discovery of the native structure of GlyT2 (A) GlyT2 secondary structure scheme (left) and molecular model based on LeuTAa (right) showing the localization of Cys-311 and Cys-320 in EL2 and Y705 in TM11. Cysteine residues are shown in red. **(B)** COS7 cells expressing GlyT2 and simple or double mutants of the EL2 cysteine pair were subjected to biotinylation as described under "Experimental Procedures" and resolved in SDS-PAGE: 6µg of total (lanes T) and 18µg of biotinylated proteins (lanes B) were subjected to Western blotting for GlyT2 detection. The bands marked with simple or double asterisk indicates dimer or monomer respectively. (C) GlyT2 and C313S were subjected to control or DTT (50mM) treatment conditions and solubilized with the specified detergents at the indicated detergent/ protein ratio and then resolved in 3-12% BN-PAGE. The bands marked with double (**) or quadruple (****) asterisk indicated dimer or tetramer respectively according to native molecular weight markers.

Figure 2. **Characterization of the stoichiometry of native GlyT2 through BN-PAGE in different expression systems. (A)** Immunoreactivity of overexpressed GlyT2 in COS7 cells or primary cortical neurons and endogenous GlyT2 in primary spinal neurons or synaptosomes showing two bands on the 3-9% gel corresponding to dimers (**) and tetramers (****) under control or DTT (50 mM) conditions. **(B, C)** Samples were subjected to pretreatment with SDS, urea or DTT at the indicated concentrations and then analyzed on BN-PAGE. The band that appears could represent the GlyT2 native monomer, simple asterisk (*).

Figure 3. Involvement of the C-terminal domain in oligomerization of GlyT2 (A). Expression of GlyT2 in different systems and Western blot with antibodies against GlyT2 N- or C-terminal epitopes. **(B)** Primary cortical neurons were transfected with several GlyT2 C-terminal deletion mutants in DIV7 and after 48 hours they were subjected to BN-PAGE under control or DTT (50mM) conditions. Mutants are labeled indicating the number of amino acids (aa) removed from the C-terminus. For comparison, a mutant is shown (-PDZ) were the last three amino acids (TQC), which conform the PDZ domain of GlyT2, were removed. **(C)** COS7 cells expressing the same GlyT2 C-terminal deletion mutants as in (B) were subjected to biotinylation as described under "Experimental Procedures" and subjected to denaturing SDS-PAGE. Tubulin immunoreactivity is shown as load control.

Figure 4. Combination of native and denaturing electrophoresis reveals oligomeric mature and immature GlyT2 (A) Transfected cortical neurons and **(B)** synaptosomes were subjected to BN/SDS-PAGE technique under control or DTT (50mM) conditions. Protein complexes solubilized in a native state in the first dimension (BN-PAGE) were rotated 90º and loaded into the second dimension (SDS-PAGE). As a control of the second dimension, a sample was loaded in the left part of the SDS-PAGE gels. Western blots are shown that were performed with the antibody against GlyT2 N-terminal (upper blots in A and B) or C-terminal (lower blots in A and B) epitope. **(C)** Representative scheme of the two-dimensional electrophoresis used.

Figure 5. (A) Effect of crosslinkers on GlyT2 oligomerization pattern. Transfected cortical neurons were crosslinked at room temperature for 30 minutes with the plasma membrane impermeable agent BS3 (5mM) and with the permeable crosslinker DSS (5mM) in the culture dish. Then, they were collected and treated - / + DTT (50mM) and subjected to BN-PAGE or SDS-PAGE. **(B)** COS7 cells were transfected with the GlyT2 transporter labeled with different tags (RFP-G2 and GFP-G2) and detected by BN-PAGE and SDS-PAGE after treatment with DTT with antibody against RFP or GFP.Note that each construction increases the molecular weight of each of the forms of the GlyT2. G2-RFP homotetramer (++++), G2-GFP homotetramer (****) and G2-RFP/G2-GFP heterotetramer (+*+*)

Figure 6. Possible GlyT2 oligomerization interface. (A) Proposed representative scheme of the possible cysteines that take part in the TM9-TM12 oligomerization interface of GlyT2. **(B)** Intracellular view of the three-dimensional surface model of GlyT2 based on dDAT crystal showing the possible assembly between monomers.

Figure 7. Mutagenesis of possible GlyT2 cysteines involved in the oligomerization interface. COS7 cells expressing the indicated cysteine mutants were assayed for glycine transport **(A)** or surface biotinylation **(B)** as described in "Experimental procedures". **(C,D,E)** Primary cortical neurons were transfected with the indicated mutants of TM9 and TM12 cysteines (C), the EL2 cysteines (D) or the N-terminal cysteine 3 used as a negative control (E) under control or DTT conditions and visualized by BN-PAGE and Western blot with the N-terminal GlyT2 antibody.

Figure 1

A

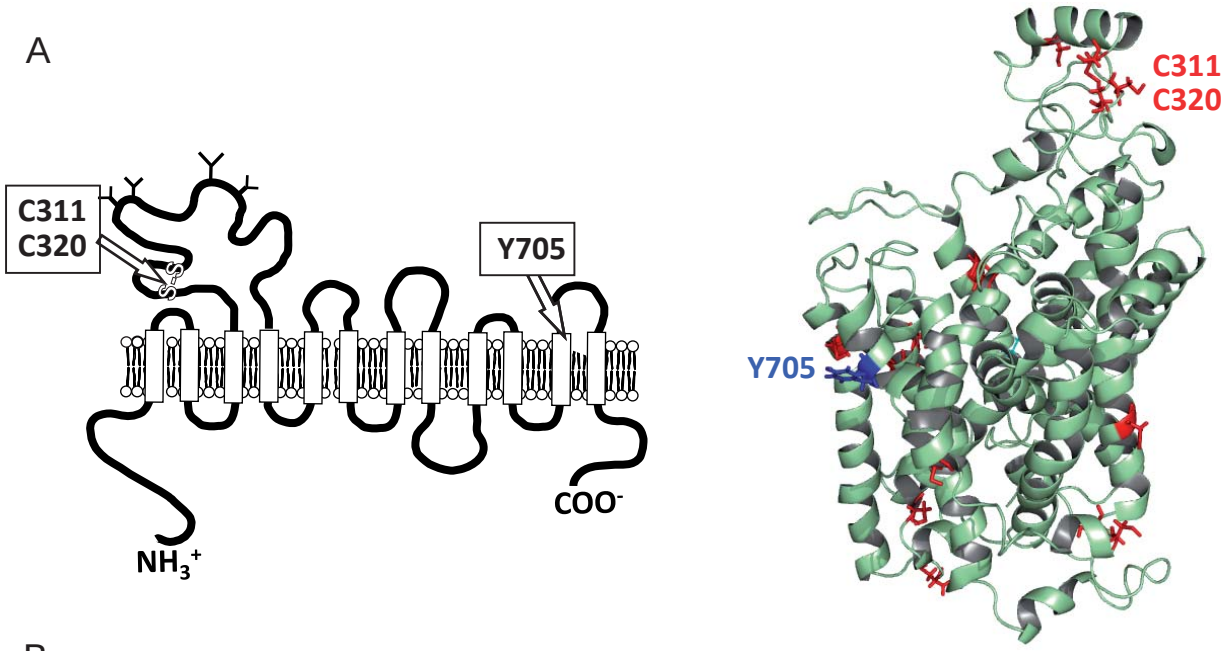
C311
C320
Y705
COO-
NH3+
C311
C320
Y705

B

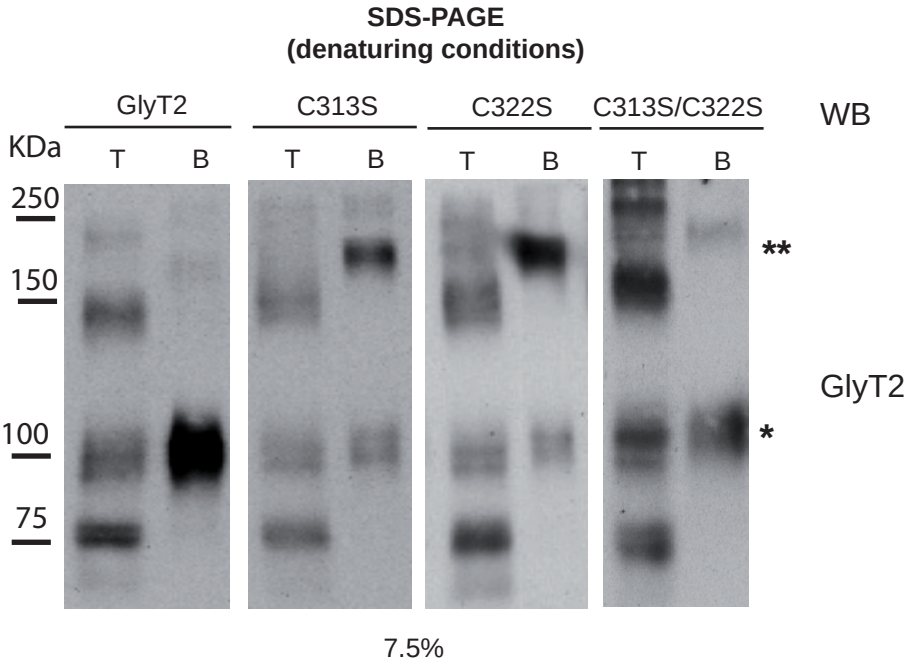
SDS-PAGE
(denaturing conditions)
GlyT2
C313S
C322S
C313S/C322S
WB
KDa
T
B
250
150
100
75
**
*
GlyT2
7.5%

C

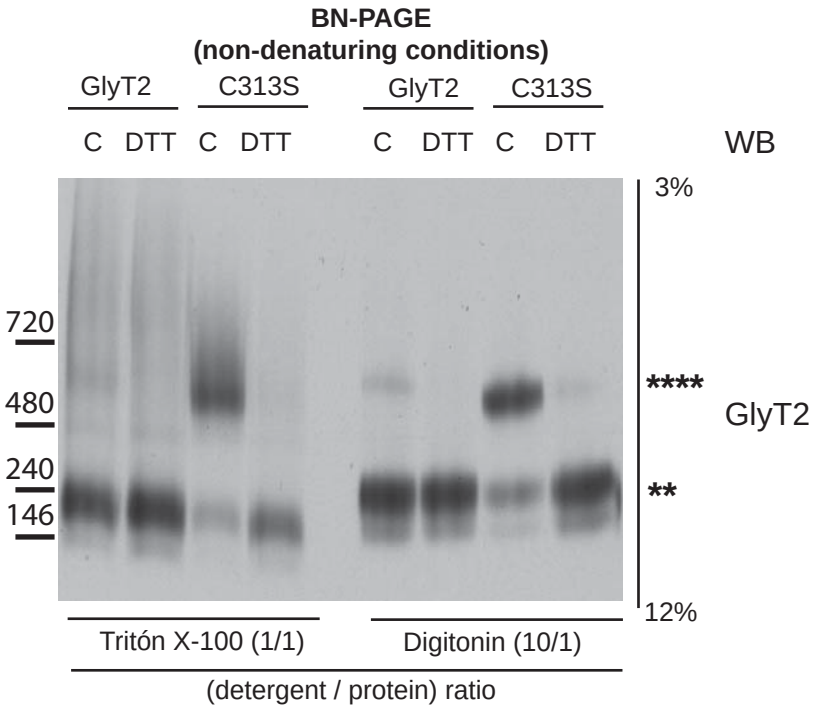
BN-PAGE
(non-denaturing conditions)
GlyT2
C313S
GlyT2
C313S
C
DTT
WB
720
480
240
146
3%
****
**
12%
GlyT2
Tritón X-100 (1/1)
Digitonin (10/1)
(detergent / protein) ratio

Figure 2

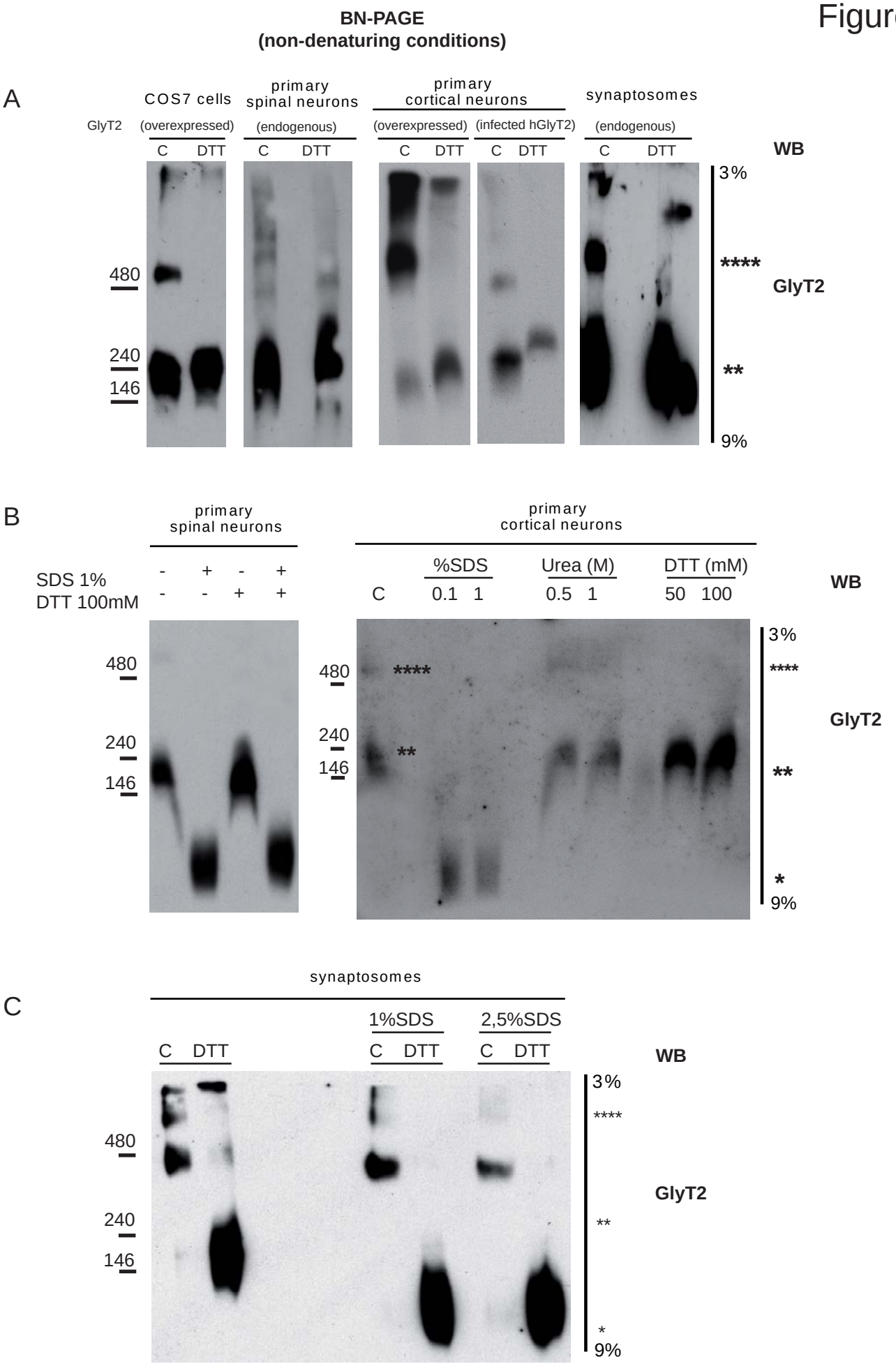
BN-PAGE
(non-denaturing conditions)
A
COS7 cells
primary spinal neurons
primary cortical neurons
synaptosomes
GlyT2
(overexpressed)
(endogenous)
(overexpressed)
(infected hGlyT2)
(endogenous)
C DTT C DTT C DTT C DTT C DTT
WB
480
240
146
3%
****
**
9%
GlyT2
B
primary spinal neurons
primary cortical neurons
SDS 1%
DTT 100mM
- + - +
- - + +
%SDS
Urea (M)
DTT (mM)
C 0.1 1 0.5 1 50 100
WB
480
240
146
****
**
3%
****
**
*
9%
GlyT2
C
synaptosomes
1%SDS
2,5%SDS
C DTT C DTT C DTT
WB
480
240
146
3%
****
**
*
9%
GlyT2

Figure 3

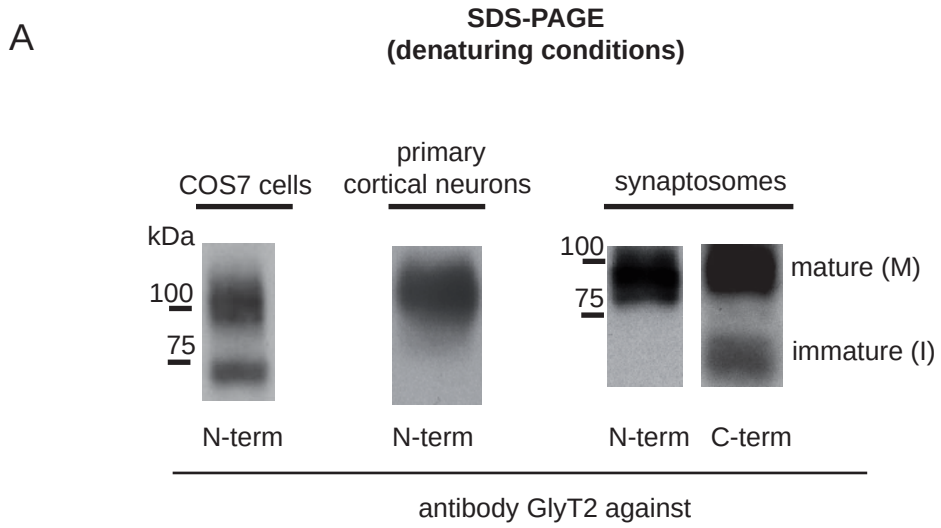
A
SDS-PAGE
(denaturing conditions)
COS7 cells
primary
cortical neurons
synaptosomes
kDa
100
75
100
75
mature (M)
immature (I)
N-term
N-term
N-term
C-term
antibody GlyT2 against

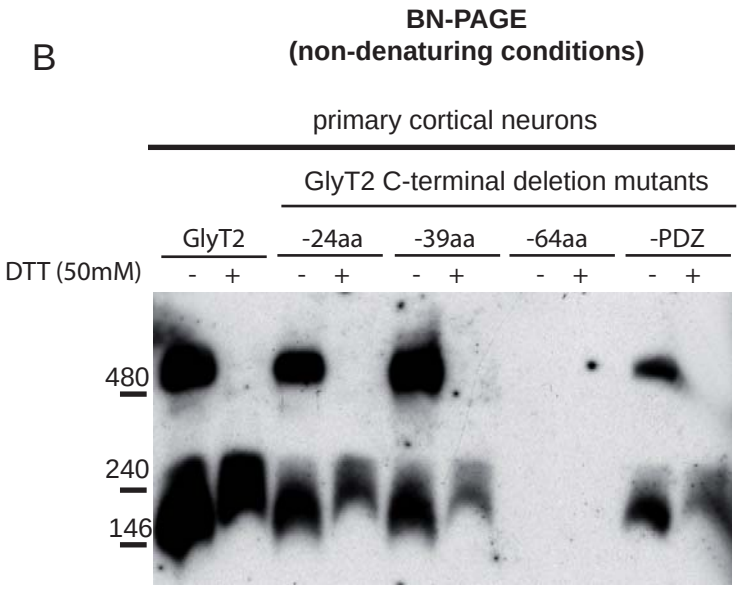
B
BN-PAGE
(non-denaturing conditions)
primary cortical neurons
GlyT2 C-terminal deletion mutants
GlyT2
-24aa
-39aa
-64aa
-PDZ
DTT (50mM)
- + - + - + - + - +
480
240
146

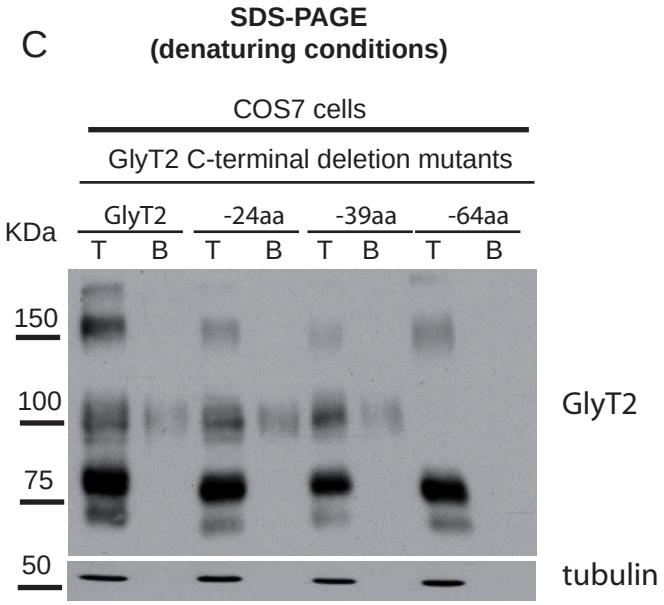
C
SDS-PAGE
(denaturing conditions)
COS7 cells
GlyT2 C-terminal deletion mutants
KDa
GlyT2
-24aa
-39aa
-64aa
T B T B T B T B
150
100
75
50
GlyT2
tubulin

Figure 4

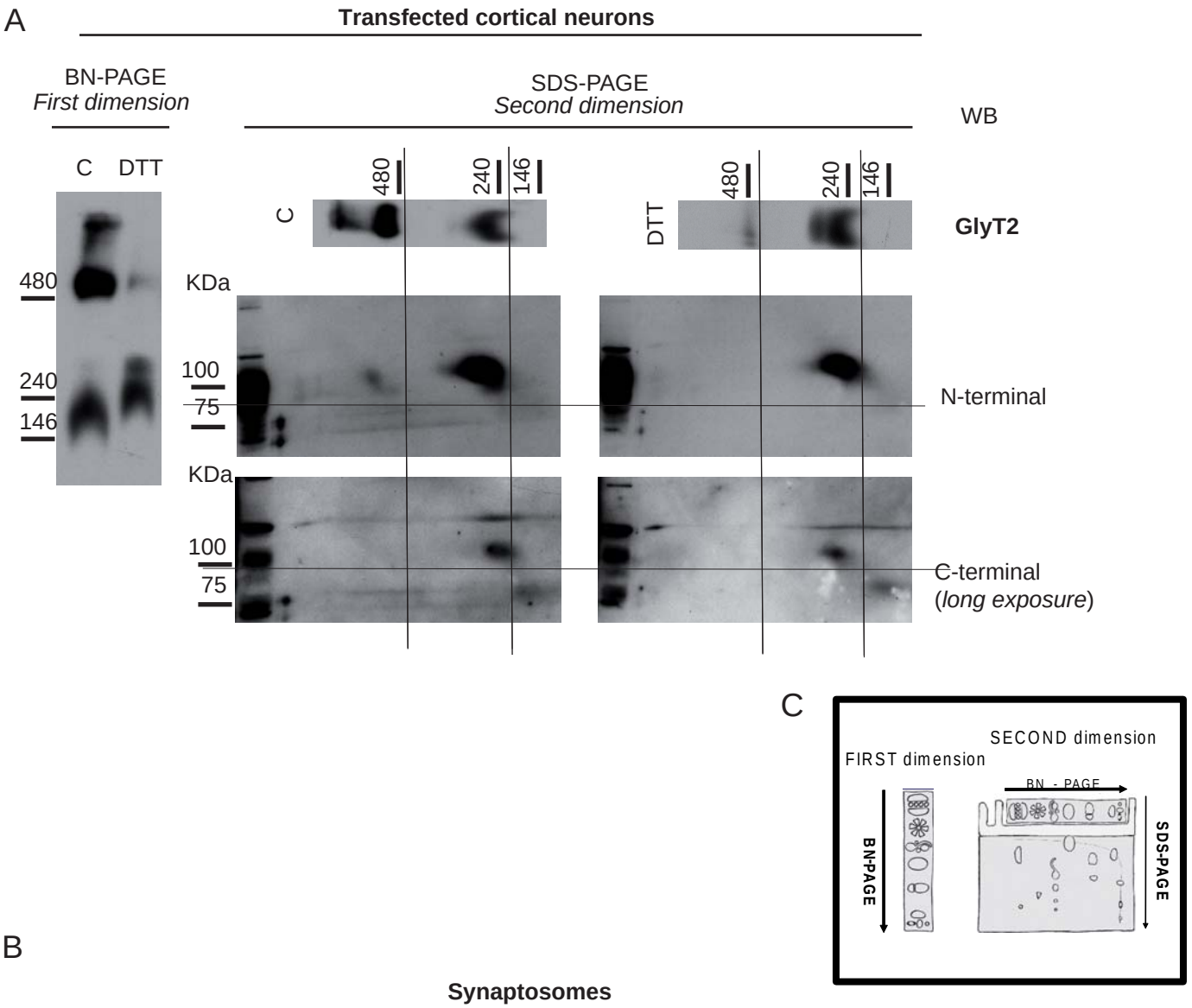
A
Transfected cortical neurons
BN-PAGE
First dimension
SDS-PAGE
Second dimension
WB
C
DTT
480
240
146
GlyT2
KDa
100
75
N-terminal
C-terminal
(long exposure)
C
SECOND dimension
FIRST dimension
BN - PAGE
BN-PAGE
SDS-PAGE
B
Synaptosomes

Figure 5

A

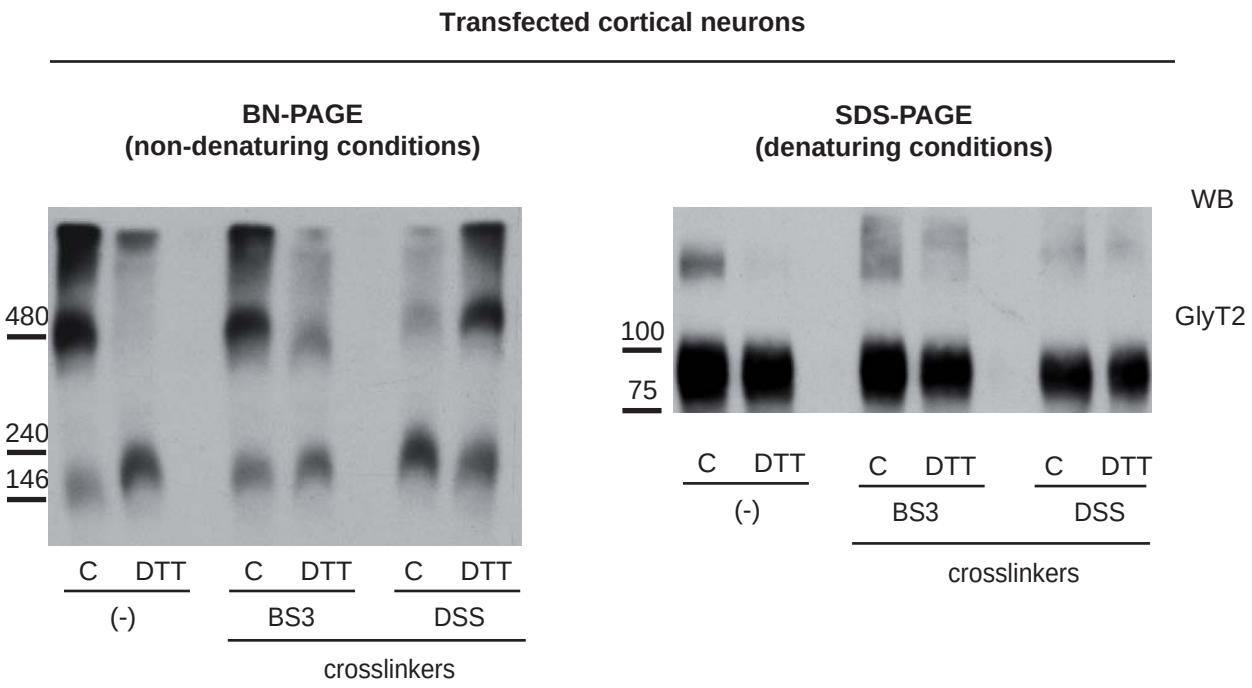
Transfected cortical neurons
BN-PAGE
(non-denaturing conditions)
SDS-PAGE
(denaturing conditions)
WB
GlyT2
480
240
146
100
75
C DTT C DTT C DTT
(-) BS3 DSS
crosslinkers
C DTT C DTT C DTT
(-) BS3 DSS
crosslinkers

B

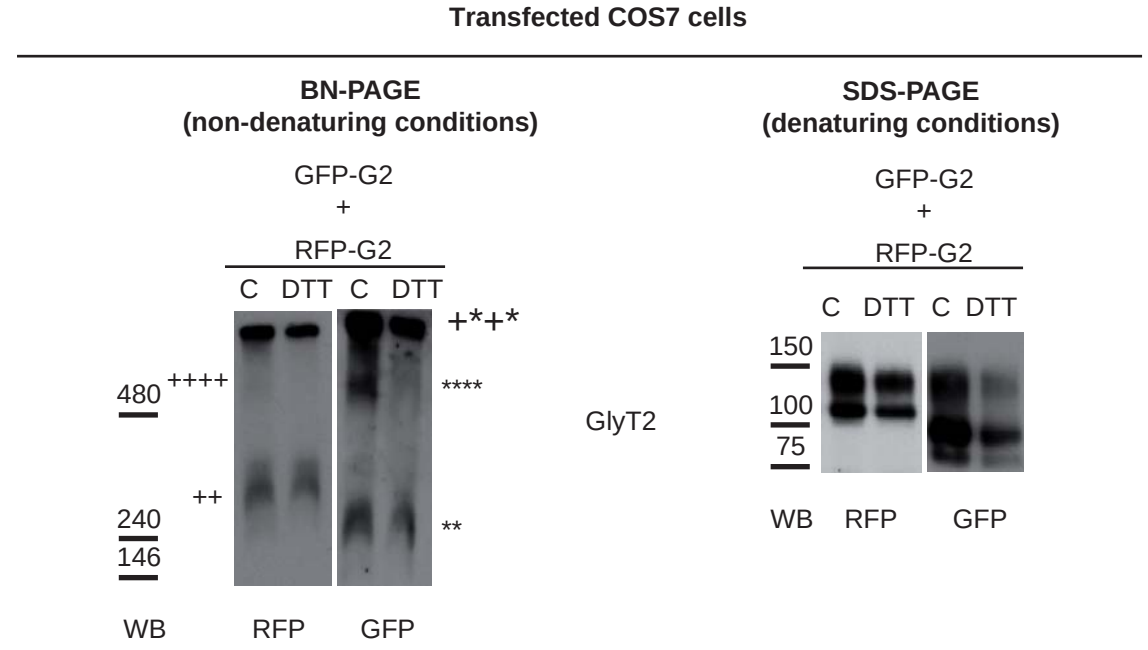
Transfected COS7 cells
BN-PAGE
(non-denaturing conditions)
SDS-PAGE
(denaturing conditions)
GFP-G2
+
RFP-G2
C DTT C DTT
+*+*
****
**
++++
++
480
240
146
WB RFP GFP
GlyT2
GFP-G2
+
RFP-G2
C DTT C DTT
150
100
75
WB RFP GFP

Figure 6

A

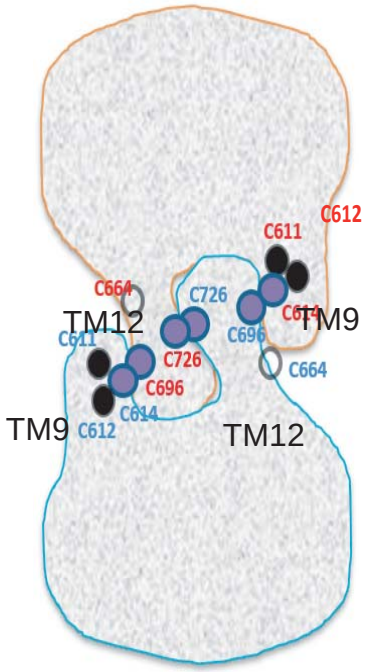
C612
C611
C664
C726
TM12
C611
C726
C696
C696
C614
TM9
C612
TM9
TM12
C664

B

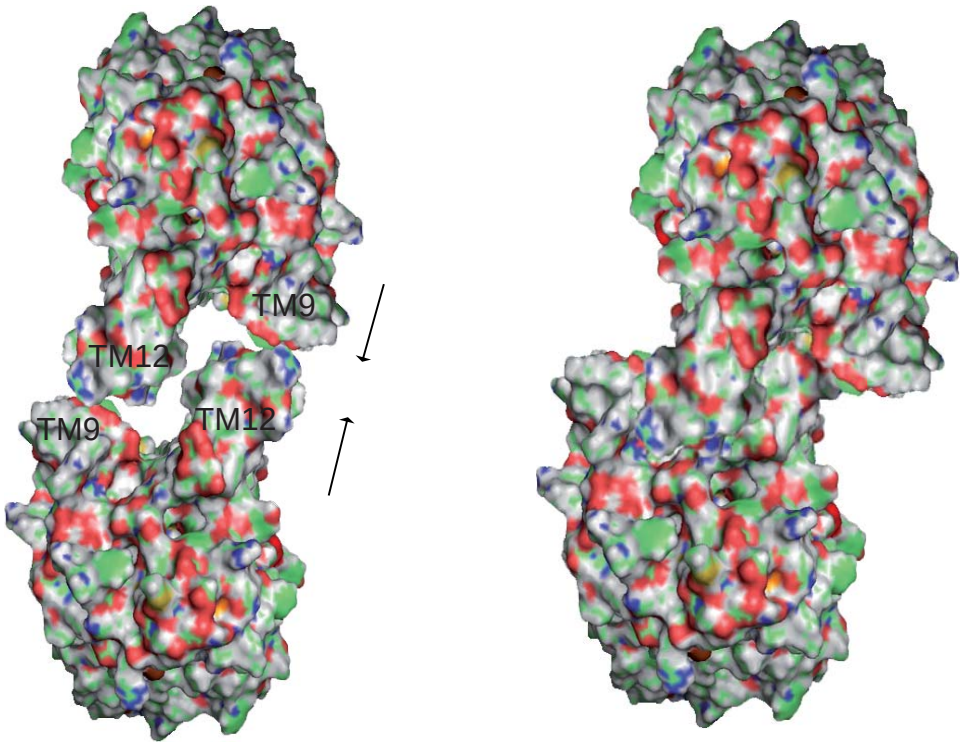
TM9
TM12
TM9
TM12

Figure 7

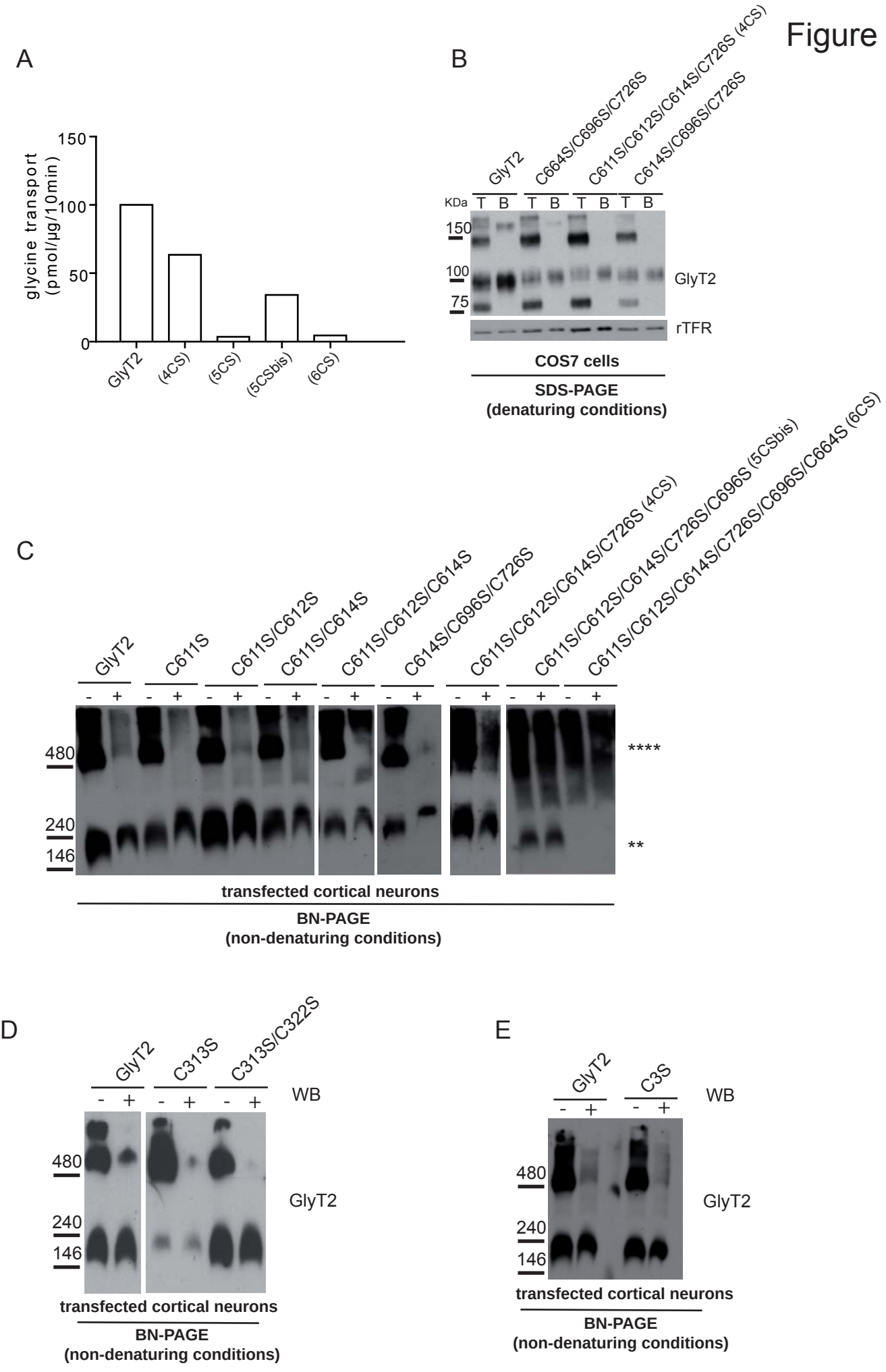
A
glycine transport (pmol/µg/10min)
150
100
50
0
GlyT2
(4CS)
(5CS)
(5CSbis)
(6CS)
B
GlyT2
C664S/C696S/C726S
C611S/C612S/C614S/C726S (4CS)
C614S/C696S/C726S
KDa
T B T B T B T B
150
100
75
GlyT2
rTFR
COS7 cells
SDS-PAGE
(denaturing conditions)
C
GlyT2
C611S
C611S/C612S
C611S/C614S
C611S/C612S/C614S
C614S/C696S/C726S
C611S/C612S/C614S/C726S (4CS)
C611S/C612S/C614S/C726S/C696S (5CSbis)
C611S/C612S/C614S/C726S/C696S/C664S (6CS)
- + - + - + - + - + - + - + - + - +
480
240
146
****
**
transfected cortical neurons
BN-PAGE
(non-denaturing conditions)
D
GlyT2
C313S
C313S/C322S
WB
- + - + - +
480
240
146
GlyT2
transfected cortical neurons
BN-PAGE
(non-denaturing conditions)
E
GlyT2
C3S
WB
- + - +
480
240
146
GlyT2
transfected cortical neurons
BN-PAGE
(non-denaturing conditions)

III. Discusión

1. Análisis de requerimientos para la síntesis de GlyT2 en la ruta secretora temprana

El conocimiento de los requisitos que son necesarios para la correcta síntesis de GlyT2 desde su inicio hasta su destino final, constituye un marco adecuado para el estudio de la biogénesis de transportadores con mutaciones asociadas a hiperplexia con posibles intervenciones terapéuticas. En este trabajo hemos abordado el estudio de algunos aspectos de la biogénesis de GlyT2 como la intervención de la N-glicosilación y algunas de las moléculas implicadas. Aunque GlyT2 es una proteína neuronal, para estudiar este proceso, se ha utilizado el sistema heterólogo de células COS7 que expresaban el transportador recombinante debido a que la proteína naciente se ha visualizado utilizando marcaje metabólico seguido de caza e inmunoprecipitación del transportador. Este método es idóneo para conocer la cinética de expresión de las proteínas en tiempo real pero requiere células creciendo en fase exponencial con una elevada tasa de síntesis y no puede ser utilizado en células postmitóticas como las neuronas. Así, aunque el trabajo requerirá confirmación mediante otros abordajes en sistemas nativos, los datos aportados son relevantes para conocer los requerimientos de la expresión en superficie de GlyT2. De acuerdo con resultados anteriores, en este sistema el transportador se detecta como un precursor inmaduro con N-glicosilación incompleta que da lugar a la forma de mayor tamaño presente en superficie (Martinez-Maza, Poyatos et al. 2001). El aumento de tamaño entre las dos formas, coincide con el esperado a partir de estudios con GlyT2 neuronal purificado donde se estableció que los azúcares constituían aproximadamente el 30% del peso molecular de GlyT2 (Nunez and Aragon 1994). El sistema ha permitido conocer la vida media del precursor (1h) y del transportador maduro (24h), lo que se asemeja a otros miembros de SLC6 con ciclos de vida largos (Pramod, Foster et al. 2013). El resultado electroforético tras digestión con distintas endoglicosidasas, que permite asignar una localización subcelular concreta (Freeze and Kranz 2010), ha revelado que el precursor inmaduro corresponde a la forma de RE o cis Golgi con glicosilación parcial, la cual se reduce al núcleo proteico tras el bloqueo completo de la glicosilación por PNGasa F o tunicamicina.

La comparación de distintas combinaciones de mutantes simples o múltiples de las cuatro asparaginas glicosiladas de GlyT2 ha establecido el papel de la N-glicosilación en algunos aspectos de la biogénesis del transportador. La pérdida progresiva de azúcares produce una alteración en los parámetros cinéticos de transporte de glicina. La V_{max} se reduce, lo que está de acuerdo con la necesidad de azúcares para la correcta migración a la membrana en células polarizadas detectada previamente por nuestro grupo (Martinez-Maza, Poyatos et al. 2001). Además, la K_m se incrementa, siendo máximo el aumento en el mutante de la Asn366 y los mutantes totalmente carentes de azúcares (N1234D ó N1234Q)

y este efecto no es dependiente de la carga pues se comportan de modo similar los mutantes de asparaginas sustituidas por aspartatos o por glutaminas. Esto sugiere que la presencia de carbohidratos contribuye al plegamiento del transportador y que la contribución a este efecto del carbohidrato en 366 es mayor. De hecho, la eliminación con PNGasa F de los azúcares de GlyT2 una vez reconstituido en liposomas, inhibe al transportador (Martinez-Maza, Poyatos et al. 2001). En el mismo sentido, la proteolisis limitada del mutante N1234D genera un patrón de fragmentos diferente al del tipo silvestre lo que apoya que la glicosilación condiciona el plegamiento y posterior tráfico a la membrana, como ocurre en otros miembros de la familia SLC6 (Melikian, McDonald et al. 1994; Tate and Blakely 1994; Li, Chen et al. 2004; Cai, Salonikidis et al. 2005). Aunque generalmente se piensa que la unión covalente de azúcares a las proteínas no produce cambios significativos en la estructura proteica sí da lugar a un incremento en su estabilidad (Lee, Qi et al. 2015) como se ha observado en DAT y GAT (Li, Chen et al. 2004; Cai, Salonikidis et al. 2005), en el caso de GlyT2 los azúcares parecen tener un efecto estabilizador más acusado que en GlyT1 (Martinez-Maza, Poyatos et al. 2001) y quizá son cruciales para la arquitectura del EL2 y para la correcta localización y unión al sustrato como predice un reciente estudio en el transportador de betaína renal (Schweikhard, Burckhardt et al. 2015). En este sentido, la importancia de EL2 en el funcionamiento de GlyT2, ha sido puesta de manifiesto en el artículo#4 donde la presencia de una sustitución a cisteína en una posición que interfiere con el puente disulfuro presente en este EL2, ocasiona un defecto no solo en la actividad de transporte sino en la biogénesis del transportador (Gimenez, Perez-Siles et al. 2012)

Dada la relevancia de la N-glicosilación en el plegamiento del transportador y que genera la señal para la entrada en el ciclo CNX/CRT, hemos investigado y caracterizado el papel de CNX en la biogénesis de GlyT2. Mediante coinmunoprecipitación tanto en el sistema heterólogo como en cultivo primario de neuronas hemos demostrado que CNX se une transitoriamente a la forma inmadura de GlyT2 y facilita su procesamiento. También hemos detectado una interacción rápida y lábil de GlyT2 con la chaperona BiP (*GRP78*) pero no con CRT, GRP94, PDI o ERP57, en nuestras condiciones experimentales. La ausencia de interacción de GlyT2 con CRT refuerza el dato bibliográfico de que los ligandos de CNX y CRT son diferentes y su especificidad no es solapante. Así, el ratón knockout para CNX, muere después de cuatro semanas debido a la incapacidad de CRT para reemplazar su actividad (Denzel, Molinari et al. 2002). Utilizando abordajes farmacológicos y mutagénesis simple o múltiple de los cuatro sitios de glicosilación de GlyT2, hemos establecido que la unión a CNX esta mediada por los azúcares y por interacciones proteína-proteína. Estos resultados confirman la hipótesis de que la unión inicial de CNX se produce con las FMG hasta que se adquiere la conformación de la proteína madura, mientras que la retención de proteínas unidas

no está mediada por glicanos sino por motivos polipeptídicos (Hammond, Braakman et al. 1994; Solda, Galli et al. 2007). Se ha descrito que el dominio globular y parte del dominio brazo de CNX son capaces de suprimir la agregación de sustratos a través de interacciones proteína-proteína bajo las condiciones variables que existen dentro del lumen del RE (Brockmeier and Williams 2006; Williams, Reed et al. 2009). De hecho, CNX puede discriminar entre distintos estados conformacionales de GlyT2 llevando a cabo una actividad chaperona independiente de su capacidad lectina. Así, la coexpresión con CNX del mutante de GlyT2 carente de azúcares (N1234D) aumenta su actividad de transporte pero no su expresión en membrana, indicando que CNX facilita la expresión en superficie de la conformación proteica más apta para la función (Stronge, Saito et al. 2001). Utilizando un sistema de cotransfección optimizado que evita saturar la maquinaria de traducción celular, hemos demostrado que los niveles de CNX correlacionan positivamente con la expresión del transportador activo. La depleción específica de CNX por RNAi reduce la expresión de GlyT2 y su sobrexpresión aumenta la expresión del transportador estabilizando su precursor y generando transportadores con un plegamiento óptimo. En levaduras, la sobrexpresión de CNX aumenta la producción de glicoproteínas virales mejorando su plegamiento y solubilidad (Ciplys, Sasnauskas et al. 2011). En hongos, la sobreexpresión de CNX y no de BiP produce un incremento de 4 a 5 veces en los niveles extracelulares de la metaloproteína peroxidasa de manganeso (Conesa, Jeenes et al. 2002). La sobrexpresión de varias chaperonas, incluida CNX, aumenta la expresión de SERT, transportador de la familia SLC6 (Tate, Whiteley et al. 1999), mientras que la sobrexpresión de CNX reduce la expresión de receptores de dopamina (Free, Hazelwood et al. 2007), lo que sugiere que el efecto de CNX es selectivo para ciertos grupos de proteínas ligando. De este modo, una buena estrategia para aumentar la expresión de GlyT2 sería actuar sobre moduladores de CNX que emulasen el efecto que produce su sobreexpresión. La cadena polipeptídica de la CNX puede incorporar modificaciones postraduccionales que regulan su actividad. Por ejemplo, las modificaciones en el C-terminal determinan su localización dentro del RE. Mientras que la palmitoilación de CNX refuerza su presencia en MAMs (mitochondria-associated membranes) donde a través de interacción con SERCA2b se regula el flujo de Ca^{2+} entre RE- mitocondria, la CNX sin modificar interviene en su función clásica en control de calidad de glicoproteínas (Lynes, Raturi et al. 2013). Se ha descrito que la capacidad de CNX está favorecida si la concentración de calcio en RE se eleva (Brockmeier and Williams 2006), lo que ha demostrado favorecer el plegamiento de mutantes que ocasionan enfermedades de depósito lisosomal (LSD) (Ong, Mu et al. 2010). Sin embargo, en el artículo #2 demostramos que en nuestras condiciones experimentales no se observan mejoras en el plegamiento de GlyT2 con tratamientos que alteran la concentración del ion, aunque no se ha llevado a cabo un estudio sistemático de este

aspecto. Otra interesante modificación de CNX es la fosforilación inducida por activación de ERK (*Extracellular signal Regulated Kinase*) que mejora su interacción con el complejo ribosoma-translocón (Hebert, Lamriben et al. 2014). La fosforilación de CNX atenúa la liberación de mutantes de α-1 antitripsina desde el RE señalando un posible mecanismo para mejorar el control de calidad de glicoproteínas (Cameron, Chevet et al. 2009).

La proteostasis resulta del balance adecuado entre la síntesis y degradación de proteínas en la célula (Okiyoneda, Apaja et al. 2011). En el caso de GlyT2, la identificación de la vía principal de degradación es crucial para diseñar tratamientos encaminados a superar el estrés de RE. Por ello se ha investigado si la vía principal de degradación del transportador es el proteasoma o el lisosoma. La inhibición del proteasoma parece impedir la biogénesis de GlyT2 eliminando la proteína madura y generando una nueva forma del transportador que coincide con el tamaño del mutante N1234D que podría representar la forma retrotranslocada y deglicosilada para ERAD. Sin embargo, la inhibición del proteasoma induce UPR en nuestras condiciones experimentales, lo que impide extraer conclusiones. Asimismo, queda por esclarecer si el mutante deficiente de azúcares es más propenso a degradación proteasomal que el genotipo silvestre, sobre todo porque las dos vías distintas de ERAD, una para sustratos glicosilados en la que interviene CNX y otra para no glicosilados donde interviene BiP pueden intercambiar sus sustratos en condiciones de estrés de RE (Ushioda, Hoseki et al. 2013). No obstante, los niveles celulares de CNX influyen en la velocidad de ERAD. Por ejemplo, la unión estabilizante de CNX con mutantes no glicosilados de la proteína proteolipído (PLP) retrasa su degradación a ERAD (Swanton, High et al. 2003). Las células carentes de CNX (células $CNX^{-/-}$) muestran una UPR constitutivamente activa con una actividad proteasomal incrementada sin mecanismos compensatorios de expresión de otras chaperonas (Coe, Bedard et al. 2008) lo que sugiere que la presencia o ausencia de CNX modula rutas específicas como ERAD para contrarrestar la carga de proteínas mal plegadas.

Finalmente, el aumento de la vida media del transportador maduro tras inhibición del lisosoma ha señalado que GlyT2 se degrada por vía lisosomal lo que está en consonancia con estudios posteriores en el laboratorio que demuestran el uso de esta vía degradativa por el transportador tras endocitosis dependiente de clatrina (de Juan-Sanz, Zafra et al. 2011; de Juan-Sanz, Nunez et al. 2013).

Los resultados presentados confirman que la biosíntesis de GlyT2 es asistida por CNX cuya concentración celular correlaciona positivamente con la expresión de GlyT2 activo, lo que hace de esta chaperona una molécula diana para posibles mutantes de hiperplexia con defectos de tráfico.

2. Estudio del efecto DN sobre el genotipo silvestre de un mutante de hiperplexia humana con defectos en el tráfico intracelular.

Después del estudio de la biogénesis de GlyT2 a través de la ruta secretora temprana, quisimos investigar porqué el mutante de hiperplexia humana que presentaba retención intracelular descrito por el grupo de Robert Harvey (School of Pharmacy, London, UK) (Rees, Harvey et al. 2006), se manifestaba en los pacientes como DN del tráfico de GlyT2. Para ello, hemos realizado un análisis detallado de los mecanismos patogénicos. De nuevo, el sistema inicial de elección fue la expresión heteróloga en células COS7 que permite expresar con alta eficiencia transportadores mutantes obtenidos por mutagénesis sobre GlyT2 recombinante y evitar interferencias con GlyT2 endógeno. La coexpresión de transportadores silvestre y mutante se utilizó como una aproximación a mimetizar la condición en el paciente portador de los alelos mutado y silvestre. Se utilizó la secuencia de GlyT2 de rata S512R (equivalente a la mutación humana S510R) debido a que las herramientas disponibles en el laboratorio como anticuerpos etc. son más convenientes que las de humano, pero todos los efectos descritos se han comprobado en el mutante de GlyT2 humano que es incluso más sensible a la mutación y al efecto descrito. En estas condiciones, hemos demostrado que S512R frena la progresión del tipo silvestre atenuando su expresión en membrana y actividad de transporte y que este efecto DN es específico de S512R sobre el tráfico GlyT2. Esta actuación verifica la definición clásica de DN donde polipéptidos mutantes sobreexpresados alteran la actividad del gen de tipo silvestre. En la bibliografía, hay muchos precedentes para este tipo de comportamiento, el oncogén p53 (Willis, Jung et al. 2004), mutantes para el cotransportador K-Cl (Ding, Ponce-Coria et al. 2013), mutantes para el receptor de la hormona de liberación de gonadotropina (Knollman, Janovick et al. 2005) podrían ser ejemplos de mutaciones dominante negativas que ocurren naturalmente (Veitia 2007).

S512R es un mutante con plegamiento defectuoso que no progresa por la vía secretora sino que queda retenido en RE y no da lugar a transportador maduro. Su procesamiento se detiene después de recibir el oligosacárido inicial que es susceptible de eliminación de glucosas (*trimming*) para producir FMG y entrar en el ciclo CNX/CRT. Por ello, como revelamos usando técnicas inmunoquímicas, S512R es un sustrato preferido de CNX semejante a lo descrito para mutantes de rodopsina (Noorwez, Sama et al. 2009). La retención de S512R se debe a la arginina introducida y no a la pérdida de la serina, pues la misma sustitución en la posición contigua N511 genera el mismo fenotipo. Esta región del TM7 contiene residuos cruciales en la coordinación de Na^+ y Cl^-, por lo que se han descrito otras sustituciones deletéreas cercanas en pacientes de hiperplexia (N511S y S515I,

respectivamente)(Carta, Chung et al. 2012). Sin embargo, nuestros datos indican que solo la introducción de aminoácidos cargados y grandes como la arginina produce plegamiento inadecuado. Podría especularse que la mutación generase la exposición de parches hidrofóbicos en la proteína que favoreciesen la unión a CNX con la consiguiente retención en RE. Estos resultados están de acuerdo con datos bibliográficos que indican que CNX tiene una asociación más prolongada y estable con moléculas mutantes de plegamiento incorrecto y una más transitoria con intermediarios silvestres (Gong, Jones et al. 2006). En el artículo #1 pudimos verificar esta afirmación comprobando que el mutante sin azúcares (N1234D) tiene una unión mucho más prolongada a CNX que el precursor de GlyT2. En el caso de S512R, también hay una dilatada unión a CNX lo que, junto con la implicación de CNX en la vía de degradación ERAD de proteínas glicosiladas, sugiere que es un sustrato preferente de ERAD (Ushioda, Hoseki et al. 2013). De hecho, la mayor intensidad de ubiquitinación y menor tiempo de vida media de S512R frente al tipo silvestre apoyan esta hipótesis.

El cristal del transportador de dopamina de *Drosophila melanogaster* resuelto recientemente (Penmatsa, Wang et al. 2013), propone que la serina homóloga a la S512 está situada en una hendidura entre el TM5 y TM7 donde aparece unida una molécula de colesterol. Se podría especular que la mutación S512R podría estar perturbando la unión de colesterol al transportador. Teniendo en cuenta que DAT, al igual que GlyT2, tiene óptima actividad en balsas lipídicas (*lipid rafts*)(Nunez, Alonso-Torres et al. 2008; Hong and Amara 2010) y que la unión de colesterol se ha propuesto podría estar estabilizando la conformación abierta hacia fuera (*outward-facing conformation*) del transportador, una mutación en esta región podría producir una importante alteración del plegamiento y/o transporte. No obstante, tras la cristalización del transportador de serotonina humano (hSERT), esta hipótesis ha perdido fuerza pues aunque SERT también es modulado por *lipid rafts* (Scanlon, Williams et al. 2001; Magnani, Tate et al. 2004) en el nuevo cristal de hSERT la molécula de colesterol se sitúa cerca del TM12a y no cerca de la S512 (Coleman, Green et al. 2016). En nuestras preparaciones, el tratamiento con metilbetaciclodextrina o la adición de colesterol no nos han permitido identificar el efecto sobre el mutante ya que la alteración de los niveles de colesterol causa estrés y compromete la función del RE (Ron and Walter 2007). Por ello, esta hipótesis deberá ser analizada en un sistema diferente como membranas aisladas o proteoliposomas. Otro dato derivado del cristal de DAT es una conexión entre la región TM5-TM7 y el sitio de unión al sustrato a través del movimiento del TM1a, implicado en el ciclo de transporte, en respuesta a la unión de colesterol. Quizá este movimiento del TM1a podría suceder como consecuencia de la mutación S512R. A su vez, también se predice que TM1a, conectado con el IL1, podría modular el extremo C-terminal del transportador y afectar a la actividad de transporte. Esta última circunstancia se ha comprobado recientemente

en SERT donde el extremo C-terminal facilita el plegamiento del transportador por su conexión con el IL1 a través de un puente salino (Koban, El-Kasaby et al. 2015) y por acoplamiento a distintas chaperonas citosólicas (El-Kasaby, Koban et al. 2014).

Un aspecto más estudiado es la intervención del extremo C-terminal en la exportación de proteínas desde el RE al Golgi. Está bien documentado para SERT y otros miembros de la familia de transportadores SLC6, que el extremo C-terminal tiene un motivo conservado (RI o RL) de unión para las distintas isoformas de Sec24, componente que recluta proteínas cargo para la formación de vesículas COPII que permiten la exportación del RE al Golgi (Sucic, El-Kasaby et al. 2011; Sucic, Koban et al. 2013) (Farhan, Reiterer et al. 2007; Fernandez-Sanchez, Diez-Guerra et al. 2008; El-Kasaby, Just et al. 2010; Sucic, Koban et al. 2013). En GlyT2, distintos mutantes de deleción del extremo C-terminal se quedan retenidos en RE (Fernandez-Sanchez, Diez-Guerra et al. 2008). Nuestro resultado de coinmunopreciptación de GlyT2 con Sec24D ha demostrado que el mutante S512R tiene una alteración estructural que reduce su unión a este componente. Aunque estas observaciones deben ser confirmadas en preparaciones neuronales, proponemos que S512R provoca una distorsión estructural en la región que puede ser transmitida al C-terminal perturbando el plegamiento y la unión a Sec24D. Sin embargo, estos dos aspectos pueden no estar asociados como se ha demostrado en SERT, donde la hélice anfipática C-terminal es necesaria para el plegamiento pero no para la exportación del RE, y por lo tanto no para la unión de Sec24, aunque SERT requiere la isoforma Sec24C en lugar de Sec24D como GlyT2 (Koban, El-Kasaby et al. 2015).

En este estudio, también hemos demostrado que las subunidades mutantes S512R forman heterómeros con GlyT2 silvestre. Para ello se incluyeron etiquetas diferenciales en el N-terminal de cada transportador (lo que no afectó a su llegaba a membrana ni a su capacidad de transporte) y se logró la coinmunoprecipitación de las formas de RE. Se comprobó que la estabilidad de los oligómeros mixtos S512R/GlyT2 es mayor que la de los homoligómeros de GlyT2 lo que hace que el tipo silvestre quede retenido en el RE y explica el efecto DN sobre el tráfico de GlyT2. Este trabajo, junto con el artículo#4, constituye la primera evidencia *in vivo* de que GlyT2 tiene estructura cuaternaria pues, aunque se ha postulado la necesidad de una adecuada oligomerización como requisito imprescindible para la salida del RE en otros transportadores de la familia (Chiba, Freissmuth et al. 2014), para GlyT2 solo existían datos *in vitro* (Bartholomaus, Milan-Lobo et al. 2008). En este trabajo previo se habían detectado formas oligoméricas de GlyT2 y GlyT1 tras entrecruzamiento oxidativo de mutantes a cisteína (T464C en GlyT2 y L343C en GlyT1). En DAT, la reintroducción de las Cys-243 y Cys-306 en un mutante *Cys-less* y posterior crosslinking genera un patrón de tetrámero, trímero y dímero indistinguible del tipo silvestre protegiéndose por inhibidores y sin ningún efecto por sustratos (Hastrup,

Sen et al. 2003). No obstante, el uso de reactivos entrecruzantes para el mantenimiento del ensamblaje en condiciones desnaturalizantes, podría estar muy alejado de la realidad. Por esta razón, resulta clave conocer la estructura cuaternaria en condiciones no desnaturalizantes. Para la visualización del transportador en condiciones nativas, hemos puesto a punto la técnica *Blue Native PAGE* (BN-PAGE) e iniciado un estudio para caracterizar las formas oligoméricas de GlyT2 y establecer la interfase de oligomerización. Para ello contamos con herramientas bioinformáticas como son los modelos del transportador dimérico realizados sobre la estructura de LeuTa y posteriormente sobre la de dDAT. Los datos preliminares indican que GlyT2 forma tetrámeros y dímeros y que la interfase de oligomerización entre ambos está sustentada por diferente tipo de interacciones. La asociación tetramérica es sensible a DTT, lo que sugiere que esta interfase está mediada por puentes disulfuro. La asociación entre dímeros no es sensible a DTT, lo que indica que esta interfase se sustenta por otro tipo de interacciones. Puesto que GlyT2 tiene 22 cisteínas de las que ocho se encuentran en localización superficial, hemos emprendido la búsqueda de las cisteínas implicadas mediante evaluación de la capacidad de oligomerización de mutantes de las cisteínas de interés de GlyT2 (Ver anexo Artículo #5 Arribas-González E. et. al, en preparación). Este trabajo permitirá abordar el análisis del papel de los multímeros en más procesos celulares. En la actualidad, se asume que cada monómero es activo pero se desconoce la contribución de la estructura cuaternaria a la actividad de transporte. En DAT, la afinidad por el ligando parece estar determinada por la combinación de protómeros concretos (Zhen, Antonio et al. 2015).

Finalmente, un aspecto relevante recogido en el artículo #2 es que la sobreexpresión CNX puede rescatar el efecto DN al aumentar la cantidad de GlyT2 de tipo silvestre que llega a la membrana plasmática y atenuar la interacción entre los transportadores silvestres y mutantes. Esto sugiere que ambos transportadores compiten por la unión a la chaperona. Sin embargo, debido a que el mutante tiene una unión más persistente a CNX que GlyT2, el rescate alcanzado refuerza la evidencia obtenida en el artículo #1 de que CNX reconoce distintos estados conformacionales de los transportadores y facilita la expresión en superficie de la conformación más adecuada para el transporte.

Los resultados obtenidos aportan las bases moleculares por las que se establece el efecto DN en los pacientes que portan esta mutación. Asimismo, hemos demostrado que este efecto puede ser revertido por sobrexpresión de CNX constituyendo una molécula diana para otros mutantes de hiperplexia con defectos de tráfico.

3. Rescate de mutantes mediante chaperonas químicas que estabilicen su plegamiento una vez reconocida la alteración estructural y el defecto de biosíntesis que presentan.

El descubrimiento de chaperones químicas como moléculas que, emulando la función clásica ejercida por chaperonas moleculares endógenas, son capaces de estabilizar proteínas mutantes y acelerar su tráfico a la superficie de modo no selectivo, ha supuesto una posible estrategia para muchas patologías asociadas a mutaciones que causan mal plegamiento o estrés de RE (Cortez and Sim 2014). El reto para que estos compuestos puedan ser agentes terapéuticos es conseguir especificidad por la molécula diana y encontrar chaperonas farmacológicas selectivas para un trastorno en particular. Un ejemplo de ello es un reciente estudio en el que se consigue mediante la estabilización de proteínas α-cristalinas una recuperación parcial de las cataratas (Makley, McMenimen et al. 2015). Con este objetivo, hemos investigado si GlyT2 podía ser rescatado del efecto DN producido por su coexpresión con el mutante S512R probando una selección de chaperonas químicas en células en cultivo y en neuronas corticales transfectadas. Al igual que sucede con la sobreexpresión de CNX, ningún compuesto recupera al mutante expresado en solitario. Sin embargo, la influencia de estos compuestos sobre el efecto DN permite especular sobre las condiciones requeridas para el correcto plegamiento de GlyT2. Los compuestos que alteran la concentración de calcio en RE como la tapsigargina que lo aumenta o el diltiazem que lo reduce, no parecen afectar demasiado a su plegamiento. Por el contrario, se observa un notable incremento de la actividad de GlyT2 utilizando el compuesto antioxidante DMSO, lo cual correlaciona positivamente con el elevado número de cisteínas presentes en GlyT2. Glicerol, taurina y betaína promueven un rescate significativo al tratarse de compuestos osmóticamente activos que presumiblemente podrían reducir el estrés de RE. Por ello, se exploró si la coexpresión de S512R con GlyT2 producía estrés de RE y, aunque no detectamos inducción de PERK a su estado fosforilado (Teske, Wek et al. 2011), sí observamos incremento en BiP lo que indica que tanto el mutante solo como coexpresado con el tipo silvestre induce un modo suave de UPR. Esto contrasta con el efecto de compuestos como activadores del proteasoma o inhibidores de la agregación para los que no observamos inducción de UPR. Estos datos requieren el estudio en un sistema más próximo al endógeno como neuronas primarias o cortes de tejido nervioso, por lo que estamos desarrollando la infección con lentivirus para expresión de los transportadores. Por otro lado, la coexpresión de

GlyT2 y S512R no produce agresomas, como se demostró mediante inmunodetección del marcador de agresomas vimentina, ni tampoco induce autofagia, lo que se probó mediante tratamiento con trehalosa, un inductor de la autofagia (Johnston, Ward et al. 1998), aunque estos resultados habrán de ser verificados en neuronas.

Imitando la función de chaperona de CNX, se analizó el efecto de otras chaperonas químicas en el rescate de GlyT2. El compuesto ácido 4-fenilbutírico (PBA) aprobado por la *Food Drug Administration* (FDA) para su uso clínico en humanos promovió un rescate significativo y restauró tanto la expresión de membrana como el transporte de glicina del GlyT2 activo co-expresado con el mutante en células heterólogas y neuronas corticales transfectadas. PBA ha demostrado actividad chaperona para otras proteínas mal plegadas como en CFTR (Loffing, Moyer et al. 1999), el transportador aniónico orgánico MRP1(ABCC1)(Iram and Cole 2012), el transportador *ATP-binding cassette transporter A1*(Sorrenson, Suetani et al. 2013). A la concentración óptima de 1mM PBA no mostró efectos tóxicos y es un compuesto interesante ya que puede pasar a través de la barrera hematoencefálica superando un fuerte impedimento para la acción de muchos fármacos. PBA se ha catalogado como agente protector en algunas enfermedades neurodegenerativas que implican estrés en RE (Leidenheimer and Ryder 2014). En pacientes de hiperplexia, cabe especular que PBA podría rescatar el efecto DN de mutantes de GlyT2 heredados en heterocigosis acelerando el tráfico a membrana de GlyT2 y afectando positivamente a la neurotransmisión glicinérgica. Además, nuestros resultados apoyan la posibilidad de que nuevas farmacoferonas selectivas puedan tener efectos terapéuticos en hiperplexia. Sin embargo, es necesario realizar experimentos *in vivo* por ejemplo con ratones transgénicos *knockin* para la mutación donde la inyección del compuesto o una dieta suplementada con 4-PBA confirme esta hipótesis.

4. Detección de nuevas proteínas que interaccionen con GlyT2 y puedan modular su tráfico y actividad.

El análisis de los péptidos detectados por espectometría de masas tras inmunoprecipitación de GlyT2 de médula espinal de rata, está permitiendo identificar posibles proteínas candidatas a interactuar con GlyT2 que podrían modular entre otras funciones, su localización celular, conformación molecular o actividad. Así, un estudio previo realizado en el laboratorio ha establecido que GlyT2 interacciona con las subunidades catalíticas α de la Na/K ATPasa (NKA) en *lipid rafts*, principalmente con la isoforma específica de neuronas α3NKA. Estas subunidades al actuar como receptores específicos de ouabaína activan mecanismos de señalización que inducen la endocitosis y degradación de la población activa de GlyT2 asociado a *lipid rafts*

en neuronas *in vitro*. Además, se comprobó que la regulación de GlyT2 a través de la NKA ocurre *in vivo* en embriones de pez cebra tras la administración de ouabaína en el medio acuático y en rata adulta tras su administración intramedular en cordón espinal, demostrando la importancia de este control de la neurotransmisión glicinérgica inhibidora conservado evolutivamente (de Juan-Sanz, Nunez et al. 2013).

Otros péptidos obtenidos en el estudio proteómico han correspondido a la bomba de calcio de membrana plasmática (PMCA) que funciona en contra del gradiente electroquímico de Ca^{2+} exportando el catión a expensas de una molécula de ATP y el intercambiador de Na^{+} y Ca^{2+} (NCX), que intercambia 3 iones sodio por uno de calcio a través de la membrana, generalmente a favor de gradiente electroquímico de sodio. Mediante el empleo de un conjunto de técnicas inmunoquímicas se han confirmado los datos proteómicos iniciales y se ha establecido que GlyT2 asocia y colocaliza con las isoformas neuronales PMCA2 y PMCA3 pero no con la ubicua PMCA4. Estos datos implican claramente a GlyT2 en la homeostasis del calcio bien a nivel de gradientes electroquímicos o quizá en señalización, pues estas bombas se localizan pre y postsinápticamente y controlan los niveles de Ca^{2+} necesarios para mecanismos reguladores dependientes de calcio (Garside, Turner et al. 2009; Boczek, Lisek et al. 2012). La interacción de GlyT2 con NCX, un intercambiador ubicuo de Na^{+} y Ca^{2+} distribuido a lo largo del SNC, crucial para el mantenimiento de la homeostasis intracelular de Ca^{2+} y Na^{+} (Brini and Carafoli 2011), apoya esta hipótesis y sugieren un complejo funcional donde el gradiente electroquímico de Na^{+} necesario para el correcto funcionamiento de GlyT2 estaría acoplado a NCX y PMCA, participantes clave en la homeostasis de Ca^{2+} y Na^{+} en microdominios específicos de membranas presinápticas glicinérgicas.

Mediante triple colocalización de GlyT2-PMCA2/3-NCX1 con el marcador de dominios raft Thy-1 se demostró que, al igual que sucede con la interacción GlyT2-NKA, estas interacciones están predominantemente presentes en *lipid rafts* donde la actividad de GlyT2 es óptima (Nunez, Alonso-Torres et al. 2008). Esto es una prueba irrefutable del carácter señalizador de la interacción pues la compartimentación de membrana favorece la interacción entre poblaciones activas de los tres candidatos proporcionando una homeostasis local presináptica de sodio y calcio durante el ciclo de transporte de glicina al interior del terminal. PMCA2/3 y NCX son las únicas proteínas de membrana plasmática responsables de la extrusión de calcio en la sinapsis y trabajan juntas en la recuperación de los niveles basales de Ca^{2+} en pequeños compartimentos de los terminales axónicos. Operan con características funcionales complementarias, mientras que PMCA2 tiene alta afinidad por calcio pero baja capacidad de transporte, NCX muestra una baja afinidad por el ion y gran capacidad para transportarlo. Aunque en condiciones basales, NCX transporta $3Na^{+}$

al interior y saca $1Ca^{2+}$ al citosol funcionando en su modo directo (Blaustein, Juhaszova et al. 2002), bajo ciertas condiciones fisiológicas como actividad neuronal o como respuesta a un incremento del Na^+ intracelular puede funcionar en su modo reverso expulsando Na^+ e introduciendo Ca^{2+} al interior celular (Roome and Empson 2013; Roome, Power et al. 2013). La reducción en el transporte causado por caloxina2a1 y KB-mes, inhibidores específicos de PMCA y NCX respectivamente, sugiere que la actividad de GlyT2 se ve afectada por cambios locales en los gradientes de Na^+ y Ca^{2+} que conducen a una reducción en el gradiente electroquímico de Na^+, fuerza necesaria para el transporte de glicina. Una regulación homeostática similar ha sido propuesta para otras proteínas como el intercambiador Na^+/Ca^{2+} y el receptor AMPA en neuronas corticales (Goldberg, Tamas et al. 2003) y la interacción de PMCA2 con el receptor nicotínico de acetilcolina en interneuronas de hipocampo (Gomez-Varela, Schmidt et al. 2012). Por tanto, parece frecuente que las isoformas de PMCA participen en complejos multiproteicos en la superficie celular. PMCA2 interactúa presinápticamente con sintaxina-1A y postsinápticamente con la proteína *scaffold* PSD95 (Garside, Turner et al. 2009). Estudios previos en nuestro laboratorio, identificaron que la interacción GlyT2-sintaxina-1A regulaba la cantidad de GlyT2 en la membrana plasmática presináptica como respuesta a un rápido incremento de Ca^{2+} durante la actividad neuronal (Geerlings, Nunez et al. 2001). Por tanto, GlyT2, sintaxina-1A y PMCA2 podrían estar formando un complejo proteico presináptico durante la liberación del neurotransmisor regulando la actividad y expresión en superficie del transportador. De hecho, las interacciones descritas para GlyT2 con sintaxina-1A, NKA, PMCA y NCX podrían ocurrir dentro del mismo complejo presináptico. De hecho, se ha detectado que NCX interacciona con NKA y esta interacción, regulada por la composición lipídica, es crucial en el acoplamiento y regulación del Ca^{2+}intracelular local (Matchkov, Gustafsson et al. 2007).

En la figura11A del artículo #3 se presenta un diagrama representativo de la regulación que proponemos. La unión de GlyT2 a PMCA2/3 y NCX en *lipid rafts* ayuda a mantener la homeostasis local de Na^+ y Ca^{2+} durante la actividad de GlyT2 en condiciones de alta demanda. Tras la liberación del neurotransmisor y la consecuente actividad de GlyT2, la alteración del gradiente de Na^+ debe recuperarse. En condiciones normales, el flujo de sodio es contrarrestado con la NKA, pero esta bomba puede verse saturada en situaciones de alta demanda debido a su baja velocidad de transporte. En situación de alta actividad de GlyT2, NCX podría localmente operar en su modo reverso expulsando $3Na^+$ por cada $1Ca^{2+}$ introducido y la PMCA completaría el complejo funcional exportando el Ca^{2+} para mantener su gradiente.

Nuestros resultados sugieren que este complejo, cuyo acoplamiento funcional es perfecto y está presente en terminales presinápticos, podría representar un mecanismo regulador que permite a GlyT2 trabajar en condiciones de alta demanda.

5. Identificación y caracterización de una nueva mutación en pacientes de hiperplexia humana.

Mediante la secuenciación de los 16 exones del gen de GlyT2 humano (*SLC6A5*) de muestras de 16 pacientes de hiperplexia proporcionadas por el Dr. Pablo Lapunzina de la Unidad de Genética del Hospital Universitario La Paz, identificamos una nueva mutación no descrita hasta el momento, presente en tres de los pacientes diagnosticados con la enfermedad originarios de España y Reino Unido. La nueva mutación A2114G, que no se encontró en el análisis de 200 genomas de individuos control, se localizó en el exón 15 y es responsable de la sustitución Y705C en el TM11 de GlyT2. El cambio se encontró en heterocigosis, lo que sugiere un genotipo dominante. Esto contrasta con la mayoría de las mutaciones descritas hasta el momento en el gen *SLC6A5* en pacientes de hiperplexia que se encuentran, bien en homocigosis o bien en heterocigosis compuesta, a excepción de la dominante negativa del tráfico estudiada en el artículo #2 (Eulenburg, Becker et al. 2006; Rees, Harvey et al. 2006).

Con estos antecedentes, un objetivo inicial de esta tesis doctoral fue la caracterización del mutante Y705C. El análisis de las propiedades bioquímicas del mutante en células COS7, reveló que la cisteína introducida afecta a varios aspectos de la función del transportador explicando así la significativa variabilidad en la presentación clínica de los pacientes. En el artículo #4 se ha demostrado que esta mutación afecta a la maduración del transportador a través de la ruta secretora y que, además, manifiesta una alteración de la dependencia de protones y zinc en su actividad de transporte. Esto revela una nueva modulación de la actividad de GlyT2 desconocida hasta la fecha. La respuesta a los cambios de pH cuando tipo silvestre y mutante están presentes, se asemeja a la detectada en el mutante, lo que indica el carácter dominante de la dependencia de protones del mutante sobre la actividad de GlyT2. Mediante reactivos específicos de grupos SH no permeables se ha confirmado que la cisteína introducida es accesible desde el exterior de la membrana plasmática. Asimismo, el tratamiento con agentes reductores como DTT consigue la exposición de algunas cisteínas, como predice el modelado molecular de GlyT2 (Perez-Siles, Morreale et al. 2011) y produce recuperación de la función de Y705C con aumento en sus niveles en superficie y su actividad de transporte. Esto es debido a que la cisteína introducida

por la mutación frena la biogénesis de este mutante como refleja la mayor proporción de forma inmadura respecto al tipo silvestre y, por tanto, su llegada a la superficie es menor. En la bibliografía se ha descrito que las cisteínas que se añaden en bucles extracelulares distorsionan la expresión de receptores acoplados a proteínas G y otras proteínas de membrana plasmática (Petaja-Repo, Hogue et al. 2002; Leskela, Markkanen et al. 2009; Williams, Reed et al. 2009). La recuperación de la función por DTT suscitó la idea que la cisteína introducida en el mutante formase un puente disulfuro con alguna de las 23 cisteínas restantes de GlyT2 y afectase negativamente a su tráfico y/o función. De hecho, el marcaje de cisteínas demostró que el mutante tiene un mayor número de puentes disulfuro que el tipo silvestre. Los transportadores de la familia SLC6 tienen un puente disulfuro conservado en el EL2 verificado en diversos cristales (Penmatsa, Wang et al. 2013; Coleman, Green et al. 2016), que en GlyT2 se produce entre el par C311-C320 (Chen, Liu-Chen et al. 1997; Chen, Wei et al. 2007). Por otro lado, los puentes disulfuro extracelulares suelen ser cruciales para mantener el plegamiento, ensamblaje y la correcta función de muchas proteínas como la fosfatasa alcalina sérica (Satou, Al-Shawafi et al. 2012). El marcaje de superficie de mutantes de las cisteínas del par se vio alterado por la presencia de la cisteína en 705, lo que indicó que la sustitución Y705C perturba el puente disulfuro endógeno del EL2. Estos datos están en consonancia con los cambios conformacionales descritos en la conformación hacia dentro (*inward-facing conformation*) donde se aproxima el EL2 al TM11 en el modelo de LeuT (Krishnamurthy and Gouaux 2012).

La diferente sensibilidad del tipo silvestre y mutante a bajas concentraciones de DTT, sugiere que el enlace disulfuro aberrante formado por el mutante es más receptivo a la disociación por el agente reductor que el puente disulfuro endógeno. Por tanto, la recuperación del mutante Y705C por DTT podría ser debida a la ruptura del puente disulfuro aberrante sin afectar al puente disulfuro endógeno. Estos datos sintonizan con que GlyT2 requiera la dimerización mediada por puentes disulfuro para la expresión en la superficie celular como ha sido descrita para otros transportadores SLC6 (Chen, Wei et al. 2007). Como se ha indicado con anterioridad, nuestros datos usando la técnica de *Blue Native-PAGE*, confirman este punto.

6. Estudio de la regulación de GlyT2 por moduladores de la neurotransmisión glicinérgica: pH y zinc.

Otro aspecto diferencial del mutante Y705C es que introduce una carga negativa local en la superficie del transportador. A pH fisiológico, tanto la Tyr-705 como la

Cys-705 estarán principalmente protonadas (pKa 10.3 y 8.3 respectivamente) pero la probabilidad de ionización en el caso del mutante es mayor. Además, un medio con alta constante dieléctrica (Dudev and Lim 2002) y la presencia de metales de transición dicatiónicos son factores que favorecen la desprotonación de cisteínas extracelulares como la Cys-705. En estas condiciones, si la Cys-705 está desprotonada, la forma protonada se vería favorecida por pH ácido.

La resistencia del mutante a la inhibición del transporte por pH ácido, sugiere que la cisteína introducida en 705 puede aceptar un protón en estas condiciones e interferir en la dependencia de protones del transportador silvestre, que podría implicar a la Tyr-705. La regulación por H^+ de algunos receptores suele implicar un residuo con un grupo hidroxilo como tirosinas o treoninas. Se han encontrado residuos de treonina en posiciones equivalentes en receptores GlyR, $GABA_a$ y $GABA_c$ sensibles a pH así como posiciones equivalentes a Tyr-705 en algunos miembros de la familia de transportadores SLC6, sugiriendo que este residuo podría tener un papel general en la modulación por protones de la actividad del transportador (Chen, Dillon et al. 2004).

Generalmente, los sitios de unión de protones y metales dicatiónicos de transición suelen ser compartidos y solapantes en proteínas sensibles a pH y Zn^{2+} (Ju, Aubrey et al. 2004; Hirzel, Muller et al. 2006; Toth 2011). El residuo Thr-112 en GlyR parece ser crucial tanto para la unión de H^+ como para Zn^{2+} y en varias proteínas de membrana presentes en sinapsis inhibidoras los sitios de unión para H^+/Zn^{2+} están constituidos por subunidades adyacentes (Krishtal 2003; Jasti, Furukawa et al. 2007). El receptor canónico NMDA formado por NR1/NR2 es fuertemente inhibido por concentraciones extracelulares elevadas de H^+ y Zn^{2+} (Traynelis, Wollmuth et al. 2010), mientras que, sorprendentemente, en los formados por NR1/NR3 la acidificación extracelular y el zinc producen una potenciación de las corrientes de glicina reduciendo su desensibilización. Ello ha sugerido la existencia de un nuevo sitio alostérico para la unión a H^+ (Cummings and Popescu 2016). Aunque inicialmente se propuso que el Zn^{2+} inhibía la actividad de DAT (Loland, Norregaard et al. 1999), parece que la concentración intracelular de Na^+ determina si el Zn^{2+} produce inhibición o activación, y a concentraciones intracelulares fisiológicas de Na^+ el transporte se activa (Li, Hasenhuetl et al. 2015). Recientemente, se ha comprobado que la unión del Zn^{2+} produce efectos bifásicos en DAT (1μM estimulación, 10μM inhibición), lo que representa una modulación alostérica de interés en mutantes con pérdida de función. Además, este modelo cinético predice una unión preferente de los metales de transición a la *outward-facing conformation* de DAT con un efecto estimulador o inhibidor del Ni^{2+} y Cu^{2+} respectivamente (Li, Mayer et al. 2017). En consecuencia, la alteración en la dependencia por H^+ y Zn^{2+}

en el mutante Y705C podría ser debida a una distorsión del sitio clásico de unión o afectar a este nuevo sitio alostérico de estos moduladores.Este aspecto requiere un estudio más profundo.

Otra interesante relación que ha sido planteada es entre oligomerización y cambios en el pH. El tetrámero y el dímero de la transtiretina (o prealbúmina) son menos estables que el monómero a medida que el pH se acidifica, lo que se ha sugerido podría ser extensible a otras proteínas (Skoulakis and Goodfellow 2003). Esta relación debería estudiarse para GlyT2 pues podría suceder que los heterómeros silvestre-Y705C tuvieran más estabilidad (al igual que ha quedado demostrado en el artículo #2 para S512R), lo que podría explicar la respuesta dominante a los protones generada por Y705C. No obstante, es importante destacar que la caracterización del mutante Y705C se ha llevado a cabo en un sistema celular (COS7) que podría estar alejado de las condiciones presentes *in vivo* en los pacientes. Así, estos datos deben ser confirmados en un sistema neuronal donde podría aumentar su carácter patogénico, a través de su interacción con otras proteínas de andamiaje o moduladoras, posibilidad que será abordada en el laboratorio en el futuro. De hecho, un trabajo reciente ha demostrado que el silenciamiento de las PMCA2/3 afecta a la homeostasis del pH celular produciendo elevaciones de Ca^{2+} citosólico (Boczek, Lisek et al. 2014). Por ello, un abordaje futuro sería reproducir la resistencia a la inhibición por pH ácido del mutante Y705C en un sistema neuronal donde están presentes las isoformas PMCA2/3 y evaluar si el efecto se acentúa a través de la interacción con PMCA2/3 descrita en el artículo #3.

Actualmente, a partir del vector de expresión dual *pLOX-Syn-DSRED-Syn-GFP* (Gascon, Paez-Gomez et al. 2008) (cedido por el Profesor Francisco Gómez-Scholl, Universidad de Sevilla) hemos generado partículas lentivirales *Syn-**hGlyT2**-Syn-GFP* y/o *Syn-**Y705C**-Syn-GFP* que infectan específicamente neuronas dentro del cultivo primario y permiten expresar mutantes de hiperplexia en sistema neuronales para caracterizar su efecto sobre la neurotransmisión glicinérgica (trabajo en preparación).

En definitiva, el conjunto de los resultados expuestos en esta tesis doctoral ha contribuido a aumentar el conocimiento sobre los mecanismos de tráfico intracelular del transportador neuronal de glicina GlyT2 y su regulación. Esta información permitirá la comprensión de las mutaciones en el gen *SLC6A5* que presentan defectos de tráfico y son causantes de hiperplexia humana. Asimismo, se han descubierto nuevos componentes del interactoma de GlyT2, cuyo papel puede ser crucial para la modulación de la neurotransmisión glicinérgica inhibidora.

IV. Conclusiones

1-GlyT2 se sintetiza como un precursor intermediario de glicosilación inmaduro en el RE que va a dar lugar al transportador maduro funcional presente en membrana plasmática.

2-La biogénesis de GlyT2 es asistida por CNX que se une transitoriamente al precursor inmaduro a través de N-glicosilación e interacciones proteína-proteína.

3-Las variaciones en la concentración de CNX producidas mediante su depleción o sobreexpresión generan cambios opuestos en la expresión y transporte de GlyT2. CNX puede distinguir distintos estados conformacionales de GlyT2 mediante actividad chaperona independiente de lectina seleccionando los intermediarios de plegamiento funcionalmente más competentes del transportador.

4-El mutante de hiperplexia S512R ejerce un efecto DN sobre el tráfico de GlyT2 reduciendo su expresión en superficie y actividad. La introducción de la arginina y no la pérdida de la serina, provoca el mal plegamiento del transportador con una deficiente glicosilación, asociación aumentada a CNX y unión alterada a Sec24D, lo que genera retención en RE.

5-El efecto DN se produce por la formación en el RE de heterómeros comunes entre GlyT2-S512R de los que GlyT2 puede ser rescatado por sobreexpresión de CNX. Esto sugiere que existe competencia entre ambos por la unión a la chaperona. La expresión de CNX podría facilitar la expresión en superficie de mutantes de hiperplexia con defectos de tráfico.

6-PBA promueve un rescate significativo del efecto DN de S512R sobre GlyT2, restaurando la expresión en membrana y el transporte de glicina del tipo silvestre en neuronas. Este compuesto tiene potencial como agente terapéutico en pacientes de hiperplexia humana.

7-La interacción funcional y exclusiva en lipid rafts de GlyT2 con la ATPasa de calcio de membrana plasmática (PMCA2-3) y el intercambiador Na^+/Ca^{2+} (NCX), dos proteínas cruciales en la homeostasis del calcio intracelular, revela una nueva modulación de la actividad del transportador por calcio.

8-El mutante de hiperplexia Y705C altera el tráfico y las propiedades bioquímicas del transportador. La cisteína introducida genera un enlace disulfuro aberrante con dos cisteínas endógenas entorpeciendo su avance hacia la superficie celular de modo recesivo. Además, la dependencia del transporte de moduladores clave de la neurotransmisión glicinérgica como son el pH y el zinc está alterada en el mutante de modo dominante.

9-La interfase de oligomerización de GlyT2 está mediada por puentes disulfuro que implican cisteínas del TM9 y TM12.

V. Bibliografía

- Adams, R. H., K. Sato, et al. (1995). "Gene structure and glial expression of the glycine transporter GlyT1 in embryonic and adult rodents." J Neurosci 15(3 Pt 2): 2524-2532.
- Alfadhel, M., M. Nashabat, et al. (2016). "Mutation in SLC6A9 encoding a glycine transporter causes a novel form of non-ketotic hyperglycinemia in humans." Hum Genet 135(11): 1263-1268.
- Anderluh, A., T. Hofmaier, et al. (2017). "Direct PIP2 binding mediates stable oligomer formation of the serotonin transporter." Nat Commun 8: 14089.
- Anderluh, A., E. Klotzsch, et al. (2014). "Single molecule analysis reveals coexistence of stable serotonin transporter monomers and oligomers in the live cell plasma membrane." J Biol Chem 289(7): 4387-4394.
- Apparsundaram, S., S. Schroeter, et al. (1998). "Acute regulation of norepinephrine transport: II. PKC-modulated surface expression of human norepinephrine transporter proteins." J Pharmacol Exp Ther 287(2): 744-751.
- Aragon, M. C., C. Gimenez, et al. (1987). "Stoichiometry of sodium- and chloride-coupled glycine transport in synaptic plasma membrane vesicles derived from rat brain." FEBS Lett 212(1): 87-90.
- Armsen, W., B. Himmel, et al. (2007). "The C-terminal PDZ-ligand motif of the neuronal glycine transporter GlyT2 is required for efficient synaptic localization." Mol Cell Neurosci 36(3): 369-380.
- Aubrey, K. R. (2016). "Presynaptic control of inhibitory neurotransmitter content in VIAAT containing synaptic vesicles." Neurochem Int 98: 94-102.
- Aubrey, K. R., A. D. Mitrovic, et al. (2000). "Molecular basis for proton regulation of glycine transport by glycine transporter subtype 1b." Mol Pharmacol 58(1): 129-135.
- Aubrey, K. R. and R. J. Vandenberg (2001). "N[3-(4'-fluorophenyl)-3-(4'-phenylphenoxy)propyl]sarcosine (NFPS) is a selective persistent inhibitor of glycine transport." Br J Pharmacol 134(7): 1429-1436.
- Bakker, M. J., E. A. Peeters, et al. (2009). "Clonazepam is an effective treatment for hyperekplexia due to a SLC6A5 (GlyT2) mutation." Mov Disord 24(12): 1852-1854.
- Balch, W. E., R. I. Morimoto, et al. (2008). "Adapting proteostasis for disease intervention." Science 319(5865): 916-919.
- Balchin, D., M. Hayer-Hartl, et al. (2016). "In vivo aspects of protein folding and quality control." Science 353(6294): aac4354.
- Bartholomaus, I., L. Milan-Lobo, et al. (2008). "Glycine transporter dimers:

evidence for occurrence in the plasma membrane." J Biol Chem 283(16): 10978-10991.

- Benveniste, M. and M. L. Mayer (1991). "Kinetic analysis of antagonist action at N-methyl-D-aspartic acid receptors. Two binding sites each for glutamate and glycine." Biophys J 59(3): 560-573.
- Bernier, V., M. Lagace, et al. (2004). "Pharmacological chaperones: potential treatment for conformational diseases." Trends Endocrinol Metab 15(5): 222-228.
- Bernier, V., J. P. Morello, et al. (2006). "Pharmacologic chaperones as a potential treatment for X-linked nephrogenic diabetes insipidus." J Am Soc Nephrol 17(1): 232-243.
- Betz, H. and B. Laube (2006). "Glycine receptors: recent insights into their structural organization and functional diversity." J Neurochem 97(6): 1600-1610.
- Blaustein, M. P., M. Juhaszova, et al. (2002). "Na/Ca exchanger and PMCA localization in neurons and astrocytes: functional implications." Ann N Y Acad Sci 976: 356-366.
- Boczek, T., M. Lisek, et al. (2014). "Plasma membrane Ca2+-ATPase isoforms composition regulates cellular pH homeostasis in differentiating PC12 cells in a manner dependent on cytosolic Ca2+ elevations." PLoS One 9(7): e102352.
- Boczek, T., M. Lisek, et al. (2012). "Downregulation of PMCA2 or PMCA3 reorganizes Ca(2+) handling systems in differentiating PC12 cells." Cell Calcium 52(6): 433-444.
- Boudanova, E., D. M. Navaroli, et al. (2008). "Dopamine transporter endocytic determinants: carboxy terminal residues critical for basal and PKC-stimulated internalization." Mol Cell Neurosci 39(2): 211-217.
- Brini, M. and E. Carafoli (2011). "The plasma membrane Ca(2)+ ATPase and the plasma membrane sodium calcium exchanger cooperate in the regulation of cell calcium." Cold Spring Harb Perspect Biol 3(2).
- Brockmeier, A. and D. B. Williams (2006). "Potent lectin-independent chaperone function of calnexin under conditions prevalent within the lumen of the endoplasmic reticulum." Biochemistry 45(42): 12906-12916.
- Brodsky, J. L. (2012). "Cleaning up: ER-associated degradation to the rescue." Cell 151(6): 1163-1167.
- Broer, S. and U. Gether (2012). "The solute carrier 6 family of transporters." Br J Pharmacol 167(2): 256-278.
- Burrows, J. A., L. K. Willis, et al. (2000). "Chemical chaperones mediate increased secretion of mutant alpha 1-antitrypsin (alpha 1-AT) Z: A potential pharmacological strategy for prevention of liver injury and emphysema

in alpha 1-AT deficiency." Proc Natl Acad Sci U S A 97(4): 1796-1801.

- Cai, G., P. S. Salonikidis, et al. (2005). "The role of N-glycosylation in the stability, trafficking and GABA-uptake of GABA-transporter 1. Terminal N-glycans facilitate efficient GABA-uptake activity of the GABA transporter." FEBS J 272(7): 1625-1638.
- Cameron, P. H., E. Chevet, et al. (2009). "Calnexin phosphorylation attenuates the release of partially misfolded alpha1-antitrypsin to the secretory pathway." J Biol Chem 284(50): 34570-34579.
- Carta, E., S. K. Chung, et al. (2012). "Mutations in the GlyT2 Gene (SLC6A5) Are a Second Major Cause of Startle Disease." J Biol Chem 287(34): 28975-28985.
- Ciplys, E., K. Sasnauskas, et al. (2011). "Overexpression of human calnexin in yeast improves measles surface glycoprotein solubility." FEMS Yeast Res 11(6): 514-523.
- Coe, H., K. Bedard, et al. (2008). "Endoplasmic reticulum stress in the absence of calnexin." Cell Stress Chaperones 13(4): 497-507.
- Coleman, J. A., E. M. Green, et al. (2016). "X-ray structures and mechanism of the human serotonin transporter." Nature 532(7599): 334-339.
- Conesa, A., D. Jeenes, et al. (2002). "Calnexin overexpression increases manganese peroxidase production in Aspergillus niger." Appl Environ Microbiol 68(2): 846-851.
- Cortez, L. and V. Sim (2014). "The therapeutic potential of chemical chaperones in protein folding diseases." Prion 8(2).
- Cubelos, B., C. Gimenez, et al. (2005). "Localization of the GLYT1 glycine transporter at glutamatergic synapses in the rat brain." Cereb Cortex 15(4): 448-459.
- Cummings, K. A. and G. K. Popescu (2016). "Protons Potentiate GluN1/GluN3A Currents by Attenuating Their Desensitisation." Sci Rep 6: 23344.
- Chen, J. G., S. Liu-Chen, et al. (1997). "External cysteine residues in the serotonin transporter." Biochemistry 36(6): 1479-1486.
- Chen, R., H. Wei, et al. (2007). "Direct evidence that two cysteines in the dopamine transporter form a disulfide bond." Mol Cell Biochem 298(1-2): 41-48.
- Chen, Z., G. H. Dillon, et al. (2004). "Molecular determinants of proton modulation of glycine receptors." J Biol Chem 279(2): 876-883.
- Chen, Z. and R. Huang (2007). "Identification of residues mediating inhibition of glycine receptors by protons." Neuropharmacology 52(8): 1606-1615.
- Chen, Z. L. and R. Q. Huang (2014). "Extracellular pH modulates GABAergic neurotransmission in rat hypothalamus." Neuroscience 271: 64-76.

- Cheong, N., M. Madesh, et al. (2006). "Functional and trafficking defects in ATP binding cassette A3 mutants associated with respiratory distress syndrome." J Biol Chem 281(14): 9791-9800.
- Chesler, M. (2003). "Regulation and modulation of pH in the brain." Physiol Rev 83(4): 1183-1221.
- Chiba, P., M. Freissmuth, et al. (2014). "Defining the blanks--pharmacochaperoning of SLC6 transporters and ABC transporters." Pharmacol Res 83: 63-73.
- Cho, J. A., X. Zhang, et al. (2014). "4-Phenylbutyrate attenuates the ER stress response and cyclic AMP accumulation in DYT1 dystonia cell models." PLoS One 9(11): e110086.
- Christianson, J. C. and Y. Ye (2014). "Cleaning up in the endoplasmic reticulum: ubiquitin in charge." Nat Struct Mol Biol 21(4): 325-335.
- Danbolt, N. C. (2001). "Glutamate uptake." Prog Neurobiol 65(1): 1-105.
- de Juan-Sanz, J., E. Nunez, et al. (2013). "Constitutive endocytosis and turnover of the neuronal glycine transporter GlyT2 is dependent on ubiquitination of a C-terminal lysine cluster." PLoS One 8(3): e58863.
- de Juan-Sanz, J., E. Nunez, et al. (2013). "Na+/K+-ATPase is a new interacting partner for the neuronal glycine transporter GlyT2 that downregulates its expression in vitro and in vivo." J Neurosci 33(35): 14269-14281.
- de Juan-Sanz, J., F. Zafra, et al. (2011). "Endocytosis of the neuronal glycine transporter GLYT2: role of membrane rafts and protein kinase C-dependent ubiquitination." Traffic 12(12): 1850-1867.
- Denzel, A., M. Molinari, et al. (2002). "Early postnatal death and motor disorders in mice congenitally deficient in calnexin expression." Mol Cell Biol 22(21): 7398-7404.
- DiAntonio, A. and L. Hicke (2004). "Ubiquitin-dependent regulation of the synapse." Annu Rev Neurosci 27: 223-246.
- Diaz, G. A., L. S. Krivitzky, et al. (2013). "Ammonia control and neurocognitive outcome among urea cycle disorder patients treated with glycerol phenylbutyrate." Hepatology 57(6): 2171-2179.
- Ding, J., J. Ponce-Coria, et al. (2013). "A trafficking-deficient mutant of KCC3 reveals dominant-negative effects on K-Cl cotransport function." PLoS One 8(4): e61112.
- Dohi, T., K. Morita, et al. (2009). "Glycine transporter inhibitors as a novel drug discovery strategy for neuropathic pain." Pharmacol Ther 123(1): 54-79.
- Dudev, T. and C. Lim (2002). "Factors governing the protonation state of

cysteines in proteins: an Ab initio/CDM study." J Am Chem Soc 124(23): 6759-6766.

- Duricka, D. L., R. L. Brown, et al. (2012). "Defective trafficking of cone photoreceptor CNG channels induces the unfolded protein response and ER-stress-associated cell death." Biochem J 441(2): 685-696.
- Dutertre, S., C. M. Becker, et al. (2012). "Inhibitory glycine receptors: an update." J Biol Chem 287(48): 40216-40223.
- El-Kasaby, A., H. Just, et al. (2010). "Mutations in the carboxyl-terminal SEC24 binding motif of the serotonin transporter impair folding of the transporter." J Biol Chem 285(50): 39201-39210.
- El-Kasaby, A., F. Koban, et al. (2014). "A cytosolic relay of heat shock proteins HSP70-1A and HSP90beta monitors the folding trajectory of the serotonin transporter." J Biol Chem 289(42): 28987-29000.
- Eulenburg, V., W. Armsen, et al. (2005). "Glycine transporters: essential regulators of neurotransmission." Trends Biochem Sci 30(6): 325-333.
- Eulenburg, V., K. Becker, et al. (2006). "Mutations within the human GLYT2 (SLC6A5) gene associated with hyperekplexia." Biochem Biophys Res Commun 348(2): 400-405.
- Farhan, H., M. Freissmuth, et al. (2006). "Oligomerization of neurotransmitter transporters: a ticket from the endoplasmic reticulum to the plasma membrane." Handb Exp Pharmacol(175): 233-249.
- Farhan, H., V. Reiterer, et al. (2007). "Concentrative export from the endoplasmic reticulum of the gamma-aminobutyric acid transporter 1 requires binding to SEC24D." J Biol Chem 282(10): 7679-7689.
- Fernandez-Sanchez, E., F. J. Diez-Guerra, et al. (2008). "Mechanisms of endoplasmic-reticulum export of glycine transporter-1 (GLYT1)." Biochem J 409(3): 669-681.
- Fernandez-Sanchez, E., J. Martinez-Villarreal, et al. (2009). "Constitutive and regulated endocytosis of the glycine transporter GLYT1b is controlled by ubiquitination." J Biol Chem 284(29): 19482-19492.
- Ferrari, D. M. and H. D. Soling (1999). "The protein disulphide-isomerase family: unravelling a string of folds." Biochem J 339 (Pt 1): 1-10.
- Forlani, G., E. Bossi, et al. (2001). "Mutation K448E in the external loop 5 of rat GABA transporter rGAT1 induces pH sensitivity and alters substrate interactions." J Physiol 536(Pt 2): 479-494.
- Fornes, A., E. Nunez, et al. (2008). "Trafficking properties and activity regulation of

the neuronal glycine transporter GLYT2 by protein kinase C." Biochem J 412(3): 495-506.

- Fornes, A., E. Nunez, et al. (2004). "The second intracellular loop of the glycine transporter 2 contains crucial residues for glycine transport and phorbol ester-induced regulation." J Biol Chem 279(22): 22934-22943.
- Forrest, L. R., Y. W. Zhang, et al. (2008). "Mechanism for alternating access in neurotransmitter transporters." Proc Natl Acad Sci U S A 105(30): 10338-10343.
- Foster, E., H. Wildner, et al. (2015). "Targeted ablation, silencing, and activation establish glycinergic dorsal horn neurons as key components of a spinal gate for pain and itch." Neuron 85(6): 1289-1304.
- Free, R. B., L. A. Hazelwood, et al. (2007). "D1 and D2 dopamine receptor expression is regulated by direct interaction with the chaperone protein calnexin." J Biol Chem 282(29): 21285-21300.
- Freeze, H. H. and C. Kranz (2010). "Endoglycosidase and glycoamidase release of N-linked glycans." Curr Protoc Protein Sci Chapter 12: Unit12 14.
- Garcia-Tardon, N., I. M. Gonzalez-Gonzalez, et al. (2012). "Protein kinase C (PKC)-promoted endocytosis of glutamate transporter GLT-1 requires ubiquitin ligase Nedd4-2-dependent ubiquitination but not phosphorylation." J Biol Chem 287(23): 19177-19187.
- Garside, M. L., P. R. Turner, et al. (2009). "Molecular interactions of the plasma membrane calcium ATPase 2 at pre- and post-synaptic sites in rat cerebellum." Neuroscience 162(2): 383-395.
- Gascon, S., J. A. Paez-Gomez, et al. (2008). "Dual-promoter lentiviral vectors for constitutive and regulated gene expression in neurons." J Neurosci Methods 168(1): 104-112.
- Gasnier, B. (2004). "The SLC32 transporter, a key protein for the synaptic release of inhibitory amino acids." Pflugers Arch 447(5): 756-759.
- Geerlings, A., B. Lopez-Corcuera, et al. (2000). "Characterization of the interactions between the glycine transporters GLYT1 and GLYT2 and the SNARE protein syntaxin 1A." FEBS Lett 470(1): 51-54.
- Geerlings, A., E. Nunez, et al. (2001). "Calcium- and syntaxin 1-mediated trafficking of the neuronal glycine transporter GLYT2." J Biol Chem 276(20): 17584-17590.
- Gether, U., P. H. Andersen, et al. (2006). "Neurotransmitter transporters: molecular function of important drug targets." Trends Pharmacol Sci 27(7): 375-383.
- Giber, K., M. A. Diana, et al. (2015). "A subcortical inhibitory signal for behavioral arrest in the thalamus." Nat Neurosci 18(4): 562-568.

- Gidalevitz, T., E. A. Kikis, et al. (2010). "A cellular perspective on conformational disease: the role of genetic background and proteostasis networks." Curr Opin Struct Biol 20(1): 23-32.
- Gimenez, C., G. Perez-Siles, et al. (2012). "A novel dominant hyperekplexia mutation Y705C alters trafficking and biochemical properties of the presynaptic glycine transporter GlyT2." J Biol Chem 287(34): 28986-29002.
- Goldberg, J. H., G. Tamas, et al. (2003). "Calcium microdomains in aspiny dendrites." Neuron 40(4): 807-821.
- Gomez-Varela, D., M. Schmidt, et al. (2012). "PMCA2 via PSD-95 controls calcium signaling by alpha7-containing nicotinic acetylcholine receptors on aspiny interneurons." J Neurosci 32(20): 6894-6905.
- Gomeza, J., W. Armsen, et al. (2006). "Lessons from the knocked-out glycine transporters." Handb Exp Pharmacol(175): 457-483.
- Gomeza, J., K. Ohno, et al. (2003). "Deletion of the mouse glycine transporter 2 results in a hyperekplexia phenotype and postnatal lethality." Neuron 40(4): 797-806.
- Gong, Q., M. A. Jones, et al. (2006). "Mechanisms of pharmacological rescue of trafficking-defective hERG mutant channels in human long QT syndrome." J Biol Chem 281(7): 4069-4074.
- Gonzalez-Gonzalez, I. M., N. Garcia-Tardon, et al. (2008). "PKC-dependent endocytosis of the GLT1 glutamate transporter depends on ubiquitylation of lysines located in a C-terminal cluster." Glia 56(9): 963-974.
- Grenningloh, G., A. Rienitz, et al. (1987). "The strychnine-binding subunit of the glycine receptor shows homology with nicotinic acetylcholine receptors." Nature 328(6127): 215-220.
- Grossman, T. R. and N. Nelson (2002). "Differential effect of pH on sodium binding by the various GABA transporters expressed in Xenopus oocytes." FEBS Lett 527(1-3): 125-132.
- Gupta, A. N., K. Neupane, et al. (2016). "Pharmacological chaperone reshapes the energy landscape for folding and aggregation of the prion protein." Nat Commun 7: 12058.
- Hammond, C., I. Braakman, et al. (1994). "Role of N-linked oligosaccharide recognition, glucose trimming, and calnexin in glycoprotein folding and quality control." Proc Natl Acad Sci U S A 91(3): 913-917.
- Han, Y. and S. M. Wu (1999). "Modulation of glycine receptors in retinal ganglion cells by zinc." Proc Natl Acad Sci U S A 96(6): 3234-3238.
- Han, Y., J. Zhang, et al. (1997). "Partition of transient and sustained

inhibitory glycinergic input to retinal ganglion cells." J Neurosci 17(10): 3392-3400.

- Hanley, J. G., E. M. Jones, et al. (2000). "GABA receptor rho1 subunit interacts with a novel splice variant of the glycine transporter, GLYT-1." J Biol Chem 275(2): 840-846.
- Haranishi, Y., K. Hara, et al. (2010). "The antinociceptive effect of intrathecal administration of glycine transporter-2 inhibitor ALX1393 in a rat acute pain model." Anesth Analg 110(2): 615-621.
- Harvey, R. J., M. Topf, et al. (2008). "The genetics of hyperekplexia: more than startle!" Trends Genet 24(9): 439-447.
- Harvey, R. J. and B. K. Yee (2013). "Glycine transporters as novel therapeutic targets in schizophrenia, alcohol dependence and pain." Nat Rev Drug Discov 12(11): 866-885.
- Hashimoto, K. (2011). "Glycine transporter-1: a new potential therapeutic target for schizophrenia." Curr Pharm Des 17(2): 112-120.
- Hastrup, H., N. Sen, et al. (2003). "The human dopamine transporter forms a tetramer in the plasma membrane: cross-linking of a cysteine in the fourth transmembrane segment is sensitive to cocaine analogs." J Biol Chem 278(46): 45045-45048.
- Hebert, D. N., L. Lamriben, et al. (2014). "The intrinsic and extrinsic effects of N-linked glycans on glycoproteostasis." Nat Chem Biol 10(11): 902-910.
- Hetz, C. (2012). "The unfolded protein response: controlling cell fate decisions under ER stress and beyond." Nat Rev Mol Cell Biol 13(2): 89-102.
- Hetz, C. and B. Mollereau (2014). "Disturbance of endoplasmic reticulum proteostasis in neurodegenerative diseases." Nat Rev Neurosci 15(4): 233-249.
- Hidvegi, T., M. Ewing, et al. (2010). "An autophagy-enhancing drug promotes degradation of mutant alpha1-antitrypsin Z and reduces hepatic fibrosis." Science 329(5988): 229-232.
- Hirzel, K., U. Muller, et al. (2006). "Hyperekplexia phenotype of glycine receptor alpha1 subunit mutant mice identifies Zn(2+) as an essential endogenous modulator of glycinergic neurotransmission." Neuron 52(4): 679-690.
- Hong, W. C. and S. G. Amara (2010). "Membrane cholesterol modulates the outward facing conformation of the dopamine transporter and alters cocaine binding." J Biol Chem 285(42): 32616-32626.
- Horiuchi, M., S. Loebrich, et al. (2005). "Cellular localization and subcellular distribution of Unc-33-like protein 6, a brain-specific protein of the collapsin response mediator protein family that interacts

with the neuronal glycine transporter 2." J Neurochem 94(2): 307-315.

- Huang, R. Q. and G. H. Dillon (1999). "Effect of extracellular pH on GABA-activated current in rat recombinant receptors and thin hypothalamic slices." J Neurophysiol 82(3): 1233-1243.
- Iannitti, T. and B. Palmieri (2011). "Clinical and experimental applications of sodium phenylbutyrate." Drugs R D 11(3): 227-249.
- Iram, S. H. and S. P. Cole (2012). "Mutation of Glu521 or Glu535 in cytoplasmic loop 5 causes differential misfolding in multiple domains of multidrug and organic anion transporter MRP1 (ABCC1)." J Biol Chem 287(10): 7543-7555.
- Ishihara, N., W. Armsen, et al. (2010). "Generation of a mouse line expressing Cre recombinase in glycinergic interneurons." Genesis 48(7): 437-445.
- Ishii, S. (2012). "Pharmacological chaperone therapy for Fabry disease." Proc Jpn Acad Ser B Phys Biol Sci 88(1): 18-30.
- Jardetzky, O. (1966). "Simple allosteric model for membrane pumps." Nature 211(5052): 969-970.
- Jasti, J., H. Furukawa, et al. (2007). "Structure of acid-sensing ion channel 1 at 1.9 A resolution and low pH." Nature 449(7160): 316-323.
- Jayanthi, L. D., D. J. Samuvel, et al. (2005). "Evidence for biphasic effects of protein kinase C on serotonin transporter function, endocytosis, and phosphorylation." Mol Pharmacol 67(6): 2077-2087.
- Jiang, L., M. D. Bechtel, et al. (2012). "Decreases in plasma membrane Ca(2)(+)-ATPase in brain synaptic membrane rafts from aged rats." J Neurochem 123(5): 689-699.
- Jimenez, E., E. Nunez, et al. (2015). "Glycine transporters GlyT1 and GlyT2 are differentially modulated by glycogen synthase kinase 3beta." Neuropharmacology 89: 245-254.
- Johnston, J. A., C. L. Ward, et al. (1998). "Aggresomes: a cellular response to misfolded proteins." J Cell Biol 143(7): 1883-1898.
- Jones, E. M., A. Fernald, et al. (1995). "Assignment of SLC6A9 to human chromosome band 1p33 by in situ hybridization." Cytogenet Cell Genet 71(3): 211.
- Ju, P., K. R. Aubrey, et al. (2004). "Zn2+ inhibits glycine transport by glycine transporter subtype 1b." J Biol Chem 279(22): 22983-22991.
- Jucker, M. and L. C. Walker (2013). "Self-propagation of pathogenic protein aggregates in neurodegenerative diseases." Nature 501(7465): 45-51.

- Jursky, F. and N. Nelson (1995). "Localization of glycine neurotransmitter transporter (GLYT2) reveals correlation with the distribution of glycine receptor." J Neurochem 64(3): 1026-1033.
- Kaneko, M. (2012). "[Molecular pharmacological studies on the protection mechanism against endoplasmic reticulum stress-induced neurodegenerative disease]." Yakugaku Zasshi 132(12): 1437-1442.
- Keller, A. F., J. A. Coull, et al. (2001). "Region-specific developmental specialization of GABA-glycine cosynapses in laminas I-II of the rat spinal dorsal horn." J Neurosci 21(20): 7871-7880.
- Kemter, E., S. Sklenak, et al. (2014). "No amelioration of uromodulin maturation and trafficking defect by sodium 4-phenylbutyrate in vivo: studies in mouse models of uromodulin-associated kidney disease." J Biol Chem 289(15): 10715-10726.
- Kilic, F. and G. Rudnick (2000). "Oligomerization of serotonin transporter and its functional consequences." Proc Natl Acad Sci U S A 97(7): 3106-3111.
- Kim, K. M., S. F. Kingsmore, et al. (1994). "Cloning of the human glycine transporter type 1: molecular and pharmacological characterization of novel isoform variants and chromosomal localization of the gene in the human and mouse genomes." Mol Pharmacol 45(4): 608-617.
- Kim, Y. E., M. S. Hipp, et al. (2013). "Molecular chaperone functions in protein folding and proteostasis." Annu Rev Biochem 82: 323-355.
- Kirsch, J., D. Langosch, et al. (1991). "The 93-kDa glycine receptor-associated protein binds to tubulin." J Biol Chem 266(33): 22242-22245.
- Knollman, P. E., J. A. Janovick, et al. (2005). "Parallel regulation of membrane trafficking and dominant-negative effects by misrouted gonadotropin-releasing hormone receptor mutants." J Biol Chem 280(26): 24506-24514.
- Koban, F., A. El-Kasaby, et al. (2015). "A salt bridge linking the first intracellular loop with the C terminus facilitates the folding of the serotonin transporter." J Biol Chem 290(21): 13263-13278.
- Kolb, P. S., E. A. Ayaub, et al. (2015). "The therapeutic effects of 4-phenylbutyric acid in maintaining proteostasis." Int J Biochem Cell Biol 61: 45-52.
- Komander, D. and M. Rape (2012). "The ubiquitin code." Annu Rev Biochem 81: 203-229.
- Kopito, R. R. (1999). "Biosynthesis and degradation of CFTR." Physiol Rev 79(1 Suppl): S167-173.
- Krishnamurthy, H. and E. Gouaux (2012). "X-ray structures of LeuT in substrate-

free outward-open and apo inward-open states." Nature 481(7382): 469-474.

- Krishtal, O. (2003). "The ASICs: signaling molecules? Modulators?" Trends Neurosci 26(9): 477-483.
- Kristensen, A. S., J. Andersen, et al. (2011). "SLC6 neurotransmitter transporters: structure, function, and regulation." Pharmacol Rev 63(3): 585-640.
- Kubota, K., Y. Niinuma, et al. (2006). "Suppressive effects of 4-phenylbutyrate on the aggregation of Pael receptors and endoplasmic reticulum stress." J Neurochem 97(5): 1259-1268.
- Kuhar, M. J. and M. A. Zarbin (1978). "Synaptosomal transport: a chloride dependence for choline, GABA, glycine and several other compounds." J Neurochem 31(1): 251-256.
- Kurolap, A., A. Armbruster, et al. (2016). "Loss of Glycine Transporter 1 Causes a Subtype of Glycine Encephalopathy with Arthrogryposis and Mildly Elevated Cerebrospinal Fluid Glycine." Am J Hum Genet 99(5): 1172-1180.
- Labrie, V. and J. C. Roder (2010). "The involvement of the NMDA receptor D-serine/glycine site in the pathophysiology and treatment of schizophrenia." Neurosci Biobehav Rev 34(3): 351-372.
- Langosch, D., L. Thomas, et al. (1988). "Conserved quaternary structure of ligand-gated ion channels: the postsynaptic glycine receptor is a pentamer." Proc Natl Acad Sci U S A 85(19): 7394-7398.
- Lee, H. S., Y. Qi, et al. (2015). "Effects of N-glycosylation on protein conformation and dynamics: Protein Data Bank analysis and molecular dynamics simulation study." Sci Rep 5: 8926.
- Legendre, P. (2001). "The glycinergic inhibitory synapse." Cell Mol Life Sci 58(5-6): 760-793.
- Leidenheimer, N. J. and K. G. Ryder (2014). "Pharmacological chaperoning: a primer on mechanism and pharmacology." Pharmacol Res 83: 10-19.
- Leskela, T. T., P. M. Markkanen, et al. (2009). "Phe27Cys polymorphism alters the maturation and subcellular localization of the human delta opioid receptor." Traffic 10(1): 116-129.
- Li, L. B., N. Chen, et al. (2004). "The role of N-glycosylation in function and surface trafficking of the human dopamine transporter." J Biol Chem 279(20): 21012-21020.
- Li, Y., P. S. Hasenhuetl, et al. (2015). "Dual Action of Zn2+ on the Transport Cycle of the Dopamine Transporter." J Biol Chem 290(52): 31069-31076.

- Li, Y., F. P. Mayer, et al. (2017). "Occupancy of the Zinc-binding Site by Transition Metals Decreases the Substrate Affinity of the Human Dopamine Transporter by an Allosteric Mechanism." J Biol Chem 292(10): 4235-4243.
- Liu, Q. R., B. Lopez-Corcuera, et al. (1993). "Cloning and expression of a spinal cord- and brain-specific glycine transporter with novel structural features." J Biol Chem 268(30): 22802-22808.
- Loffing, J., B. D. Moyer, et al. (1999). "PBA increases CFTR expression but at high doses inhibits Cl(-) secretion in Calu-3 airway epithelial cells." Am J Physiol 277(4 Pt 1): L700-708.
- Loland, C. J., L. Norregaard, et al. (1999). "Defining proximity relationships in the tertiary structure of the dopamine transporter. Identification of a conserved glutamic acid as a third coordinate in the endogenous Zn(2+)-binding site." J Biol Chem 274(52): 36928-36934.
- Lynes, E. M., A. Raturi, et al. (2013). "Palmitoylation is the switch that assigns calnexin to quality control or ER Ca2+ signaling." J Cell Sci 126(Pt 17): 3893-3903.
- Madden, D. R. (2002). "The structure and function of glutamate receptor ion channels." Nat Rev Neurosci 3(2): 91-101.
- Magnani, F., C. G. Tate, et al. (2004). "Partitioning of the serotonin transporter into lipid microdomains modulates transport of serotonin." J Biol Chem 279(37): 38770-38778.
- Makley, L. N., K. A. McMenimen, et al. (2015). "Pharmacological chaperone for alpha-crystallin partially restores transparency in cataract models." Science 350(6261): 674-677.
- Marques-da-Silva, D. and C. Gutierrez-Merino (2014). "Caveolin-rich lipid rafts of the plasma membrane of mature cerebellar granule neurons are microcompartments for calcium/reactive oxygen and nitrogen species cross-talk signaling." Cell Calcium 56(2): 108-123.
- Martinez-Maza, R., I. Poyatos, et al. (2001). "The role of N-glycosylation in transport to the plasma membrane and sorting of the neuronal glycine transporter GLYT2." J Biol Chem 276(3): 2168-2173.
- Martinez-Villarreal, J., N. Garcia Tardon, et al. (2012). "Cell surface turnover of the glutamate transporter GLT-1 is mediated by ubiquitination/deubiquitination." Glia 60(9): 1356-1365.
- Mata, A. M. and M. R. Sepulveda (2005). "Calcium pumps in the central nervous system." Brain Res Brain Res Rev 49(2): 398-405.
- Matchkov, V. V., H. Gustafsson, et al. (2007). "Interaction between Na+/K+-pump and Na+/Ca2+-exchanger modulates intercellular communication." Circ Res 100(7): 1026-1035.

- McIntire, S. L., R. J. Reimer, et al. (1997). "Identification and characterization of the vesicular GABA transporter." Nature 389(6653): 870-876.
- Melikian, H. E., J. K. McDonald, et al. (1994). "Human norepinephrine transporter. Biosynthetic studies using a site-directed polyclonal antibody." J Biol Chem 269(16): 12290-12297.
- Melzack, R. and P. D. Wall (1965). "Pain mechanisms: a new theory." Science 150(3699): 971-979.
- Merianda, T. T., A. C. Lin, et al. (2009). "A functional equivalent of endoplasmic reticulum and Golgi in axons for secretion of locally synthesized proteins." Mol Cell Neurosci 40(2): 128-142.
- Milner, H. E., R. Beliveau, et al. (1994). "The in situ size of the dopamine transporter is a tetramer as estimated by radiation inactivation." Biochim Biophys Acta 1190(1): 185-187.
- Miller, E. A., T. H. Beilharz, et al. (2003). "Multiple cargo binding sites on the COPII subunit Sec24p ensure capture of diverse membrane proteins into transport vesicles." Cell 114(4): 497-509.
- Muchowski, P. J. and J. L. Wacker (2005). "Modulation of neurodegeneration by molecular chaperones." Nat Rev Neurosci 6(1): 11-22.
- Niggli, V. and E. Sigel (2008). "Anticipating antiport in P-type ATPases." Trends Biochem Sci 33(4): 156-160.
- Niggli, V., E. Sigel, et al. (1982). "The purified Ca2+ pump of human erythrocyte membranes catalyzes an electroneutral Ca2+-H+ exchange in reconstituted liposomal systems." J Biol Chem 257(5): 2350-2356.
- Nishimura, T., Y. Fukata, et al. (2003). "CRMP-2 regulates polarized Numb-mediated endocytosis for axon growth." Nat Cell Biol 5(9): 819-826.
- Nong, Y., Y. Q. Huang, et al. (2003). "Glycine binding primes NMDA receptor internalization." Nature 422(6929): 302-307.
- Noorwez, S. M., R. R. Sama, et al. (2009). "Calnexin improves the folding efficiency of mutant rhodopsin in the presence of pharmacological chaperone 11-cis-retinal." J Biol Chem 284(48): 33333-33342.
- Nunez, E., P. Alonso-Torres, et al. (2008). "The neuronal glycine transporter GLYT2 associates with membrane rafts: functional modulation by lipid environment." J Neurochem 105(6): 2080-2090.
- Nunez, E. and C. Aragon (1994). "Structural analysis and functional role of the

carbohydrate component of glycine transporter." J Biol Chem 269(24): 16920-16924.

- Nunez, E., G. Perez-Siles, et al. (2009). "Subcellular localization of the neuronal glycine transporter GLYT2 in brainstem." Traffic 10(7): 829-843.
- Ohno, K., M. Koroll, et al. (2004). "The neuronal glycine transporter 2 interacts with the PDZ domain protein syntenin-1." Mol Cell Neurosci 26(4): 518-529.
- Okiyoneda, T., P. M. Apaja, et al. (2011). "Protein quality control at the plasma membrane." Curr Opin Cell Biol 23(4): 483-491.
- Olzmann, J. A., L. Li, et al. (2008). "Aggresome formation and neurodegenerative diseases: therapeutic implications." Curr Med Chem 15(1): 47-60.
- Ong, D. S., T. W. Mu, et al. (2010). "Endoplasmic reticulum Ca2+ increases enhance mutant glucocerebrosidase proteostasis." Nat Chem Biol 6(6): 424-432.
- Parodi, A. J. (2000). "Protein glucosylation and its role in protein folding." Annu Rev Biochem 69: 69-93.
- Penmatsa, A., K. H. Wang, et al. (2013). "X-ray structure of dopamine transporter elucidates antidepressant mechanism." Nature 503(7474): 85-90.
- Perez-Siles, G., A. Morreale, et al. (2011). "Molecular basis of the differential interaction with lithium of glycine transporters GLYT1 and GLYT2." J Neurochem 118(2): 195-204.
- Perez-Siles, G., E. Nunez, et al. (2012). "An aspartate residue in the external vestibule of GLYT2 (glycine transporter 2) controls cation access and transport coupling." Biochem J 442(2): 323-334.
- Perri, E. R., C. J. Thomas, et al. (2015). "The Unfolded Protein Response and the Role of Protein Disulfide Isomerase in Neurodegeneration." Front Cell Dev Biol 3: 80.
- Petaja-Repo, U. E., M. Hogue, et al. (2002). "Ligands act as pharmacological chaperones and increase the efficiency of delta opioid receptor maturation." EMBO J 21(7): 1628-1637.
- Pey, A. L., M. Ying, et al. (2008). "Identification of pharmacological chaperones as potential therapeutic agents to treat phenylketonuria." J Clin Invest 118(8): 2858-2867.
- Pramod, A. B., J. Foster, et al. (2013). "SLC6 transporters: structure, function, regulation, disease association and therapeutics." Mol Aspects Med 34(2-3): 197-219.
- Praveen, V., S. K. Patole, et al. (2001). "Hyperekplexia in neonates." Postgrad Med J 77(911): 570-572.
- Punnakkal, P., C. von Schoultz, et al. (2014). "Morphological, biophysical and synaptic properties of glutamatergic neurons of the mouse spinal dorsal horn." J Physiol 592(4): 759-776.

- Ramirez, O. A., S. Hartel, et al. (2011). "Location matters: the endoplasmic reticulum and protein trafficking in dendrites." Biol Res 44(1): 17-23.
- Rees, M. I., M. Andrew, et al. (1994). "Evidence for recessive as well as dominant forms of startle disease (hyperekplexia) caused by mutations in the alpha 1 subunit of the inhibitory glycine receptor." Hum Mol Genet 3(12): 2175-2179.
- Rees, M. I., K. Harvey, et al. (2006). "Mutations in the gene encoding GlyT2 (SLC6A5) define a presynaptic component of human startle disease." Nat Genet 38(7): 801-806.
- Rees, M. I., T. M. Lewis, et al. (2002). "Hyperekplexia associated with compound heterozygote mutations in the beta-subunit of the human inhibitory glycine receptor (GLRB)." Hum Mol Genet 11(7): 853-860.
- Ron, D. and P. Walter (2007). "Signal integration in the endoplasmic reticulum unfolded protein response." Nat Rev Mol Cell Biol 8(7): 519-529.
- Roome, C. J. and R. M. Empson (2013). "The contribution of the sodium-calcium exchanger (NCX) and plasma membrane Ca(2+) ATPase (PMCA) to cerebellar synapse function." Adv Exp Med Biol 961: 251-263.
- Roome, C. J., E. M. Power, et al. (2013). "Transient reversal of the sodium/calcium exchanger boosts presynaptic calcium and synaptic transmission at a cerebellar synapse." J Neurophysiol 109(6): 1669-1680.
- Routledge, K. E., V. Gupta, et al. (2010). "Emergent properties of proteostasis-COPII coupled systems in human health and disease." Mol Membr Biol 27(8): 385-397.
- Roux, M. J. and S. Supplisson (2000). "Neuronal and glial glycine transporters have different stoichiometries." Neuron 25(2): 373-383.
- Rozeboom, A. M., B. N. Queenan, et al. (2015). "Evidence for glycinergic GluN1/GluN3 NMDA receptors in hippocampal metaplasticity." Neurobiol Learn Mem 125: 265-273.
- Rudnick, G., R. Kramer, et al. (2014). "The SLC6 transporters: perspectives on structure, functions, regulation, and models for transporter dysfunction." Pflugers Arch 466(1): 25-42.
- Rutkowski, D. T., S. M. Arnold, et al. (2006). "Adaptation to ER stress is mediated by differential stabilities of pro-survival and pro-apoptotic mRNAs and proteins." PLoS Biol 4(11): e374.
- Saenz-Lope, E., F. J. Herranz-Tanarro, et al. (1984). "Hyperekplexia: a syndrome of pathological startle responses." Ann Neurol 15(1): 36-41.
- Safory, H., S. Neame, et al. (2015). "The alanine-serine-cysteine-1 (Asc-1) transporter controls glycine levels in the brain and is required

for glycinergic inhibitory transmission." EMBO Rep 16(5): 590-598.

• Sagne, C., S. El Mestikawy, et al. (1997). "Cloning of a functional vesicular GABA and glycine transporter by screening of genome databases." FEBS Lett 417(2): 177-183.

• Sanders, C. R. and J. K. Myers (2004). "Disease-related misassembly of membrane proteins." Annu Rev Biophys Biomol Struct 33: 25-51.

• Sato, K., H. Betz, et al. (1995). "The recombinant GABA transporter GAT1 is downregulated upon activation of protein kinase C." FEBS Lett 375(1-2): 99-102.

• Sato, K. and A. Nakano (2003). "Oligomerization of a cargo receptor directs protein sorting into COPII-coated transport vesicles." Mol Biol Cell 14(7): 3055-3063.

• Sato, S., C. L. Ward, et al. (1996). "Glycerol reverses the misfolding phenotype of the most common cystic fibrosis mutation." J Biol Chem 271(2): 635-638.

• Satou, Y., H. A. Al-Shawafi, et al. (2012). "Disulfide bonds are critical for tissue-nonspecific alkaline phosphatase function revealed by analysis of mutant proteins bearing a C(201)-Y or C(489)-S substitution associated with severe hypophosphatasia." Biochim Biophys Acta 1822(4): 581-588.

• Scanlon, S. M., D. C. Williams, et al. (2001). "Membrane cholesterol modulates serotonin transporter activity." Biochemistry 40(35): 10507-10513.

• Scheper, W. and J. J. Hoozemans (2015). "The unfolded protein response in neurodegenerative diseases: a neuropathological perspective." Acta Neuropathol 130(3): 315-331.

• Schweikhard, E. S., B. C. Burckhardt, et al. (2015). "Role of N-glycosylation in renal betaine transport." Biochem J 470(2): 169-179.

• Shiang, R., S. G. Ryan, et al. (1993). "Mutations in the alpha 1 subunit of the inhibitory glycine receptor cause the dominant neurologic disorder, hyperekplexia." Nat Genet 5(4): 351-358.

• Skoulakis, S. and J. M. Goodfellow (2003). "The pH-dependent stability of wild-type and mutant transthyretin oligomers." Biophys J 84(5): 2795-2804.

• Solda, T., C. Galli, et al. (2007). "Substrate-specific requirements for UGT1-dependent release from calnexin." Mol Cell 27(2): 238-249.

• Song, Y., G. Fang, et al. (2012). "Human surfactant protein A2 gene mutations impair dimmer/trimer assembly leading to deficiency in protein sialylation and secretion." PLoS One 7(10): e46559.

• Sorkina, T., S. Doolen, et al. (2003). "Oligomerization of dopamine

transporters visualized in living cells by fluorescence resonance energy transfer microscopy." J Biol Chem 278(30): 28274-28283.

- Sorrenson, B., R. J. Suetani, et al. (2013). "Functional rescue of mutant ABCA1 proteins by sodium 4-phenylbutyrate." J Lipid Res 54(1): 55-62.
- Springer, S., P. Malkus, et al. (2014). "Regulated oligomerization induces uptake of a membrane protein into COPII vesicles independent of its cytosolic tail." Traffic 15(5): 531-545.
- Stronge, V. S., Y. Saito, et al. (2001). "Relationship between calnexin and BiP in suppressing aggregation and promoting refolding of protein and glycoprotein substrates." J Biol Chem 276(43): 39779-39787.
- Sucic, S., A. El-Kasaby, et al. (2011). "The serotonin transporter is an exclusive client of the coat protein complex II (COPII) component SEC24C." J Biol Chem 286(18): 16482-16490.
- Sucic, S., F. Koban, et al. (2013). "Switching the clientele: a lysine residing in the C terminus of the serotonin transporter specifies its preference for the coat protein complex II component SEC24C." J Biol Chem 288(8): 5330-5341.
- Swanton, E., S. High, et al. (2003). "Role of calnexin in the glycan-independent quality control of proteolipid protein." EMBO J 22(12): 2948-2958.
- Tate, C. G. and R. D. Blakely (1994). "The effect of N-linked glycosylation on activity of the Na(+)- and Cl(-)-dependent serotonin transporter expressed using recombinant baculovirus in insect cells." J Biol Chem 269(42): 26303-26310.
- Tate, C. G., E. Whiteley, et al. (1999). "Molecular chaperones stimulate the functional expression of the cocaine-sensitive serotonin transporter." J Biol Chem 274(25): 17551-17558.
- Teske, B. F., S. A. Wek, et al. (2011). "The eIF2 kinase PERK and the integrated stress response facilitate activation of ATF6 during endoplasmic reticulum stress." Mol Biol Cell 22(22): 4390-4405.
- Thomas, R. C. (2009). "The plasma membrane calcium ATPase (PMCA) of neurones is electroneutral and exchanges 2 H+ for each Ca2+ or Ba2+ ion extruded." J Physiol 587(2): 315-327.
- Thomas, R. C. (2011). "The Ca(2+): H(+) coupling ratio of the plasma membrane calcium ATPase in neurones is little sensitive to changes in external or internal pH." Cell Calcium 49(6): 357-364.
- Thomas, R. H., S. K. Chung, et al. (2013). "Genotype-phenotype correlations in hyperekplexia: apnoeas, learning difficulties and speech delay." Brain 136(Pt 10): 3085-3095.

- Toth, K. (2011). "Zinc in neurotransmission." Annu Rev Nutr 31: 139-153.
- Traynelis, S. F., L. P. Wollmuth, et al. (2010). "Glutamate receptor ion channels: structure, regulation, and function." Pharmacol Rev 62(3): 405-496.
- Turturici, G., G. Sconzo, et al. (2011). "Hsp70 and its molecular role in nervous system diseases." Biochem Res Int 2011: 618127.
- Ushioda, R., J. Hoseki, et al. (2013). "Glycosylation-independent ERAD pathway serves as a backup system under ER stress." Mol Biol Cell 24(20): 3155-3163.
- Veitia, R. A. (2007). "Exploring the molecular etiology of dominant-negative mutations." Plant Cell 19(12): 3843-3851.
- Wang, M. and R. J. Kaufman (2014). "The impact of the endoplasmic reticulum protein-folding environment on cancer development." Nat Rev Cancer 14(9): 581-597.
- Wang, M. and R. J. Kaufman (2016). "Protein misfolding in the endoplasmic reticulum as a conduit to human disease." Nature 529(7586): 326-335.
- Wang, W., Z. Wu, et al. (2013). "Glycine metabolism in animals and humans: implications for nutrition and health." Amino Acids 45(3): 463-477.
- Wenthold, R. J., R. A. Altschuler, et al. (1990). "Immunocytochemistry of neurotransmitter receptors." J Electron Microsc Tech 15(1): 81-96.
- Williams, S. E., A. A. Reed, et al. (2009). "Uromodulin mutations causing familial juvenile hyperuricaemic nephropathy lead to protein maturation defects and retention in the endoplasmic reticulum." Hum Mol Genet 18(16): 2963-2974.
- Willis, A., E. J. Jung, et al. (2004). "Mutant p53 exerts a dominant negative effect by preventing wild-type p53 from binding to the promoter of its target genes." Oncogene 23(13): 2330-2338.
- Woycechowsky, K. J. and R. T. Raines (2000). "Native disulfide bond formation in proteins." Curr Opin Chem Biol 4(5): 533-539.
- Xiong, W., S. R. Chen, et al. (2014). "Presynaptic glycine receptors as a potential therapeutic target for hyperekplexia disease." Nat Neurosci 17(2): 232-239.
- Yamashita, A., S. K. Singh, et al. (2005). "Crystal structure of a bacterial homologue of Na+/Cl--dependent neurotransmitter transporters." Nature 437(7056): 215-223.
- Yang, Z., E. Taran, et al. (2012). "Stoichiometry and subunit arrangement of alpha1beta glycine receptors as determined by atomic force microscopy." Biochemistry 51(26): 5229-5231.
- Zafra, F., C. Aragon, et al. (1995). "Glycine transporters are

differentially expressed among CNS cells." J Neurosci 15(5 Pt 2): 3952-3969.

- Zafra, F. and C. Gimenez (1989). "Characteristics and adaptive regulation of glycine transport in cultured glial cells." Biochem J 258(2): 403-408.
- Zafra, F. I., I. Giménez, C. (2016). "Glycinergic transmission: glycine transporter GlyT2 in neuronal pathologies." Neuronal Signaling.
- Zeilhofer, H. U. (2008). "Loss of glycinergic and GABAergic inhibition in chronic pain--contributions of inflammation and microglia." Int Immunopharmacol 8(2): 182-187.
- Zeilhofer, H. U., B. Studler, et al. (2005). "Glycinergic neurons expressing enhanced green fluorescent protein in bacterial artificial chromosome transgenic mice." J Comp Neurol 482(2): 123-141.
- Zeitlin, P. L., M. Diener-West, et al. (2002). "Evidence of CFTR function in cystic fibrosis after systemic administration of 4-phenylbutyrate." Mol Ther 6(1): 119-126.
- Zhen, J., T. Antonio, et al. (2015). "Dopamine transporter oligomerization: impact of combining protomers with differential cocaine analog binding affinities." J Neurochem 133(2): 167-173.